



# Kent Academic Repository

**Nevill, Andrew John (1991) *A foot pressure measurement system utilising PVdF and copolymer piezoelectric transducers*. Doctor of Philosophy (PhD) thesis, University of Kent.**

## Downloaded from

<https://kar.kent.ac.uk/86116/> The University of Kent's Academic Repository KAR

## The version of record is available from

<https://doi.org/10.22024/UniKent/01.02.86116>

## This document version

UNSPECIFIED

## DOI for this version

## Licence for this version

CC BY-NC-ND (Attribution-NonCommercial-NoDerivatives)

## Additional information

This thesis has been digitised by EThOS, the British Library digitisation service, for purposes of preservation and dissemination. It was uploaded to KAR on 09 February 2021 in order to hold its content and record within University of Kent systems. It is available Open Access using a Creative Commons Attribution, Non-commercial, No Derivatives (<https://creativecommons.org/licenses/by-nc-nd/4.0/>) licence so that the thesis and its author, can benefit from opportunities for increased readership and citation. This was done in line with University of Kent policies (<https://www.kent.ac.uk/is/strategy/docs/Kent%20Open%20Access%20policy.pdf>). If y...

## Versions of research works

### Versions of Record

If this version is the version of record, it is the same as the published version available on the publisher's web site. Cite as the published version.

### Author Accepted Manuscripts

If this document is identified as the Author Accepted Manuscript it is the version after peer review but before type setting, copy editing or publisher branding. Cite as Surname, Initial. (Year) 'Title of article'. To be published in *Title of Journal*, Volume and issue numbers [peer-reviewed accepted version]. Available at: DOI or URL (Accessed: date).

## Enquiries

If you have questions about this document contact [ResearchSupport@kent.ac.uk](mailto:ResearchSupport@kent.ac.uk). Please include the URL of the record in KAR. If you believe that your, or a third party's rights have been compromised through this document please see our [Take Down policy](https://www.kent.ac.uk/guides/kar-the-kent-academic-repository#policies) (available from <https://www.kent.ac.uk/guides/kar-the-kent-academic-repository#policies>).

**A FOOT PRESSURE MEASUREMENT SYSTEM  
UTILISING PVdF AND COPOLYMER  
PIEZOELECTRIC TRANSDUCERS**

by

**ANDREW JOHN NEVILL**

*A thesis presented for the degree of  
Doctor of Philosophy in Electronic Engineering  
at the University of Kent at Canterbury*

1991

## **ACKNOWLEDGEMENTS**

A very special thanks go to my supervisor, Dr. M.G.Pepper for his cheerful enthusiasm and encouragement and his invaluable advice and guidance throughout the course of this research. Many thanks also to all the members, past and present, of the Medical Electronics group at UKC who always made themselves available.

I would like to acknowledge the staff of the Electronic Engineering laboratories at UKC for their assistance and cooperation, and also the staff from the Medical Physics department and the library at Kent and Canterbury Hospital for their help.

Special thanks also go to Mr. M.Whiting, my clinical tutor, and the staff at Leaf Hospital, Eastbourne who have offered invaluable clinical advice and assistance.

At the other end of the country, I would like to thank Prof. D.I.Rowley and the members of the Orthopaedic and Trauma Surgery department, Dundee Royal Infirmary for their considerable clinical support.

Downs Surgical plc, and particularly Mr D.Bevan have my thanks for their involvement and initial funding of the project.

My appreciation also goes to all those individuals, too numerous to mention, who in one way or another have offered advice and assistance throughout this research.

Last but by no means least, a very special thanks must go to Emma who has managed to put up with me during the writing of this thesis.

To;

My Mother and Father

## CONTENTS

	Page	
Acknowledgements	(ii)	
Contents	(iv)	
Abstract	(vii)	
<b>Chapter 1</b>	<b>Introduction and aims of project</b>	<b>1</b>
1.1	Introduction	2
1.2	Anatomy of the human foot	4
1.2.1	Osteology	4
1.2.2	Arthrology	6
1.2.2.1	Arches of the foot	8
1.2.3	Myology	9
1.2.4	Major load bearing areas of the plantar surface	9
1.3	Methods of study of human gait	10
1.3.1	A dictionary of terms	11
1.3.2	Kinematics of gait	13
1.3.3	Kinetics of gait	13
1.3.4	EMG detection to describe gait	14
1.3.5	In-shoe pressure measurement	14
1.3.6	The normal human gait cycle	15
1.4	Polyvinylidene fluoride and copolymer piezoelectric film	16
1.4.1	Uses and application for piezoelectric film	17
1.4.2	Direct force measurement	18
1.4.3	A review of transducer materials and methods for gait analysis studies	19
1.5	A summary	20
<b>Chapter 2</b>	<b>Historical review</b>	<b>21</b>
2.1	Introduction	22
2.2	Methodology	22
2.2.1	Complete analysis of human gait	23
2.2.2	Foot pressure measurement systems	23
2.2.2.1	Barefoot to floor techniques	24
2.2.2.2	In-shoe techniques	28
2.2.2.3	Other related techniques	32
2.3	Clinical observation	33
2.3.1	Normal static foot loading	33
2.3.2	Normal dynamic foot loading	34
2.3.2.1	The vertical component of reaction force	36
2.3.2.2	Centre of foot pressure	36
2.3.2.3	Plantar distribution of load	38
2.3.3	Foot pressure measurement to investigate pathological conditions	39
2.4	Conclusions	41
<b>Chapter 3</b>	<b>Properties of PVdF and copolymer film</b>	<b>43</b>
3.1	Introduction	44
3.2	Production of PVdF and copolymer piezoelectric film	46
3.3	Polymer film piezoelectricity	47
3.3.1	Definition of piezo film axes	47
3.3.2	The direct and converse piezoelectric effect	48
3.3.3	The piezoelectric constants	49
3.3.4	Piezoelectric strain or charge constant	50
3.3.5	Piezoelectric stress or voltage constant	51

3.3.6	Secondary piezoelectric effects	51
3.3.7	Piezoelectric strength - a material comparison	52
3.4	Mechanical to electrical transduction	53
3.4.1	Relationship between transducer and measurement site areas - stress measurement in the thickness mode	54
3.4.1.1	The effect upon transducer sensitivity of using non-conducting adhesives for fabrication	57
3.4.2	Feasibility of direct shear force measurement using piezo film	59
3.5	Inherent measurement artifacts	60
3.5.1	Pyroelectric effect	61
3.5.2	Bending effects	62
3.6	Conclusions	67
<b>Chapter 4</b>	<b>Transducer development</b>	<b>69</b>
4.1	Introduction - a tough transducer for a tough environment	70
4.2	The foot transducer interface	72
4.2.1	Insole fabrication	73
4.3	Vertical force transducer construction	73
4.3.1	Bonding piezoelectric films	74
4.3.2	Electroding and lead attachment	76
4.3.3	Final transducer fabrication	78
4.3.3.1	First copolymer prototype transducer set - DSHSDN	79
4.3.3.2	Second copolymer prototype transducer set - BHHHDN	79
4.3.3.3	Fabrication jig	80
4.3.3.5	Prototype PVdF transducer - BSHSDN	80
4.3.4	Latest modifications	82
4.4	Shear force measurement	83
4.5	Conclusions	84
<b>Chapter 5</b>	<b>System development</b>	<b>86</b>
5.1	Introduction and design philosophy	87
5.2	Electronic system	88
5.2.1	Amplification techniques for piezoelectric transducers	91
5.2.2	Charge amplification stage - First stage	98
5.2.3	Frequency compensation stage - Second stage	106
5.2.4	Transducer calibration	112
5.3	System construction and enclosures	116
5.3.1	Design and construction of the patient ankle boxes	116
5.3.2	Design and construction of the waist box	118
5.3.3	Design and construction of the main equipment console	118
5.4	Computer interfacing	119
5.5	Software development	120
5.5.1	Data acquisition and control - GSACQU	121
5.5.2	Data display and analysis - GSPOST	124
5.5.3	Software calibration - GSETUP	128
5.6	Conclusions	129
<b>Chapter 6</b>	<b>System performance</b>	<b>131</b>
6.1	Introduction	132
6.2	The transducer	132
6.2.1	Frequency response	132
6.2.2	Calibration	135
6.2.3	Repeatability	137
6.2.4	Linearity and hysteresis	140
6.2.5	Temperature coefficient of transducer sensitivity	141
6.2.6	Bending tests	142
6.2.7	Humidity susceptibility	144

5.3	Calibration unit	145
5.3.1	Frequency response	145
5.3.2	Calibration	147
5.4	Electronic system	150
5.4.1	Frequency response	150
5.4.2	Calibration and noise measurement	153
5.4.3	Computer data acquisition	156
5.5	Conclusions	156
<b>Chapter 7</b>	<b>Clinical measurement</b>	<b>159</b>
7.1	Introduction	160
7.2	Measurement procedure	161
7.3	Measurement results	167
7.3.1	A normal patient	167
7.3.2	Measurement repeatability	172
7.3.3	Knee failure and its effect upon foot loading	175
7.3.4	Results from a patient with heel pain	178
7.3.5	Results from orthotic insert investigations	182
7.3.6	System performance and measurement artifacts	184
7.4	A summary - clinical validity	185
<b>Chapter 8</b>	<b>Conclusions and discussion</b>	<b>187</b>
8.1	A review of the research project	188
8.1.1	Transducer development	188
8.1.2	Instrumentation	189
8.1.3	Clinical measurement	190
8.2	Outline for future development	191
8.2.1	Transducer design and development	191
8.2.2	A shear force transducer	192
8.2.3	An insole incorporating a matrix of piezoelectric film sensors	192
8.2.4	Automatic calibration for piezo film transducers	194
8.2.5	Instrumentation developments	195
8.2.6	Software developments	195
8.2.7	Combined gait analysis studies	196
8.2.8	Clinical measurement	197
8.3	Conclusions	198
References		199
Appendix I	General properties of PVdF and piezoelectric PVdF film	211
Appendix II	Gaitscan installation and operating manual	215
Appendix III	Printed circuit templates, component layout and connection diagrams	246
Appendix IV	Transducer prototype codes	252
Appendix V	Costing	255

## **ABSTRACT**

Foot pressure measurement provides valuable information in the quest for complete analysis of human gait.

In the search for accurate assessment of pathological foot conditions and subsequent successful intervention of a surgical or orthotic nature, it is desirable to be able to quantify the in-shoe load distribution under major anatomical sites of the plantar surface.

Commercially there is a trend towards barefoot, single foot strike systems. The few attempts at in-shoe pressure measurement have resulted in unreliable data, primarily due to transducer problems.

In the research detailed within this thesis PVdF and copolymer piezoelectric film has been successfully designed into novel transducers, sixteen of which have subsequently been incorporated into two insoles. These transducers provide signals allowing absolute measurement (< 10%) of vertical in-shoe loading for multiple footsteps of both feet simultaneously.

A computer based system named Gaitscan has been built around these transducers that, together with its associated electronics and computer processing, affords data collection of the required in-shoe pressure measurements during gait. Gaitscan also allows retrieval and analysis of this comprehensive information, being of use to the researcher and, as designed, to the clinician for diagnostic purposes.

Clinical trials have been carried out together with comparative measurements with other commercial foot pressure measurement systems. Gaitscan has been proven to provide a useful addition to the armoury of equipment available to the podiatrist and orthopaedic surgeon.

## **Chapter One**

**1**

# **INTRODUCTION AND AIMS OF PROJECT**

## 1.1 Introduction

The overall project aim is to define and develop an in-shoe foot pressure measurement system for use in a clinical environment to measure discrete absolute pressure values at pre-defined anatomical sites of interest to within 10%. A major part of the work will be to perform feasibility tests upon novel pressure transducer fabrications using piezoelectric polymer films.

Due to our civilised existence and the mere fact that we wear shoes, changes in the functions required of the modern foot are unavoidable. It is thought that many disorders are caused because man has only recently adapted to an upright stance and locomotion, before completeness of the evolutionary process to allow this has taken place (Hutton, 1976). Around 40% of the western adult population, primarily people over the age of 50, suffer from foot disorders of some description (M. Whiting, personal communication). Disorders such as hallux valgus are associated with the wearing of shoes, but conclusive reasons for such conditions are difficult to obtain (Stokes *et al*, 1979; Hutton and Dhanendran, 1981). Other reasons for problem feet include injuries, particularly sports injuries, and diseases, such as diabetes which is a cause of neuropathic or vascular ulceration of the plantar surface of the foot (Lord *et al*, 1986; Ciercteko *et al*, 1981).

Gait analysis is the study of how we walk and can be sectioned into the assessment of foot function, the detection of electrical muscle activity and the a study of the changing geometry of the lower limb. Present day diagnostic methods primarily involve only physical examinations and this is chiefly due to the unavailability of appropriate measurement instrumentation to enable quantifiable gait analysis or the complexity of existing systems. Thus for the orthopaedic surgeon and podiatrist the task of reliable diagnosis and assessment of all types of foot disorder has its difficulties. The few centres using gait analysis equipment on a routine basis chiefly employ methods based around force plates or pressure mats, which only allow analysis of the barefoot over a single foot strike. Commercially available systems are also primarily of this nature and attempts at in-shoe foot pressure measurement have resulted in unreliable or only coarse relative pressure indication.

Function of the shod foot can be analysed by considering the loading at a few anatomical sites of interest, namely the five metatarsal heads, the heel and the great toe. Of course, measurement under the entire plantar surface of the foot with good spatial resolution would provide a considerable amount of information. However few centres are in a position to make use of this abundance of data and

variably concentrate the analysis upon the aforementioned anatomical sites (Hughes *et al*, 1987). The engineering expertise required, complexity and cost for such a system to investigate in-shoe pressure distribution would be substantial (Hennig *et al*, 1982), such that it would no longer be considered a clinical, but a research tool.

It is clear that there is a need for an in-shoe pressure measurement system to analyse loading upon a few discrete anatomical areas. Pre- and post-operative comparisons could then be quantified for the shod foot over multiple foot steps. The absolute calibrated data would also be available for comparative tests using barefoot systems and the effects of orthotic intervention could be quantified. For pathological feet it cannot be assumed that analysis would be confined to the previously mentioned anatomical sites, therefore flexibility in the form of transducer mobility is important. Positionable transducers are also required when investigating the normal foot as all feet differ anatomically and further more because the foot positions itself uniquely inside each item of foot wear. With this background in perspective it is proposed that the research concentrate on the development of an accurate (<10%), absolute measurement transducer to monitor in-shoe pressure under pre-defined anatomical sites. A gait analysis system is required and is to be built around this transducer to enable clinical diagnosis of pathological feet. Clinical trials at two centres will be discussed.

This thesis contains eight chapters, brief details of which follow.

The introduction outlines the aims of the research, describes the anatomical structure of the foot and introduces gait analysis. Piezoelectric film is presented as a useful and versatile transducer material with particular application to dynamic pressure measurement. Chapter two is a comprehensive review of methodology and of clinical and research analysis techniques to date. Gait analysis as a whole subject is considered with emphasis upon the directly related area of in-shoe foot pressure measurement. Chapter three discusses the properties of piezoelectric film, the nature of its piezoelectricity and the theoretical response expected for detecting mechanical stress. Details of all areas of the transducer development including materials and methods used are described in chapter four, along with prototype construction procedures. Chapter five is an account of the instrumentation implementation and describes the development of the gait analysis system in terms of hardware and software. The performance of individual system components and of the system as a whole are

detailed in chapter six, which includes results from bench trials. In chapter seven some results from the many clinical trials undertaken are analysed and discussed along with a measurement protocol. Chapter eight contains conclusions drawn from the research and a discussion on areas for future work.

## 1.2 Anatomy of the human foot

The anatomy of the foot bears some resemblance to that of the hand. Consisting of 26 bones, 11 muscles and a network of ligaments and tendons, it has two important functions to perform; the support of body weight when standing and to act as a lever to propel the body during locomotion. An anatomical description of the foot goes some way to describing how it performs these functions and certainly clarifies the reasoning behind the use of force measurements to describe gait. Study of the foot at this level also enables the cause and consequences of dysfunction and clinical intervention to be more easily understood. The important mechanical structures of the foot include: the skeletal structure (see section 1.2.1), which together with the ligaments provide rigidity; the muscles (see section 1.2.3), which together with their tendons enable movement; the fascias, which holds the foot together. Arthrology of the foot, or a description of the joints, is given in section 1.2.2, including the structure and function of the arches (see figures 1.3 and 1.4).

### 1.2.1 Osteology

The skeleton of the foot can be sectioned into three regions, as shown in figure 1.1:

- (i) a posterior region - the *Tarsus*
- (ii) a middle region - the *Metatarsus*
- (iii) an anterior region - the *Phalanges*

The tarsus consists of roughly cubical bones that make up the posterior half of the foot and provide the link between the foot and the bones of the leg. It comprises seven bones that form a proximal and a distal row, with one bone interconnecting the two rows. The *calcaneum* and the *talus* form the proximal row. The *calcaneum*, being the largest and strongest of the tarsal bones, lies indirectly beneath the *talus* which in turn is part of the ankle joint and is the principle link to the bones of the leg. The distal row comprises four bones, the *medial cuneiform*, the *intermediate cuneiform*, the *lateral*

TARSUS

- 1 Calcaneum
- 2 Talus
- 3 Navicular
- 4 Medial Cuneiform
- 5 Intermediate Cuneiform
- 6 Lateral Cuneiform
- 7 Cuboid

METATARSUS

- 8 First Metatarsal
- 9 Second Metatarsal
- 10 Third Metatarsal
- 11 Fourth Metatarsal
- 12 Fifth Metatarsal

PHALANGES

- 13-17 Proximal Phalanges
- 18 Distal Phalange
- 19-22 Middle Phalanges
- 23-26 Distal Phalanges

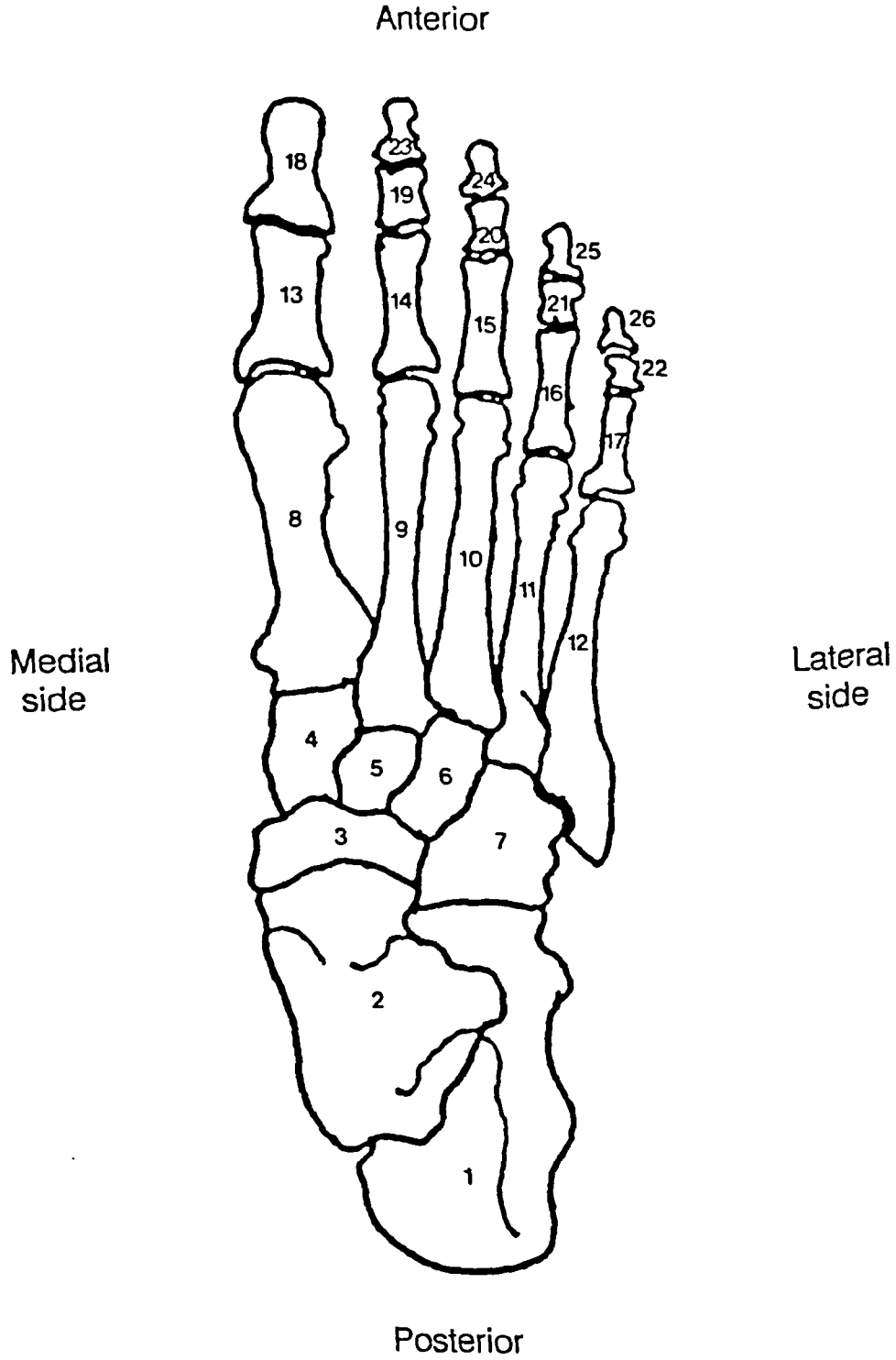


Figure 1.1 The skeletal right foot dorsal surface

*cuneiform* and the *cuboid*. Together these bones form a transverse arch. On the medial side of the foot and connecting the talus to the medial three bones of the distal row is the *navicular*.

The metatarsus comprises five miniature long bones, numbered from the medial to the lateral side. Situated in the anterior part of the foot they lie between the tarsus and the phalanges. The base of these bones join with the distal row of the tarsus and with one another and the head of each bone joins with a corresponding proximal phalange. Embedded in the tendons at the first metatarsophalangeal joint there exist two rounded nodules of bone known as the *sesamoid bones*, the medial one being the larger of the two. Sesamoid bones may also be found at other metatarsophalangeal joints and at the interphalangeal joints of the great toe.

The phalanges are miniature bones that form the toes. Two make up the great toe and three make up each of the other toes, namely the *proximal*, *middle* and *distal phalanges*.

## 1.2.2 Arthrology

The joints of the foot can be divided into six main groups:

(i) the *Ankle joint*

(ii) the *Intertarsal*

(iii) the *Tarsometatarsal*

(iv) the *Intermetatarsal*

(v) the *Metatarsophalangeal*

and (vi) the *Interphalangeal joints*

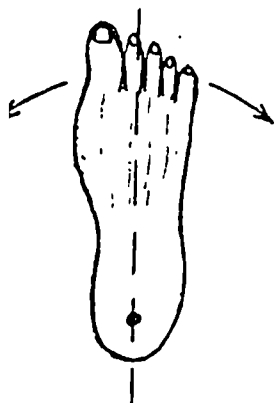
The movements of the foot which are described in this section are illustrated in figure 1.2.

The ankle joint is a hinge type joint and is where the lower end of the tibia meets the talus. It allows dorsiflexion and plantarflexion of the foot and also has slight side to side movement.

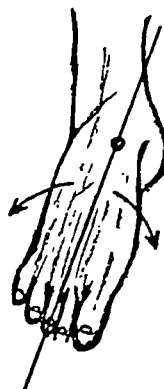
Seven joints comprise the intertarsal group. The *talocalcanean* and *talocalcaneonavicular* joints have considerable gliding and rotatory movement which subsequently allows inversion of the foot. The *calcaneocuboid* joint has slight gliding and rotatory movement which also allows inversion, as well as eversion, of the foot. Slight gliding movement is afforded by the remaining four of the group, the *cuneonavicular*, the *cubonavicular*, the *intercuneiform* and the *cuneocuboid* joints. During load bearing the movement of these joints increases the overall suppleness of the foot.

uction

Abduction

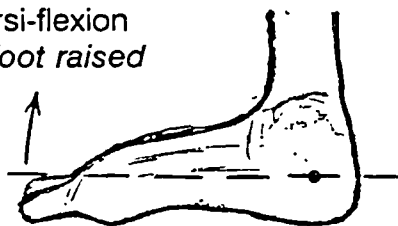


Inversion  
pressure on medial  
side of heel



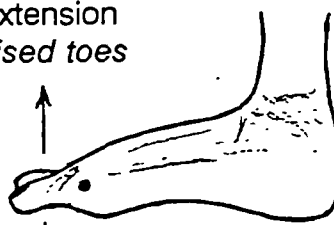
Eversion  
pressure on lateral  
side of heel

orsi-flexion  
efoot raised



Plantar-flexion  
forefoot lowered

Extension  
raised toes



Flexion  
lowered toes



Supination  
eversion & abduction  
during load baring



Pronation  
inversion & adduction  
during load baring

Figure 1.2 Movements of the foot

The interfaces between the posterior of the metatarsal bones and the tarsus produce the tarsometatarsal joints that have a very limited range of gliding action. The exception to this is the joint between the first metatarsal bone with the medial cuneiform where considerable movement is possible.

The bases of the four lateral metatarsal bones are connected together with ligaments and form the tarsometatarsal joints; the bases of the first and second metatarsal bones are free from connection. Transversely all the metatarsal heads are connected indirectly by ligaments and slight gliding occurs when the foot is under load.

The metatarsophalangeal joints are where the rounded heads of the metatarsal bones locate in the shallow cavities of the phalanges. Up to 90° of extension is possible, but only a few degrees of flexion. Adduction of the foot is associated with flexion of these joints and abduction with extension. All the interphalangeal joints are of the hinge type and allow extension and flexion of the foot.

#### 2.2.1 Arches of the foot

It is required for the foot to support body weight while standing and act as a lever to propel the body during locomotion. So it should be able to conform to uneven surfaces, thus making good contact with the ground, and also be able to form a rigid lever that will not collapse under body weight. These multi tasks are possible due to a series of arches shaped by the bones, as shown in figures 1.3 and 1.4.

The medial and lateral longitudinal arches are relatively solid in nature; the medial being the more

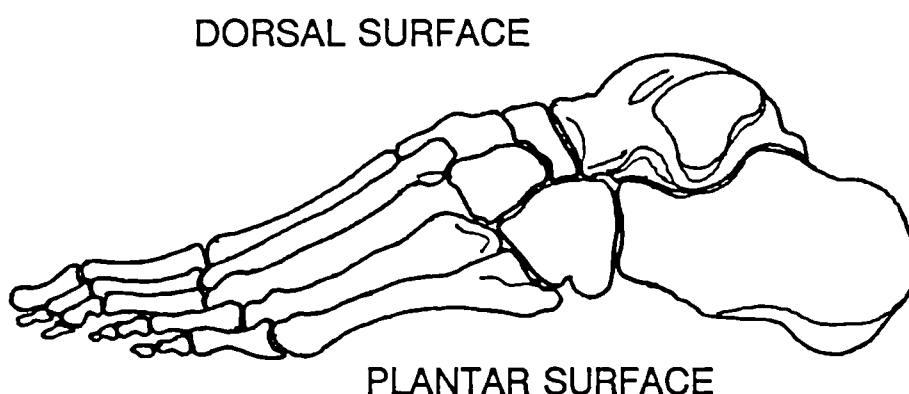


Figure 1.3 The skeletal left foot, lateral view

POSTERIOR

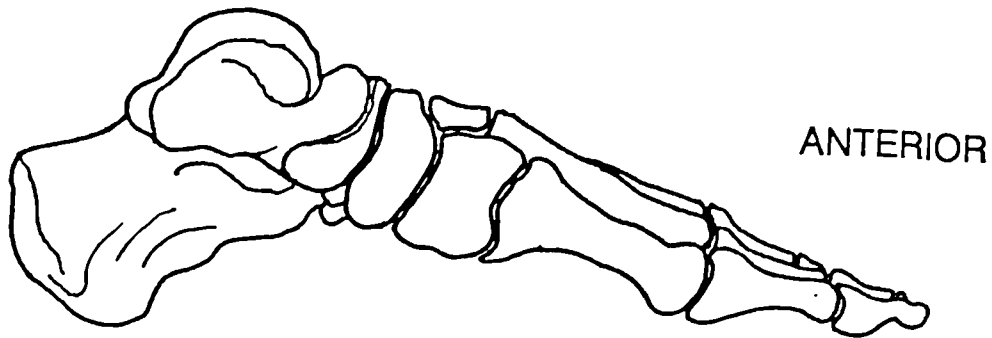


Figure 1.4 The skeletal left foot, medial view

resilient of the two. A series of transverse arches exist, however these are more like half-domes around the middle of the tarsus. These transverse arches are quite resilient, remaining formed with the foot above the ground and becoming more flattened when the foot bears load. The arches of the foot are supported by a network of muscles and tendons providing the strength, flexibility and movement necessary for correct function.

### 1.2.3 Myology

The muscles of the foot can be divided into dorsal and plantar groups. The dorsal group comprises of just one muscle, the *digitorum brevis* that acts upon the phalanges. The plantar group comprises of a multitude of muscles subdivided into four layers. During locomotion all muscles of the lower limb are actively involved, each being in contraction and relaxation at different times. As well as propelling the body forwards, some muscles are involved in preserving balance and maintaining the arches of the foot.

### 1.2.4 Major load bearing areas of the plantar surface

Over the years there has been much debate around the definition of a normal pattern of weight bearing during standing and the mid-stance phase. It is evident from anatomical study that longitudinal and transverse arches exist (see section 1.2.2.1), which alter their shape when the foot is load bearing. Early theories on normal weight distribution are reviewed by Lord (1986), Cavanagh

1987) and Barnett (1956). Dickson and Dively's *tripod* theory is discussed where it was assumed that the load was evenly distributed between the heel, the first and the fifth metatarsal heads. The longitudinal and transverse arches were therefore considered to be incompressible. Conversely, Frankfort's theory was the other extreme; he considered that the perfect foot collapses completely when bearing weight so that all the arches disappear. It is now widely accepted that initially all the load is taken by the heel and transfers across to the forefoot in locomotion, where the metatarsal heads take most of the forefoot loading (Hutton, 1976). The lateral arch collapses during this cycle enabling support of the foot along the length of the arch. It can thus be deduced that the heel and the metatarsal heads are the major load bearing areas of the plantar surface of the foot.

### 3 Methods of study of human gait

This section introduces and briefly describes the various areas of the measurement of gait. Complete gait analysis can only be achieved by observing foot function along with the changing geometry of the lower limb and electrical muscle activity (see section 2.2.1).

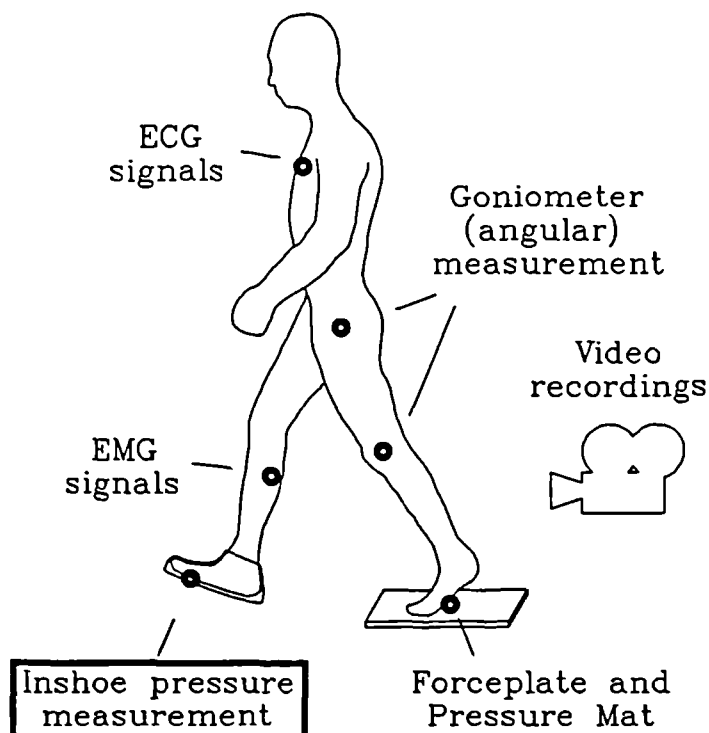


Figure 1.5 The complete gait analysis system

However, due to the complexity of such a set up, clinical gait analysis systems usually concentrate

olely on the measurement of foot loading. It has been observed that most clinical centres employing gait analysis instrumentation will refer patients to a more comprehensive centre if satisfactory diagnosis cannot be achieved based upon foot loading information (if such a centre is accessible). Results from many gait analysis systems are unique because of the absence of calibrated, absolute measurements, often making comparison and correlation between different systems difficult or impossible. Research groups usually concentrate on a particular selection of the many available gait parameters and develop systems around the measurement of these parameters. Commercially produced systems are usually limited in what they are able to investigate due to added constraints, which are not present in a research environment.

### 3.1 A dictionary of terms

An understanding of the function of the foot requires description of the phases of a normal gait to which reference can be made during pathological analysis. The way in which gait is described can vary in accuracy depending upon methods used and the expertise of those who perform the diagnosis (Wall, 1987). However, a widely accepted terminology exists for the general description of the gait cycle, which will subsequently be detailed.

*Spatial* representation of results is the consideration of the relative positions of contact and gives rise to a few gait parameters. With reference to figure 1.6, the *step length* is a measure of distance with which a foot is placed in front of the trailing foot, using the same anatomical positions for each foot. While *stride length*, is the distance between two consecutive points of contact of the same foot. *Heel strike* is the occurrence of initial foot contact and *toe off* represents the end of foot contact with the ground.

The *temporal* phases of gait are considered by looking at the sequence of events for one or both feet with respect to time over consecutive cycles. So from a temporal perspective, further nomenclature can be explained. From straight forward time and distance measurements the average *velocity* of gait can be calculated, also known as the *cadence*. Figure 1.7 shows the time with which both feet are in contact with the ground. Considering just the right foot, initial contact is at *heel strike*,  $H_2$  and contact with the ground continues until *toe-off*,  $T_2$ . This is the *support phase*. From toe-off,  $T_2$  to the second heel strike,  $H_4$ , the foot is being moved above the ground, which is known as the *swing phase*.

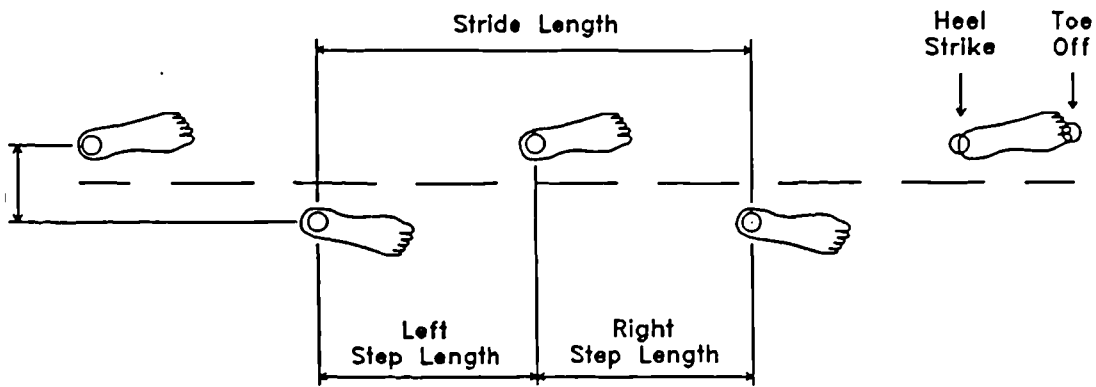


Figure 1.6 Spatial representation of four consecutive normal foot steps

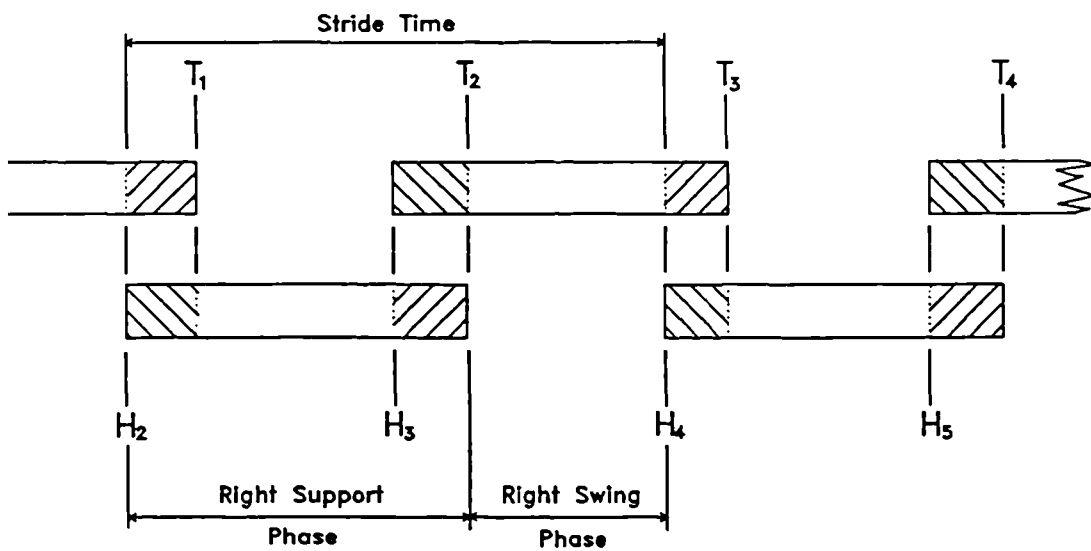


Figure 1.7 Temporal phases for four consecutive normal foot steps

*stride time* is the time for one cycle of the pattern,  $H_2$  to  $H_4$ .

Considering the temporal events for both feet, it can be seen that between right heel strike,  $H_2$  and left toe off,  $T_1$ , both feet are in contact with the ground, which is known as a *double support phase*.

$T_1$  initiates the phase in which the body is only being supported by the right foot, which is known as a *single support phase*.

When analysing abnormal gait, the above definitions may not directly apply (Wall, 1987). Analysis of the load distribution over the plantar surface of the foot will give information about the points of contact with the ground and corresponding temporal parameters. For example, some pathologies affect gait, such that *forefoot loading occurs before hind-foot loading*. It can be seen that the description of anatomical patterns such as this requires careful consideration.

### 3.2 Kinematics of gait

An important area of gait analysis is the measurement of spatial and temporal parameters of the lower limb (Crouse, 1987; Law, 1987) and its changing geometry in locomotion. Photographic, closed circuit television and electromechanical techniques have been used by many researchers (Jhanendran, 1979). Early photographic methods were expensive and laborious, however new computerised devices such as the commercially available Vicon video camera system have substantially reduced measurement durations and eased the analysis of results. The relative movement of various joints of the lower limb can be studied using goniometers (MIE Ltd; Penny & Giles Blackwood Ltd), which give angular information in three planes using groups of potentiometers. Such a system is described by Isacson who furthers the work initiated by Hannah *et al* (Isacson *et al*, 1986).

### 3.3 Kinetics of gait

The measurement of forces that are exerted between the foot and the ground or a shoe can provide valuable information about the function of the lower limb of the foot and of general postural control during stance phases and locomotion. The approaches and methods of such measurement vary and their relative importance are individually assessed by each research group depending upon their particular discipline. A full review of this methodology is detailed in chapter two.

### 3.4 EMG detection to describe gait

For a complete analysis of human locomotion, knowledge of the muscle activity of the lower limb is required. EMG data on its own can provide limited information, however, correlation of this data with data from other areas of study such as kinetic measurement can afford useful analysis. The EMG data can be collected using surface or needle electrodes placed at the appropriate sites of a selection of lower limb muscles. These muscles of importance could include: soleus, rectus femoris, biceps femoris, vastus medialis and tibialis anterior (Arsenault *et al*, 1986). The raw EMG data requires some initial signal processing such as rectification and filtering to provide a signal representative of the muscle activity. Most importantly an indication of whether a muscle has fired and the corresponding level of muscle activity is the information required from such measurements. Superimposed with other parameters of gait this EMG information can provide a useful indication of function or dysfunction of the lower limb.

It is intended that future research in the gait analysis field should include EMG detection and analysis, however this particular area is only addressed on one further occasion in this thesis; see future development, section 8.2.

### 3.5 In-shoe pressure measurement

While in locomotion, modern society spends a large percentage of the time wearing shoes. In-shoe reaction forces need to be accurately quantified to allow comparison with the bare foot if our modern ambulatory functions are to be analysed. Accurate investigation of dynamic activities such as running, analysis of multiple consecutive foot steps and the effect of orthotic or surgical intervention are examples of other areas that require an in-shoe pressure measuring system. Also, shoe design and the effects of shoe wear would be able to be investigated. Often a pathological condition exists affecting one foot only, however changes in gait, i.e. the pressure distribution for both feet, may result. To measure both feet simultaneously, enabling assessment of the step-by-step variability, has obvious advantages. Technically care must be taken in the design of such a system so that the introduction of transducers at the foot-shoe interface does not unacceptably affect the pressure distribution that is being measured.

For clinical systems it is desirable to restrict the number of parameters of measurement to a minimum.

is favours the method of selecting a number of anatomical sites at which to place the transducers; opposed to measurement of the entire plantar surface. Useful measurements can be obtained by concentrating upon the loading under the metatarsal heads, the heel and the great toe. Pressure mats of high spatial resolution attempt to resolve the entire distribution which can be of importance for the location of abnormally high pressure areas and for the production of certain results, such as the centre of pressure curve. From an engineering view, an insole incorporating a complete matrix of transducers is very complex, as can be seen from Hennig and Cavanagh's insole system (Hennig, 1982) using 499 piezoelectric ceramic elements. This approach is akin to systems of a purely research nature. Even though a sacrifice is made in order to concentrate on the accurate pressure measurement at important anatomical sites, a large amount of data will still be produced. The clinician will then be able to concentrate analysis upon this limited data in order to interpret the results. As the plantar pressure varies considerably in successive steps, calculation of a *typical* footstep will require the application of statistical methods of analysis. In most instances this limitation is far from being a disadvantage. It is apparent that the analysis of data obtained from systems measuring the pressure distribution over the entire plantar surface is isolated to the aforementioned anatomical sites. Much of the information from such systems is therefore redundant.

A comprehensive review of in-shoe techniques investigated by other researchers is presented in chapter two (section 2.2.2.2).

### 3.6 The normal human gait cycle

A complete gait cycle is the period of one stride or between two consecutive contacts with the ground of the same foot. Measurements with men during normal walking have shown that the stance phase is around 60% of the gait cycle and the swing phase around 40% (Murray *et al*, 1964). Figures 1.6 and 1.7 show the cycle and its divisions. A few researchers have compiled data for various spatiotemporal gait parameters that are generally considered to represent a *normal* walking pattern. Murray *et al* (1964) produced a set of results with a system using stroboscopic methods to obtain direct measurements from multiply exposed photographic frames, indicating the positions of reflective markers attached to the skin. Temporal factors are usually referred to in terms of a percentage of the walking cycle, as they change only very slightly with changes in walking rate (Hutton *et al*, 1976).

In the joints and muscles of the lower limb contribute to the reaction forces and torque at the heel/foot interface (Rehman *et al*, 1948), the relative angular movements of the hip, knee and ankle (Murray *et al*, 1964) the rotations of the pelvis, femur and tibia (Levens *et al*, 1948) and the movements of the subtalar joint about its axis (Wright *et al*, 1964). These movements and forces for a normal subject are fully explained in a description of the foot in walking by Hutton *et al* (1976).

It is essential for the assessment of the abnormal foot to have comprehensive *normal* data, so allowing comparative analysis. Normal barefoot loading and pressure, and the associated measurement techniques chiefly based around force plates and pressure mats, are well documented (Aharonson, 1980; Alexander *et al*, 1990; Lord, 1986). The vertical component of the reaction force and the centre of foot pressure both have characteristic shapes (see section 2.3.2). Discrete loads under localised areas of the plantar surface vary greatly between subjects in peak magnitudes, however the pressure/time traces are more similar (Betts *et al*, 1980). Clarke and Cavanagh (1981) and Soames (1985) report values for peak pressures using normal patients. The collection of *normal* in-shoe data is severely limited in quantity and quality due to the lack of calibrated measuring systems. Commercial systems such as Novel's EMED in-shoe device have had many problems with obtaining calibrated results. Only a few research systems have managed to produce useful results such as the complex insole developed by Hennig *et al* (1982) using a multitude of piezoelectric elements. However, as a research tool, routine clinical data collection necessary to build up *normal* information is impractical.

#### **4 Polyvinylidene fluoride and Copolymer piezoelectric film**

Piezoelectricity is the reversible conversion of mechanical energy into electrical energy. This property is exhibited in materials such as quartz, lead titanate zirconate and lithium niobate. In the 1960's it was discovered that many organic materials including some polymers also exhibit piezoelectric properties. Kawai (1969) in the late 1960's made the discovery that elongated and polarised films of inert polyvinylidene fluoride (PVdF) exhibit piezoelectric and pyroelectric characteristics. Since then other copolymers (most importantly P(VdF-TrFE)) have been found to possess similar properties, each with a slightly different set of characteristic constants. A huge variety of devices utilising these piezoelectric films have been proposed and developed by many research groups throughout the world

(see section 1.4.1), although thorough developmental work is thin on the ground. Marketable product development has been slow due to the specialist nature of the field, however, with applications help from the PVdF film manufactures, industry is slowly turning it's attention to this versatile transducer material. The film has numerous modes of operation and the mode applicable to the proposed application, direct pressure measurement, is introduced in section 1.4.2 and explained in detail in chapter 3. The use of this for this application is novel however many other transducers have been used for gait analysis systems; these are reviewed in section 1.4.3.

#### 4.1 Uses and applications for piezoelectric film

Due to it's highly versatile nature piezoelectric film lends itself to many transducer configurations. Thus the applications are very diverse and cover areas such as switches, acoustics and hydrophones, high sensitivity sensors, infrared detectors and medical instruments (Carlisle, 1986; Chatigny, 1987; Cleaver *et al*, 1982; Fox, 1986; Halvorsen, 1986; Richardson, 1989; Robinson, 1978). Piezoelectric film has military interest because of it's hydrophone applications. It is particularly efficient in this area due to it's low acoustic impedance ( $2.7 \times 10^6 \text{kg/m}^2\text{sec}$ ) compared to other piezoelectric materials, resulting in a desirable impedance match to that of water and likewise to that of human tissue and adhesive systems. It should be noted that all the applications are at relatively low temperature, as PVdF begins to lose it's piezoelectric properties above temperatures of 120°C. The manufacturers' technical manuals provide comprehensive applications information (Pennwalt Ltd, 1987; Yarsley Ltd, 1982). A few examples of such applications are detailed below.

Accurate measurement of a static force, such as is required for commercial scales, can be achieved using two pieces of piezoelectric film attached to either face of a resonant membrane (Halvorsen, 1986; Pennwalt Ltd, invention record #F9). The film is used in the dynamic mode, one piece as an oscillator driving the membrane at it's resonant frequency and one as a contact microphone providing feedback in order to maintain resonance. This configuration is known as a *singing plate*. If an external force is applied to the membrane, it's resonant frequency alters, and so to monitor this change is therefore to monitor the value of the applied force.

The Volvo car company were involved in a research project whereby PVdF elements were implanted under the skin of the head of a dummy, so that facial damage during accidents could be investigated

DeReggi, 1976; Nilsson, 1987; Warner, 1986).

amorph configurations, where layers of film are placed together back-to-back, have several applications such as sensitive switches, low power actuators and small vibrating fans (Toda, 1979, 1981). This configuration is specifically useful where possible artifacts from pyroelectric effects need to be minimised.

PVdF has been successfully utilised in various medical applications (DeReggi *et al*, 1981; Kobayashi *et al*, 1981; Ohigashi *et al*, 1982). Miniature piezoelectric polymer probes have been used in mapping beams from ceramic ultrasound transducers and have been proposed for identifying the location of biopsy needles in relation to deep tissues. High fidelity measurements of heart sound, pressure and flow can be achieved by mounting PVdF transducers on catheter tips. These catheters can be inserted into blood vessels or the oesophagus. PVdF films can be used in phonocardiograms (Richardson, 1989) which when mounted on the mother can be used for fetal monitoring. Polymer sensors could be mounted on limb prostheses to give information about touch pressures and contact location which then could be transmitted to the wearer. In a similar area, tactile sensors have been developed for robotic applications (Dario *et al*, 1985; Dvorsky *et al*, 1987; Park *et al*, 1987). Detection of the position and orientation of objects has been tackled using a planar matrix of 16 x 16 circular PVdF sensors supported on a printed circuit board (Dario *et al*, 1982). It is hoped that in the future that PVdF will make possible the development of sensors with skin like properties (DeRossi *et al*, 1986).

#### 4.2 Direct force measurement

Depending upon the application a transducer incorporating piezoelectric film may utilise the film in one of a number of various modes. That is, an ultrasonic transceiver, infra red detector and precision load cell all have very different design requirements. Being a dynamic material it develops an electrical charge proportional to any change in mechanical stress. Decay of this induced charge means that only a *quasi static* mode of operation is possible. The time constant for this decay is determined by the internal resistance and the dielectric constant of the film, as well as the impedance of interface electronics. Considering an element of 28 $\mu$ m PVdF film measuring 1cm<sup>2</sup>: with a resistivity of  $5 \times 10^{13} \Omega \text{m}$  the leakage resistance will be  $4.2 \times 10^{12} \Omega$  and with a dielectric constant of around 12 the

capacitance will be 380pF. Therefore the intrinsic RC time constant for this disc will be of the order 26 minutes. For a 500 $\mu$ m copolymer film element of the same area the time constant will be around 10 minutes (see also section 5.2.1). In designing an in-shoe force transducer consideration should be given to the effect of bending as the film is sensitive to stress in all three orthogonal directions. This implies that the transducer should be of a rigid construction, and so the use of hard sandwiching layers is required. As the application imposes dimensional constraints upon the transducer then this can be seen to be a disadvantage. In order to measure an applied force knowledge of the direction of application of the force with respect to the film is required. To detect vertical in-shoe forces the line of action of the applied force will have to be perpendicular to the film surface. The theoretical magnitude of this force can then be calculated using the appropriate piezoelectric coefficient. The transducer is therefore to be designed in such a way as to provide a direct charge output due to the applied force transmitted through it's, and hence the film's, thickness.

#### 4.3 A review of transducer materials and methods for gait analysis studies

There are a multitude of transducers used for medically related measurement systems and transducer choice very much depends upon the area of application (Payne, 1989). The review of methodology found in chapter two details all the methods used for investigating foot loading. Confining the discussion to transducer materials capable of measuring in-shoe loading and pressure distribution, the list is somewhat smaller. Inside the confines of the shoe bulky transducers, like those used for pressure mats and force plates, can no longer be used. Various systems have been devised using a variety of piezo-metric transduction techniques; see section 2.2.2.2 for a review of all such systems. For investigating biomechanic forces the following transducer methods have been used: wire and semiconductor strain gauges (Lerheim *et al*, 1973; Pratt *et al*, 1979; Ranu, 1986, 1987, 1989; Soames *et al*, 1982); capacitive transducers (Bauman *et al*, 1963; Miyazaki *et al*, 1986; Nicol *et al*, 1978); piezoelectric materials (Bhat *et al*, 1989; Hennacy *et al*, 1975; Hennig *et al*, 1982; Pedotti *et al*, 1984); conductive films (Durie *et al*, 1979; Miller *et al*, 1979); force sensitive resistive films (Interlink Ltd; Maalej *et al*, 1989; Servodata Ltd); Magneto resistive elements (Tappin *et al*, 1980). All these methods have their advantages and disadvantages depending upon the specific application. It is the researchers' particular expertise and preferences along with the relative merits of each method that determines

high transducer material is to be used.

## 5 A summary

From the many techniques used to qualify and quantify gait, in-shoe methods have many advantages, as detailed in section 1.2.6. In developing an in-shoe pressure measuring system it is intended to provide the orthopaedic surgeon and podiatrist with a means to accurately measure discrete absolute pressure values at predetermined anatomical sites of interest. Such a system is not currently available as a clinical tool and would be invaluable for accurate assessment of foot function as well as providing data for the comparison of different systems. Concentrating on the measurement of absolute and not relative pressure is the only way in which comparative studies can hope to be performed. Many existing systems rely on the results from a single foot strike, whereas to record data from multiple consecutive foot steps would enable a more accurate and comprehensive picture to be obtained. VdF and copolymer films, with their multitude of applications, has advantages over other transducer materials when used to measure in-shoe loading. As it is a passive transducer then no electrical supply or energisation signal is required. Its flexibility is also advantageous for some applications, however in order to have control over the nature of the signal produced, it will have to be utilised in rigid transducer construction.

At present some variation exists in the presentation of data from gait analysis systems. However there are a few techniques used that are widely familiar to those concerned. So for initial clinical assessment of a new system it would be advantageous for it to present data using similar methods, thereby maximising critical clinical input. With the diagnosis of foot disorders still primarily relying upon visual inspection at the clinic, it is hoped that the intervention of this technology will improve the accuracy of diagnosis and assess the efficacy of treatment, and will ultimately be of benefit to the patient. Along the guidelines of BS5724, equipment will require construction to appropriate electrical safety standards.

## **Chapter Two**

**2**

# **HISTORICAL REVIEW**

## 1 Introduction

Many researchers and clinical groups have been studying the structure and function of the foot over the centuries in an attempt to understand the mechanics of the healthy and pathological foot. As early as 1882, Beely (1882) describes a method he used to try and detect the greatest weight bearing areas of the foot. Patients were asked to stand on a thin sack filled with plaster of Paris and a cast of the impression was subsequently taken. Unfortunately this method captured the shape of the foot rather than the pressure pattern.

The parameters of gait can be subdivided into five areas (section 2.2.1) and all of these are of importance in terms of providing useful information for gait analysis. The following review concentrates upon the area relevant to this thesis, static and dynamic floor reaction forces, and is divided into a methodology part (section 2.2) and a following clinical observation part (section 2.3). There exists a great variety of measurement systems and therefore a spread of results the nature of which depending upon the purpose of the investigation. This often means that direct comparison of results from different systems is not possible (Stewart *et al*, 1989; Lord *et al*, 1986). The comprehensive review of methodology will include all systems of importance but will have emphasis upon in-shoe techniques (section 2.2.2.2). The various results obtainable from foot loading measurement systems along with the importance of, and applications for, these results will be given in the clinical observation sections of this review. Expected results for normal subjects will also be discussed. Section 2.4 concludes the review with a discussion on techniques and methods of importance and also the problems and trends of present day measurement practices.

## 2 Methodology

The analysis of human gait has long interested many orthopaedic surgeons, podiatrists, and researchers and as a direct result many ingenious systems for quantifying gait have evolved. This review concentrates on the area relevant to this research, that of pressure measurement and specifically in-shoe techniques. For comparative purposes other methods previously used for performing measurements to describe ambulatory foot function and static foot loading are also detailed.

## 2.1 Complete analysis of human gait

A comprehensive analysis of human gait concerns the measurement of many kinetic and kinematic parameters (refer to figure 1.5), these can be sectioned into five areas as follows:

- (i) static and dynamic floor reaction forces
- (ii) spacial and temporal parameters
- (iii) joint and limb movements
- (iv) muscular activity
- (v) metabolic cost

To perform measurements of all these parameters in order to obtain highly detailed analysis requires a great deal of sophisticated equipment (Gifford and Hughes, 1982). Clinically this is not possible due to time and financial constraints, so this sort of analysis is restricted to research or specialist based usage. Therefore a typical clinical system will measure a particular subset of these parameters selected by the clinician. Thereby providing enough information to aid the diagnosis and assessment and treatment for a particular group of patients. An example of this are the studies carried out by Betts *et al* (1980) based on the use of Chodera's pedobarographic equipment (Chodera *et al*, 1979 cited Lord, 1981) for the assessment of corrective procedures for children suffering from paralytic deformities, mainly due to spina bifida. Betts considered that foot contact shape, high spatial resolution and a readily available image was of importance, therefore this optical technique was used. The Dundee limb fitting centre clinic has a system of devices enabling all parameters but the metabolic rate to be measured. This is considered a research facility, however it has clinical use for specialist areas.

## 2.2 Foot pressure measurement systems

Approaches to the measurement of foot pressure vary considerably and the relative importance of which methods are individually assessed by each research group depending upon their particular discipline. Generally it is thought that measurements of the vertical forces during static loading and locomotion are of the greatest importance. Therefore most of the efforts of research groups have been to develop systems in this area. The horizontal, or shear, forces and torque also play an important role in some diagnostic procedures, providing information directly related to skin stresses

d to the magnitude and direction of the total reaction vector. The three following measurement interfaces can be examined in order to obtain foot-ground pressure information:

- (i) plantar surface of barefoot to ground
- (ii) shoe outsole to ground
- (iii) plantar surface of the foot to shoe insole

Each of these has advantages and disadvantages depending upon the particular application. Most researchers have developed systems to measure reaction forces at interface (i) because of the relative ease of transducer development. All methods of measurement can be loosely divided into the following overlapping categories:

- (i) printing techniques
- (ii) direct visualisation techniques
- (iii) force plates and pressure mats
- (iv) load cells
- (v) inshoe transducers and insole methods

### 2.2.1 Barefoot to floor techniques

The barefoot plantar surface to ground interface is considered the easiest at which to obtain force and pressure distribution information. Most commercial systems are based around force plates, pressure mats and measurement platforms, which when placed along a walkway effectively sensitise a small area of the floor.

#### Printing techniques

For certain applications the fast and effective use of printing techniques are still employed, an example of this being the Harris footprinting mat, distributed by Downs Surgical Ltd. Originating from Morton's netograph (Morton, 1935), the technique was further developed by researchers such as Silvino (1980) who also attempted to quantify the data obtained from the mat. The mat is a rubber layer with angular ridges cut into the underside which print an area of ink proportional in size to the locally applied force from the foot. Applications include the Canadian Army foot survey, performed by Harris and Beath (1947). Henry *et al* (1975) also used the Harris mat to assess the results of operations for hallux valgus. Various printing methods were developed by other researchers (Bauman *et al*, 1963;

ritomi *et al*, 1983; Grieve *et al*, 1984), however all such methods have the drawback of only providing qualitative results.

#### **Visualisation and barographic techniques**

Early visualisation techniques were being developed during the same period as the advent of Morton's cinematograph. Elftman (cited from Lord, 1981) developed his Barograph which has certain similarities to the Harris mat except that the underside deformations of a patterned rubber mat were viewed using a cinecamera through a glass plate. A variation to this fundamental design is described by Arcan and Hull (1976) who observed the interference patterns underneath a platform of still transparent plastic produced by a matrix of rigid protrusions during foot loading.

Barnett developed his plastic pedograph (Barnett 1954, 1956), which involved filming the depression of a matrix of rods into a rubber mat. Further developments of the barograph followed, based on different optical principles (Hertzberg, 1955; Chodera *et al*, 1979; West, S., 1987; West, P., 1987), leading to the formation of the present day pedobarograph. The early pedobarograph had the drawback of having an extremely slow response, and so was only used as a static foot-loading measurement device. Much work has been published by Betts and Duckworth (1978, 1980) on the use of such systems in clinical practice. Technological advances have allowed sophisticated electronic processing of the images and automatic microprocessor analysis is now used, as outlined by Duckworth *et al* (1982). Dynamic pressure patterns are currently being investigated using a pedobarograph by Hughes at Northwich Park (West, S., 1987). A commercial device is available in the UK from John Drew Ltd, which they market under the name of pedobaroscope. Similarly in the biomechanics market a system which is known as their dynamic pedobarograph. These devices have good resolution (1 pixel), but unfortunately still suffer from having a relatively low high frequency response of 12.5Hz.

#### **Force plates and load cells**

A force plate can be summarised as being a flat plate used to measure the forces exerted by the foot during walking. The design of the plate determines the data provided, the major variations being due to the spatial resolution and relative sensitivities to forces in the three orthogonal directions. The greatest single drawback arising from the use of force plates is the possible alteration of a subject's usual walking pattern in his/her attempt to strike the plate centrally. Grundy *et al* (1975) describes the

problem in detail when using the Skorechi and Channley plate in his studies. Early force plate techniques are described by Lord (1981) and S. West (1987).

A significant development was reported by Hutton *et al* (1972) who detailed a force plate constructed from twelve parallel beams 9.5mm in width and 300mm in length with a 2mm separation gap. Strain gauges were used to measure the vertical component of load during the stance phase of the gait cycle. This construction was inserted into a 7m walkway and could be rotated through 90° to facilitate the measurement of either mediolateral or anteroposterior pressure distribution. Further work on this system was carried out by Stokes *et al* (1974) who also incorporated the use of an inked mat to give spatial information of the foot, however they experienced difficulties in obtaining repeatable results. Development was taken further by Dhanendran *et al* (1978; Hutton *et al*, 1979) to a full matrix force plate consisting of 128 cells, each supported by a strain gauge ring. A PDP11 computer was used to process the information on-line and to provide various displays of the data. Beverly (1985) used this system to assess silastic arthroplasty of the hallux and Hutton *et al* (1981) used it to investigate the mechanics of the hallux.

A variation of this beam technique is described by Manley (1979) where he used sixteen transparent parallel beams mounted in a walkway transverse to the direction of walking. Total load and the centre of pressure were measured using force transducers and a camera was placed under the beams to provide an image of the footprint. A second camera was used to provide spatial information from a lateral view of the foot and leg, thus providing both spatial and force information. A drawback of these beam-type systems is that the resolution is poor; determined by the size and number of beams.

Arvikar and Seireg (1980) developed a platform of six rings sensitised using strain gauges. They were used to measure the vertical load under each metatarsal head and the heel, however this system had problems related to the nature of support of the feet.

Raganich *et al* (1980) report a unique system combining a piezoelectric force plate measuring the three components of force and a matrix of switches. This matrix enabled the measurement of foot contact area in a digital form as a sequence of switch closures, however its use as a clinical tool is questioned (West, P., 1987).

Amongst the vast range of piezo-instrumentation that Kistler Instruments Ltd manufacture is their multicomponent measuring platform which is widely used in the bioengineering field. It measures any

ces and moments applied in three orthogonal directions using four load cells, one positioned in each corner of the platform. Accurate, reliable and calibrated measurements are obtained from Kirtley's system and so consequently they are used at research centres engaged in accurate gait analysis (Kirtley *et al*, 1985).

#### Pressure mats

Modern transducer technology advanced many researchers, and certainly companies, turned their attention to developing high resolution pressure mats thus allowing the entire plantar surface of the foot to be investigated. A commercially available system based upon a matrix of 32 x 16 conductive rubber transducers was developed at Musgrave Park Hospital in Belfast by W.M.Automation. Recently the company has upgraded its *Musgrave Footprint* system so that a plate of the same initial dimensions contains 2048 sensors. The system is supported with a powerful and easy to use software package, however its value as a system able to provide absolute pressure data is limited due to poor transducer performance.

A sophisticated system developed by the German company Novel<sub>gmbh</sub> is currently being marketed as their *EMED* system. Powerful software packages are employed enabling visual representation of the data. This system is favoured by many researchers due to the comprehensive product support offered by Novel and because of the high number of research projects the company has been involved in. The company also claim that the system is the most comprehensive and accurate (Seitz, personal communication). The pressure mat itself is based upon the *Nicol mat* developed by Nicol and Hennig (1978). Nicol and Hennig describe a force transducer matrix consisting of 16 x 16 conducting strips incorporated into a flexible rubber mat. An applied force alters the capacitance across two perpendicular strips which is subsequently detected by the instrumentation. The signals are fed to a computer which also controls the scanning of the matrix and the processing and display of results. Gerber (1982) describes an improved method for the representation of results from the Nicol mat.

A commercially available system called *Orthomat* using piezoelectric film is marketed by an Italian company, Polysens s.p.a. The pressure mat consists of 1024 sensors that can be scanned at selectable rates. Dedicated software allows the processing of specific gait parameters and also the subsequent display of the results using an IBM pc. Polysens ran into technical difficulties with the

nsducer and so consequently there were only 5 systems produced for the general market. The Belgian company Clinical Interactive Research market two systems based around their multi-sensor mat: the *electroposturgraph* (ELP) and the *electropodograph* (EPG). The mat consists of 1024 sensors and is based upon the Nicol mat. Analysis of static and dynamic foot loading as well as postural sway is possible. Much emphasis has been put upon the software development thus enabling detailed presentation of the results. The clinical validity for this system is thought to be as good as the other pressure mat systems, however actual pressure data is only presented as relative percentage values.

## 2.2.2 In-Shoe Techniques

This section presents a review of in-shoe methodology, and is categorised into transducer techniques.

### Capacitive

The foot to insole interaction has been investigated using a variety of measurements techniques. As early as 1947 a system was reported by Schwartz and Heath (1947) using small capacitive disc transducers, however many calibration and performance difficulties were encountered. Bauman *et al* (1963) also developed a system using capacitive transducers, and later this system was redesigned by Hennacy and Gunther (1975) who used piezoelectric crystal elements as an alternative transducer material. Dynamic calibration was accomplished although through using a relatively slowly varying pressure at frequencies between 20 and 70/min, which is not fast enough to calibrate for a normal dynamic walking pattern where pressure variations up to and beyond 50Hz a frequency of are possible. Lord (1981) in her review has cited the early research techniques in some detail.

Iiyazaki *et al* (1986) also used a capacitive technique, this time to monitor total foot loading. An insole was constructed from a 2mm sponge rubber sheet sandwiched between two 50 $\mu$ m copper foils, the whole constituting a capacitor. An audible tone is generated when the desired load is achieved during physiotherapy sessions.

The duration of load bearing under discrete areas of the foot has been investigated by Miller and Stokes (1979) using simple switch pads located under the heel, the metatarsal heads and the great toe. Temporal gait patterns were compiled for normal and hallux valgus feet.

One commercially available system, the Computer Dyno Graph (CDG), using special slippers with 8 pre-

positioned transducer sites is marketed by a Dutch company (Infotronic). The transducers are capacitive and are of relatively large dimensions measuring 30 x 30 x 1.5mm. An emphasis on software development has resulted in powerful analysis of results providing data in the form of force-time graphs, force histograms, centre of pressure curves and a cyclogram. This system provides an overall idea of foot loading, although appears limited in its value as an accurate diagnostic tool.

Developments include a thin flexible insole as part of their EMED system for dynamic pressure measurement, based on the capacitive pressure mat developed by Nicol and Hennig (1978). Trials using the insole have been undertaken at the Royal Liverpool Hospital (Klenerman, personal communication) however troublesome operation resulted due to internal breakages. The insole is a matrix of only around 70 transducer elements, so to that effect the spatial resolution is relatively coarse.

#### Strain Gauge

James *et al* (1982) developed sixteen transducers having a beryllium copper body with a centrally pivoted cantilever. A semiconductor strain gauge was mounted on the cantilever to provide a signal due to its bending, upon application of a force. Unfortunately a flat rigid surface beneath the transducer was required for accurate results, so measurements could only be taken using the unshod foot on a firm floor.

Arreim and Serek-Hanssen (1973) embedded five transducer discs, measuring 12mm diameter and 5mm thick, into a PVC insole in an attempt to produce a system for clinical use. Silicon beam strain gauges were used and the integral beam was deflected via the deflection of a top membrane due to the applied force. Transducer positioning was determined using an X-ray and repositioning was necessary if the whole foot was to be studied.

Cost and Cass (1981) describe a system of load cells that are individually mounted into holes of 3mm diameter cut from a rubber insole having a thickness of 1.6mm. Each transducer is constructed from a sandwich of two thin circular rubber slugs, 6mm in diameter in between which is centrally embedded a resistive strain gauge. Mounting of the transducers within the holes of the insole is somewhat precarious as they are held in place solely by the lead-out wires and so run a high risk of being worn out during use. This system also suffers from bending artifacts and so the insole had to be worn on the bare foot and used on a flat floor.

ansby-Zachary *et al*, (1990) use an ultra thin (0.9mm) Entran silicon strain gauge transducer to measure forefoot pressure at predetermined sites on the sole of the foot. They use the transducer to make assessments of the effect of footwear and insoles, by measuring peak height, the pressure time integral, and step duration.

An unusual study of the pressures in ballet pointe shoes was carried out by Teitz *et al* (1985). Small strain gauge pressure transducers with a sensitive area of 2.7mm<sup>2</sup> were applied to the tips of the first and second toes to investigate ballet technique and pointe shoe design.

#### Force sensitive resistive film (FSR)

Conductive and resistive films have featured quite prominently in recent techniques. A French research group (Péruchon *et al*, 1989) has used a matrix insole produced by a French company (Midi-aptours). The insole consists of a conductive elastomeric sheet which is laid upon a flexible Kapton layer with 2 x 127 printed electrodes. Mechanical abrasion of the rubber layer resulting in a restricted transducer life of around 100 uses and the modest electromechanical properties of the conductive rubber were the main difficulties encountered. Extensive software development has allowed data presentation.

FSR is now readily available (Interlink Electronics) and has been used in a number of recent foot pressure measurement systems. Due to the ease of fabrication of transducers using FSR compared to other transducer materials, systems have appeared on the market very quickly, and before many research teams have published results of experimental findings. Langer Biomechanics Group introduced their Electrodynogram (EDG) around 1982. The system is based on 14 flexible force transducers that are positioned on discrete locations of the plantar surface of the foot. Langer's latest developments, using FSR, have resulted in a new transducer details of which are currently unavailable, however initial trials are to be carried out at Dundee Royal Infirmary. Data from the transducers is collected via a microprocessor controlled self-contained waist pack and post-analysis of results are carried out on a second microcomputer. Clinical applications of the Electrodynogram are detailed by McKechny (1986).

Belgian biomedical company (Clinical Interactive Research) has developed their LEGA system which uses two flexible printed insoles available in 6 different sizes. There are eight fixed transducer sites, and again the material is FSR. Some problems have been experienced with the insole performance

due to bending artifacts. Using Interlink FSR, Maalej *et al* (1989) describe a conductive polymer pressure sensor array to investigate the in-shoe movement and the pressure distribution of the second metatarsal head for one subject. A 4 x 4 array transducer was constructed and each element measured 5 x 5mm. They concluded that the diameter of the sensor should be at least 7mm in order to cover the peak pressure location under the metatarsal heads.

A complex flexible insole with a matrix of hundreds of elements (TecScan) has been initially developed for the shoe manufacturer Scholl. The insole is formed by two polymer layers each deposited with thin strips of FSR material, one longitudinally and the other transversely. The rows and columns of the FSR come into contact after the two layers have been glued together. A network of printed connections take the signals to an ankle box which subsequently stores the data of just one footstep. In connection to a computer the data is transferred and can be analysed. This system is currently under trial around the country and was aimed for use mainly in Scholl's own high street shoe stores. FSR has the drawback of being an active transducer material and so requires an energising signal. It has been found to be difficult to calibrate due to its aging and wear characteristics and its relatively high temperature coefficient of sensitivity, especially around body temperature.

#### Piezoelectric

A number of research groups have used piezoelectric materials to develop their transducers. Pedotti *et al* (1984) used 200µm PVdF film to produce a very thin insole with 16 aluminium deposited electrode sites, each 6mm in diameter. All 16 signals from these sites were multiplexed and integrated before being processed by a Digital MINC11 computer. The insole had technical difficulties, the most serious being an inability for each of the 16 sensor sites to provide a calibrated pressure signal due to localised bending. The authors concentrated on the analysis of temporal measurements rather than the absolute values of pressure exerted in a specific instant on a particular area of the plantar surface of the foot.

A very detailed system was reported by Hennig *et al* (1982) who developed a flexible silicon rubber sole embedded with 499 lead zirconate titanate piezoelectric elements. The instrumentation was complicated as 499 charge amplifiers were used, their outputs being multiplexed and then processed using an Apple II and PDP 11/34 computer. The transducers were tested using a mechanical loading frame and a Kistler type 9322A quartz reference transducer. Each transducer was calibrated

eparately using this equipment.

recent system using small PZT piezoelectric transducers, 4.83x4.83x1.3mm, has been developed by Gross and Bunch (1988). Eight transducers were positioned under selected areas of the plantar surface of the foot enabling dynamic measurement of discrete vertical in-shoe stress. Measurements were taken using a treadmill and some results were detailed.

A group from the University of Wisconsin, USA has recently published various papers on transducer development including a general purpose transducer constructed from Kynar PVdF film (Bhat *et al*, 1989). PVdF, 52µm in thickness, is sandwiched in between two insulating mylar film layers and the hole is taped to a metal backing plate, total dimensions being 42x19x2mm. Charge amplification is used to process the raw signals. The group intend to use the transducer to carry out pressure measurements under the bony prominences of the foot.

#### Shear force measurement

The important area of shear force measurement has been tackled by one group quite effectively (Appin *et al*, 1980). Transducers 15.96mm in diameter and 2.3mm in thickness were constructed with integral magnetoresistive elements. They were attached to particular areas of the foot using double sided tape. Research is currently being carried out using these transducers and some earlier results investigating types of footwear is detailed by Pollard *et al* (1983).

### 2.2.3 Other Related Techniques

Only a small amount of work has been reported on the measurement of shoe-floor reactions. Force plates and pressure mats have mainly been used for such investigations, however a number of specialist devices have been developed based around instrumented shoes. These are especially useful when assessing replacement limbs and to assist in the rehabilitation of amputees.

Manu (1987, 1989) describes a shoe upon the sole of which are mounted five triaxial load cells measuring 19 x 19mm and 8mm in thickness. Each load cell was constructed from 4 loops of load bearing elements placed symmetrically around a 12.5mm square element which is located at the center of the load cell. A total of 16 small foil-type strain gauges were used to achieve triaxial force output with minimal cross talk. Pressure against time curves and the centre of pressure were computed and these results were obtained in various trials with amputee patients.

the ground reaction force and its point of action were investigated by Kljajic *et al* (1987) who built eight or nine transducers into the soles of a shoe. Each force transducer measures 27 x 12mm and 0.5mm in thickness and is a specially constructed steel beam with a protuberance in the middle. Four semiconductor strain gauges are stuck symmetrically to the beam and connected to instrumentation allowing the detection of vertical ground reaction force. The system was aimed towards the analysis of gait in hemiplegic patients. It was impossible for the patients to undergo the long lasting and exhausting trials required by force plate testing and so a shoe based system was considered to be the only alternative.

### **3 Clinical observation**

There is a large variation in the measurements that different researchers have found to be of the greatest importance in providing useful diagnostic information. The major measurement techniques include:

- (i) static loading
- (ii) dynamic loading - total reaction force
- (iii) centre of foot pressure
- (iv) pressure distribution
- (v) discrete small area pressure measurement

The nature of the investigation determines what quantities should be measured and analysed. For example the detection of high loading could identify a potential skin lesion site, and can best be achieved by using the data from a pressure map with good spatial resolution. Whereas accurate measurement of the loading of the metatarsophalangeal joint of a shod foot can only be achieved using an absolutely calibrated discrete transducer.

With the growing availability of various techniques for foot pressure measurement there has been increased application to specific clinical areas (section 2.3.3) and to the assessment of orthopaedic and podiatric treatment techniques.

#### **2.3.1 Normal static foot loading**

There have been a number of conflicting theories about how the body weight is distributed under the

not when standing (Cavanagh *et al*, 1987). It is considered rather more advantageous to observe the dynamic rather than the static foot, as this is its primary function, and so due to this there have only been a few cited studies based upon static foot pressure data. Detailed below are the most widely accepted findings for the normal static pressure pattern.

On a firm flat surface the normal foot distributes almost the entire body weight over the heel and the forefoot whilst the midfoot carries very little load (Hutton *et al*, 1977). A number of investigative groups have suggested ratios for this heel and forefoot loading based upon their studies. Hutton *et al* (1977) found that a comfortable stance could be achieved with the heel carrying between one and three times the forefoot load. The toes were found to carry only 5 to 10% of the forefoot load, however progressively more as weight is transferred to the front of the foot, by rocking forward. The load distribution across the transverse arch of the metatarsal heads is such that higher loads are found in the middle, thus suggesting a convex arch (Arvikar *et al*, 1980; Leduc *et al*, 1979). This result was probably true for the majority of the subjects in their study, however it is more correct to suppose that loading can be greatest at any point across the transverse arch of the metatarsal heads for normal subjects. There is also frequent and rapid alteration in this load distribution across the forefoot in order to maintain balance.

### 3.2 Normal dynamic foot loading

The primary function of the foot is locomotion, therefore it follows that analysis upon the foot should be performed while walking. In order to diagnose disorders of the foot or lower limb knowledge of normal dynamic foot loading is required for comparison. It is expected that abnormal foot function will reflect in an abnormal plantar distribution while in locomotion. Unfortunately there is little literature on normal gait as most research groups have concentrated upon obtaining measurements from patient groups with particular foot disorders.

Specific spatial and temporal parameters of normal gait are explained in section 1.2.6. There are a number of important kinetic parameters that can be measured and used to describe normal foot loading. The vertical component of reaction force against time is explained in section 2.3.2.1, also of importance are the horizontal forces and turning moments that can be measured using the Kistler force plate (section 2.2.2.1). The centre of foot pressure is a well documented result with a

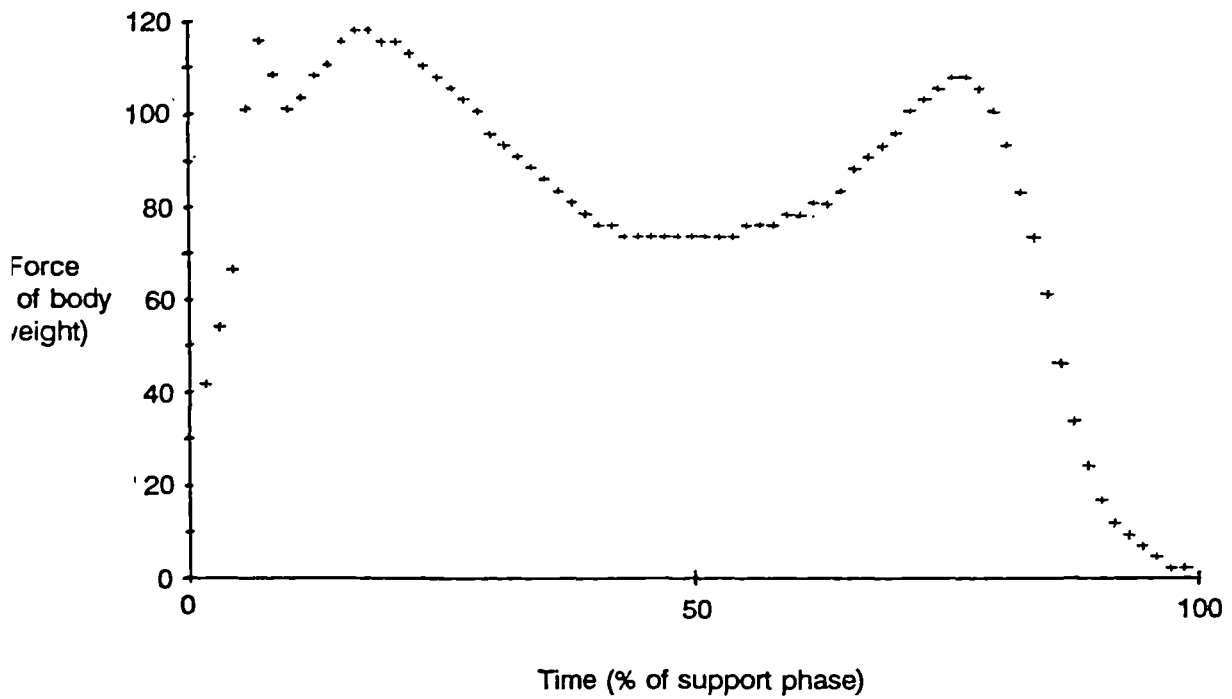


Figure 2.1 A graph of the vertical component of reaction force against time for a normal subject, obtained from a Kistler force plate system.

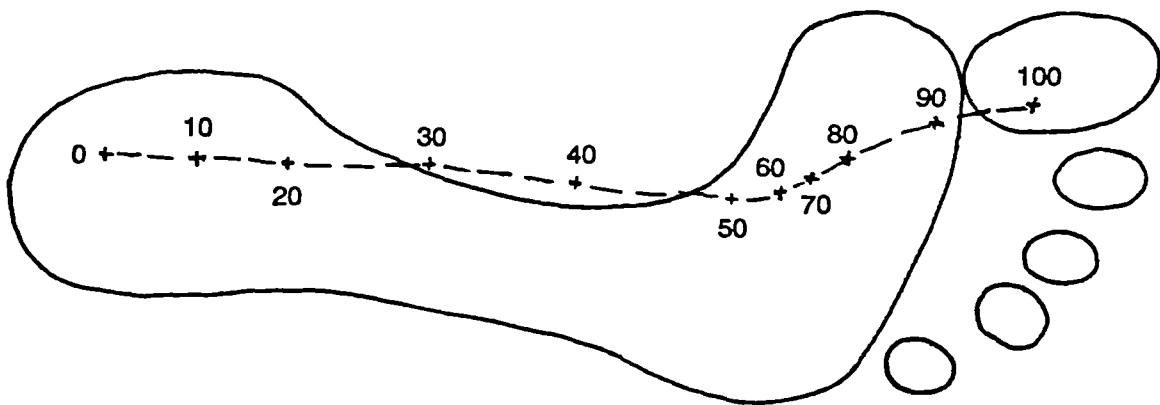


Figure 2.2 A modelled typical centre of foot pressure locus for a normal subject. Timing points are indicated as percentages of the support phase.

characteristic shape, this is discussed in section 2.3.2.2. The plantar load distribution, discrete pressure measurements and the course of pressure with time are all important parameters which are discussed in section 2.3.2.3. The frequency content of force signals obtained during gait has been reported by a number of researchers. It is cited by Pedotti *et al* (1984) that a system with a frequency response up to 50Hz is sufficient to capture the gait signal during walking. However Peruchon *et al* (1989) use a system with a frequency response of up to 100Hz. Pratt (1988) uses a spectral analysis technique in order to compare the shock attenuating properties of different insole materials: the analysis is performed upon walking subjects, in the frequency range 10 to 150Hz.

### 2.3.2.1 The vertical component of reaction force

When plotted against time the vertical component of the reaction force has a well documented symmetrical double hump form (Lord, 1986), as typically depicted in figure 2.1. The Kistler force plate system produces the most accurate results of this form, as well as providing similar results for the horizontal forces and the turning moments. It must be noted that this is a representation of the resultant vertical reaction during foot strike and is best achieved using a force plate. The data from pressure mats once mathematically analysed will produce the same result, however the summation of signals from a number of discrete transducers will only produce an approximation to the true shape. With reference to figure 2.1, the foot initially makes contact with the floor at heel strike where a short duration spike may occur. As the foot progressively makes contact with the floor the vertical reaction force builds up to its first peak, which is usually around 10 to 20% above bodyweight. During midfoot contact it falls off to just below bodyweight and then rises again during forefoot contact to a second peak which is similar in magnitude to the first. At the end of the step it rolls off to zero at toe-off. Grundy *et al* (1975) describes the course of this vertical reaction force and compares it with the centre of foot pressure (section 2.3.2.2) and plantar contact. A detailed account of the vertical reaction force and how it relates to other measurements is given by Hutton *et al* (1976) in their chapter on the mechanics of the foot.

### 2.3.2.2 Centre of foot pressure

With reference to figure 2.2 the centre of pressure (CFP) is the locus during the support phase of the

ation where the resultant force vector would act if its point of application was considered to be a single point. The shape of the CFP shown is characteristic of a normal subject. Immediately after heel strike there is a progression forward of the CFP. The line followed is slightly medial of the midline of the foot and is well away from the contact of the lateral border of the foot. This suggests that the midfoot plays a very small role in transferring the load from the hindfoot to the forefoot. As all the load is taken on the forefoot there is a clustering of time markers under the metatarsal head area indicating that the duration of load-bearing at this area is a relatively high proportion of the support phase. The CFP tends medially as the load is transferred onto the toes, and it terminates around the first and second toes at toe-off.

The concept of CFP has been used to describe both normal and pathological gaits (Cavanagh, 1978; Patton and Dhanendran, 1979; Grundy *et al*, 1975; Simkin and Stokes, 1982). This particular form of data representation has been made a feature of most systems that are able to provide vertical force distribution data (Kaliszer *et al*, 1989). It is also possible to construct a crude approximation to the actual CFP using the information provided by systems utilising only a small number of discrete transducers.

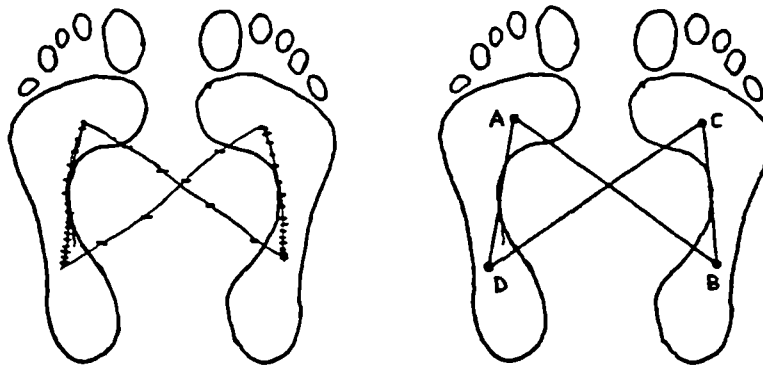


Figure 2.3 The resultant centre of pressure (RCP) trace. A: right heel strike; B: left toe-off; C: left heel strike; D: right toe-off. With reference to figure 1.7, the sequence is  $H_2, T_1, H_3, T_2, H_4, T_3, H_5, T_4$ , etc.

As with most kinetic gait parameters there is considerable step-to-step variability, a major cause of which is probably being mediolateral sway. Averaging is therefore necessary if the CFP is to be of real benefit.

a clinical situation. Cavanagh (1978) discusses a technique for averaging centre of pressure paths on a force platform. As well as indicating the nature of progressive foot loading this measurement of value in the discussion of the ankle, knee and hip in gait.

Closely related to CFP is the resultant centre of pressure (RCP) which is shown in figure 2.3. Calculation of a RCP is possible with the aid of a system capable of measuring the plantar pressure distribution of multiple consecutive footsteps for both feet, and essentially it is the combination of the CFP traces for both feet. The RCP is typically butterfly in shape for normal subjects and can vary considerably for pathological cases (Peruchon *et al*, 1989). Infotronic have a similar representation of the RCP which they call a *cyclogram*, produced by their CDG system.

### 3.2.3 Plantar distribution of load

The peak magnitudes of discrete loads under localised areas of the plantar surface vary greatly between subjects during walking. However it has been noted that the general shape of a pressure centre trace for a particular location is very similar from subject to subject (Betts *et al*, 1980). In order to provide useful information of diagnostic value the magnitude and duration of plantar load have been the two parameters of measurement most favoured by all users of measurement systems. Systems measuring barefoot plantar load distribution (pressure mat systems) have always provided the bulk of this information. Table 2.1 shows some reported peak pressure values for normal subjects obtained from a selection of papers.

For normal subjects the medial side of the heel is first to load after heel strike. At around 5% into the support phase the forefoot will come into contact with the ground and then there is a gradual transfer of load from the heel to the forefoot until the heel leaves the ground at around 30% into support phase. While in contact with the ground the distribution of load carried by the heel can be said to be regularly contoured. The midfoot carries very little load during the support phase. The distribution of load on the forefoot is shared predominantly by the metatarsal heads and as for static loading (section 2.3.1) the percentage of load carried by each of the metatarsal heads varies between subjects. During the latter part of the support phase the toes play an increasing part in supporting a foot until at toe-off it is usual for the first and second toes to be last to leave the ground.

Source	Peak Pressure (kPa)			
	Hindfoot	Midfoot	Forefoot	Toes
Marke and Cavanagh (1981)	391 lateral 433 medial	79 lateral 59 medial	324 lateral 319 medial	160 lateral 379 medial
Watts <i>et al</i> (1980), estimated by Lord (1986) from graphs	370	-	350/420/380/280/130 1st/2nd/3rd/4th/5th	420 hallux
James (1985), estimated by Lord (1986) from graphs	800 posterior 480 medial 400 lateral	100 posterior 150 anterior	480/480/560/470/350 1st/2nd/3rd/4th/5th	430 hallux 280 second 100 fifth
Winks <i>et al</i> (1983), estimated from graphs	590	215	450/450/1170/680/1000 1st/2nd/3rd/4th/5th	400 hallux
Lu <i>et al</i> (1989), estimated from graphs	400 posterior 390 anterior	-	360/440/350/270 1st/2nd/4th/5th	310 hallux
Dieve <i>et al</i> (1984)	208	88 anterior 47 posterior	163/212/197/160/97 1st/2nd/3rd/4th/5th	178 hallux

Table 2.1 A summary of reported values for mean peak pressures for normal patient groups during barefoot gait under different areas of the plantar surface of the foot (partially adapted from Lord, 1986)

Hughes and Klenerman (1987) report investigations of this nature. They used three different systems but unfortunately due to equipment incompatibilities absolute peak pressure values were not available for comparison and so measurements were reported as percentages. Gerber (1982) reports the use of an improved system based upon the Nicol mat enabling the measurement of pressure distribution, however no values for pressure are given. Hennig *et al* (1982) use their insole of 500 piezoelectric elements to describe the in-shoe vertical force distribution and its variation with time. Discrete transducers are able to provide information on a particular area, however information on the entire plantar surface of the foot is forfeited. Where systems provide calibrated pressure data it is usually expressed in kg/cm<sup>2</sup> units, whereas the more correct unit to use would be the kilopascal (1kg/cm<sup>2</sup> = 3.1kPa). The former units have been used because the analysis of results has usually been carried out by clinical staff, and so ease of interpretation (relation to body weight) was important.

### 3.3 Foot pressure measurement to investigate pathological conditions

The majority of reports from clinical studies are in the orthopaedic area and particular attention is given to hallux valgus (a lateral deviation of the hallux towards the middle line of the foot at the metatarsophalangeal joint), varus (deviation medially) and rigidus (restricted motion of the 1st metatarsophalangeal joint) pathologies, however foot pressure measurement systems have been used

for a diversity of applications. Some of the major studies performed by investigative groups are mentioned in this section, which aims to highlight and also indicate the divergence of these areas of study.

Maliszewski *et al* (1989), report using the Musgrave Footprint system to investigate hallux valgus patients. Similar investigations and also the effects of Kellers operation are described in numerous reports Miller *et al*, 1979; Henry *et al*, 1975; Grundy *et al*, 1975; Betts *et al*, 1980; Stokes *et al*, 1979). Soames *et al*, (1982) used their systems of discrete transducers to investigate patients with arthritic foot conditions. An apparatus was also described by Hutton and Drable (1972) for evaluating treatment for arthritic feet. The gait of patients with osteoarthritis of the hip was investigated by Khodadadeh (1987) who used a force plate. Minnis and Craxford (1984) compared static and dynamic methods of assessment for patients with rheumatoid arthritis.

The accurate measurement of gait and effective rehabilitation methods for amputee patients have been reported by Cunningham and Brown (1952); with the use of a force plate they measured the load in an artificial leg. Ranu (1987) has also investigated amputee patients using his triaxial load cells. Spina bifida has been an area of investigation: Betts *et al* (1980) used a pedobarographic technique to investigate the pressure distribution for a group of patients with this disease. The rehabilitation of stroke victims was discussed by Hermens *et al* (1986). They reported on results from measurements taken using a set of 16 transducers that were attached to shoe out soles.

The use of pressure measurement to help design corrective footwear has been reported on several occasions. Derbyshire and Platts (1989) described a system that initially measured pressure distribution and then aided the fabrication of moulded shoe insoles using the impression from the foot obtained by the system. Stokes *et al* (1977) also described the effect of shoe inserts that were positioned to redistribute load.

Diabetic patients are particularly susceptible to neuropathic and vascular changes which can affect the foot function. Ulceration is a particular problem caused by high pressure peaks around the bony prominences of the foot, this has been investigated by Stokes *et al* (1974, 1975), who also used the same equipment for the assessment of Kellers operation. Several other groups have investigated the diabetic foot using a variety of methods (Ctercteko *et al*, 1981; Zhu *et al*, 1989 and Boulton *et al*, 1984). The neuropathic ulceration of feet affected by leprosy was investigated by Chandrasekaran

1980). Pollard et al (1983) used shear force transducers (Tappin et al, 1980) to investigate diabetic ceration.

Other researchers have used various foot pressure measurement techniques to study particular disorders such as metatarsalgic feet (Silvino et al, 1980), or orthopaedic surgical techniques such as metatarsophalangeal fusions and Swanson arthroplasties (Duckworth et al, 1982) and silastic arthroplasty (Beverly, 1985).

#### 4 Conclusions

It has been shown that a great variety of systems capable of measuring foot loading have been developed since Beeley's initial research in the area. Of particular notice is the recent software explosion. Now that virtually all systems are based around a computer, the use of dedicated software to carry out sophisticated signal and image processing is common place. A typical example of this is the Musgrave colour footprint (section 2.2.2.1) which displays a wealth of highly colourful graphics on screens. Unfortunately transducer technology appears to be the short fall of many system development endeavours, and this is particularly so for in-shoe techniques. The EMED system was designed around a capacitive pressure mat, and when Novel<sub>gmbh</sub> used similar technology to develop their insoles many problems were encountered. It is clearly important that the correct system should be used in order to provide relevant data for a particular application or disorder. Any one system will measure a subset of all the available parameters of gait, and each a different set. This means that the comparison of results is often difficult or even impossible because of this variation in the data provided, and also due to the predominantly uncalibrated nature of this data. There is a great need for standardisation of measurement procedures and, together with research groups, this has to be the job for a leading manufacturer: if a pressure mat system is used to investigate plantar loading then it should be clear how many steps should be taken before striking the mat; how many captured steps should be averaged before providing results. If an insole system is used it should be clear which areas of the plantar surface of the foot results should be provided for; what footwear should be worn by the subject under examination. A significant step towards standardisation would be the development and use of reliable, repeatable and calibrated equipment. The diversity of equipment reviewed in this chapter collectively produces a great variety of data. If this data was of a calibrated

ture then the task of comparing the results obtained from different systems would be considerably simplified. It can therefore be seen that the development of an in-shoe pressure measurement system that could provide calibrated data to within 10% uncertainty would be a valuable addition to the repertoire of existing gait analysis systems.

## **Chapter Three**

**3**

# **PROPERTIES OF PVdF AND COPOLYMER FILM**

## Introduction

The aim of this chapter is to determine the response expected from a transducer constructed from a piezoelectric film to measure in-shoe foot loading.

Pierre and J Curie first discovered the piezoelectric effect in certain crystalline materials in 1880. A rough review of the early history of piezoelectric crystals can be found in Cady's classic work *Piezoelectricity* (Cady, 1964). In the 1940's piezoelectric effects were noticed in polycrystalline materials and links were made between their high dielectric constants, ferroelectricity and the creation of useful piezoelectric ceramics. The discovery of the poling process was the final step in the understanding of piezoelectricity in ceramics; that is, application of a high voltage sufficient to align the electric moments of spontaneously polarized regions in the material. Historical details of the discovery of piezoelectric ceramics can be found in Jaffe *et al* (1971).

In 1969 Kawai (1969) discovered that elongated and polarized films of polymers possessed piezoelectric qualities and from his studies poly(vinylidene) fluoride (PVdF) film (figure 3.1) was found to be of particular importance. More recently a copolymer film, P(VDF-TrFE) (figure 3.2), has been found to possess equally useful qualities. When referring generally to piezoelectric film, that is, PVdF or P(VDF-TrFE) film, throughout this chapter, the abbreviation *piezo film* will be used. An account of the manufacturing process for the production of piezo film is given in section 3.2.

Section 3.3 provides the necessary theoretical background to enable design calculations to be made, that is, that the expected response of an element of piezo film used to measure mechanical stress can be assessed. The conventional coordinate system used to denote piezo film axes, and hence clarify the meaning of the vector and tensor notation used throughout the chapter is described in section 3.3.1. Section 3.3.2 introduces the basic piezoelectric equations and the piezoelectric constants are defined in sections 3.3.3, 3.3.4 and 3.3.5. Of the various modes of operation in which piezo film may be used (section 3.4), the thickness mode is applicable if it is desirable to detect stress applied perpendicular to the plane of the film. The theoretical response for piezo film used in this mode is discussed in section 3.4.1. Two shear modes of operation are possible, and film sensitivity to a directly applied shearing force is discussed in section 3.4.2.

Piezo film has pyroelectric properties, which can be undesirable for some applications. Treated as an artifact, this effect is discussed in section 3.5.1. Similarly, bending the film can introduce

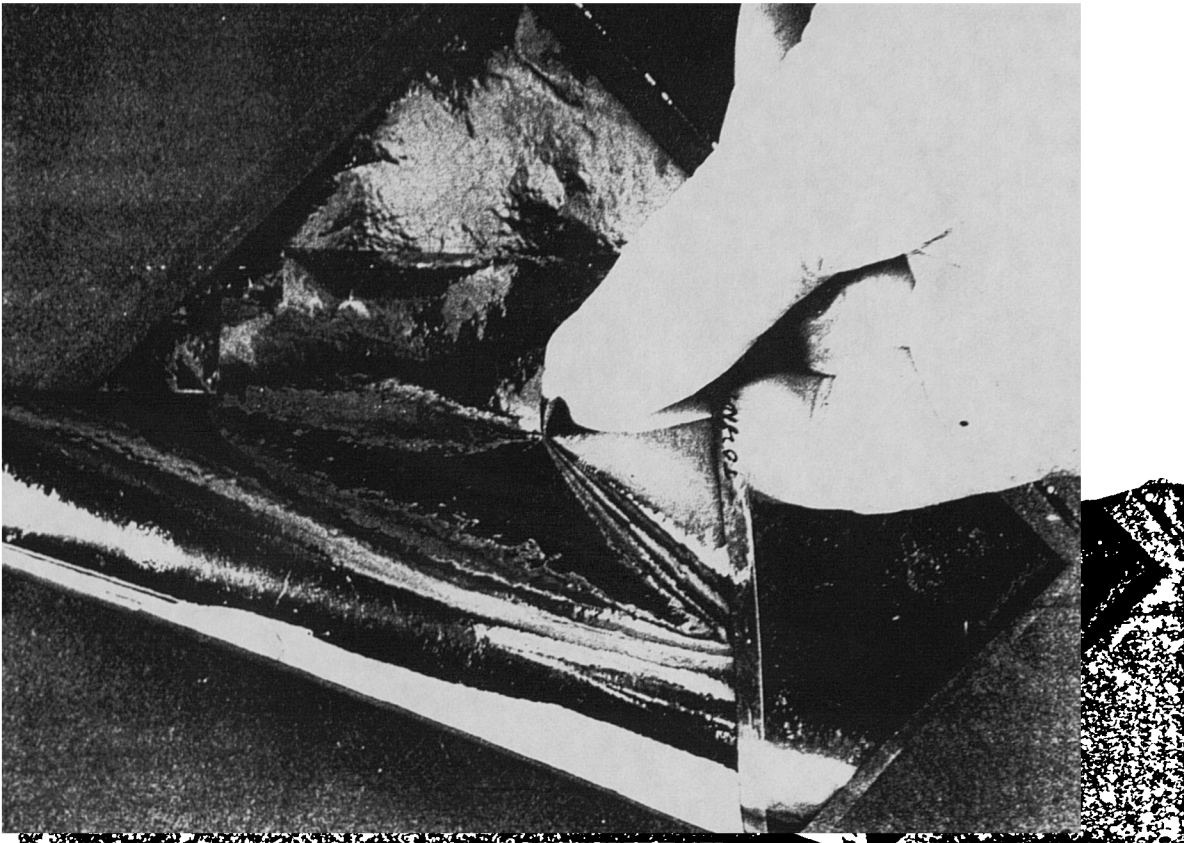


Figure 3.1 Kynar 28µm metallised PVdF film

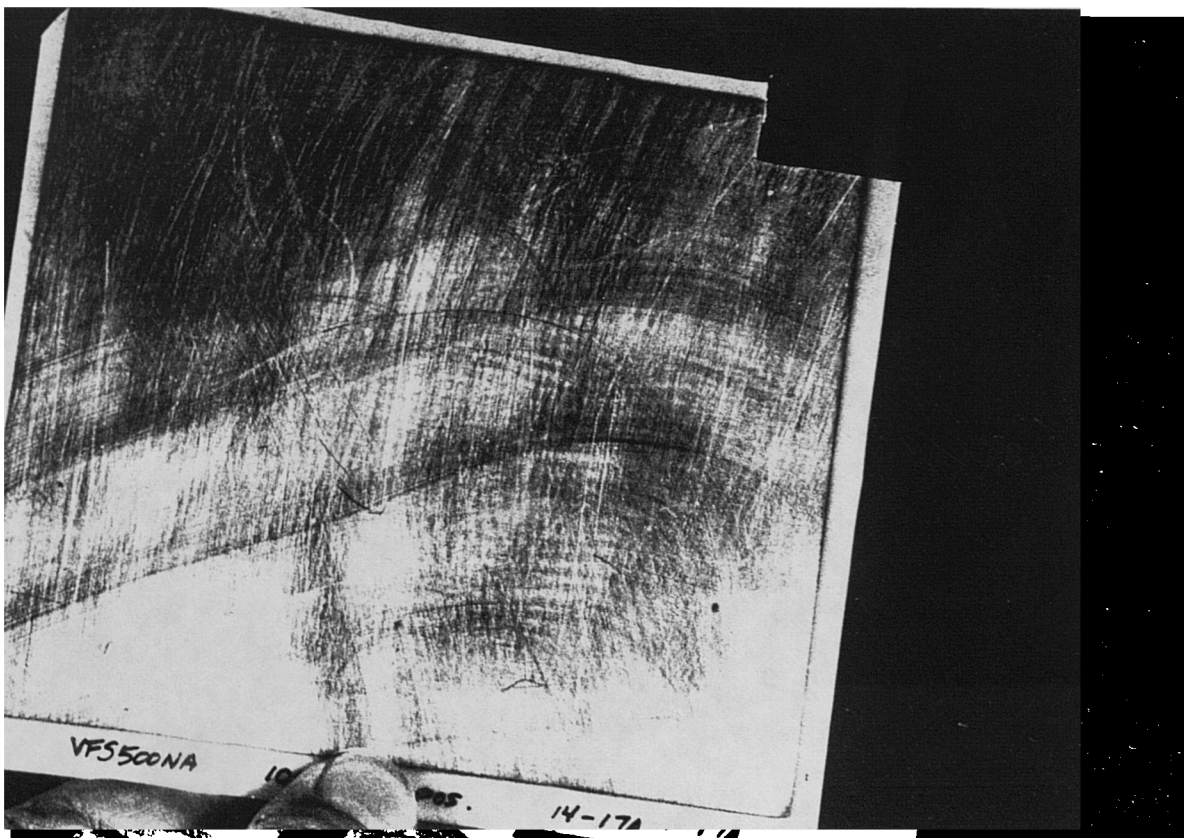


Figure 3.2 Kynar 500µm metallised copolymer film

membrane stresses so producing undesirable signals (section 3.5.2). Electroding the film and lead connection is a major design problem, complicating transducer construction. Using non conducting adhesives to mount the film has advantages due to the widespread availability of such adhesives, however their use can have a detrimental effect upon the detected charge from a transducer; the mitigation of this effect is given in section 3.4.1.1.

### **Production of PVdF and Copolymer piezoelectric film**

PVdF and its copolymers are currently the only commercially available piezoelectric polymer films. Synthesis of the polymers is reported, with particular emphasis on polymer chemistry, by Ferran and *et al*, (1988). In general, the properties of piezo film depend heavily on the nature of its crystalline structure. Three common crystalline phases for piezo film are designated alpha, beta and gamma.

#### **Production of PVdF**

PVdF is formed following the polymerisation of the Difluoroethylene monomer  $CH_2=CF_2$ . Extruded and cooled from a melt, PVdF crystallises primarily into a non-polar alpha phase polymorph. The polymer is then oriented by mechanically stretching it at temperatures below 130°C. This stretching causes a packing of unit cells into parallel planes and transforms the film from alpha phase to the polar beta-phase. In order to obtain the desired piezo- and pyroelectric activity the oriented film requires polarisation to align all the internal dipoles relative to the applied field direction. Several techniques can be used for poling the film, but conventionally the thermal technique is used, where both surfaces of the film are electroded and an electric field of about 0.5MV/cm is applied across the electrodes at a temperature of 80-100°C. The film is then cooled in the presence of the electric field, result in a permanent orientation of molecular dipoles within the polymer.

#### **Production of the P(VDF-TrFE) copolymer**

The copolymer has a mixed composition of Difluoroethylene,  $CH_2=CF_2$ , and Trifluoroethylene,  $CF_2=CF_2$ , monomers. The ratio of these monomers determines the final properties of the copolymer, which is sometimes referred to as  $VF_2/VF_3$ . Manufacture is somewhat simplified by the fact that crystallisation in a polar form takes place from the melt. This eliminates the need for an orienting process, however poling is still required in order to obtain significant piezoelectric activity. To achieve

high value for the electromagnetic coupling factor (section 3.3.7) of the material it is necessary to enhance crystallisation by annealing prior to or during the poling process (Ohigashi, 1982). From a practical point of view, not having to orient the film has advantages in the fabrication of some devices.

### 3.3.1 Polymer film piezoelectricity

Without familiarization with any branch of crystal physics, including piezoelectricity, is not possible without at least a slight acquaintance with the principles of crystallography. It is not within the scope of this thesis to take a comprehensive look at the subject, however relevant theory is given in section 3.3.2, and basic piezoelectric theory will be referred to throughout this section where appropriate. This section is also subdivided into the following specific areas.

The axes and notation used to denote direction relative to the film is explained in section 3.3.1. A subset of the eighteen piezoelectric constants can be used to describe the piezoelectric characteristics of any material, those applicable to piezo film are given in section 3.3.3. Piezo film is sensitive to mechanical stress applied in particular directions. In calculating the electrical response to an applied stress (or vice versa), one of four equations may be used, these are defined in sections 3.3.4 and 3.3.5. Whether detecting voltage or charge will determine the presence or not of a secondary piezoelectric effect, this is discussed in 3.3.6. Finally, the electromagnetic coupling factor is a useful guide to the overall piezoelectric strength of a material; values for piezo film are compared to those for other materials in section 3.3.7.

#### 3.3.1 Definition of piezo film axes

At a crystalline and molecular level, piezo film has asymmetry due to the poling and stretching processes carried out during manufacture (section 3.2). This means that the piezoelectric electro-mechanical and mechano-electrical activity is dependent upon direction relative to the film, and so piezo film is anisotropic. In order to enable the tabulation of properties relating vectors of polarisation to electrical field to tensors of mechanical stress or strain, a coordinate system is required. The film axes are identified as shown in figure 3.3.

The polarization axis is always the thickness or 3 axis. Axis 1 is the length, or the longitudinal direction, and is the direction in which the film was drawn. Axis 2 is the width, or transverse direction.

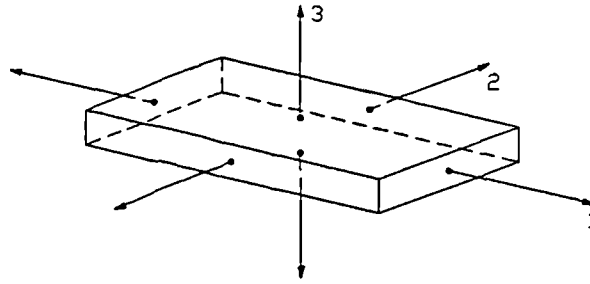


Figure 3.3 The numerical classification of axes for piezo film

generally accepted to consider the sign convention for applied stress as: positive when tensile, extensional; negative when compressive.

## 2 The direct and converse piezoelectric effect

Piezoelectric materials can be classified into 32 crystal classes depending upon the relative positions and orientations of the *symmetry elements*, or groups of symmetrically arranged atoms (Nye, 1957 76-83). Each crystal class has a unique set of properties, and each class is also grouped into one of seven *crystal systems* depending on the particular symmetry characteristics it possesses. All classes devoid of a centre of symmetry are piezoelectric, with one exception, class 29, where other symmetry elements combine to exclude the piezoelectric property. The reversible nature of the piezoelectric effect implies that piezoelectric materials must be anisotropic, which means that their physical properties must depend on the direction of the axes within the material. Such materials do not have a centre of symmetry because if one existed the reversal of an applied field could have no significance relative to the material's internal structure.

Uniaxially drawn and poled PVdF and copolymers of vinylidene fluoride are in the 3rd, or *orthorhombic*, system and possess *mm2 symmetry* which puts them in class 7. All materials in this class possess piezo- and pyroelectric<sup>1</sup> properties.

The *direct* piezoelectric effect can be represented simply as:

$$P = d \sigma \quad (3.1)$$

---

<sup>1</sup>piezo and pyro are derived from Greek words meaning *to press* and *fire*

where  $d$  is the ratio of developed polarization,  $P$ , to applied stress (force per unit area),  $\sigma$ . By definition this polarization is represented as polarization charge per unit area taken perpendicular to direction of polarization. Likewise the *converse* effect can be represented simply as:

$$S = dE \quad (3.2)$$

where here  $d$  is the ratio of developed strain (ratio of the change in a dimension to the original),  $S$ , applied electric field,  $E$ .

### 3 The piezoelectric coefficients

Piezoelectricity can be represented by a third-order tensor quantity. By definition this implies that there are 27 independent moduli, or components of  $d$  (from equation 3.1) of the form  $d_{ijk}$ . However, these coefficients are always denoted by just two numbered subscripts and this is because a reduction in the number of independent moduli can be performed, and a different notation used so that the second and third subscripts are replaced by a new *matrix* notation (Nye, 1957 pp110-5). The history of this reduction is not considered in this chapter as it is only important to understand the meaning of the matrix notation in order to be familiar with the piezoelectric coefficients.

The matrix array for  $d_{ij}$  can be written as:

$$d = \begin{bmatrix} d_{11} & d_{12} & d_{13} & d_{14} & d_{15} & d_{16} \\ d_{21} & d_{22} & d_{23} & d_{24} & d_{25} & d_{26} \\ d_{31} & d_{32} & d_{33} & d_{34} & d_{35} & d_{36} \end{bmatrix} \quad (3.3)$$

In short, 9 components of  $d_{ijk}$  have been eliminated and new single subscripts have been used for the second and third of  $d_{ijk}$ , defined as follows:

tensor notation	11	22	33	23,32	31,13	12,21
matrix notation	1	2	3	4	5	6

The first subscript of  $d_{ij}$  identifies the axis of polarisation or applied electric field (1, 2 or 3) while the second subscript indicates the nature of the applied mechanical stress or developed strain, where 1, 2 or 3 are normal components and 4, 5, and 6 are shear components.

In a piezo film the matrix of piezoelectric coefficients has five non zero elements and can be defined

Nix, 1986):

$$d = \begin{bmatrix} 0 & 0 & 0 & 0 & d_{15} & 0 \\ 0 & 0 & 0 & d_{24} & 0 & 0 \\ d_{31} & d_{32} & d_{33} & 0 & 0 & 0 \end{bmatrix} \quad (3.4)$$

h piezoelectric material will have a unique set of piezoelectric coefficients, as for all the other sets material coefficients such as elastic compliance and permittivity. Actual values for these coefficients piezo film and their use in calculating the expected charge output due to an applied stress will be illed in section 3.4.

#### 4 Piezoelectric strain or charge constant

n equation 3.1, the strain or charge constant  $d$  expresses the ratio of the developed polarisation applied stress along specified axes, under electrically free conditions (short circuit). Generally:

$$\begin{aligned} d_{ij} &= \frac{\text{Polarization along the } i \text{ axis}}{\text{Stress applied along the } j \text{ axis}} = \frac{P_i}{\sigma_j} \left[ \frac{C m^{-2}}{N m^{-2}} \right] \\ &= \frac{\text{Charge per electrode area}}{\text{Stress applied along the } j \text{ axis}} = \frac{Q_i}{\sigma_j A} \quad [C N^{-1}] \end{aligned} \quad (3.5)$$

versely (see equation 3.2), the same constant determines the amount by which an applied field ses dimensional changes in the film in all three axes, under mechanically free conditions (no hanical restraint). Generally:

$$d_{ij} = \frac{\text{Strain developed along } j \text{ axis}}{\text{Electric field applied along } i \text{ axis}} = \frac{S_j}{E_i} \quad [m V^{-1}] \quad (3.6)$$

ation 3.5 will be used in section 3.4 to determine the theoretical charge sensitivity of transducers orporating piezo film, due to applied stress in the thickness (3) direction.

## 3.5 Piezoelectric stress or voltage constant

As well as for the  $d$  constant, values for the stress or voltage constant,  $g$ , are usually quoted by manufacturers of piezo film. It is related to the  $d$  constant, under mechanically free conditions, by the dielectric constant,  $\epsilon$ , where:

$$g = \frac{d}{\epsilon} \quad (3.7)$$

The  $g$  constant is the ratio of the electric field developed due to the stress applied along a specific axis, under electrically clamped conditions (open circuit). Generally:

$$g_{ij} = \frac{\text{Electric field developed along } i \text{ axis}}{\text{Stress applied along } j \text{ axis}} = \frac{E_i}{\sigma_j} \quad [VmN^{-1}] \quad (3.8)$$

So, the same constant gives the ratio of the amount of strain developed under mechanically free conditions, to the applied polarisation. Generally:

$$g_{ij} = \frac{\text{Strain developed along the } j \text{ axis}}{\text{Applied charge per electrode area}} = \frac{S_j A}{Q_i} \quad [m^2C^{-1}] \quad (3.9)$$

The  $g$  constant is usually used when making design calculations in order to determine the voltage response of piezo film due to applied stress.

## 3.6 Secondary piezoelectric effects

When a piezoelectric element is under mechanical stress, the direct effect gives rise to an electric polarisation (equation 3.1) which, except under special boundary conditions, in turn gives rise to an electric field. According to Voigt's theory (Cady, 1964 vol2, pp260-83), this field, through the action of the converse effect, causes certain components of strain in addition to those due to the mechanical stress. Similar reasoning applies for the converse situation where an applied electric field causes the secondary polarisation (equation 3.2).

Electrical boundary conditions are of importance when considering the piezoelectric response of material under mechanical stress, and there are two such conditions: electrically *clamped* and electrically *free*.

An element should be considered electrically clamped when conditions are such that there is no overall polarisation or, more generally when the polarisation is constant; an isolated, or open circuit element is therefore practically in the electrically clamped state.

The electrically free state is applicable where the surrounding medium has infinite dielectric permittivity. This condition is realised by making the entire surface equipotential; by shorting the electrodes or by allowing time for surface charges to be neutralised by leakage. So there will be no field in the element, and if it is mechanically stressed the piezoelectric polarisation is not diminished by counter-polarisation.

In order to reduce the secondary piezoelectric effect it is beneficial to use a piezoelectric element in the electrically free state (charge amplification) rather than in a clamped state (voltage amplification), although this effect has little practical significance, particularly for the application of this work.

#### 4.7 Piezoelectric strength - a material comparison

An overall assessment of the strength of a piezoelectric effect within a material is often desired and probably the best single measurement of this is the coupling factor,  $k$ . This is a measurement of the fraction of the electrical energy converted to mechanical energy when an electric field is applied, or vice versa when an element is stressed. The energy transformation ratio is the square of the coupling constant (Kynar technical manual, 1983) and can be defined as:

$$k^2 = \frac{\text{mechanical energy converted into electrical energy}}{\text{input mechanical energy}} \quad (3.10)$$

This is always an incomplete process, and so  $k^2$  is always less than 1.

Table 3.1 shows comparative values of  $k$  for a few piezoelectric materials (Jaffe, 1971 p10; Ohigashi, 1982). Currently manufacturers are developing copolymer films in an attempt to further increase the coupling factor.

Material	Coupling Factor
Barium titanate	0.4
Lead titanate zirconate	0.5 - 0.7
Quartz	0.1
Rochelle salt	0.9
PVdF	0.2
P(VDF-TrFE)	0.3

Table 3.1 The electromechanical coupling factor for various materials

### Mechanical to electrical transduction

There are many mechano-electrical applications for piezo film (Kynar technical manual, 1987; Yarsley technical manual, 1982). For each application the film will be used in a particular mode, and the five main modes that an element may operate in due to stress applied normal to the axes are as follows (the mechano-electric shear modes are described in section 3.4.2):

**Thickness mode.**

The element is free to move in the 1 and 2 directions and a charge is developed in the 3 direction due to an applied stress in the 3 direction. The constant  $d_{33}$  applies.

**Clamped thickness mode.**

The element is clamped in the 1 and 2 directions and a charge is developed in the 3 direction due to an applied stress in the 3 direction. The constant  $d_t$  applies.

**Longitudinal mode.**

The element is free to move in the 2 and 3 directions and a charge is developed in the 3 direction due to an applied stress in the longitudinal (1) direction. The constant  $d_{31}$  applies.

**Transverse mode.**

As for the longitudinal mode except that the stress is applied in the transverse (2) direction.

The constant  $d_{32}$  applies.

**Hydrostatic mode.**

The element is free to move in all directions and a charge is developed in the 3 direction due to hydrostatic forces in which the pressure field stresses all surfaces of the element equally.

The constant  $d_h$  applies ( $d_h = d_{31} + d_{32} + d_{33}$ ).

Clamped thickness and hydrostatic modes are special cases where the corresponding piezoelectric constants have been defined for particular practical conditions. These two modes are the two exceptions to the double numeric subscript system for denoting the piezoelectric constants.

In-shoe foot pressure measurement a discrete transducer should be sensitive to the average loading experienced in the thickness direction. Construction of the transducers is described in chapter four, but basically an element of film is sandwiched between two stiffening materials and is therefore operating in the clamped thickness mode. In practice the adhesive used to mount the element will not provide a truly rigid bond, and so will allow a small amount of lateral movement. It is therefore expected that the actual sensitivity for a practical transducer will be somewhere between two values for  $d_t$  and  $d_{33}$ , however  $d_t$  will be used when making design calculations. The value  $d_t$  is around two thirds of the value for  $d_{33}$ . Values for the  $d$  constants for Kynar piezo film are given in table 3.2.

Constant [pC/N <sup>-1</sup> ]	Material	
	PVdF	P(VDF-TrFE)
$d_{31}$	23	7
$d_{32}$	3	6
$d_{33}$	-33	-25
$d_t$	-22	-17
$d_h$	-7	-12

Table 3.2 Piezoelectric strain or charge constant values for Kynar piezo film,  $d$  [pC/N<sup>-1</sup>]

1 Relationship between transducer and measurement site areas - stress measurement in the thickness mode.

If a compressive force,  $F$ , acts upon a piezo film element of area  $A_p$  in the thickness mode, then an equivalent stress,  $\sigma$ , is experienced by the element if this force is distributed over  $A_p$ . The resulting deformation causes a change in the surface charge density of the material so that a charge,  $Q$ ,

ears across the electrodes, as shown in figure 3.4. If the force becomes tensile then the resulting charge produced would be of reverse polarity.

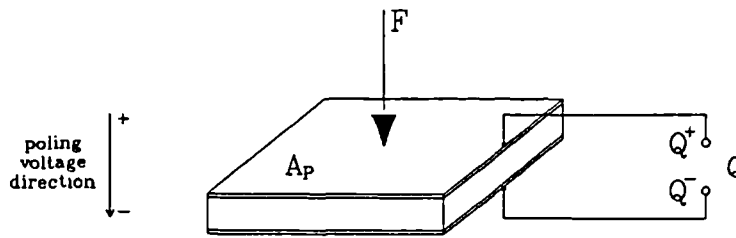


Figure 3.4 Piezo film element operating in the thickness mode

In equation 3.5 the charge produced can be expressed as:

$$Q = d_t F \quad (3.11)$$

In terms of applied stress,  $\sigma$ , as:

$$Q = d_t \sigma A_p \quad (3.12)$$

In the application of this work the quantity to be measured by a piezo film transducer is the loading at particular anatomical sites (section 1.2.4), that is, the average stress or pressure experienced by the site, or the equivalent force. In practice the anatomical site under investigation will not evenly distribute its load over the surface of the transducer. To help show this the structure of the foot should be considered (section 1.2). For example, the metatarsal heads are roughly spherical bones beneath the epidermis, so it is expected that a pressure map would have the appearance of ring like contours. The transducer response due to such loading will now be considered.

Generally, for an element of piezo film supported on a rigid flat surface, the stress experienced will be a map of  $n$  small areas each having a discrete value. From equation 3.12 the charge response can be expressed as:

$$Q = d \sum_{i=0}^n \sigma_i A_i \quad (3.13)$$

each individual small area is contributing to the overall charge and an averaging process takes place. This element is therefore sensitive to the average stress applied over its area.

The problem of bending artifact will be addressed in section 3.5.2, and it will be shown that this problem can be reduced by sandwiching a piezo film element between stiffening layers. A top stiffening layer will have the effect of mechanically averaging the applied stress, and so to determine charge response equation 3.12 can be used directly.

Therefore it can be seen that the charge response for a piezo film transducer suitable for in-shoe pressure measurement is proportional to average stress and this can be equated to a force value if required.

After giving consideration to the published results of studies carried out by other researchers, the range below was chosen (see section 2.3.2.3):

Dynamic pressure measurement range = 0 to 2MPa

A charge of 1 nC for an element of area 1cm<sup>2</sup>, corresponds to a force range of 0 to 200N. Using equation 3.11, the expected charge response for this range is given below in table 3.3.

Table 3.2.

Applied Stress [kPa]	Force [N]	Charge Produced [nC]	
		PVdF	P(VDF-TrFE)
50	5	110pC	85pC
500	50	1.1	0.85
1000	100	2.2	1.7
2000	200	4.4	3.4

Table 3.3 Theoretical charge output for a piezo film element 1cm<sup>2</sup> in area, operating in the clamped thickness mode

In order to analyse the relationship between the measurement sites and a transducer it is important to establish exactly what a transducer will quantify. This is particularly important if it is intended to compare results against those obtained from other systems. The force exerted by the heel is spread out over the whole hind foot which can be area of around 30cm<sup>2</sup>. Whereas the force exerted by a metatarsal head may be exerted over an area of as little as a few square millimetres. In order to associate a transducer response with an assumed applied force, it must have been ensured that the

ial force was distributed wholly over the area of the transducer. Then equation 3.11 may be used, it can be seen that the result is independent of the size of the transducer. For the heel situation, will not be the case as the force will be distributed over an area much greater than that which is ared by the transducer. A transducer will thus provide an indication of the average stress at the icular area under the heel it is positioned.

### 1.1 The effect upon transducer sensitivity of using non-conducting adhesives for fabrication

necessity of constructing rigid transducers (section 3.5.2) has resulted in the use of strong esives, and a non-conducting epoxy has proved most successful for this purpose (see chapter However, if non-conducting adhesive is used to secure the film to stiffening layers, which also e as the electrodes, then the capacitance of the glue film will be presented in series with the piezo element. This will have the effect of reducing the sensitivity of the transducer, which will now be nated, with reference to figure 3.5.

Material	Dielectric Constant $\epsilon$
PVdF	12
P(VDF-TrFE)	8.5
Epoxy Resin	2.95

Table 3.4 The dielectric constants for piezo film and epoxy adhesive

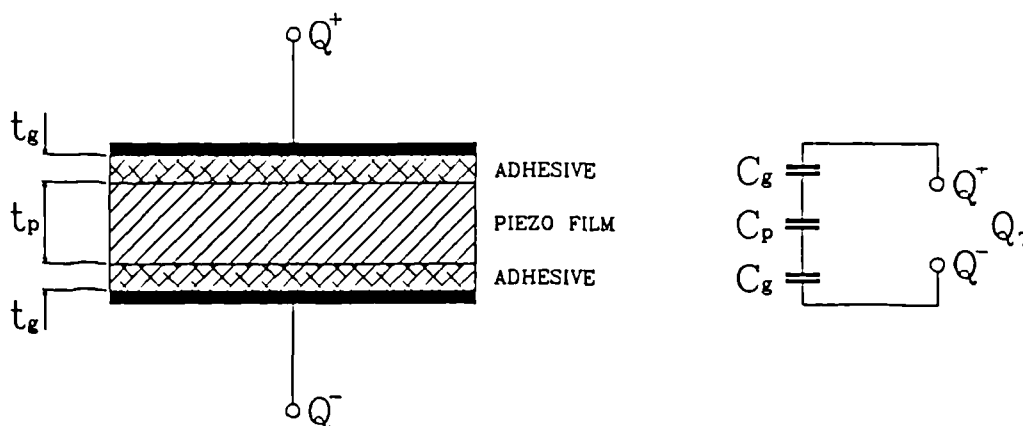


Figure 3.5 Equivalent circuit for a piezo film element adhered between two electrodes using non-conducting adhesive

It is assumed that the top and bottom adhesive layers are the same thickness, and the area of the element is A, then the capacitance of the piezo film,  $C_p$ , is:

$$C_p = \epsilon_0 \frac{\epsilon_p A}{t_p} \quad (3.14)$$

where  $t_p$  is the thickness of the piezo film; and the capacitance of each adhesive film,  $C_g$ , is :

$$C_g = \epsilon_0 \frac{\epsilon_g A}{t_g} \quad (3.15)$$

where  $t_g$  is the thickness of the adhesive film. So the combined capacitance for the transducer,  $C_T$ , can be expressed as:

$$C_T = \frac{C_p C_g}{2C_p + C_g} \quad (3.16)$$

The voltage across the transducer,  $V_T$ , is equal to the voltage across the piezo film,  $V_p$ , assuming no net charge across the  $C_g$ , so the charge output,  $Q_T$ , can be expressed as:

$$Q_T = \frac{V_p C_p C_g}{2C_p + C_g} \quad (3.17)$$

Since  $Q_p = C_p V_p$ , then substituting for  $V_p$  in equation 3.17 will give:

$$\frac{Q_T}{Q_p} = \frac{C_g}{2C_p + C_g} \quad (3.18)$$

the *adhesive factor*,  $\nu$ , be defined as:

$$\nu = \frac{\text{Output charge from transducer}}{\text{Charge developed by piezo film}} = \frac{Q_T}{Q_p} \quad (3.19)$$

A convenient expression for  $\nu$  can be obtained by substituting for  $C_g$  and  $C_p$  from equations 3.14 and 3.15, to give:

$$\nu = \frac{e_g t_p}{2e_p t_g + e_g t_p} \quad (3.20)$$

Therefore the charge sensitivity of a transducer constructed using non-conducting adhesive is always down by a factor  $\nu$ , compared to the sensitivity of the piezo film element; the voltage sensitivity remains the same.

The reduction in sensitivity for PVdF and copolymer transducers constructed using non-conducting adhesive can now be estimated using equation 3.20. So assuming the glue thickness to be  $20\mu\text{m}$ , the adhesive factor for a PVdF transducer ( $52\mu\text{m}$  film thickness) will be:

$$\nu_{\text{PVdF}} = 0.24$$

and the adhesive factor for a copolymer transducer ( $500\mu\text{m}$  film thickness) will be:

$$\nu_{\text{P(VDF-TrFE)}} = 0.81$$

It can be seen that film thickness is a major factor affecting transducer sensitivity ( $\nu_{\text{PVdF}} = 0.75$  for  $10\mu\text{m}$  film), and so it is desirable to use piezo film of at least  $500\mu\text{m}$  in thickness in order to maintain sensitivities of greater than 75%.

## 3.2 Feasibility of direct shear force measurement using piezo film

PVdF and copolymer film have two non-zero shear coefficients (equation 3.4),  $d_{24}$  and  $d_{15}$ . Values for PVdF film are  $-23\text{pC/N}$  and  $-27\text{pC/N}$  respectively; no known values are available for copolymer film. Polarization due to the direct shear effect (shear between the top and bottom surfaces of the film) can be expressed by two equations as follows:

$$P_2 = d_{24} Y_4 \quad P_1 = d_{15} Y_5$$

generally

$$P_i = d_{ij} Y_j \quad (i = 2,1; j = 4,5) \quad (3.21)$$

mentioned in section 3.3.3, the tensor notation for stress can be abbreviated to a convenient form, that the two tensor subscripts are replaced by one. The applied shear stress  $Y_4$  represents shear perpendicular to the 3 direction, along the 2 axis and  $Y_5$  represents shear perpendicular to the 3 direction, along the 1 axis.

denoted by the first subscript of  $d_{ij}$ , in order to detect an electrical response due to an applied shear stress, electrodes would have to be placed along the appropriate edges of the film. Due to the dimensions of the film, the actual charge produced would be relatively extremely small, as  $P_i$  is the polarization charge per unit area ( $A_e$ ), where  $A_e$  is the area of the electroded edge.

The magnitude of in-shoe shear force experienced by discrete areas of the plantar surface of the foot is of the same order of magnitude as the vertical force experienced by the same area (Tappin *et al*, 2000). So as an example, if a 30N force is to be measured by a PVdF element 1cm<sup>2</sup> in area and is applied in the 1 direction, the applied shear stress would be 300kPa, and so the polarization produced would be,  $P_1 = d_{15} Y_5 = 27 \times 10^{-12} \times 300 \times 10^3 = 8.1 \times 10^{-6} \text{Cm}^{-2}$ . If the thickness of the film is 100 $\mu\text{m}$  then the charge produced would be,  $Q = P_1 A_e = 8.1 \times 10^{-6} \times 1 \times 10^{-6} = 8.1 \text{pC}$ . Therefore sophisticated instrumentation would be necessary in order to detect this charge due to direct shear stress. If a polymer film of thickness 500 $\mu\text{m}$  is used instead of the PVdF element,  $A_e$  would be 5 times greater, so if  $d_{15}$  is assumed to be the same then the charge produced would also be 5 times greater. Hence, it is advantageous to use thicker piezo film elements so that a greater charge is produced for the same applied stress.

### Inherent measurement artifacts

For measurements of practically any description, artifacts can present difficulties when attempting to extract the required parameter(s) from a signal. Artifact due to temperature and bending are expected to present problems that require consideration when designing a transducer using piezoelectricity, and these are addressed in the following two sections of this chapter.

## Pyroelectric effect

When thermal energy is absorbed by a piezo film there is a corresponding rise in the temperature that produces an electrical response. This pyroelectric effect is linearly reversible upon cooling. The electric effect is complicated by the fact that a pyroelectric material is also always piezoelectric. A change in temperature of a free element causes a deformation, and this in turn produces a secondary polarisation of piezoelectric origin, superimposed upon the primary pyroelectric polarisation. Measurement of the relative magnitudes of the primary and secondary effects is difficult and so actual values for a material are not usually known. In general, however, it was found that the primary effect is small but not negligible, and was around one fifth of the total effect. This ratio will vary for different materials, but the greater part of the pyroelectricity for all materials is secondary (Nye, 1957: 180-81, 189-91). The pyroelectric constant,  $\rho$ , can therefore be defined as the sum of the primary,  $\rho_p$ , and secondary,  $\rho_s$ , pyroelectric constants:

$$\rho = \rho_p + \rho_s \quad (3.22)$$

The pyroelectric coefficient,  $\rho$ , for a piezo film is around an order of magnitude lower than for commonly used ceramics; the value quoted for Kynar PVdF is  $-25 \times 10^{-8} \text{Cm}^{-2}\text{K}^{-1}$  and the value for copolymer film can be assumed to be the same (Don Halvorsen, Atochem Ltd, personal communication). The presence of secondary pyroelectricity is an important consideration when designing transducers, as the use of a clamp to clamp an element in the 1 and 2 directions would reduce pyroelectric effects. For an element of piezo film adhered between a brass layer and a double sided circuit board layer using epoxy adhesive (type BHHHDN transducers, see section 4.3.3.2), the pyroelectric response can be estimated as follows. The coefficients of linear expansion,  $\alpha$ , for brass, epoxy resin, piezo film and double sided circuit board are 18, 39, 72 and  $25 \times 10^{-6} \text{C}^{-1}$  respectively. So the piezo film will expand an amount approximately 4 times that of the sandwiching layers and 2 times the thin glue layers. Therefore qualitatively it can be presumed that the sensitivity to changes in temperature for this transducer construction will be reduced from that of a mechanically free piezo film element. However, for pyroelectric calculations the worse case will be assumed, and  $\rho$  will be used.

The pyroelectric coefficient,  $\rho$ , relates to the product of the film area,  $A$ , and the change in

perature,  $\Delta T$ , thus:

$$Q = \rho A \Delta T \quad (3.23)$$

a  $1\text{cm}^2$  element of piezo film, the charge produced due to a  $1^\circ\text{C}$  change in temperature will be  $1\text{C}$ . As for the piezoelectric response of a piezo film transducer, the pyroelectric response is a.c., due to the intrinsic time constant (leakage) of the film and that of the interfacing electronics. A transducer used inside a shoe will therefore be sensitive to a change in temperature, and the initial charge developed due to the temperature difference between room temperature and in-shoe temperature will decay (section 7.3.6). For comparison, an applied compressive force produces a positive charge output whereas an increase in temperature produces a negative charge output.

The choice of materials will affect the pyroelectric response of a transducer in that if materials with low thermal conductivities are used to contain a piezo film element then the transducer would have greater sensitivity to peripheral temperature change. So a transducer constructed using double sided circuit board elements ( $k = 0.52\text{Wm}^{-1}\text{K}^{-1}$ ) will be less sensitive to temperature change than a transducer constructed using brass elements ( $k = 106\text{Wm}^{-1}\text{K}^{-1}$ ).

#### Temperature coefficient for $d_t$ and $d_{33}$

The piezoelectric strain constants,  $d_t$  and  $d_{33}$ , will vary with changes in ambient temperature. For the temperature range  $10\text{-}40^\circ\text{C}$  it can be assumed that the temperature coefficient for  $d_{33}$  of PVdF is linear, and has a value of  $0.18\text{pCN}^{-1}\text{K}^{-1}$  (Kynar technical manual, 1983, 1987). There is no theoretical value available for copolymer film, however it is thought to be some degree lower (Don Halvorsen, Atochem personal communication). The effect upon the temperature coefficient values of mechanically loading an element is also unknown; this is investigated experimentally and is discussed in section 5.

## 2 Bending effects

In order to estimate the effect of the bending of a piezo film transducer it is necessary to consider the bending of a uniform beam. It is quite probable that a transducer will at some time be positioned over a bony part of the foot and this being the case, spherical bending will occur. Alternatively, the

umstances may be that the transducer is forced into bending along one axis, and it is expected : the maximum deflection due to uniaxial bending will be greater than for spherical bending. The ory necessary to estimate transducer errors due to spherical bending is very complex and so essment is carried out experimentally (see section 6.2.6), however it will be useful to consider a plified case of uniaxial bending of a beam.

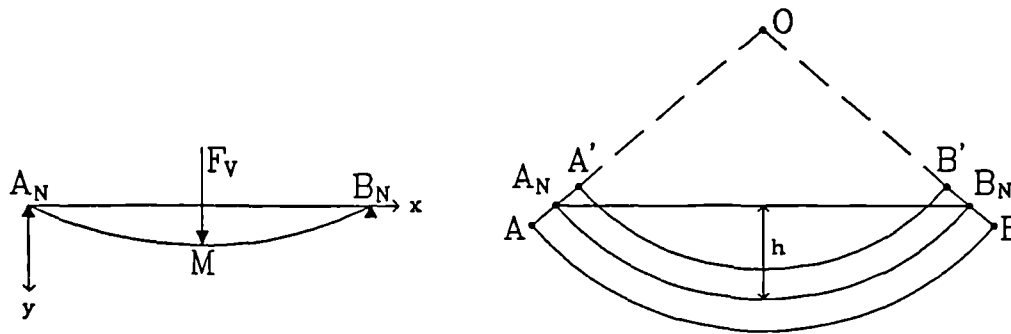


Figure 3.6 Shows a beam resting on two supports  $A_N$  and  $B_N$  at its ends, bending due to an applied force. The cross sectional view through its thickness shows the different radii of curvature of the top and bottom surfaces and the neutral axis.

In this analysis a uniform beam of length and width  $a$ , thickness  $t$  and negligible weight will rest in a horizontal position on supports at its ends,  $A_N$  and  $B_N$  (figure 3.6). A vertical force,  $F_v$ , will be applied at the centre of the beam,  $M$ , ( $x = a/2$ ), and an expression for the maximum deflection,  $h$ , will be obtained. The bending will be assumed to be only slight and so the arcs  $AB$ ,  $A_N B_N$  and  $A' B'$  will be assumed to be circular. Arc  $A_N B_N$  is called the *neutral line* of the cross section, and is neither stretched nor contracted during bending. However if an element of piezo film is rigidly adhered to the top surface  $A B$  then it will be stretched, and conversely, if an element is adhered to the bottom surface  $A' B'$  then it will be compressed. The deflection  $h$  at the centre of the beam was obtained by considering the Bernoulli-Euler law of flexure for a beam (Green and Gliddon, 1966 pp114-33; Adlington and Ramsay, 1962 pp252-60), and can be expressed as:

$$h = \frac{1}{48} \frac{F_v a^3}{Y_s I} \quad (3.24)$$

where  $Y_s I$  is the flexural rigidity of the beam, and for this cross section  $I$  can be expressed as:

$$I = \frac{1}{12} t^3 a \quad (3.25)$$

substituting for I in 3.24 gives:

$$h = \frac{1}{4} \frac{F_v a^2}{Y_s t^3} \quad (3.26)$$

Therefore it can be seen that the bending of a transducer due to an applied force depends upon the length and thickness of the transducer and the Young's modulus,  $Y_s$ , of the material. If a laminate of materials with different Young's moduli are used then this will affect the position of the neutral axis, nearer the film is positioned to the neutral axis the less it will be stressed as a result of the bending. So transducer construction can minimise or accentuate unwanted signals due to transducer bending. In view of this, a piezo film element sandwiched between two identical materials will be the most favourable construction.

In order to determine by how much the arcs AB and A'B' extend and contract by, an expression for the radius of curvature of  $A_N B_N$  needs to be found. Trigonometric relationships will be considered and figure 3.7, which presents information in addition to figure 3.6, will be referred to.

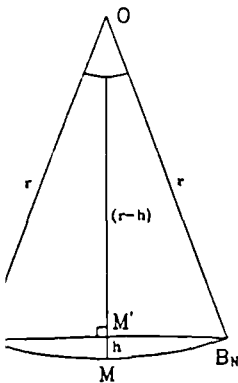


Figure 3.7

The length of arc  $A_N B_N$  can be written as:

$$a = r \theta$$

where  $\theta$  is measured in radians. So from triangle  $A_N O M'$  in figure 3.7:

$$r \cos \frac{\theta}{2} = r - h$$

$$h = r \left( 1 - \cos \frac{\theta}{2} \right) \quad (3.27)$$

if the bending is slight, then

$\theta$  is small ( $\ll 1^\circ$ ) and the small angle identity,  $\cos \theta = 1 - \theta^2/2$ , may be used ( $< 1\%$  error for  $\theta < 37^\circ$ ),

so equation 3.27 becomes:

$$h = r \left( 1 - 1 + \frac{a^2}{8r^2} \right)$$

The relationship for the radius of curvature  $r$  for arc  $A_N B_N$  can be expressed as:

$$r = \frac{a^2}{8h} \quad (3.28)$$

The lengths of arcs AB and A'B' can be written as:

$$\left( r + \frac{t}{2} \right) \theta \quad \text{and} \quad \left( r - \frac{t}{2} \right) \theta$$

Therefore the top and bottom material surface lengths change by an amount equal to  $(t/2)\theta$ . If the perpendicular distance from the neutral axis to the material surface is  $n$ , then using equation 3.28, the change in material surface lengths,  $\Delta a$ , can be expressed as:

$$\Delta a = \frac{8hn}{a} \quad (3.29)$$

Substituting for  $h$  from equation 3.26 gives:

$$\Delta a = \frac{2F_v n a}{Y_s t^3} \quad (3.30)$$

If an element of piezo film is adhered to one of the surfaces, and its stiffness is considered negligible, then the displacement  $\Delta a$  will cause a stress,  $\sigma_1$ , to be developed, which can be written as:

$$\sigma_1 = \frac{\Delta a}{a} Y_p \quad (3.31)$$

where  $Y_p$  is the Young's modulus for the piezo film. From equation 3.5 the resulting charge,  $Q_3$ , due

to this stress, can be written as:

$$Q_3 = d \sigma_1 A_e \quad (3.32)$$

where  $A_e$  is the area of the film ( $A_e = a^2$ ) and  $d$  is either  $d_{31}$  or  $d_{32}$ , depending upon the orientation of the film with respect to the bending axis. So substituting equation 3.31 into 3.32 gives:

$$Q_3 = \frac{d Y_p A_e \Delta a}{a} \quad (3.33)$$

Therefore by substituting for  $\Delta a$  in equation 3.33, from 3.30, an expression can be obtained for the amount of charge developed due to the applied vertical force  $F_v$ :

$$Q_3 = \frac{2 d Y_p F_v A_e n}{Y_s t^3} \quad (3.34)$$

From this simplified analysis for uniaxial bending of a beam, the charge developed by an element of film rigidly bonded to the beam can be estimated. It can be seen that if the piezo film element is sandwiched between two equal layers of another material then the neutral axis of the film will lie along the neutral axis of the laminate, i.e.,  $n=0$  in equation 3.3.4, and so there will be no charge produced due to bending. Using equation 3.3.4, the charge developed by an element of copolymer film ( $d=7 \times 10^{-12} \text{CN}^{-1}$ ,  $Y_p=2 \text{GPa}$ ,  $A_e=1 \times 10^{-4} \text{m}^2$ ) sandwiched between two layers of double sided circuit board ( $Y_s=5.7 \text{GPa}$ ,  $t=3.2 \times 10^{-3} \text{m}$ ) due to a vertical force of 30N will be 6pC or less if the positions of the neutral axes of the film and the laminate differ by  $13 \mu\text{m}$  or less. This is less than 1% of the charge developed due to the vertical force (0.6nC for 20pC/N transducer sensitivity). Type DSHSDN transducers (section 4.3.3.1) are of this construction, however the machined cable groove in the bottom layer will destroy uniformity and so the neutral axis of the laminate is expected to move away from this layer. For type BHHHDN transducers (section 4.3.3.2) the piezo film element is sandwiched between two different materials of differing thicknesses, and so the neutral axis of this configuration will be displaced due to these differences and also due to the cable groove in the bottom layer. In

order to aid the selection of materials and thicknesses for transducer components so that the neutral axis of the laminate lies along that of film, the following equation may be used:

$$l_1 A_1 Y_1 = l_2 A_2 Y_2 \quad (3.35)$$

where  $l_1$  and  $l_2$  are called the *lever lengths* and are the distances of the neutral axes the two materials from that of the laminate,  $A_1$  and  $A_2$  are areas of the materials (in this case can be the thicknesses due to the common width) and  $Y_1$  and  $Y_2$  are the Youngs moduli of the materials. As an example, for a  $100\mu\text{m}$  copolymer film transducer, the ideal thickness,  $t_1$ , for a brass top layer ( $l_1=0.25+t_1/2$ ,  $A_1=t_1$ ,  $Y_1=100$ ) with double sided circuit board as the bottom layer ( $l_2=1.05$ ,  $A_2=1.6$ ,  $Y_2=5.7$ ) is calculated using equation 3.35 as being 0.25mm.

Another practical factor that is not considered in this analysis is the effect of support under the transducer, which will be provided by the shoe insole and will have the effect of reducing this error due to bending.

### 3.6 Conclusions

It has been shown that piezo film has piezo- and pyroelectric qualities analogous to those defined for classic crystalline materials. With this in mind the valid piezoelectric constants could be defined and the appropriate equations used to determine the theoretical charge sensitivity of transducers incorporating piezo film. For this application the direct piezoelectric equation is used together with the charge (or strain) constant, which takes into account the applicable electrical and mechanical boundary conditions (electrically and mechanically free). More generally, piezo film can be used in one of seven (including two shear) mechano-electrical modes. The transducer constructions described in chapter 4 are such that the piezo film element is sandwiched between two stiffening layers, and so the clamped thickness mode of operation applies. This means that the element is mechanically constrained in the 1 and 2 directions, however because the bond will not be truly rigid, operation will actually be somewhere between the thickness (mechanically free) and the clamped thickness mode. Careful consideration should always be given to the relationship between the measurement site and the transducer. It has been shown that the quantity being measured by a piezo film transducer is the

verage vertical stress applied over the area of the transducer, or the equivalent applied force, and this is regardless of whether a stiffening top layer exists or not. Raw PVdF was initially used as an inert lining material for chemical containers; in its piezoelectric thin film form the inert properties remain which means that obtaining good adhesive bonds is problematic. Copolymer film is less inert, and the best bonds have been accomplished using a special non-conducting epoxy adhesive (the same is true for PVdF film, following fluorocarbon adhesive pre-treatment). The presence of this glue layer means that the piezo film element is capacitively coupled to the interfacing electronics and so the detected charge signal will be appropriately diminished. It has been shown how the glue can affect the output signal by developing theory to describe the expected drop in signal magnitude. Temperature and bending artifact are the two main areas of measurement artifact that require consideration when using piezo film for in-shoe foot pressure measurement. These areas have been addressed and quantified so that the appropriate allowances could be made during further system design.

## **Chapter Four**

**4**

# **TRANSDUCER DEVELOPMENT**

## 4.1 Introduction - a tough transducer for a tough environment

This chapter contains details of the development of the discrete pressure transducer for measuring in-shoe loading, as shown in figure 4.1. All design criteria and constructional methods are described, however only the latest three transducer designs are described in detail (section 4.3.3). The present transducer system has evolved after giving consideration to various approaches: utilising whole sheets of PVdF with isolated sensor sites; discrete transducers interconnected using flexible circuit laminates and stand-alone discrete transducers. Eight transducers (section 1.3.5) are used to obtain the required data from each foot, and currently all sixteen transducers used for clinical measurements are constructed using copolymer film. As with any device used to measure a physical parameter, the introduction of a transducer will affect the parameter being measured. Therefore the introduction of a pressure transducer into a subject's shoe should be designed to have minimal effect upon the desired measurand. The feasibility of meeting this requirement is addressed in section 4.2.

Numerous design and development features have been given careful consideration, and some of the more important areas are as follows:

- Optimum transducer dimensions
- Providing electrical connections
- Adhesive bonding techniques
- Transducer bending artifacts

These areas are discussed in the relevant sections of this chapter.

From a view of developing a clinical system, material costs must be given consideration. A sheet of 28 $\mu$ m Kynar PVdF film measuring 150 x 300mm costs around £75 and a sheet of 500 $\mu$ m Kynar copolymer film half this area costs around £250 (prices for Nov 1990), therefore small area discrete transducers will have a low material cost. Current fabrication techniques are complex and time consuming (around 10 hours total fabrication time is required for each transducer) and so from an economic viewpoint, material costs are insignificant in comparison. With this in mind the transducers are to be reusable and should have a life span in excess of 100 uses. Thus robust design is essential (section 4.3). The transducers are to be integrated into a custom insole (section 4.2.1) designed and fabricated for each individual subject (figure 4.2). The cables from the eight transducers for each foot are wired into a plug which connects to an ankle box (section 5.3.1). This assembly of transducers is termed the

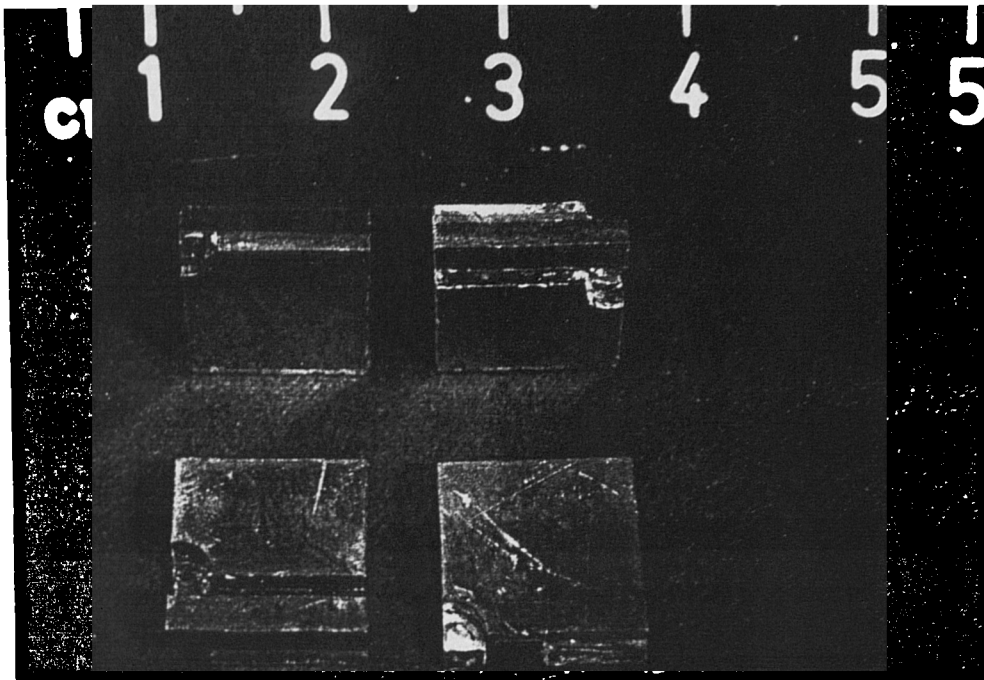


Figure 4.1 Photograph showing various views of a type BHHHDN transducer.

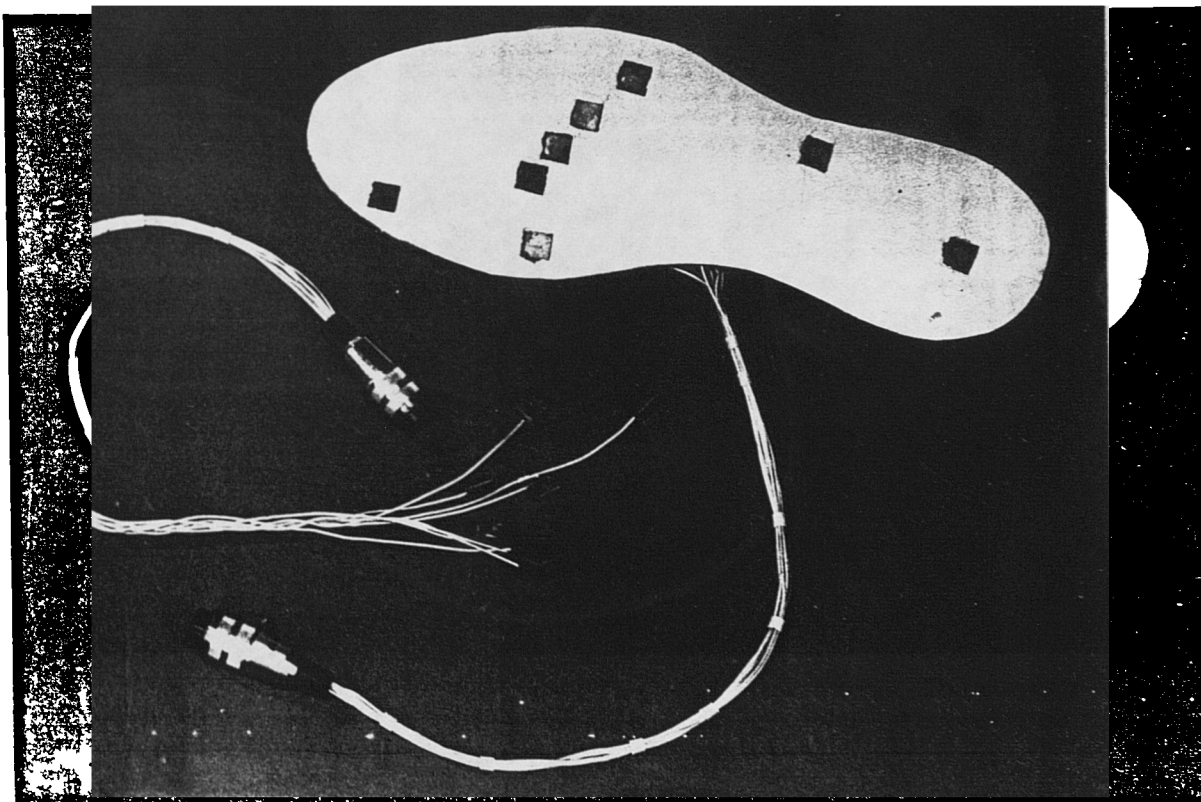


Figure 4.2 Two sets of prototype transducers used for clinical measurements. This shows a loose set referred to as the spider (type BHHHDN) and it illustrates how a set is positioned in an insole (type DSHSDN) ready for measurements.

order, and so away from the insole this spider is free from any structural constraint. Early work also involved a brief look at shear force measurement (section 4.3).

Each prototype transducer has been given a unique code that describes the materials and adhesives used, this code is explained in appendix IV, which also provides a useful summary of all the materials and adhesives used.

## 4.2 The foot transducer interface

Having been placed at the foot-insole interface, the presence of the ideal transducer will not alter the pressure at this interface or modify normal gait. Space limitations at this confined measurement site dictate that the transducer should have minimal thickness. Unfortunately the transducer must not be permitted to bend and so stiffening layers are required to minimise  $d_{31}$  and  $d_{32}$  sensitivities (section 4.4). Also, reliable lead attachment is essential. The constraint for minimal interference to gait requires that the transducer should have a thickness of the order of a few millimetres, as described in section 4.4. These transducers are incorporated in an insole of equal thickness and the use of materials for the fabrication of this insole is described in section 4.2.1. The shoe fit is also important such that the foot does not inadvertently move about. The transducers are located in fixed positions in the insole, and hence the shoe, so excessive foot movement may cause the anatomical sites under investigation to move away from these transducer locations. Conversely, the introduction of the insole should not make the shoe fit too tightly, hence become uncomfortable and affect gait. It has been shown (Maalej *et al*, 1989) that the movement of a metatarsal head with the foot secure in such a shoe is contained to a circular area of diameter 7mm. Simple tests using card insoles and inked feet were performed and it was found that for normal feet the movement tended to be less than that previously stated. A size for the transducer had to be chosen where the main requirement is to ensure that the anatomical sites of interest fall over the transducers, and that with normal movement of the foot metatarsal head pressures were still reliably measured. Square transducers of 10 x 10mm were developed; although the body has no sharp corners, square shapes are easier to fabricate than circular. These transducers are too large for childrens' or small ladies' feet due to cluttering of the metatarsal head region. For shoe sizes less than 3 (UK adult size) transducers of around 7.5 x 7.5mm would be more suitable.

## 2.1 Insole fabrication

The direct use of transducers more than a fraction of a millimetre in thickness would lead to artificially high pressure areas at the transducer sites because of the redistribution of load under the foot around these sites, it is therefore necessary to slot the transducers into strategically placed holes in an insole equal in thickness to that of the transducers. Tests showed that *moulding leather* was the best available material to use for such an insole due to it being relatively incompressible (Abboud, 1989). However during clinical trials this material was found to be too stiff, as well as having an unacceptable variation in thickness and a relatively high cost. The stiffness was found to be a problem for two main reasons: firstly, the transducers tended to catch against the edges of the holes cut from the insole causing undesirable 'blips' in the obtained waveforms; secondly, subjects under examination reported that the *feel* of their shoes with the insole in place was very different compared to that of the shoe alone. It was very important to consider this comfort factor as any discomfort or notable change in *feel* would be very likely to alter the subject's usual gait. Rubberised cork (Footman & Co Ltd) was chosen as a substitute for the leather and no problems were experienced with its use. Of the two types of transducers utilised for clinical measurements (section 4.3.3), 1/8" rubberised cork was used with type DSHSDN transducers (see appendix IV for code translation) and 1/16" rubberised cork laminated to 1.2mm card or regenerated leather board (Footman & Co Ltd) for type BHHHDN transducers. A custom insole must be produced for each subject and upon a change in footwear for the same subject to ensure the transducers are located correctly. After performing many clinical trials an efficient technique for constructing the insoles has been devised which is outlined in section 7.2.

## 2.3 Vertical force transducer construction

Many of the transducer design and construction requirements are determined solely through giving consideration to the harsh in-shoe environment these transducers are to be exposed to. PVdF is an extremely chemically inert material (appendix I) however the copolymer P(VdF-TrFE) is slightly less inert. Obtaining a reliable bond to the film surfaces therefore presents its difficulties. Numerous adhesive methods have been used to bond the film in different transducer configurations ranging from instant cyanoacrylates to double sided tape (section 4.3.1). To adapt a well known phrase: a transducer is only as good as its weakest point, and this usually refers to its electrical lead

connection. A robust *through body connection* design has been implemented and successfully tested in a clinical situation. An effective means of collecting the surface charge, following the film's polarisation, has been obtained using silver loaded epoxy for the first copolymer prototype transducer (section 4.3.3.1). The second copolymer prototype utilises capacitive coupling as a non conducting epoxy is used to bond the layers together (section 4.3.3.2), as does the PVdF prototype after the film surface had been etched (section 4.3.3.4). Electroding and lead attachment is given consideration in section 4.3.2. Early prototype transducers were machined from a large prefabricated laminate, which was extremely time consuming and problems were often experienced with delamination during the machining process. As the transducer design became more refined and foreseeable changes were thought to be only of a minor nature it became evident that a much quicker method of constructing transducer prototypes was required. Pre-machined component parts were used and transducers were glued together individually or as a set in a purpose built fabrication jig, as described in section 4.3.3.3. Late design modifications are given in section 4.3.4; these came to attention while the system was undergoing clinical trials at the two collaborating centres.

### 4.3.1 Bonding piezoelectric films

It is extremely difficult to achieve a good bond to the very inert film surface. Copolymer film is a little less inert than PVdF and is therefore easier to bond to. It should be noted that all the adhesive tests performed were qualitative, that is, no equipment was used to measure bond strength. Evaluations were made using simple tests whereby laminates were subjected to forces similar to those expected inside the shoe. In initial adhesive tests a suitable bond to PVdF was not discovered. During these tests a sample of copolymer film was obtained, which was successfully bonded to other materials using an epoxy adhesive (#ER1436, Design Resins Ltd). Nevertheless, early tests with PVdF led to the successful construction of a prototype measuring 20 x 10mm, as shown in figure 4.3. This transducer was bonded together using a sample of double sided tape, #303, supplied by Advance Tape Ltd. The tape has a high tack which is ideal for use with materials such as PVdF. The drawback with this particular design was that uneven internal stresses were present due to the two small areas of silver loaded epoxy used to make the electrical connections. From a project perspective this prototype aided the evolution of the insole by providing a usable discrete transducer.

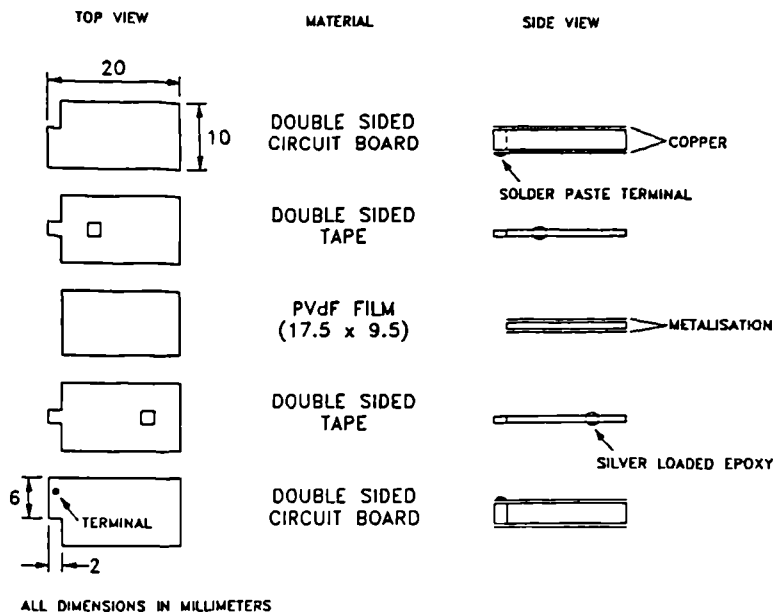


Figure 4.3 Elements of a prototype transducer

Further development concentrated upon the use of uniform adhesive layers, which provide direct or capacitive electrical coupling for the charge produced by the film, as well as mechanical bonding. Silver loaded epoxy (RS Components Ltd) produced a successful bond between copolymer and copper, although this adhesive was difficult to work with due to its high viscosity. After some initial consultation with the technologist of Design Resins Ltd, trials were performed using a careful selection of non-conducting adhesives. Very good adhesion was obtained using their tough epoxy, #ER1436. Copolymer film dissolves (with difficulty) in highly polar solvents such as N.N - Dimethyl Formamide (Vang *et al*, 1988). Solvent welding techniques were investigated following advice from the Thorn EMI central research labs (Nix, personal communication). Laminates of copolymer were successfully fused using a 70% Acetone 30% N.N-Dimethyl Formamide solution, although fusion to metal substrates such as copper was unsuccessful. At this stage in the project 3M released their double sided conducting transfer tape, #9703. It is necessary to use this tape to adhere two metallic layers in order to obtain the desired electrical connection. This is because its construction is that of a criss cross of material cores carrying the acrylic adhesive, in between which are tiny silver balls that provide the conduction. Therefore the ratio of the tape area providing conduction to the total tape area is small and so the collection of charge from an unelectroded film element will be inefficient. The tape is however useful

for prototyping, particularly when speed of construction is a key factor. Loctite have recently introduced a polyolefin primer, #757, for use with their cyanoacrylate adhesives. This is claimed to increase the bonding strength when using *difficult* materials such as PTFE. The #757 primer was used with Loctite #406 adhesive (formulated for plastics and rubbers) but a successful bond was not obtained. While investigating this technique attention was cast to other special pre-bonding preparations for PTFE. A fluorocarbon PTFE etchant, Tetra Etch, is supplied by W.L.Gore Ltd and an amount was obtained for tests. PVdF has a similar chemical structure to that of PTFE and the surface molecules are attacked by the etchant in a similar manner. Trials were successful and considerable bond strengths were obtained using various thicknesses of etched PVdF. It was found necessary to re-heat the film to 50°C and then to submerge it in the etchant for 18 hours; this method differs to that recommended by the manufacturers for etching PTFE. Copolymer film required no heating and only a few seconds of treatment due to its less inert characteristics.

#### Adhesive selection

Epoxy adhesives were used for the two sets of prototype copolymer film transducers that were used extensively for clinical trials: silver loaded epoxy for the first set (section 4.3.3.1); and a tough non conducting epoxy (section 4.3.3.2) for the second set. The latest transducers have been constructed using etched 52µm PVdF film and the same non conducting epoxy adhesive.

### 4.3.2 Electroding and lead attachment

The effective collection of charge developed by a film element using electrodes, and the transfer of this charge to electronic circuitry using electrical leads are two interrelated areas that are considered separately in this section.

#### Electroding

The charge developed upon the surface of the film requires collection if it is to be detected by electronic circuitry. This means that the surface should be metallised and a connection to this metallisation should be made. Alternatively the unmetallised surface of the film, if separated from a metal electrode equal in area by a thin adhesive layer, will be capacitively coupled to this electrode. Stochem Ltd can supply film with a variety of types of metallisation; PVdF is supplied as standard with a 150Å nickel base layer, a 400Å aluminium intermediate layer and a 150Å nickel cover layer. It is

inconvenient to use metallised film for prototyping purposes, however as transducer development progressed this became unnecessary. Electrical coupling must be provided by a uniform adhesive layer if an applied force is to be transmitted to, and a resulting signal received from, a film element. Therefore the requirements for mechanical and electrical coupling should be considered as one of the prime concerns when designing an accurate force transducer using piezoelectric film.

#### Lead attachment

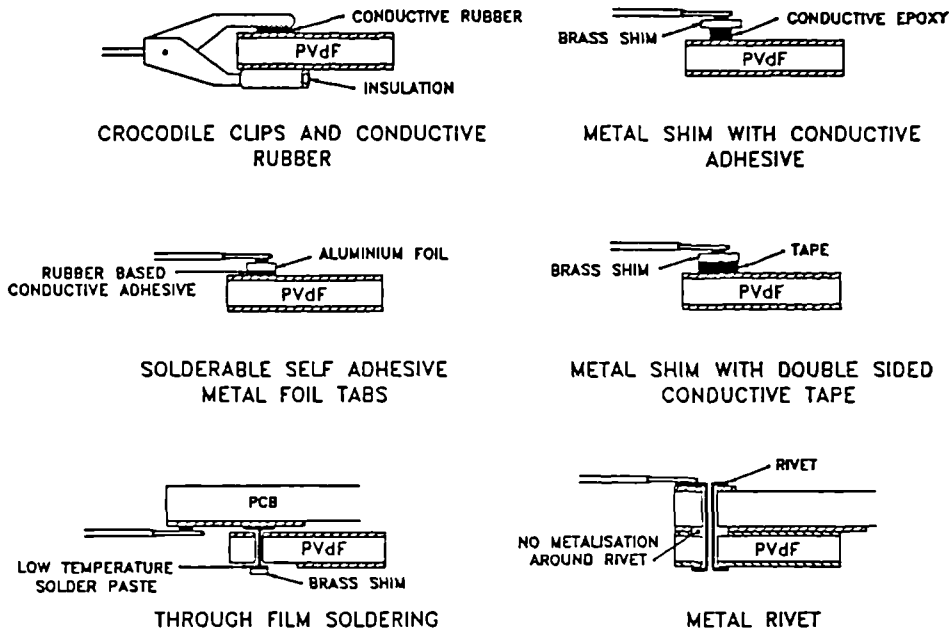


Figure 4.4 Methods of lead attachment

There are many methods that can be utilised to achieve an electrical connection to the film surface. Figure 4.4 shows some of the methods used during transducer development. It is important to consider the effect of such connections upon the force response of a transducer. With this in mind only indirect lead attachment was considered, that is, no direct electrical connection was to be made to the film. Instead connections were made to electrodes which were in turn coupled to the film either directly or capacitively. This helps ensure that any mechanical stress on the leads is not directly coupled to the film. This technique also allows maximum sensitivity to be achieved from the film element in that the lead attachment does not require extra film area; all that is stressed is sensed. Strain relief of the lead terminations is an important consideration, especially when using low temperature solder pastes which have a lower strength than regular solder. This requirement is dealt

with through implementation of the through body connection design whereby the lead is cemented into a 1mm square groove cut into the bottom double sided circuit board transducer component. Here this lead appears from the transducer body then becomes the weakest point.

### 4.3.3 Final transducer fabrication

This section contains details of the construction of the two sets of transducers used for clinical trials and that for the etched PVdF transducer, along with development details of the fabrication jig.

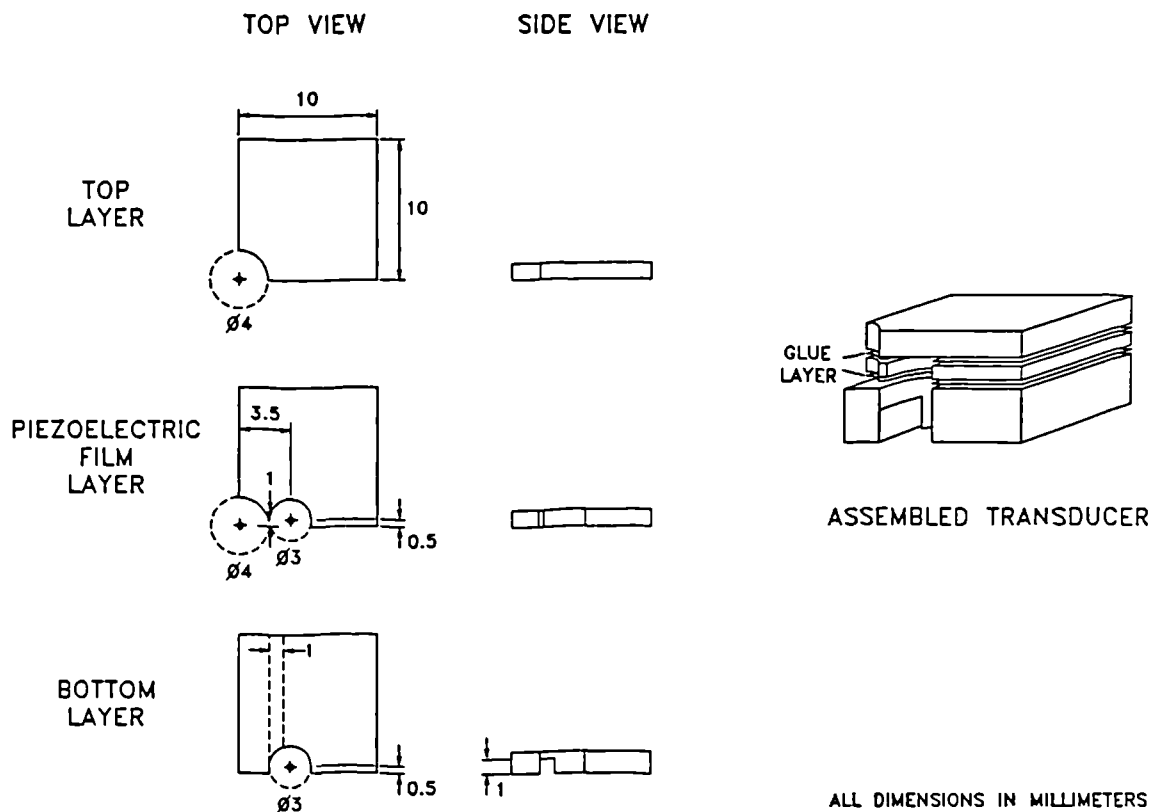


Figure 4.5 The typical transducer

The development and prototyping of transducers is an on-going process and so it was necessary to produce a *working* set of transducers at a convenient break point in this development in order to enable clinical trials of the system as a whole to be carried out. Section 4.3.3.1 outlines the construction of the first of such a set which were used extensively for initial laboratory trials and with a second set (section 4.3.3.2) for clinical trials. The initial technique used for fabricating these transducers was considered to be too time consuming and necessitated a simpler method and hence

a development of a purpose built jig which is described in section 4.3.3.3. The final transducer design is shown in figure 4.5 which provides exploded top and side views of the transducer components and also an isometric view of the complete unit.

### 3.3.1 First copolymer prototype transducer set - DSHSDN

These eight transducers were fabricated from a single laminate measuring 40 x 40 x 3.7mm thick. To form the laminate a 500 $\mu$ m copolymer film layer (H) was bonded between two double sided circuit board layers (D)(1.6mm in thickness) using silver loaded epoxy adhesive (S)(RS Components Ltd). The laminate was cut into nine equal elements after allowing 7 days for the adhesive to fully cure. Each element was then milled to desired dimensions and the appropriate details were machined as shown in figure 4.5. During this machining process the stress experienced by the transducer was occasionally sufficient to cause delamination, so express care was necessary and a good bond was essential. The code given to each of these transducers was DSHSDN. A low temperature solder paste, type #BI52 supplied by Multicore Solders Ltd, having a melting point of 96°C was used to terminate the coax cable appropriately, after the cable ends had been cut and shaped accurately and tinned. It was necessary to use this solder paste because the film loses its piezoelectricity if exposed to temperatures greater than 120°C. The transducer terminals were also tinned before the tinned lead was terminated. Thorough tinning was necessary as minimal soldering time is desirable. Finally the table was slotted into the bottom channel and encapsulated using quick set epoxy adhesive (RS Components Ltd). A multipin connector was used to bring the cables from all eight transducers together and *loops* of heat shrink tubing were spaced along the length of the grouped cables to hold them tidily together. Figure 4.2 shows these transducers embedded in an insole.

### 3.3.2 Second copolymer prototype transducer set - BHHHDN

These eight transducers were fabricated in a similar way to those of the first set in that they were machined from a laminate. The 500 $\mu$ m copolymer film layer (H) was bonded between a brass top layer (B) and a bottom double sided circuit layer (D) using #ER1436 epoxy adhesive (H)(Design Resins Ltd). Hence the code given to each of these transducers was BHHHDN. The top brass layer was 0.7mm (22 gauge), therefore the transducer had an overall thickness of 2.8mm, 0.9mm less than

type DSHSDN. Figure 4.1 shows various views of a constructed transducer. The thermal stability time of the transducer will be lower as the thermal conductivity for the top brass component ( $106 \text{ Wm}^{-1}\text{K}^{-1}$ ) is higher compared to the value for double sided circuit board ( $0.2 \text{ Wm}^{-1}\text{K}^{-1}$ ). The coax lead was connected in a similar way to that of the first set, but it was found that the soldering time required in order to achieve a good bond between the coax screen and the brass terminal was around four times longer because of the larger volume of metal of the top brass component compared to the volume of the copper layer of the double sided circuit board, so acting as a more efficient heat sink. The sensitive +Q electrode was the lower conductive layer (top copper layer of the double sided circuit board) and the ground electrode was the top brass layer, thus keeping the sensitive electrode as enclosed and protected as possible.

### 3.3.3 Fabrication jig

The fabrication jig was developed to allow transducers to be constructed from individual components; up to 16 transducers can be fabricated at any one time. Figure 4.6 shows a third angle orthographic drawing of jig components. Brass top layer transducer pads and double sided circuit board bottom layer pads were accurately ( $10 \times 10\text{mm} \pm 0.01\text{mm}$ ) machined and were used together with the required film and adhesive to form the transducers. Essentially the jig holds these components so that they are aligned correctly and applies an adjustable pressure along the transducer thickness axis while the adhesive cures. An aerosol PTFE dry lubricant (Electrolube Ltd) is sprayed to cover all the internal surfaces of the jig prior to use so that the transducers do not glue to the jig, alternatively other adhesive release agents may be used. Once cured the transducers were removed using an extraction plate (not shown in figure 4.6), which is of the same form as the bottom plate except that the *tenon* part is deeper. This plate is pressed from the underside of the jig after the bottom plate has been removed and this ensures that the transducers remain parallel to the edges of the jig while being pressed out, thus virtually eliminating the possibility of delamination. Acetone and alcohol can be used to clean the jig after use and dichloromethane can be used to remove deposits of epoxy resin.

### 3.3.4 Prototype PVdF transducer - BSHSDN

Transducers have been successfully fabricated using etched  $52\mu\text{m}$  non-electroded PVdF film (S). Pre-

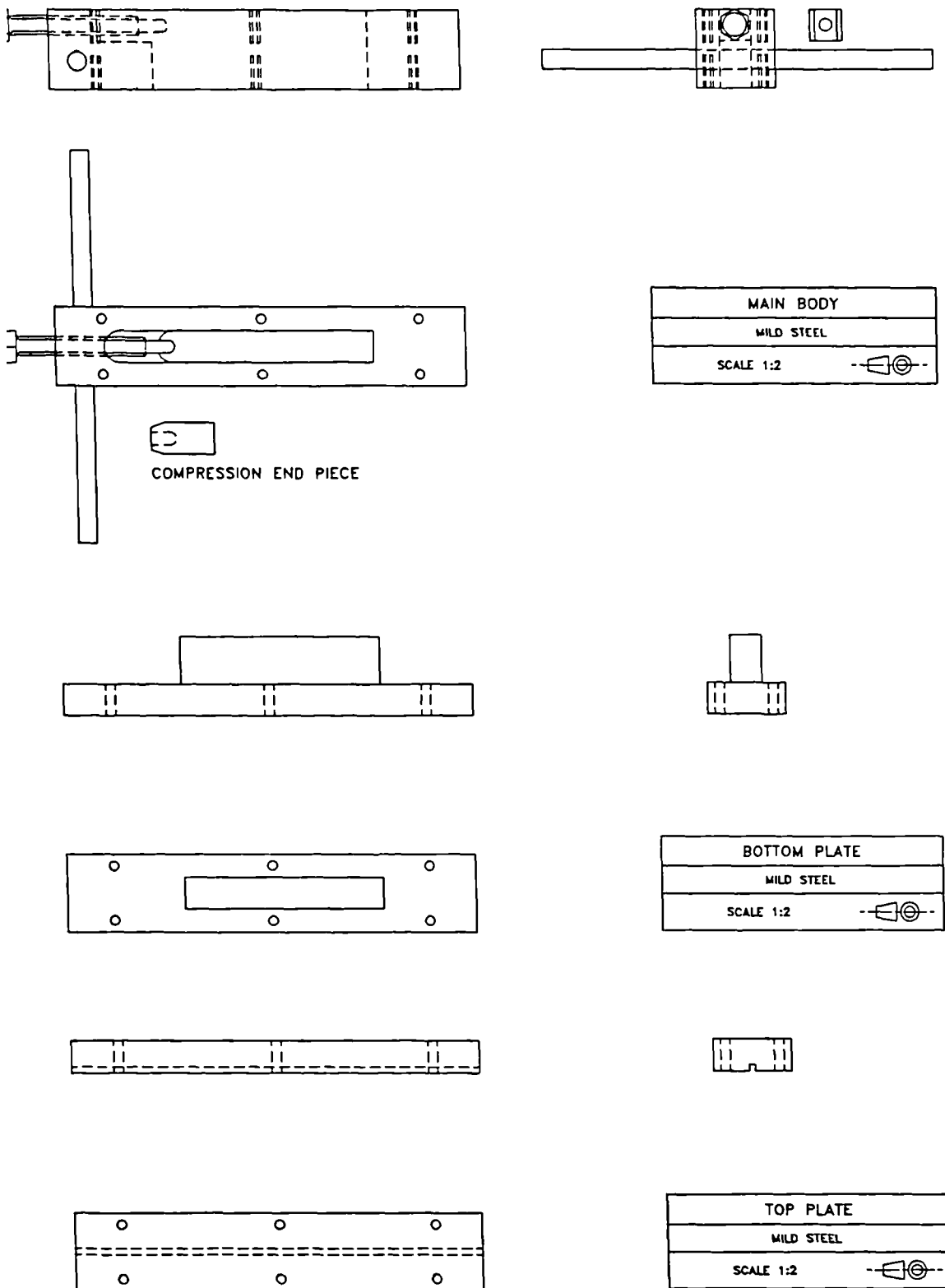


Figure 4.6 Scale orthographic drawing of the individual components of the fabrication jig.

machined brass (B) and double sided circuit board (D) components were used together with the film, which was cut to size (10 x 10mm). The PTFE etchant, Tetra Etch (W.L.Gore Ltd), was used to treat the film prior to fabrication using the jig. In order to minimise the time taken to solder the connecting pad the transducer terminals were tinned before fabrication. As for the second copolymer prototype transducer set, the type of adhesive used was #ER1436 epoxy (Design Resins Ltd).

### 3.4 Latest modifications

After around 400 sets of measurements (each of around 20 foot steps) fatigue of the coax connection pads was noticed for 3 transducers. This occurred at their interface with the transducer body, and the lead had to be repaired. This is the weakest point and transducer failure is expected to be due to this fatigue. The modification suggested is one of user education. Clinical users tend not to be automatically aware of the delicacy of the transducers and it has been frequently observed that transducers have been removed from a no longer required insole by their leads. Thus fatigue is an inevitable outcome, however transducer lifespan will be increased if these points are stressed before any user embarks upon fabricating insoles.

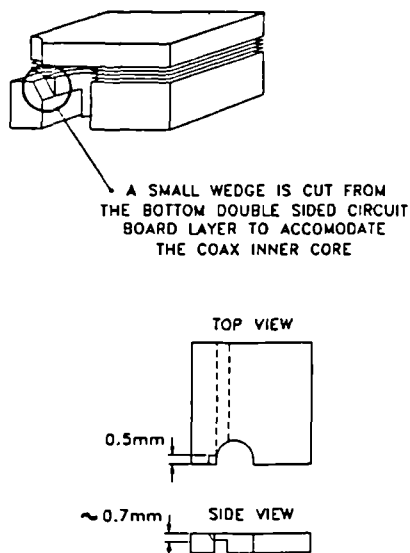


Figure 4.7 Etched PVdF transducer modification

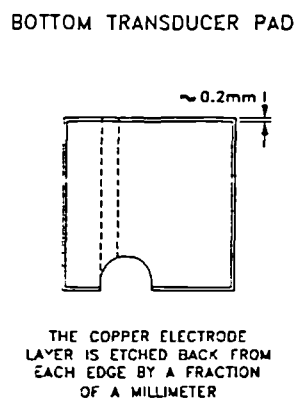


Figure 4.8 Modification to increase transducer insulation

Since the success of fabricating transducers using etched PVdF it was necessary to cut a small wedge from the bottom double sided circuit pad to allow the inner core of the coax lead (diameter

mm) to pass through, as shown in figure 4.7.

#### transducer insulation

charge will leak away from any exposed part of the sensitive electrode of the transducer if the environment is humid, ie sweaty feet. Due to this it has been necessary to insulate the transducer faces and electrode terminal using a polyurethane lacquer. An alternative method of providing this insulation is shown in figure 4.8. The sensitive electrode copper layer is etched back from the edges a fraction of a millimetre and so this gap will be filled with insulating epoxy adhesive during fabrication in the jig.

#### Shear force measurement

Only a single reference has been found relating to the shear force measuring capabilities of a piezoelectric film (Nix and Ward, 1986). In his paper Nix describes how he obtained values for the two piezoelectric shear coefficients,  $d_{15}$  and  $d_{24}$ . No firm specifications were offered by the film

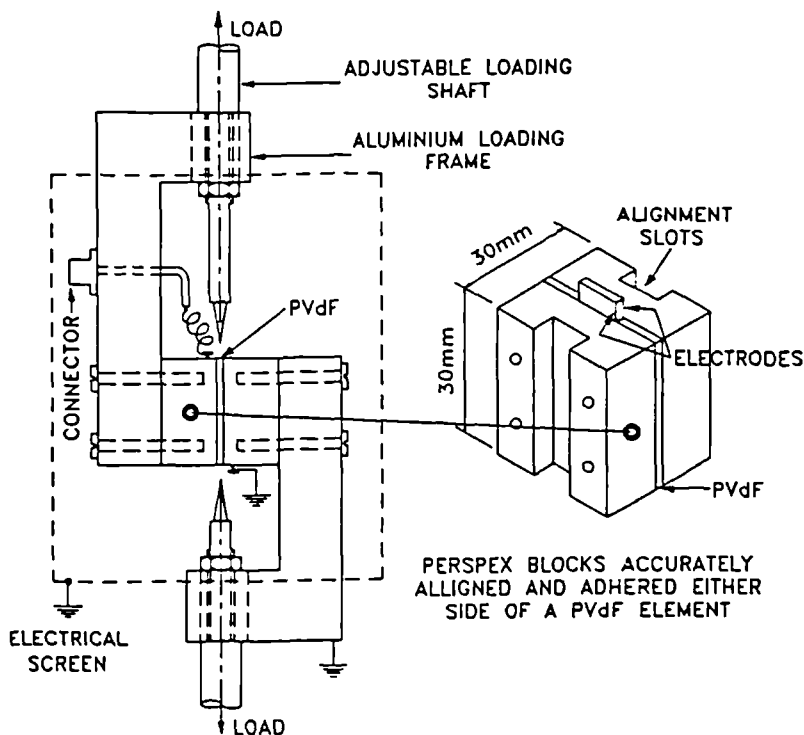


Figure 4.9 Shear test jig, based upon the rig reported by Nix and Ward (1986)

suppliers (Atochem Ltd) for the shear performance of their film. In order to use elements of film to measure solely vertical load, it was necessary to prove that no charge is developed across the film

ces due to shearing forces. This result is expected due to the film symmetries and hence the number of valid piezoelectric coefficients (section 3.3.3). A jig, shown in figure 4.9, similar to the one reported by Nix was constructed to enable 3 x 3cm sheets of film to be deformed in simple shear. The jig was suspended from a bench clamp and loading masses were applied to the bottom half using a hook. A tensile testing machine would provide more accurate loading, however access to such a machine was not possible, nor necessary for the test. Double sided tape was used to adhere the film element to the perspex blocks, and electrical connections to the metallised film surfaces were made using aluminium tape with conductive adhesive (3M electrical tape, #1170). Shear transducers utilising the film in modes other than direct shear as above are possible to fabricate, however they are likely to be bulky due to their relatively complex mechanical construction. Such a prototype has been designed and constructed that has the ability to sense a uniaxial shear force: the film element is stressed due to the force in tension in the 1 direction. This transducer was fabricated purely to test the idea and no extensive tests were performed. A discussion on the further development of a shear force transducer is given in section 8.2.2.

## 5 Conclusions

Transducer development and fabrication has evolved after giving consideration to the harsh environment in which it is required to operate, along with the constraints present due to the type of transducer, piezoelectric film, being used. A system of building a custom insole around a set of pre-fabricated transducers provides the easiest and most accurate way of measuring the loading under defined areas of the plantar surface of the foot. It is important for the transducers to accurately reflect the quantity for which it is being used to detect. Unfortunately the film is sensitive to stretch along both axes perpendicular to its thickness, therefore bending other than along its neutral axis will yield an output of the same order of magnitude as the vertical force experienced. Two stiffening layers are bonded to the film to minimise any errors in the output signal due to this bending. Transducer fabrication is carried out using a jig that has been specially developed to simplify this process. The best transducers have been fabricated using PVdF, pre-treated with a PTFE etchant, and copolymers. The most successful adhesive used to bond the transducer components together has been E1436 epoxy resin, developed by Design Resins Ltd. This adhesive provides an extremely strong

id insulating bond. The charge developed by the film element is effectively coupled by these adhesive layers to the metal electrodes of the other two transducer components and a sub-miniature coax cable is attached to the metal electrodes using a low temperature solder paste. The problem with lead breakages and terminal fatigue has been virtually eliminated by designing cable strain relief into the transducer; the cable is bonded into a small channel cut in the bottom of the transducer. A robust, reliable and accurate force transducer has resulted from the careful design and fabrication techniques detailed in this chapter.

## **Chapter Five**

**5**

# **SYSTEM DEVELOPMENT**

## 2.1 Introduction and design philosophy

In this chapter the system design criteria and its implementation in hardware and software will be outlined. The success of any measurement system relies upon accurate transduction of the measurand such that the signal conditioning system does not introduce unacceptable errors (<10%), and so that measurements can therefore be termed as reliable. This is of prime importance for the assessment of in-shoe foot pressures. Through electronic and software processing it should then be possible to provide information useful to the user. The acceptance of any *high technology* tool into a clinic, or moreover by a medical / clinical user relies upon these requirements being met.

Along with the engineering requirements an important factor in the design of the system is the cost. In order that it is appealing to the small and specialised market a cost of around £4k should be the target, including a personal computer. Therefore a modular approach to the system design is necessary, enabling its use with existing computers if the department cannot go to the expense of a dedicated machine. It is also important that the equipment is safe to use and as far as is practicable meets the safety requirements for medical equipment stipulated by the standard BS5724 Part 1 for class IB equipment.

The raw charge signal from a piezo film transducer (chapter 3) requires processing by electronic circuitry, which usually requires the use of a charge amplifier employing a high precision operational amplifier and components of extreme values (resistance  $>10^9\Omega$ ), in order to achieve an accuracy of a few percent and a low frequency response down to under 1Hz (Kynar technical manual, 1987). In general it is not straightforward to meet these requirements for reasons that will be explained in this chapter, and so a dual stage technique has been designed to reduce these difficulties.

Initial testing and calibration of the transducers while under development was achieved by developing a calibration unit which was designed as a single channel charge amplifier able to deal with a wide range of inputs (2pC to 8nC) and having an overall uncertainty equivalent to 1pC, or 5% of 1N, the smallest input signal. The essential parameters common to both the main patient equipment and the calibration equipment are summarised below:

Operating temperature range	10 - 40°C
Force measurement range	0 - 200N
Average transducer sensitivity	20pC/N
Frequency response	0.01 - 200Hz

A knowledge of these operating parameters is required to enable circuit design and error analysis. This force range was determined after giving consideration to published results of studies carried out by other researchers (sections 2.3.2.3 and 3.4.1). Likewise for the system frequency response; an upper limit of 200Hz was chosen so that the system would have the capability of detecting the higher frequency signals present during running and other high activity (section 2.3.2), however for normal walking the acceptable upper frequency would be 50Hz.

Under test the subject is linked to the main equipment console via a multicore cable, or *umbilical cord*. An *ankle box* is strapped to each leg, each containing eight charge amplification channels; receiving the input from the transducers set in an insole positioned inside the subject's shoes. Linked to a junction *waist box*, the umbilical cord transmits the signals from the first stage electronics contained in the ankle boxes, and also supplies their power. The data from the sixteen transducers is acquired utilising a 12-bit A/D converter card and stored in computer RAM. After acquisition a data file is created and stored on disc. The entire file can be accessed and simple analysis achieved using the postacquisition analysis software developed as part of the research. This permits rapid examination of the waveforms of selected single or multiple footsteps from the test. Figure 5.1 shows a block diagram of the whole system, which consists of four main parts: pressure transducers; electronic instrumentation; data acquisition / software control and finally the postacquisition software analysis.

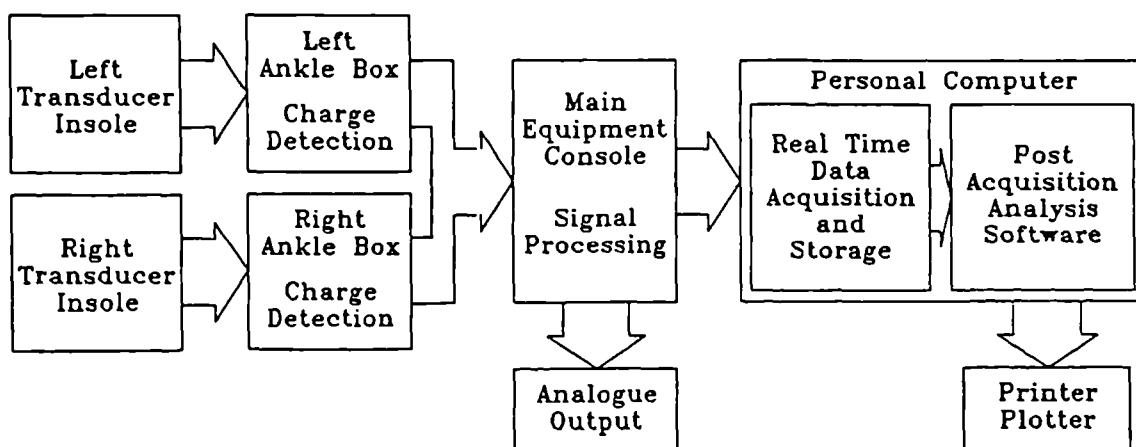


Figure 5.1 System Block Diagram

## 5.2 Electronic System

A piezo film element acts as a capacitor,  $C_T$ , in parallel with a very high resistance,  $R_T$ , and it may be

considered as either charge source,  $Q_T$ , in parallel with  $C_T$  or as a voltage source,  $V_T$ , in series with  $C_T$ , as shown in figure 5.2. For reasons pertaining to the high impedance of the film (resistivity,  $\rho$  for PVdF is of the order of  $1.5 \times 10^{13} \Omega\text{m}$ ) and the requirement for independence to changes in input,  $C_{IN}$ , and cable,  $C_C$ , capacitances, there are advantages in using charge amplification for an initial electronic interfacing stage; this is explained in section 5.2.1.

For a charge amplifier it will be shown that a compromise for the values of the capacitive and resistive feedback components are necessary so that requirements for both the gain and the frequency response can be met. For an initially selected value for the feedback capacitor of 1.5nF, a resistive component in the order of  $10^{10}\Omega$  would be necessary in order to obtain the desired low frequency cut-off point of 0.01Hz. Using such a component will require a relatively large volume of space, and circuit layout and environment would also be critical (section 5.2.1).

For a clinical system it is also necessary to minimise lead length between the transducer and charge amplifier in order to minimise the noise due to cable movement and EMI. Therefore it was decided to design sixteen charge amplification channels into two boxes and to strap one to each leg just above the ankle. In order to minimise interference to the subject's gait these ankle boxes should be as small and as light as possible. With this and circuit design and performance in mind it was decided to use a two stage amplification technique for each channel.

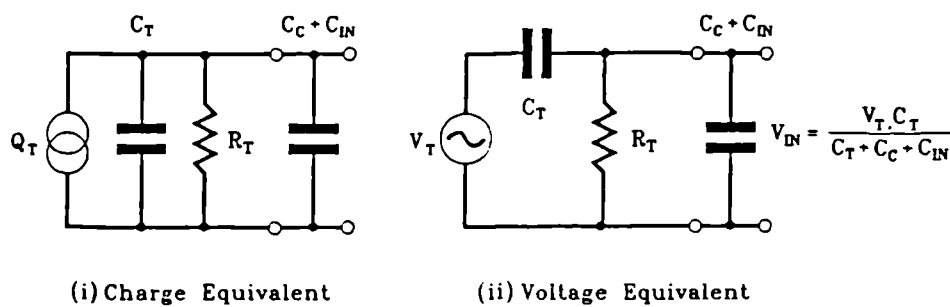
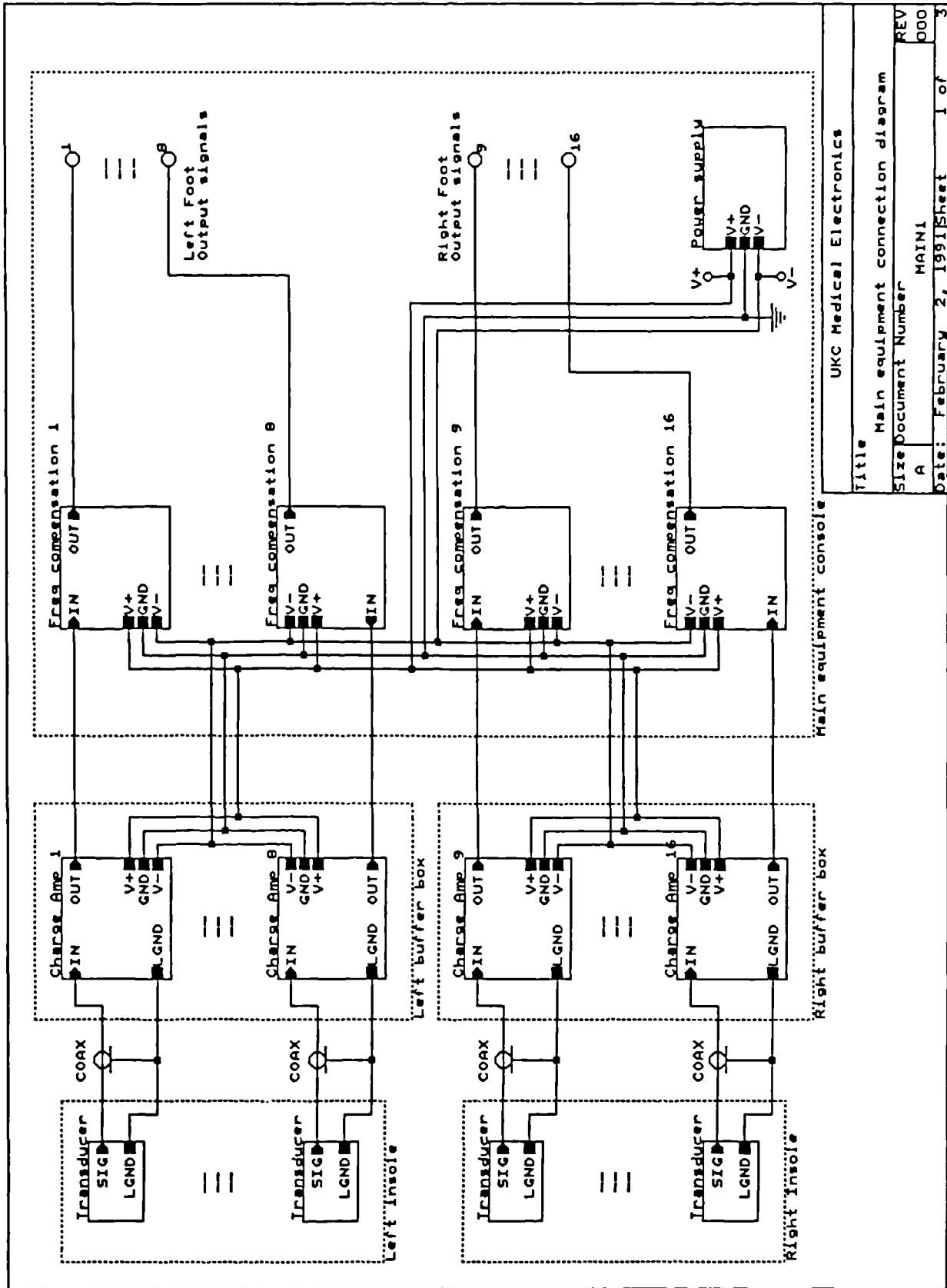


Figure 5.2 Equivalent circuits for piezoelectric film with connection cable

The first stage is a charge amplifier with a low frequency cut off point of around 1Hz and employs components which help meet the size, weight and layout criteria. The second stage performs low frequency compensation to provide a response down to 0.01Hz. The electronics for these sixteen second stage channels is situated in the main equipment console near the personal computer. These



UKC Medical Electronics  
 Title Main equipment connection diagram  
 Size Document Number A MAIN1  
 REV 000  
 Date: February 2, 1991 Sheet 1 of 3

Figure 5.3 Connection diagram for the patient equipment

two stages are described in sections 5.2.2 and 5.2.3 respectively. Figure 5.3 shows the connection diagram for this patient equipment. For transducer testing and initial circuit analysis an accurate self contained single channel unit was built and housed in the main equipment console. Transducer calibration was also performed using this unit (section 5.2.4). Photographs of the equipment are shown in figures 5.19 and 5.20.

### 5.2.1 Amplification techniques for piezoelectric transducers

In chapter 3 the theoretical electrical response of a piezo film element was derived and from equation 3.8 for constant charge (open circuit) conditions the voltage developed across a piezo film element,  $V_3$ , operating in the clamped thickness mode, due to an applied stress,  $\sigma_3$ , can be expressed as:

$$V_3 = g_t \sigma_3 t \quad (5.1)$$

where  $g_t$  is the voltage constant and  $t$  the thickness of the element. Similarly, from equation 3.5 for constant voltage (short circuit) conditions the charge,  $Q_3$ , developed across the same piezo film element can be expressed as:

$$Q_3 = d_t \sigma_3 A_T \quad (5.2)$$

where  $d_t$  is the charge constant and  $A_T$  the area of the element. Two techniques can be used for the detection of these signals: voltage and charge detection (see figure 5.2), and these will be described below.

#### Voltage Detection

For the circuit of figure 5.4 the transfer function can be shown to be:

$$V_{in} = V_T \cdot \frac{Z_{IN}}{Z_{CT} + Z_{IN}} \quad (5.3)$$

where  $Z_{IN}$  is the parallel combination of  $R_T$ ,  $C_C$ ,  $C_{IN}$  and  $R_B$  (op-amp bias resistor). This becomes:

$$V_{in} = V_T \cdot \frac{C_T}{C_T + C_C + C_{IN}} \cdot \left[ \frac{1}{1 + \frac{1}{j\omega R [C_T + C_C + C_{IN}]}} \right] \quad (5.4)$$

where  $R$  is the parallel combination of  $R_T$  and  $R_B$ . Thus for frequencies above the 3dB point, where:

$$f_{3dB} = \frac{1}{2\pi R [C_T + C_C + C_{IN}]} \quad (5.5)$$

the transfer function becomes:

$$V_{in} = V_T \cdot \frac{C_T}{C_T + C_C + C_{IN}} \quad (5.6)$$

and is frequency independent.

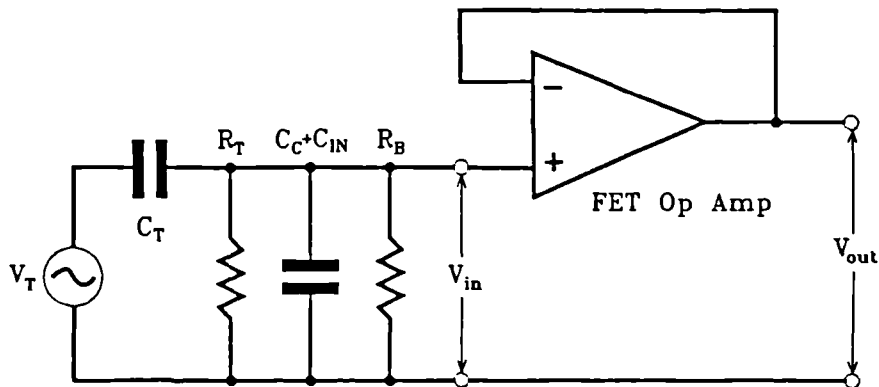


Figure 5.4 Piezo film connected to a voltage follower

However there are several problems faced with using this configuration because of the properties of piezo film and the non-ideal characteristics of the circuit. The main problems are related to the effect of the impedance of the film, connection cable and input capacitance, and the resistance of the

amplifier on the realisable frequency response of the circuit.

Piezoelectric transducers have a relatively high impedance at low frequencies. For bulk material, the resistance of an element,  $R_T$ , is given as:

$$R_T = \frac{\rho t}{A_T} \quad (5.7)$$

where  $\rho$  is the volume resistivity. So for a copolymer film element measuring  $1\text{cm}^2$  by  $500\mu\text{m}$  thick, the resistance is calculated as  $7.5 \times 10^{13}\Omega$ . The capacitance,  $C_T$ , of a piezo film element can be expressed as:

$$C_T = \frac{\epsilon_0 \epsilon_r A_T}{t} \quad (5.8)$$

and for the same copolymer film element this capacitance is calculated as  $15\text{pF}$ . The impedance of a piezo film element is therefore comparable with the input impedance of most FET input op-amps ( $R_{in} \approx 10^{12}\Omega$ ,  $C_{in} \approx 10\text{pF}$ , so  $f_{3dB} \approx 0.015\text{Hz}$ ). However the input impedance will be limited by the op-amp input bias current and a realisable bias resistor ( $R_B$ ), which would typically be of the order of  $10^8$ - $10^9\Omega$ . Hence in order to maximise signal transfer, it can be seen from equation 5.6 that  $C_{in} + C_c$  should be minimised. However if  $R_{in} \leq 10^9\Omega$  and  $C_c \approx 200\text{pF}$  then  $f_{3dB} \approx 0.8\text{Hz}$ . Thus in order to reduce  $f_{3dB}$   $C_{in}$  and  $C_c$  have to be increased, which in turn reduces the signal transfer.

It can therefore be seen that the required frequency response could not be achieved with the available piezo film and op-amp technology, and furthermore there are also other difficulties in using a voltage detection technique, which will now be discussed.

Because of the high impedances involved, the front end will be very susceptible to induced noise such as  $50\text{Hz}$  EMI, and so great care would have to be taken in screening the transducers and connecting cables. Another major problem with detecting the voltage is that any cable and input capacitance will have a detrimental effect upon the detected signal. This is because the charge developed by the transducer is shared across the plates of all input and cable capacitances. Therefore as the voltage seen by the amplifier is inversely proportional to the total capacitance (equation 5.6) then a change in this capacitance will result in a change in the detected voltage. Calibration difficulties would arise

due to this as the input and cable capacitance would have to be known and kept constant. Piezoelectric film has a voltage sensitivity (calculated using the stress constant,  $g_{33} = -339 \times 10^{-3} \text{ VmN}^{-1}$ ) of around an order of magnitude higher than that for other piezoelectric materials, and so for some applications requiring relative (frequencies higher than  $\approx 1\text{Hz}$ ) and indicative measurements, e.g. contact switches, it may be possible to use voltage amplification, so taking advantage of this fact.

### Charge Detection

Charge detection has many advantages over the above voltage technique and is chosen to be the method used. The piezoelectric transducer can be represented as a charge source in parallel with a capacitance, as well as a voltage source in series with a capacitance (see Figure 5.2) and so the signal produced is a function of  $\omega$ , the frequency of the applied force. Amplification with an inherent  $1/\omega$  response is therefore required so that overall independence to frequency is obtained. An ideal charge amplifier achieves this and is characterised below, together with a derived expression for its sensitivity.

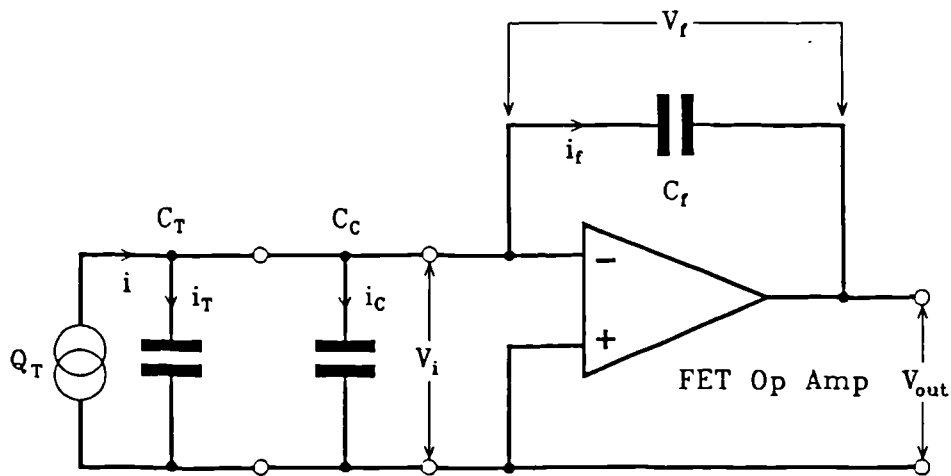


Figure 5.5 Ideal charge amplifier and piezoelectric transducer

In figure 5.5 an FET ( $R_{in} \approx 10^{12} \Omega$ ) operational amplifier is used as a charge amplifier. A piezoelectric film element is connected to its input, so providing a charge signal due to an applied force,  $F$ . For the following derivations it is assumed that the input resistance of the amplifier is infinite and the transducer capacitance  $C_T$ , the connecting cable capacitance  $C_C$ , and the feedback capacitor  $C_f$  are all ideal with loss factors of zero.

From Kirchhoff's laws:

$$i = i_T + i_C + i_f \quad (5.9)$$

and

$$V_f = V_i - V_{out} \quad (5.10)$$

So for a developed charge  $Q_T$ , a current  $i$  is generated. This charge is shared by the three capacitors  $C_T$ ,  $C_C$  and  $C_f$  and currents  $i_T$ ,  $i_C$  and  $i_f$  flow to the transducer, the cable and the feedback capacitances respectively.

If  $A$  is the open loop gain of the amplifier then:

$$V_{out} = -A V_i \quad (5.11)$$

If  $Q_f$  is the charge on the feedback capacitor, then:

$$i_f = \frac{dQ_f}{dt} = C_f \frac{dV_f}{dt} \quad (5.12)$$

Similarly

$$i_T = C_T \frac{dV_i}{dt} \quad (5.13)$$

and

$$i_C = C_C \frac{dV_i}{dt} \quad (5.14)$$

As

$$Q_T = \int i dt \quad (5.15)$$

then after substituting for  $i_T$ ,  $i_C$  and  $i_f$  in equation 5.9 and integrating,  $Q_T$  can be expressed as:

$$Q_T = \int \left( C_T \frac{dV_i}{dt} + C_C \frac{dV_i}{dt} + C_f \frac{dV_f}{dt} \right) dt$$

$$Q_T = C_T V_i + C_C V_i + C_f V_f \quad (5.16)$$

Substituting for  $V_i$  from equation 5.11 and  $V_f$  from equations 5.10 and 5.11 gives:

$$Q_T = -V_{out} \left[ \frac{1}{A} (C_T + C_C) + C_f \left( 1 + \frac{1}{A} \right) \right] \quad (5.17)$$

For an ideal operational amplifier  $A \rightarrow \infty$  so there becomes a simple linear relationship between the charge generated by the transducer and the output voltage which is independent of transducer, cable and input capacitances:

$$V_{out} = -\frac{Q_T}{C_f} \quad (5.18)$$

Alternatively, for an ideal op-amp the signal gain for this configuration can be expressed as a simple ratio of the feedback impedance,  $Z_f$ , to the input impedance,  $Z_{in}$ :

$$\frac{V_{out}}{V_i} = -\frac{1}{j\omega C_f} j\omega (C_T + C_C) = -\frac{(C_T + C_C)}{C_f} \quad (5.19)$$

where  $V_i$  is the voltage produced by the transducer and can be expressed in terms of a developed charge,  $Q_T$ :

$$V_i = \frac{Q_T}{C_T + C_C} \quad (5.20)$$

And so after substituting for  $V_i$  in equation 5.14, the expression for  $V_{out}$  becomes:

$$V_{out} = -\frac{Q_T}{C_f} \quad (5.21)$$

Thus, as with the above derivation, the output voltage is independent of frequency and transducer, cable and input capacitances. By substituting for  $Q_T$  from equation 5.2 an expression can now be obtained for the charge amplifier output voltage in terms of an applied stress:

$$V_{out} = -\frac{d_t \sigma_3 A_T}{C_f} = -\frac{d_t F}{C_f} \quad (5.22)$$

### Practical Considerations

Due to the amplifiers bias current requirements, continuous charging of  $C_f$  would occur causing the output to drift into saturation. A resistance  $R_f$  connected in parallel with  $C_f$  is therefore required in order to provide a d.c. path for the bias current. Unfortunately the presence of the resistor  $R_f$  limits the low frequency 3dB point of the charge amplifier, such that the transfer characteristic,  $A(\omega)$  is frequency dependent and becomes:

$$|A(\omega)| = \frac{\omega R_f C_T}{(1 + \omega^2 R_f^2 C_f^2)^{1/2}} \quad (5.23)$$

with

$$f_{3dB} = \frac{1}{2\pi R_f C_f} \quad (5.24)$$

In order to obtain a low frequency response down to 0.01Hz using the chosen value for  $C_f$  (1.5nF), it can be seen from equation 5.24 that  $R_f$  is required to be not less than  $10^{10}\Omega$ . As has been mentioned in the introduction, such resistances tend to be bulky (around 3-4cm in length) and their use would impose stringent environmental and circuit layout restrictions, and so the construction of

a relatively small eight channel amplification unit would not be possible. Hence a two stage system was preferred for the patient measuring system, enabling the component value requirements for the first, charge amplifier, stage to be relaxed.

If a lower capacitance value was chosen for  $C_p$ , the required value for  $R_f$  would be correspondingly lower, however the charge gain would also increase, limiting the dynamic range of the circuit. So when choosing a value for  $C_p$ , the maximum charge that would be produced by a transducer due to an applied force of 200N (upper limit, see section 3.4.1) was considered. This was calculated to be 6.6nC (taking the transducer charge constant upper limit to be that of  $d_{33}$  for PVdF), and so if  $C_f = 1.5nF$  the corresponding output voltage would be 4.4V. As the circuit power rails are  $\pm 7.5V$ , this allows ample head room for baseline drift.

### 5.2.2 Charge Amplification Stage - First Stage

This section deals with the practical implementation of the charge amplification stages used for the sixteen piezo film transducers. The first and second (see section 5.2.3) stages of electronics are interdependent, especially when considering the ways of minimising the various error signals present, and so some cross referring will be made between this section and section 5.2.3.

Figure 5.6 shows the circuit configuration for this stage and if the transducer is considered as a voltage source,  $V_T$ , in series with a capacitance,  $C_T$  (see section 5.2), then the transfer function,  $A(j\omega)$ , can be expressed as:

$$A(j\omega) = -\frac{Z_f}{Z_{in}} = -\frac{j\omega R_2 C_T}{1 + j\omega(R_2 C_1 + R_1 C_T) - \omega^2 R_2 C_1 R_1 C_T} \quad (5.25)$$

If the magnitude response for this transfer function is plotted against frequency, the plot shown in figure 5.7 is obtained.

The operation of this circuit is as described in section 5.2.1. So from equation 5.21, the passband ( $\omega R_1 C_T > 1$ ,  $\omega R_2 C_1 < 1$ ) charge gain will be:

$$V_{out} = -\frac{Q_T}{C_1} \quad (5.26)$$

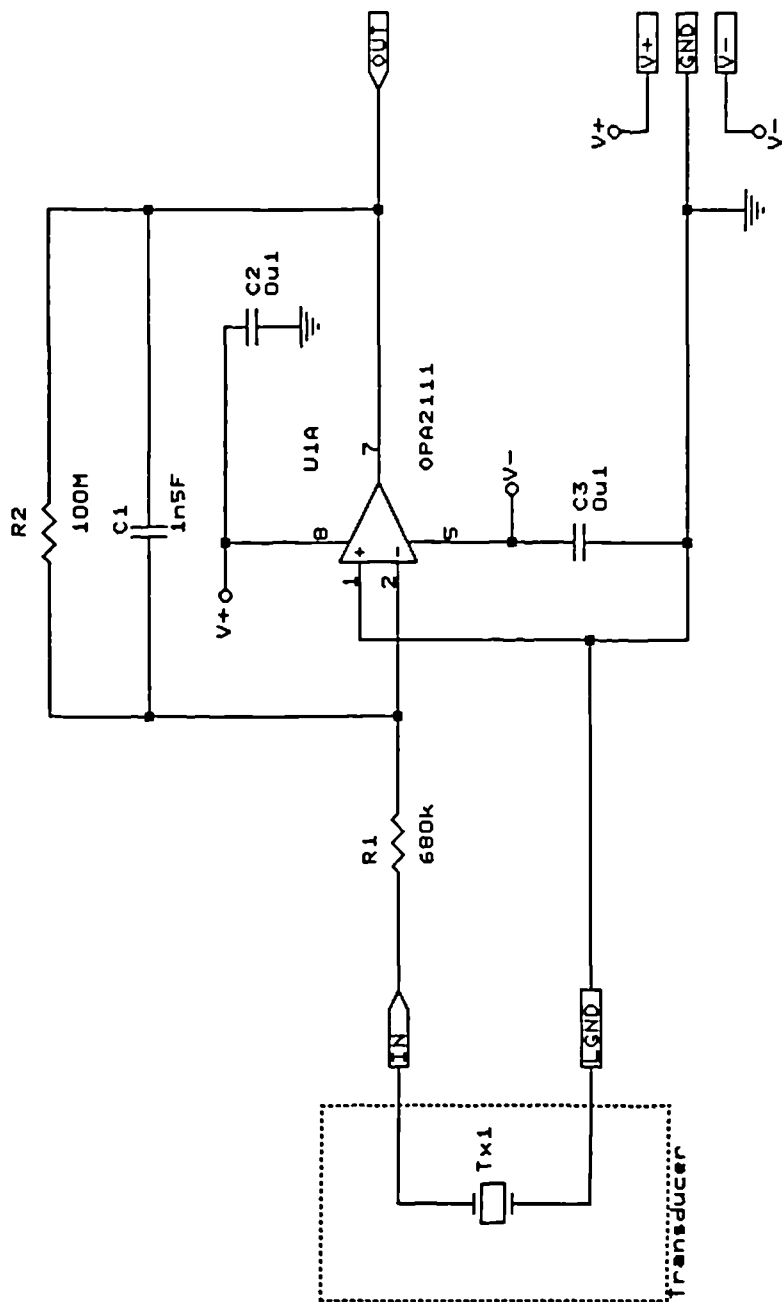


Figure 5.6 Circuit diagram for the first electronic stage - charge amplifier

UKC Medical Electronics	
Title	Charge amplifier - first stage
Size	A
Document Number	MAIN1_2
REV	000
Date:	February 2, 1991
Sheet	2 of 3

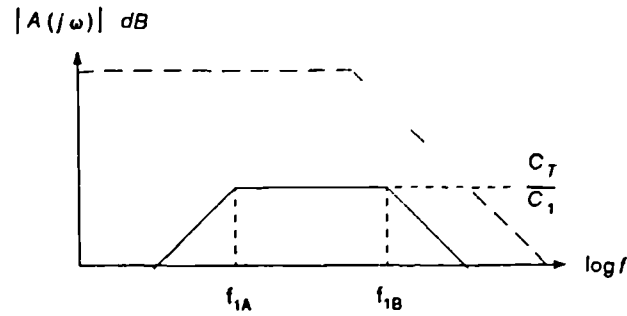


Figure 5.7 First stage frequency response - Bode plot.

The lower 3dB point,  $f_{1A}$ , where:

$$f_{1A} = \frac{1}{2\pi R_2 C_1} \quad (5.27)$$

is controlled by  $R_2$  and  $C_1$  and chosen values for these are 100M $\Omega$  and 1.5nF respectively, so for these component values  $f_{1A}$  is calculated to be 1.06Hz.

Likewise, the higher 3dB point,  $f_{1B}$ , where:

$$f_{1B} = \frac{1}{2\pi R_1 C_T} \quad (5.28)$$

is controlled by  $R_1$  and  $C_T$ , but as the value for  $C_T$  depends upon the transducer used, choosing a value for  $R_1$  in order to determine this higher 3dB point is not straightforward. The higher the transducer capacitance, the lower this cut-off frequency, for a fixed value for  $R_1$ , so as  $f_{1B}$  is required to be 200Hz, it was necessary to predict a maximum value for  $C_T$  to use in the calculation: for a 9 $\mu$ m PVdF transducer 1cm<sup>2</sup> in area,  $C_T \approx 1.2$ nF. So a 680k $\Omega$  resistor was chosen which gives a corresponding value for  $f_{1B}$  of 198Hz. If a 500 $\mu$ m copolymer transducer of the same area is used, the upper response frequency will be  $\approx 15$ kHz.

In addition to those given in section 5.1, the input signal parameters and error tolerances necessary for circuit design can be summarised below:

Input charge signal range	0 to 4nC
Measurement resolution	1N (20pC)
Accuracy	$\pm 10\%$

All sources of error within the circuit should be considered and are listed in the table below.

Input Offset Voltage $V_{io}$	Temperature Drift of $V_{io}$
Input Bias Current $I_b$	Temperature Drift of $I_b$
Input Offset Current $I_{io}$	Temperature Drift of $I_{io}$
Voltage Noise	Current Noise
External Interference Noise	Component tolerance and temperature dependence

Table 5.1 Sources of error within the circuit

Consideration should also be given to the fact that the second stage will have a d.c. gain of 100, although within the passband (0.01 to 200Hz) a signal gain of unity. This means that d.c. offsets due to both stages are amplified a hundred times. However because the voltage signal acquired by the computer can be manipulated with ease some of the requirements for error specification can be relaxed. There is therefore no need to cancel out the d.c. offsets electronically, assuming they are of a reasonable magnitude, i.e not greater than around 250mV (10% F.S.D).

#### Offset voltages and currents

Analysis of these errors is necessary because the presence of a d.c. offset at the output will lower the dynamic range of the circuit, as mentioned above. As explained in section 5.2.1,  $R_2$  is required to provide the bias current,  $I_b^-$  for U1A (figure 5.6). If this resistor is any higher than the chosen value (100M $\Omega$ ) environmental circuit protection and very careful circuit layout would become necessary (so that leakage to adjacent components is minimised and humidity, for example, does not present problems), also the physical size of a higher value resistor is unacceptable. The resistance of the piezo film element,  $R_p$ , is so large ( $\approx 10^{13}$ ) that the bias current  $I_b^-$  is wholly supplied through  $R_2$  and so to maintain a d.c. output offset voltage,  $V_e(I_b^-)$ , of below  $\approx 1$ mV an operational amplifier with an  $I_b$  of the order of picoamps is required. The effect of  $I_b^-$  can be expressed in terms of an equivalent voltage,  $V_{IB}$  connected directly to the input terminal of U1A, as shown in figure 5.8 which also shows the other error voltage sources connected to the non-inverting input.

The equivalent error voltage due to  $I_b^-$  can be expressed as:

$$V_{IB} = -I_b^- R_s \quad (5.29)$$

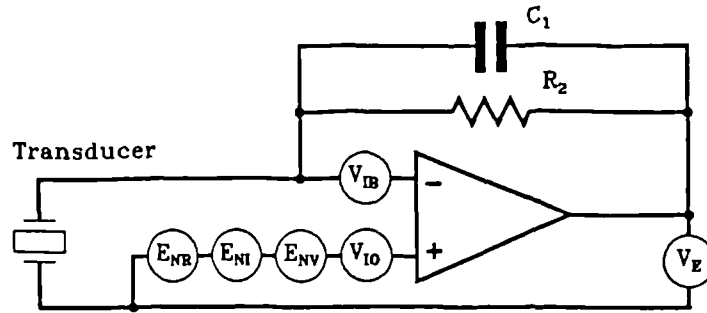


Figure 5.8 Input offset voltage, bias current and noise represented by error generators at the input of an ideal operational amplifier.

where  $R_s$  is the effective source resistance connected at the input terminal (parallel combination of all resistive paths to ground). It is possible to reduce the output offset due to input bias current by connecting a resistance from the non inverting input to ground having a value  $R_2/(R_T+R_1)$ . This allows the input offset current  $I_o$  to be used for calculating the output offset; a smaller error current. For the op-amp selected (Burr Brown OPA2111)  $I_o$  was only a fraction smaller than  $I_b$  and so due to this and component space limitations this additional resistance was not included in the circuit.

The worse case total equivalent input offset voltage,  $V_{os}$ , can be expressed as:

$$V_{os} = |V_{io}| + |V_{ib}| \quad (5.30)$$

Therefore for the OPA2111 at 25°C,  $I_b=3\text{pA}$  and  $V_{io}=0.3\text{mV}$  so  $V_{os}$  becomes:

$$V_{os} = (0.3 + 0.3) = 0.6 \text{ mV} \quad (5.31)$$

Signals applied directly to the amplifier input terminals appear at the output multiplied by the closed loop gain,  $1/\beta$ , which in this case is a value approaching unity. So generally:

$$V_E(V_{os}) = \frac{1}{\beta} V_{os} \quad (5.32)$$

where in this case the output offset error  $V_E(V_{os})$  is equal to the total equivalent input offset voltage,  $V_{os}$ .

Drift due to temperature will have an effect upon this value for  $V_{os}$ . Errors will be lower than above in the temperature range 10 to 25°C, so only the range 25 to 40°C will be considered. In this temperature range the bias current,  $I_b$ , will have a range of 3 to 7.5pA (doubles every 10°C), and the offset voltage will have a range of 0.3mV  $\pm$ 0.2mV ( $dV_{os}/dT = \pm 8\mu V^\circ C^{-1}$ ). Therefore using equation 5.30,  $V_{os}$  will have a worse case value at 40°C of:

$$V_{os} = (0.5 + 0.75) = 1.25 \text{ mV} \quad (5.33)$$

So from equation 5.32, the worse case output offset will also be 1.25mV. As the d.c gain of the second stage is 100 then this output will appear at the output of the second stage as 125mV. Taking the difference of the two offset values for 40 and 20°C (equations 5.33 and 5.31), the average drift of the output offset over the range 25 to 40°C is calculated to be:

$$\frac{\Delta V_E(V_{os})}{\Delta T} = 43 \mu V^\circ C^{-1}$$

This is equivalent to a 4.3mV°C<sup>-1</sup> change at the output of the second stage, which is in turn equivalent to a 6.5pC°C<sup>-1</sup> input charge applied to the first stage (1N=20pC). The other component temperature drift ( $\pm 60$  ppm/°C for  $C_{11}$ ,  $\pm 50$  ppm/°C for the resistors) are negligible in comparison.

#### Noise voltages and currents

The required measurement resolution is 1N, so the combined equivalent peak-to-peak input charge noise is required to be less than 10% that of the smallest input signal (<2pC), in order to fulfil the accuracy requirement.

In order to consider the noise signals within the circuit, the spectral distributions of the input noise sources should be considered. These spectral distributions are multiplied by the frequency dependant noise gain,  $1/\beta$ . For this charge amplifier stage there are four sources of noise to consider: the op-amp generated noise voltage and current sources and the two noise sources due to resistors  $R_1$  and  $R_2$ . The spectral distributions of the equivalent input voltages for these noise sources are shown in figure 5.9, which will now be discussed.

The r.m.s. noise voltage due to Johnson noise for a resistor can be calculated using:

$$E_{NR} r.m.s (f_1 - f_2) = 0.13 \sqrt{R(f_2 - f_1)} \mu V \quad (5.34)$$

where R is in MΩ. So for R<sub>1</sub> this equates to 1.5μV and the noise density is shown by plot (a) in figure 5.9. However for R<sub>2</sub> the voltage noise will be reduced because the noise bandwidth is reduced due to the feedback capacitor, C<sub>1</sub>. The equivalent noise density is shown by plot (b) in figure 5.9 and providing the bandwidth of the op-amp is much greater than for the RC network the r.m.s. noise voltage due to this resistor is independent of resistance and can be calculated using:

$$E_{NR} r.m.s = \sqrt{\frac{kT}{C}} \mu V \quad (5.35)$$

which equates to 1.6μV for R<sub>2</sub>.

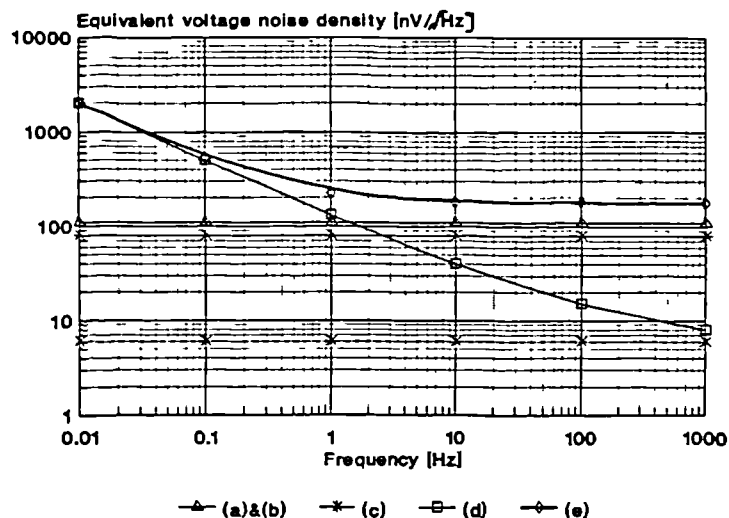


Figure 5.9 Equivalent input and output voltage spectra for the charge amplifier.  
 (a)&(b) Noise due to R<sub>1</sub> and R<sub>2</sub>.  
 (c) Noise due to op-amp input current noise.  
 (d) Op-amp input voltage noise.  
 (e) Output equivalent noise voltage density.

The input current noise is effectively white noise for the desired frequency range, and can be calculated using:

$$I_{NI} r.m.s (f_1 - f_2) = n_w \sqrt{(f_2 - f_1)} \quad A \quad (5.36)$$

where  $n_w$  is the white noise amplitude. This current noise flows through  $R_2$  so the equivalent input noise voltage (plot (c) in figure 5.9) due to the current noise is:

$$E_{NI} r.m.s (0.01 - 200Hz) \approx 1.1 \mu V \quad (5.37)$$

The input voltage noise (plot (d) in figure 5.9) is a combination of white and  $1/f$  noise and the total r.m.s. noise contributed by both components for the frequency range  $f_1$  to  $f_2$  is calculated using:

$$E_{NV} r.m.s. (f_1 - f_2) = n_w \sqrt{\left[ f_0 \log_e \frac{f_2}{f_1} + (f_2 - f_1) \right]} \quad V \quad (5.38)$$

where  $n_w$  is the white noise density and  $f_0$  is the  $1/f$  corner frequency (1kHz for OPA2111) (Clayton, 1985 pp72-93). So using the information supplied in the data sheet for the OPA2111:

$$\therefore E_{NV} r.m.s (0.01 - 200Hz) \approx 0.6 \mu V \quad (5.39)$$

The combined effect of these random noise sources is found by root sum of the squares addition of the r.m.s. values of the separate sources:

$$E_N = \sqrt{(E_{NV}^2 + E_{NI}^2 + E_{NR}^2)} \quad (5.40)$$

Addition of the individual noise densities can provide information upon dominating noise sources, this is indicated by plot (e) of figure 5.9 which is the combined output voltage noise density. It can be seen that the op-amp input voltage noise is the most dominant noise source for frequencies less than 0.1Hz. Equation 5.40 also has the effect of emphasising larger noise quantities and it is often possible to ignore the smaller quantities, however in this case all the noise sources are included in the

calculation, which gives:

$$E_N r.m.s. \approx 2.5 \mu V \quad (5.41)$$

As a general rule of thumb the peak-to-peak noise is calculated by multiplying the r.m.s. value by a factor of 6, so:

$$E_N p-p \approx 15 \mu V \quad (5.42)$$

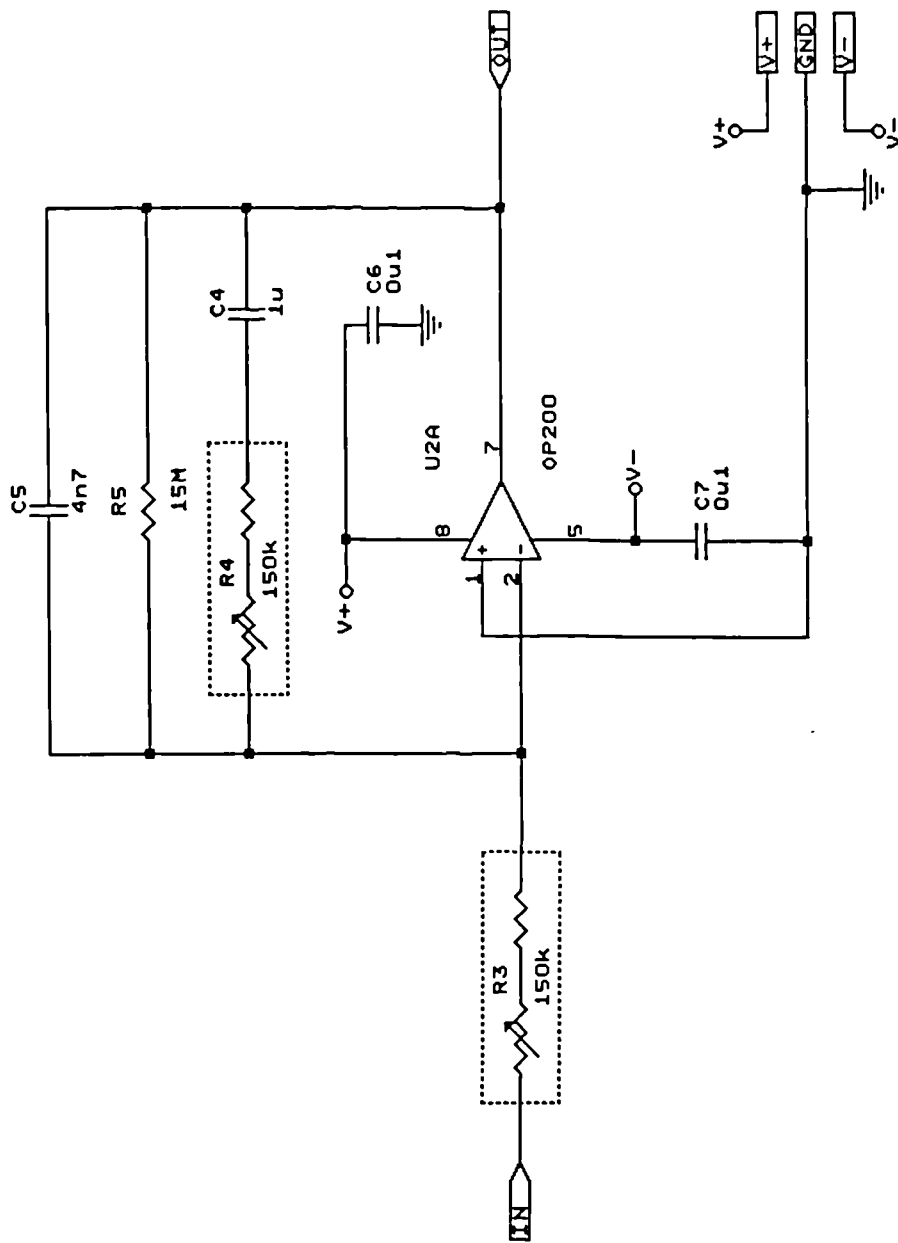
The output noise voltage,  $V_E(E_N)$ , due to the peak-to-peak noise  $E_N$  is therefore equal to  $E_N$ , as the noise gain is unity, and as the response of the noise gain has the same shape as the signal gain (figure 5.8), then the noise bandwidth is similarly limited. This output noise voltage is equivalent to an input charge of 23fC, so it is estimated that the circuit is expected to have an accuracy of better than 0.01% for steady state temperature conditions.

In conclusion to this section, the uncertainty of measurement is attributed to the random component generated noise, and is expected to have a value of around  $15 \mu V$  p-p (equivalent to 0.01% of 1N). The total d.c. offset for this stage was required to be of the order of millivolts so that the resulting output offset after the second stage (d.c. gain = 100) was maintained of the order of hundreds of millivolts. The requirements for these d.c. offsets are not critical, and they do not have to be particularly low (i.e. < 10mV) because any d.c. offset can be removed using software techniques. So they do not present a problem as long as the total d.c. offset plus the expected maximum signal ( $\approx 4.5V$ ) is less than the power rail ( $\pm 7.5V$ ). However, it is desirable to keep offsets as low as possible because of the base line drift caused by changes in transducer temperature (section 3.5.1 and 7.3.6): a greater offset means less signal head room and so possibly quicker op-amp saturation due to the d.c. drift.

### 5.2.3 Frequency compensation stage - second stage

This section deals with the practical implementation of the frequency compensation stages used for the sixteen piezo film transducers. The previous section is closely related and will be referred to.

Figure 5.10 shows the circuit configuration for this stage, and the transfer function,  $A(j\omega)$ , can be



UKC Medical Electronics	
Title	Frequency compensation - second stage
Size	Document Number
A	MAIN1_3
REV	000
Date:	February 2, 1991
Sheet	3 of 3

Figure 5.10 Circuit diagram for the second electronic stage - augmenting integrator

expressed as:

$$A(j\omega) = -\frac{R_5}{R_3} \left[ \frac{1 + j\omega C_4 R_4}{1 + j\omega C_4 R_5 + j\omega C_5 R_5 + j\omega C_4 R_4 (1 + j\omega C_5 R_5)} \right] \quad (5.43)$$

If the magnitude response for this transfer function is plotted against frequency, the plot shown in figure 5.11 is obtained.

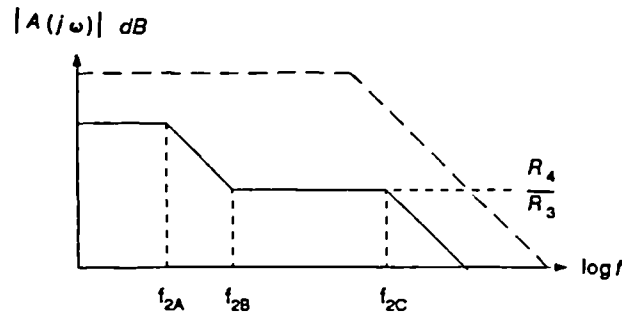


Figure 5.11 Second stage frequency response - Bode plot.

The required transfer function for this electronic stage was determined by studying the effect of  $R_2$  upon the transfer function of the first stage. That is, for signals lower in frequency than  $f_{1A}$  (see figure 5.6) the output of the first stage is proportional to the differential of the input signal. So to compensate for this effect in order to achieve an overall low frequency cut-off of 0.01Hz, the transfer function for the second stage is required to be the inverse of that of the charge amplifier. Practically the circuit is an *augmenting* integrator and will integrate signals between  $f_{2A}$  and  $f_{2B}$ , where:

$$f_{2A} = \frac{1}{2\pi R_5 C_4} \quad , \quad f_{2B} = \frac{1}{2\pi R_4 C_4} \quad (5.44)$$

and have a flat response up to a higher bandwidth limit,  $f_{2C}$ , where:

$$f_{2C} = \frac{1}{2\pi R_3 C_5} \quad (5.45)$$

For the chosen components,  $f_{2A}=0.01\text{Hz}$ ,  $f_{2B}=1.06\text{Hz}$  (which coincides with  $f_{1A}$ , equation 5.27) and  $f_{2C}=225\text{Hz}$ . The sum of the bode plots for both electronic stages gives the overall frequency response for the two electronic stages, as shown in figure 5.12.

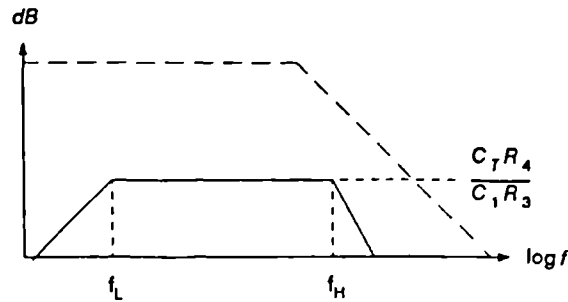


Figure 5.12 Overall frequency response for both stages

Therefore for the combined circuit the lower 3dB point,  $f_L$ , is as for  $f_{2A}$  (determined by  $R_5$  and  $C_4$ ) and the higher 3dB point,  $f_H$ , is as for  $f_{2C}$  (determined by  $R_3$  and  $C_3$ ). In figure 5.12 it is indicated that the higher 3dB points for both stages ( $f_{1B}$  and  $f_{2C}$ ) coincide, and so there will be two poles of filtering. Practically this is unlikely to occur as  $f_{1B}$  is determined by the transducer capacitance and so varies according to the transducer used, as explained in the previous section.

In analysing the sources of error within the circuit (see table 5.1) consideration will also be given to the errors from the first stage electronics in order to estimate the output errors due to the combined circuit. As with the previous section, firstly d.c. offsets will be considered and secondly analysis of frequency dependant noise within the circuit will be discussed.

#### Offset voltages and currents

For the selected op-amp (PMI OP200) at  $25^\circ\text{C}$ ,  $I_b = 0.1\text{nA}$  and  $V_p = 80\mu\text{V}$ . So from equation 5.29 the equivalent error voltage,  $V_B$ , due to  $I_b$  is calculated to be  $15\mu\text{V}$ . Therefore from equation 5.30, the total equivalent input offset voltage,  $V_{OS}$ , becomes:

$$V_{OS} = 95\mu\text{V} \quad (5.46)$$

The closed loop d.c. gain for the circuit has a value of 101, so from equation 5.32 the output offset error,  $V_E(V_{OS})$ , is thus:

$$V_E(V_{OS}) = 9.5mV \quad (5.47)$$

Over the temperature range 25 to 40°C the bias current will have a range of 0.1 to 0.2nA (estimated from data sheet graphs), and the offset voltage will have a range of 80μV ±9μV ( $dV_{OS}/dT = \pm 0.6\mu V^\circ C^{-1}$ ). So using equation 5.30,  $V_{OS}$  will have a worse case value at 40°C of 119μV.

So from equation 5.32, the worse case output offset will be 12mV. It was shown that the output offset from the first stage will appear at the output of this second stage as 125mV (equation 5.33), so the worse case output offset for the combined circuit is therefore 137mV. Hence the second stage contributes only 9% of the total output offset, which indicates the importance of maintaining low offset errors for the first stage in order to reduce the total output offset errors for the combined circuit.

The average output offset drift over the range 25 to 40°C is calculated to be:

$$\frac{\Delta V_E(V_{OS})}{\Delta T} = 167 \mu V \text{ } ^\circ C^{-1}$$

This is equivalent to a 0.3pC/°C<sup>-1</sup> input charge applied to the first stage. The equivalent drift due to the first stage was calculated to be 6.5pC/°C<sup>-1</sup>, and so the drift for this stage is virtually insignificant in comparison (4%). It is assumed that the temperature of the circuitry will remain constant while measurements are being taken, i.e. for a duration of 15 seconds, and so the output offset error due to  $V_{OS}$  will be a d.c. value that can be filtered by the software.

#### **Noise currents and voltages**

For this electronic stage there are five sources of noise to consider: the op-amp generated noise voltage and current sources and the three Johnson noise sources due to  $R_3$ ,  $R_4$  and  $R_5$ , and in addition there is the noise from the first stage which will appear at the output multiplied by the second stage signal gain.

Figure 5.13 shows the equivalent input and output voltage spectral distributions for these noise sources and it can be seen that the output voltage noise due to the second stage, (c), is dominant compared to that due to the first stage, (d). Analysing further, the input current noise for the OP200 is the most dominant noise source for the whole circuit. Plot (e) shows the total output voltage noise

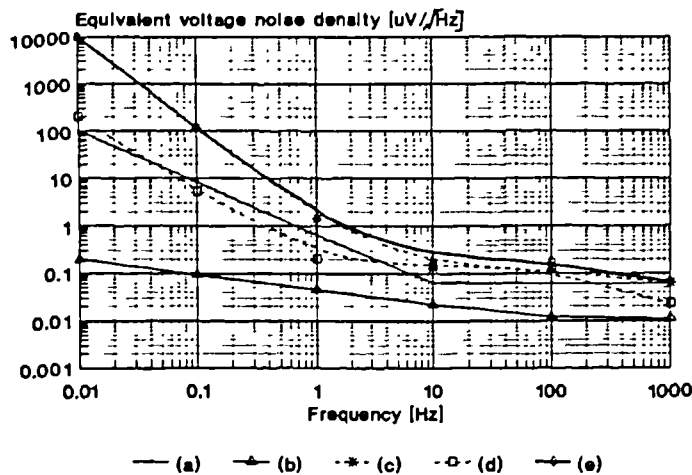


Figure 5.13 Equivalent input and output voltage spectra for the augmenting integrator.  
 (a) Noise due to op-amp input current noise.  
 (b) Op-amp input voltage noise.  
 (c) Output equivalent noise due to second stage.  
 (d) Output equivalent noise due to first stage.  
 (e) Total output voltage noise density.

density and using equations 5.36 and 5.38 the r.m.s. noise voltage in the frequency range 0.01 to 200Hz is estimated to be:

$$V_E(E_N)_{r.m.s} = 0.22 \text{ mV} \quad (5.48)$$

which is equivalent to a peak-to-peak voltage of 1.3mV, or 2pC input charge, or 10% of 1N applied force, therefore satisfying the accuracy requirement as stipulated in the previous section.

In conclusion to this section, the uncertainty of measurement for the combined circuits of stages one and two is estimated to be 2pC (10% of 1N, the smallest input signal), and is due to random component generated noise. The most dominant source of error within the combined circuit is the input current noise for the OP200 of the second stage. The d.c. output offset is expected to be below a few hundred millivolts (137mV maximum) and the second stage only contributes around 10% of this offset. As explained in the previous section, this does not present a problem and any offset can be nulled using software techniques. As it is assumed that the component temperatures will remain constant over the duration of a test, changes in offsets and component values due to ambient temperature change are considered negligible.

### 5.2.4 Transducer calibration

In order to permit the reliable and accurate measurement of the charge developed by the transducers a calibration unit with an accuracy of measurement of <5% was designed and constructed. This description of the calibration system is divided into two parts. The first describes the electronic calibration unit, and the second describes the mechanical jig which enabled known forces to be applied to the transducers.

#### Electronic calibration unit

Figure 5.15 shows the circuit configuration for this unit, which is essentially a charge amplification stage and a frequency compensation stage as described in sections 5.2.2 and 5.2.3, followed by extra inverting and non-inverting amplifiers. This unit was designed and constructed to enable transducer to be tested during their development and so component values were chosen so that a wide input charge range of 2pC to 8nC could be possible. The required input measurement range (see figure 6.15) was selectable through the use of interlocking pushbutton switches mounted on the front panel (SW1 to SW4 in figure 5.15). For the chosen component values the charge amplifier frequency response is shown in figure 5.14, where the gain ranges A to D correspond to switch settings SW1 to SW4 respectively.

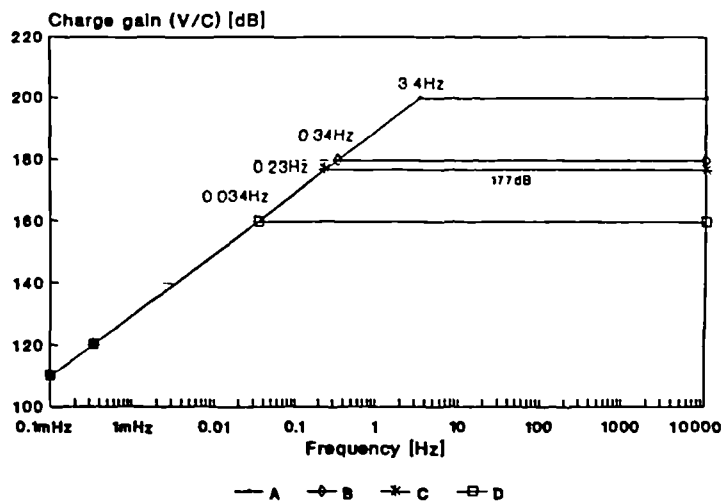
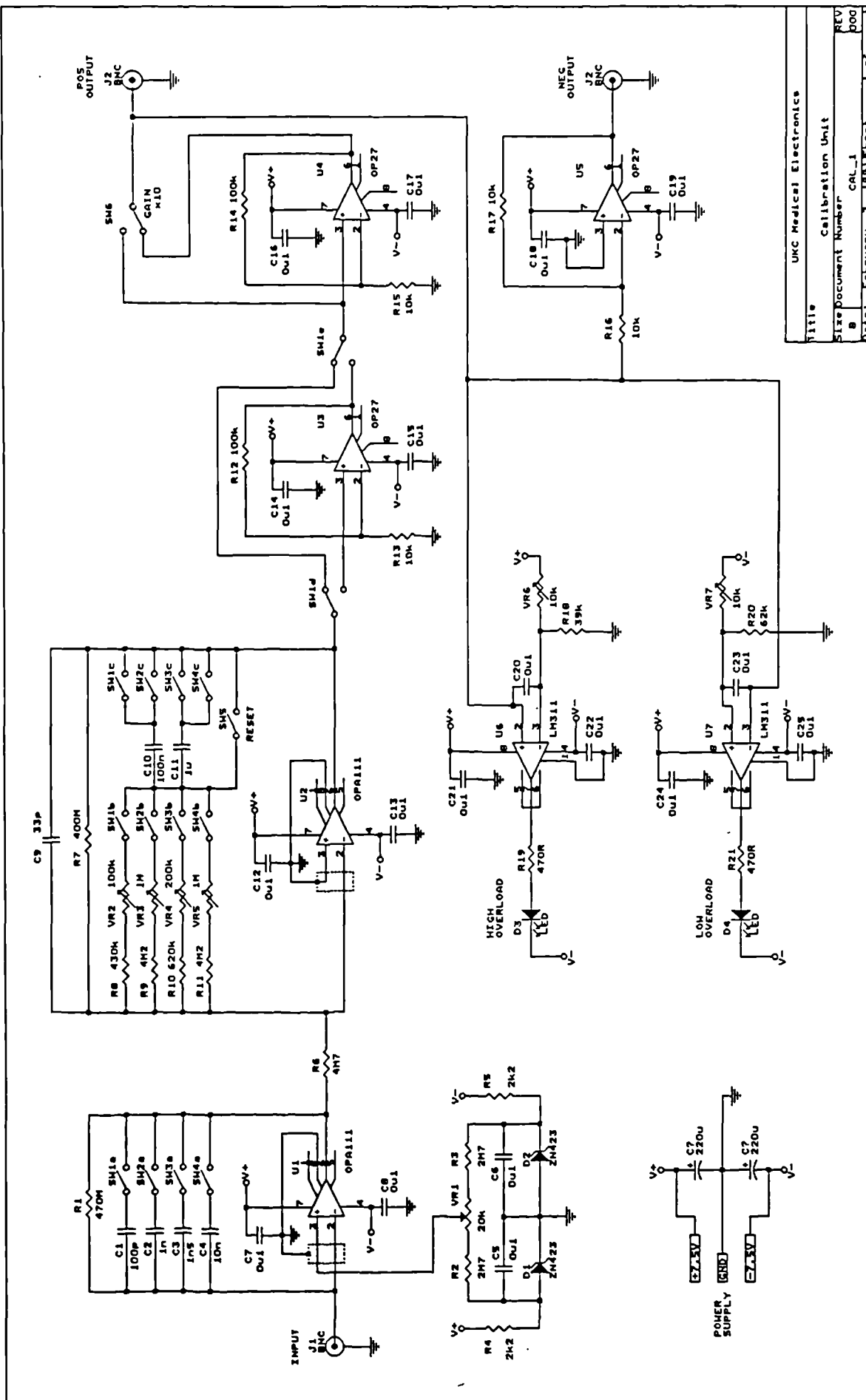


Figure 5.14 Charge amplifier frequency response for the four gain ranges of the calibration unit

Furthermore, figure 5.16 shows the frequency response for the second stage and the combined response is as for figure 5.12 where  $f_l$  is 0.4mHz for the gain settings A and B and 4mHz for the gain settings C and D, and  $f_H$  is 1kHz (determined by  $R_6$  and  $C_6$ ). The worse case input offset voltage



Title	UNC Medical Electronics
Size	Calibration Unit
Document Number	CAL 1
REV	000
Date:	February 2, 1991 Sheet 1 of 3

Figure 5.15 Circuit diagram for the calibration unit

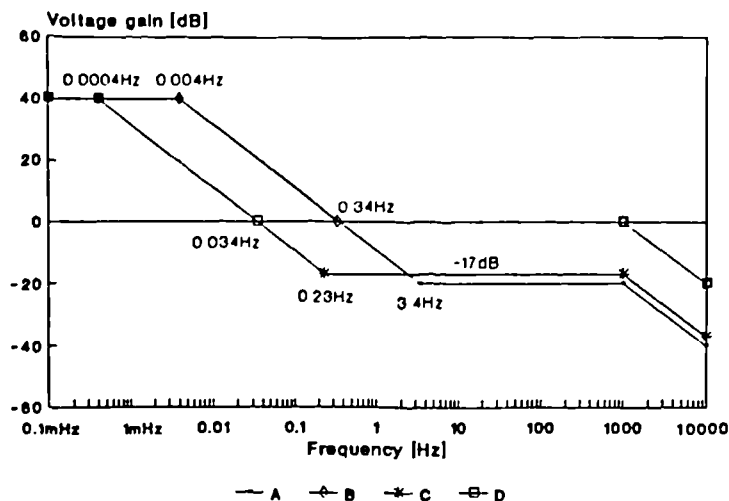


Figure 5.16 Second stage frequency response for the four gain ranges of the calibration unit

for the first stage will be around 1.1mV ( $I_B=2\text{pA}$ ,  $V_{IO}=145\mu\text{V}$  at  $40^\circ\text{C}$ ). The noise gain for this stage is a value approaching unity and so the output offset voltage for this stage will also be 1.1mV. The worse case input offset voltage for the second stage is expected to be around  $154\mu\text{V}$  and so the combined input offset voltage for this stage will be around 1.3mV. The second stage has a d.c. gain of 85 and so the worse case output offset from this stage will be around 110mV. Offset adjustment is carried out by applying an adjustable voltage ( $\pm 5\text{mV}$ ) to the non-inverting input of U1 from a voltage reference source.

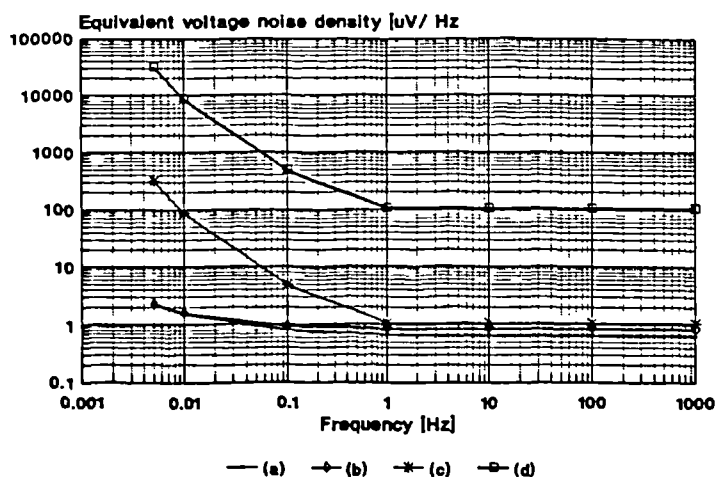


Figure 5.17 Equivalent input and output voltage spectra for the calibration unit

- (a) Output noise from charge amplifier.
- (b) 2nd stage input noise due to 2nd stage.
- (c) Output noise from 2nd stage.
- (d) Maximum output noise for calibration unit.

As with the main patient equipment the accuracy of the circuit is determined by the random component generated noise. Figure 5.17 shows the spectral distributions for the input and output noise voltages at various stages of the circuit.

These spectral densities have been obtained after giving consideration to all the noise sources within the circuit and the appropriate noise gains. Plot (d) is for the worse case situation, that is, with the signal passing through all the amplification stages of the circuit and the r.m.s. noise voltage is estimated to be:

$$V_E(E_N)_{r.m.s} \approx 1.5 \text{ mV} \quad (5.49)$$

which is equivalent to a peak-to-peak voltage of 9mV, or 0.9pC (10V/nC charge gain), or 5% of 1N applied force.

#### Mechanical calibration jig

Conventional calibration (2% uncertainty) weights were used to apply loading to the transducers. The jig basically permitted a vertical shaft to rest upon a transducer which had a top platform upon which weights could be placed, as shown in figure 5.18.

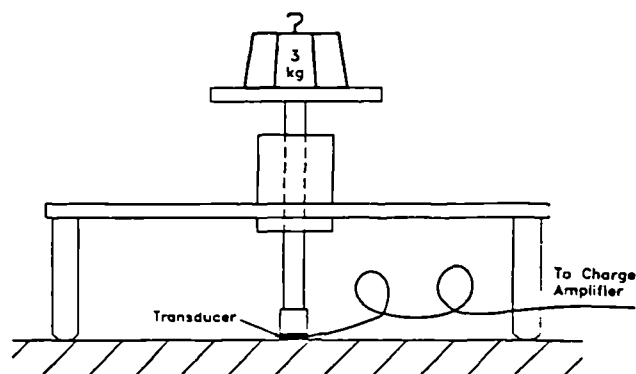


Figure 5.18 The mechanical calibration jig

Removable perspex blocks of varying shapes and sizes (see also section 6.2.6) could be attached to the end of the vertical shaft, known as *styli*. The stylus used throughout most of the calibration measurements was a 1cm cube. The calibration procedure and use of this jig is described in section 6.2.2.

### **5.3 System construction and enclosures**

The hardware enclosures and constructional methods are described in this section; figure 5.19 shows a photograph of the equipment. For reasons explained in section 5.2, ankle boxes (figure 5.20) are attached to the distal leg just above the talocrural joint. These enclosures and the technique for securing them are described in section 5.3.1. Screened multicore leads are used to connect the ankle boxes to a waist box (section 5.3.2), which in turn is connected to the main equipment console (section 5.3.3) via the umbilical cord.

All printed circuit boards were designed with the aid of a drawing package, EasyPC (Number One Systems Ltd), and were subsequently fabricated using the usual PCB prototyping procedures (see appendix III for templates).

#### **5.3.1 Design and construction of the patient ankle boxes**

Figure 5.20 shows a photograph of a patient ankle box which are aluminium two-part enclosures measuring 76x51x25mm, obtained from Maplin professional supplies. Due to space limitations and in order to ease construction all wire connections from the plug and socket were to a mother board which was secured to one side of the box. Two circuit boards, each carrying four charge amplifiers were designed to fit into the remaining space. When plugged into the mother board they stack one on top of the other, separated by insulating foam rubber. There was no further need to secure the boards as they were held firmly in place with the lid screwed down. A miniature 12-way screw lock socket was used to receive the transducer signals, and in order to fit this socket so that minimal space was occupied inside the box, a small collar was used. A 15-way compact 'D' type connector was used to receive the lead from the waist box. Two power rails and an earth were supplied and eight signal lines were used.

While taking measurements in the clinic it is important to ensure that all leads are secure and that the equipment feels comfortable to the patient under examination. For this reason screw down connector hoods were used throughout and special straps were used to fasten the ankle boxes to the legs. These straps were crafted at the orthotics department at Dundee Royal Infirmary and consisted of a flexible plastic plate with a layer of foam rubber for patient comfort and adjustable straps of silicon rubber for fastening. It was found that silicon rubber was the only material that prevented the straps

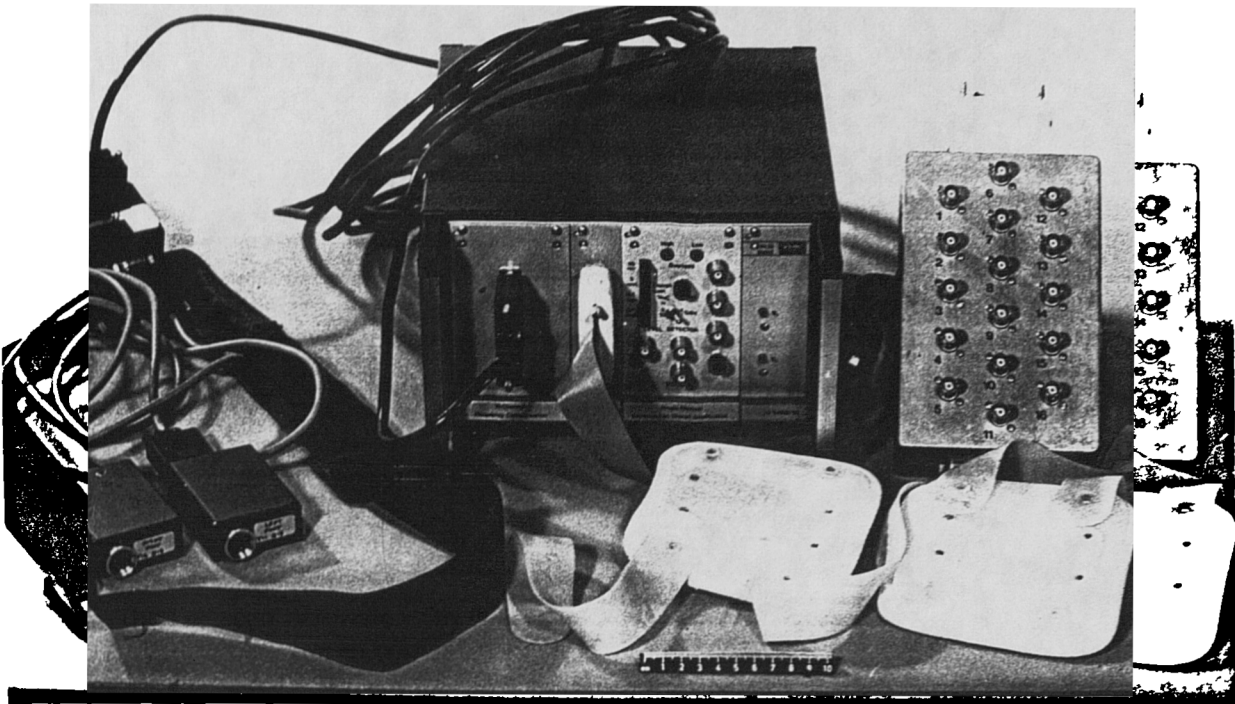


Figure 5.19 The Gaitscan hardware. On the left, in front of and connected to the waist box, are shown two ankle boxes. The waist box is connected to the main equipment console by the umbilical cord. The patch box is shown on the right which receives signals from the main console and relays them to the computer (not shown). Just behind the scale to the right are shown the two ankle straps.

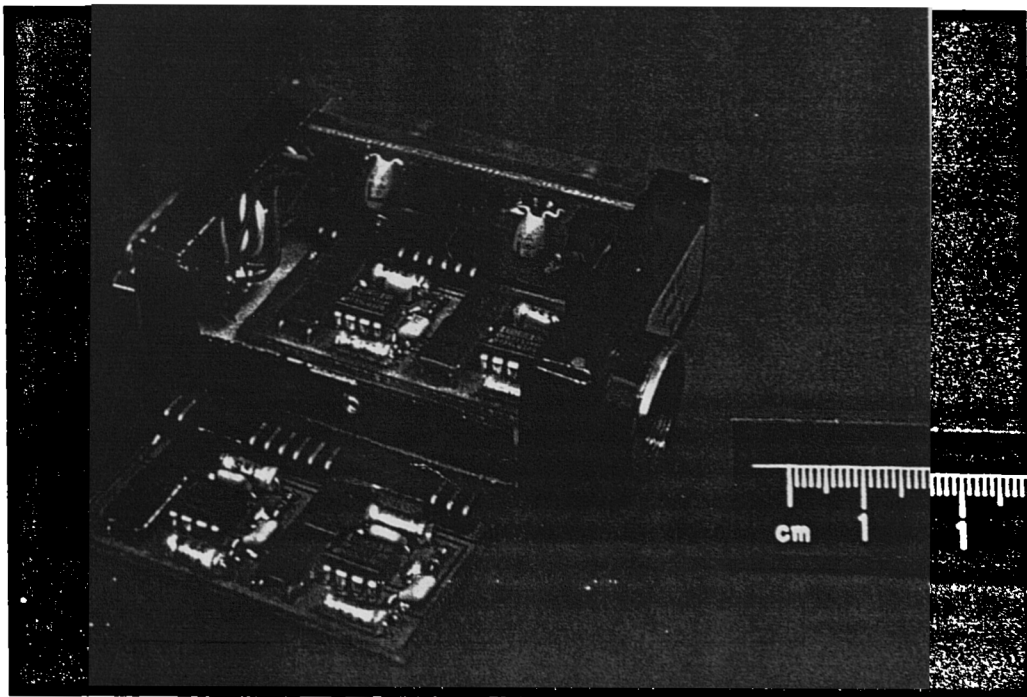


Figure 5.20 A patient ankle box showing the internal construction. Wires are fed to a mother board from connectors on either side of the box. Four charge amplifier channels are contained on each of the plug-in circuit boards which are stacked inside the box.

slipping if the patient wore stockings. A large velcro pad was used to attach the ankle box to the plastic plate once the strap was in position. The total weight of the ankle box is 115g and the strap weighs 60g.

### **5.3.2 Design and construction of the waist box**

A small plastic box measuring 78x61x39mm was used solely for interconnecting the umbilical cord to the two ankle box leads (figure 5.19). This box is secured around the patient's waist using a rucksack style strap. Two 15-way compact 'D' type sockets were used for the ankle box leads and a 37-way compact 'D' type plug was used for the umbilical cord. This arrangement is very comfortable, and if necessary a substantial amount of equipment could be housed in this fashion if required during further system development.

### **5.3.3 Design and construction of the main equipment console**

Because of the nature of a research project, it is wise practice to develop a modular approach to hardware design. This adds flexibility to the system and cuts down the time taken when modifying or updating. With this in mind the main equipment console was chosen to be a KM6 3U multitrack system, obtained from Verospeed (figure 5.19). This allows the development of individual, self contained or interconnected modules as development of the system progresses. Interconnection is straight forward as each module plugs into strip connectors secured to the rear of the console. The electronics for the second stage is contained in one module, with a single 37-way standard 'D' type socket mounted on the front for the umbilical cord. A screw down connector hood can be used to secure the umbilical cord to its module, however following clinical experience it is advisable to permit rapid and easy cable disconnection where mobile patients are concerned, as they may occasionally fail to stop at the end of cable pay-out. Therefore it was found more effective to leave the umbilical cord just pushed in place at the waist box. Twelve meters of 25-way multicore cable was used for the umbilical cord which allowed ample patient mobility for tests. Even though the cable measured 7mm in diameter, its presence did not seem to cause any problems during walking. Two identical circuit boards were used for the second stage module, and wires carrying the processed signals from this module were routed to a 25-way standard 'D' socket mounted on a small front panel. This output

provides the signals for a 16 channel patch box and ultimately for the A/D converter card at the rear of the computer. The patch box is constructed from diecast aluminium and has 16 BNC sockets mounted on its lid. Each channel can thus be monitored as necessary.

The calibration unit circuitry is contained in another module which has BNC connectors for input and output connections. All the hardware is powered by a commercial power supply (Verospeed type PK30/Bivolt) which is housed in the main console. This dual rail adjustable power supply can deliver up to 1A, and the voltage is set to  $\pm 7.5V$ , as some specialised operational amplifiers (particularly CMOS op-amps) have a maximum supply voltage specification of  $\pm 8V$ , and so this setting allows their use without further adjustment of the power rails. Mains power is provided through a euro connector block which is also fused and has an integral medical grade filter.

#### 5.4 Computer Interfacing

The function of a data acquisition system is to convert the raw outputs from one or more transducers into corresponding digital signals that may then be used for further processing by a computer or microcontroller. The signals from the 16 transducers, after being processed by the electronic hardware described in sections 5.2.2 and 5.2.3, are interfaced to a pc-AT using a Metrabyte DAS16 data acquisition and control card (Keithley Instruments Ltd). There are many parameters that require consideration in determining the most appropriate card to use, and in most cases the DAS16 card fulfils these requirements more than adequately. An important parameter concerning the selection of this, rather than an inferior card, was availability. In addition to those given in section 5.1, the main parameters requiring consideration, along with numeric values where relevant, are as follows:

Number of transducers	16
Measurement resolution	1N
Input signal range to card	4.4V
On-board timer	

Additional multiplexing circuitry was not considered, so 16 A/D analog input channels were required, one for each of the 16 transducers. To permit acquisition of all the desired details of the waveforms an adequately high sampling rate is required. According to the Nyquist sampling theory, the sampling rate should be at least twice the highest signal frequency (200Hz) to be digitised. In practice the

sampling rate is often between 3 and 10 times the maximum frequency of interest. It was decided to sample at 1kHz per channel and so an overall acquisition rate of 16kHz was required. The hardware of most cards can enable acquisition rates in excess of this (60kHz maximum throughput rate for the DAS16 card), however the host pc and/or software speeds are usually the limiting factors (section 5.5.1). Clock speed differences between machines are common, so as it was desirable to sample at a known rate without having to adjust for machine speed, an on-board timer was required. The DAS16 card has an Intel 8254 3-channel programmable interval timer. The required amplitude resolution is the last of the main parameters of concern. This is the smallest difference that can be distinguished between two values and is directly related to the required measurement resolution, chosen to be 1N. When specifying the number of bits to represent an amplitude in a practical situation it is necessary to be aware of the linear dynamic range of the system, that is, the maximum output voltage swing. As described in section 5.2.1, this was calculated to be 4.4V (considering a maximum applied force of 200N and taking the transducer charge constant upper limit to be that of  $d_{33}$  for PVdF). The card has a dynamic input range of  $\pm 10V$ . If the dynamic input range of the card had matched the range of the electronic system, the number of quantums or levels required to give 11.3mV resolution (equivalent output voltage for an applied force of 1N - taking the transducer charge constant lower limit to be that of  $d_t$  for copolymer film) would be 390. However, because of the difference in the dynamic ranges of the input signal and card, the number of levels actually required was 1770. It can be seen that if a signal being sampled has a dynamic range less than that of the card then the amplitude resolution will be less, that is, the two should be matched in order for the setup to be most efficient. If gain stages of magnitude 4 were added to the outputs of the electronic system then 9-bit resolution would be sufficient. As it is, 11-bit resolution is sufficient. The DAS16 card has 12-bit resolution which satisfies these conditions.

## 5.5 Software development

It was soon evident that the commercial data acquisition software used for early clinical trials in addition to the Gaitscan hardware (section 7.2) was not sufficient to enable adequate acquisition rates. CODAS (the commercial data acquisition package supplied by Metrabyte) handled a maximum total sampling rate of only 4kHz which was considerably lower than the required rate of 16kHz. The

commercial software also had the disadvantage of having a limited data presentation ability. Display of the data was possible only in a raw format and measurements were difficult to extract from this. Also, it was virtually impossible to obtain feedback from clinical staff because they were unable to interpret the data displayed in this raw form. Therefore custom designed software was necessary and the main requirements for this software are given below.

It was necessary to display the data in a way more akin to foot pressure measurement systems, enable the manipulation of large data files produced from measurements and incorporate hard copy facilities for records. At the time of embarking upon this software development measurements were being carried out upon just one foot. So one of the most important advantages of this development was that upgrading to enable the measurements of both feet, and likewise, general alterations, would be relatively straight forward. A major clinical objective was to examine a series of consecutive foot steps, this is specially important while examining patients having intermittent gait abnormalities. This means that a large amount of data (up to 480kbytes - see section 5.5.1) required storing, and subsequently it was necessary to examine this data as a whole and in parts.

Three programs have been written in Turbo Pascal. The first, referred to as *gsacqu*, controls the data acquisition and storage (section 5.5.1). The second, referred to as *gspost*, enables the data within the file created by *gsacqu* to be observed and to a certain extent analysed (section 5.5.2). Finally the third, referred to as *gsetup*, permits the creation and alteration of a calibration data file which is in turn used by *gsacqu* and *gspost* so that the information presented by these programs is in a calibrated form (section 5.5.3). Flow charts for these programs are given in the relevant sections however specific details about the code is not given. The floppy disc attached to this thesis contains all the pascal, executable and support files which may be referred to. Chapters 8 to 10 of the installation and instruction manual (appendix II) also contain details on these programs and diagrams of the graphics screens.

### **5.5.1 Data acquisition and control - GSACQU**

The program *gsacqu* initialises the DAS16 card, controls data acquisition to RAM and creates data files containing this captured information and finally writes files to disc. This complete measurement process will be referred to as the *test*. Figure 5.21 shows a flow chart of this program.

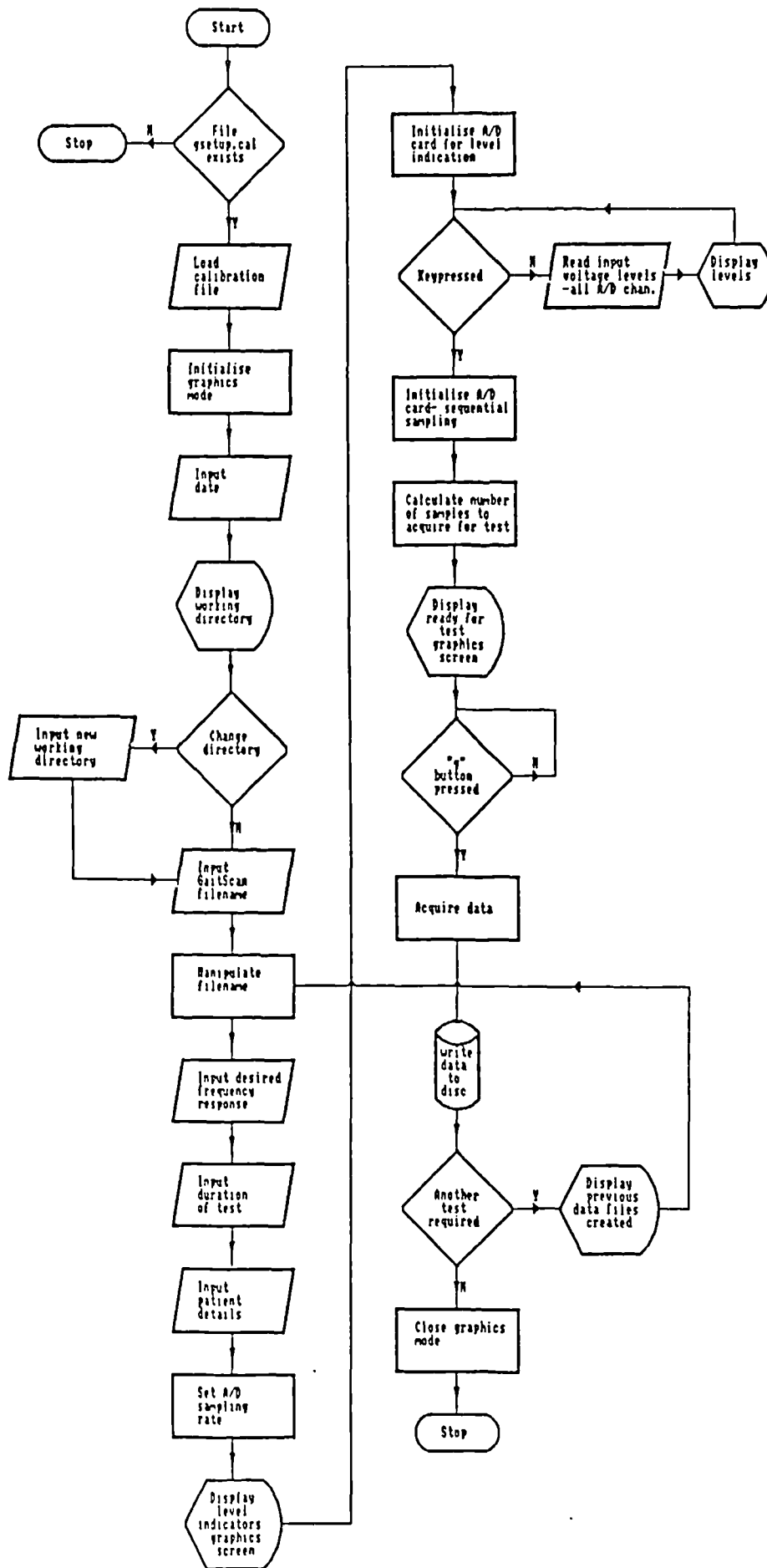


Figure 5.21 Flow chart for the data acquisition and control program GSACQU

In a clinical setting the available length of clear floor space where tests could be performed varies considerably and it is not usual to have more than 10 to 15 meters at disposal. In order to optimise data collection it was therefore necessary to have an adjustable test duration, which would be determined by the user. An upper test duration limit of 15 seconds was chosen, which was ample for all the clinical trials performed. Design of the software was focused around the actual acquisition procedure. Sampling rate limitations were caused by software execution time restrictions and so the code had to be optimised so that machine time spent executing the acquisition procedure (*acquire data* in figure 5.21) was kept to a minimum. This was achieved in a number of ways: firstly, each byte of the acquired data was read from the two appropriate card ports and directly converted into binary which is the simplest data form. This binary information was sequentially written to arrays in the RAM, or *heap*, which had previously been initialised. There could be no time consuming user interaction during acquisition and so the amount of data required, that is the total number of samples, was calculated beforehand through knowing the desired test duration and sampling rate. A simple count was kept during acquisition and when this count was reached acquisition was terminated. Finally the *acquire data* procedure was enclosed by the simplest repetitive control loop, a *for...to...*, loop, which enabled the fastest software execution times thus enabling acquisition at the required rate (section 6.5.3).

It was desirable to set the sampling rate to a known value, so the on-board interval counter was used to control the A/D triggering. Upon execution, sequential sampling takes place and the software services an *EOC* flag (Metrabyte DASH-16/16F technical manual, 1986) produced by the card at the end of every conversion and subsequently reads in data.

Including the encoded channel number, the amount of data that requires storage at the maximum rate of 16kHz is 32kbytes/sec, as the card has 12-bit resolution. The maximum memory requirement for a test of duration 15s is therefore 480kbytes. However IBM RAM is structured into blocks of 64kbytes and so most commercial data acquisition software packages only enable 64kbytes of data to be acquired at speeds in excess of a few thousand samples per second and furthermore multiple channel sampling is not supported. The Turbo Pascal programming package enables this memory limitation problem to be overcome by allowing user management of the heap memory. The memory limitation then becomes the size of the base memory, 640kbytes. The program and the acquired data share

this space and so the amount of memory available for data storage is around 520kbytes, which satisfies the memory requirement for this particular application.

Aside from data acquisition gsacqu performs a number of other tasks. Although not fully developed, patient details such as age and weight are prompted for upon initial execution. This information is added to the data along with a date stamp and other essential parameters of the test to form a data file, which is written to the hard disc once the test had been completed. As the program does not support real time display of the data during a test some means of being able to monitor the output of the transducers just before a test was desirable. A sixteen channel bar-graph type display performs this task and so a pre-test system check is therefore possible without the aid of ancillary equipment. Structurally the code is split into three units: a main controlling program (gsacqu.pas); a collection of global variables (gsacqu\_g.pas) and a unit of procedures and functions (gsacqu\_1.pas).

### **5.5.2 Data display and analysis - GSPOST**

The program gspost reads a data file produced by gsacqu and loads its contents into heap memory. This data is then displayed in various forms on EGA or VGA screens which enables visual inspection of the results and allows peak pressure measurements to be taken from selected footsteps. Figure 5.22 shows a flow chart of the program.

Initially pressure-time waveforms for the entire test are displayed (refer to figure 7.3). Having the whole data file stored in the heap enables quick access to any section of the file. Early versions of gspost read an appropriate section of a data file from the hard disc each time that section required viewing, and this technique was found to be too time consuming. The program uses the mouse for many operations. For example, any section of the file can be zoomed into and selected using the mouse cursor.

In order to reduce the time spent regeneration graphics screens, two EGA graphics pages are utilised. The main screen is the most complex and has the longest regeneration time (the time it takes to draw all the waveforms); this screen is always page #0. Subsequently displayed screens are less complex and are page #1. By flipping between these graphics pages the program can be operated 2 or 3 times faster. While in the main screen simple waveform manipulation is supported, which enables them to be displayed as required, that they can be moved around the screen and magnified. After

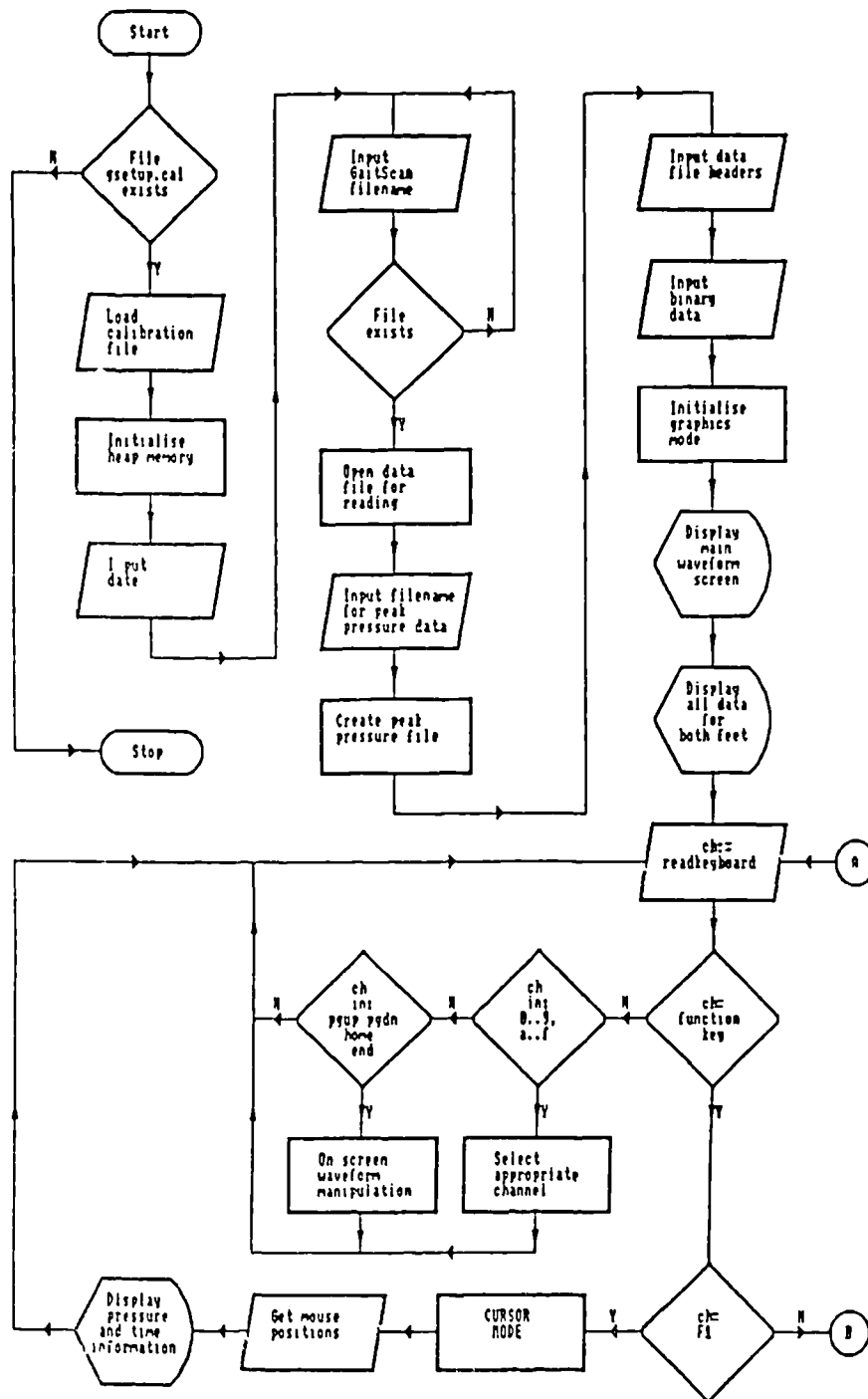


Figure 5.22(a) Flow chart for the data display and analysis program GSPOST (part a)

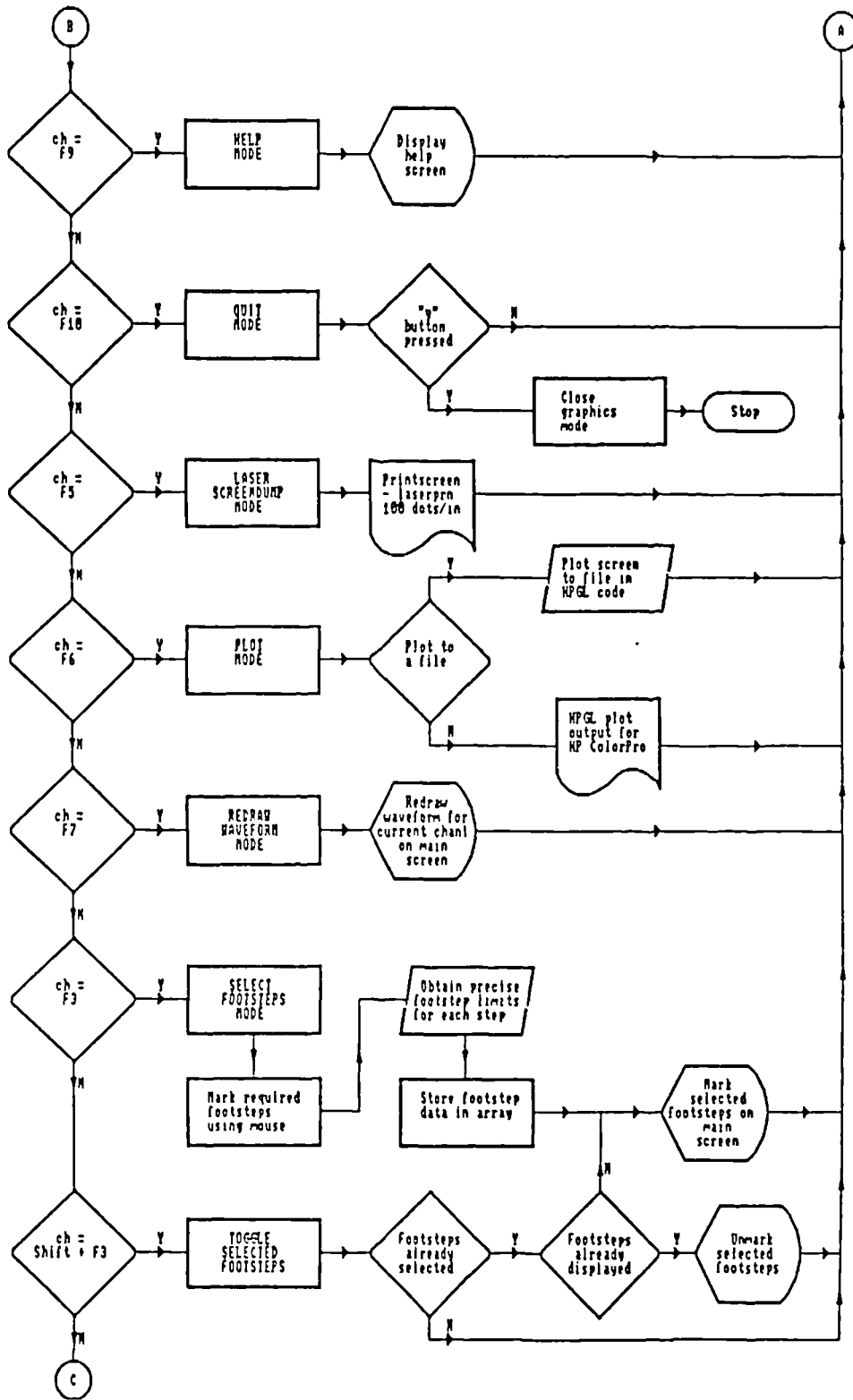


Figure 5.22(b) Flow chart for the data display and analysis program GSPOST (part b)

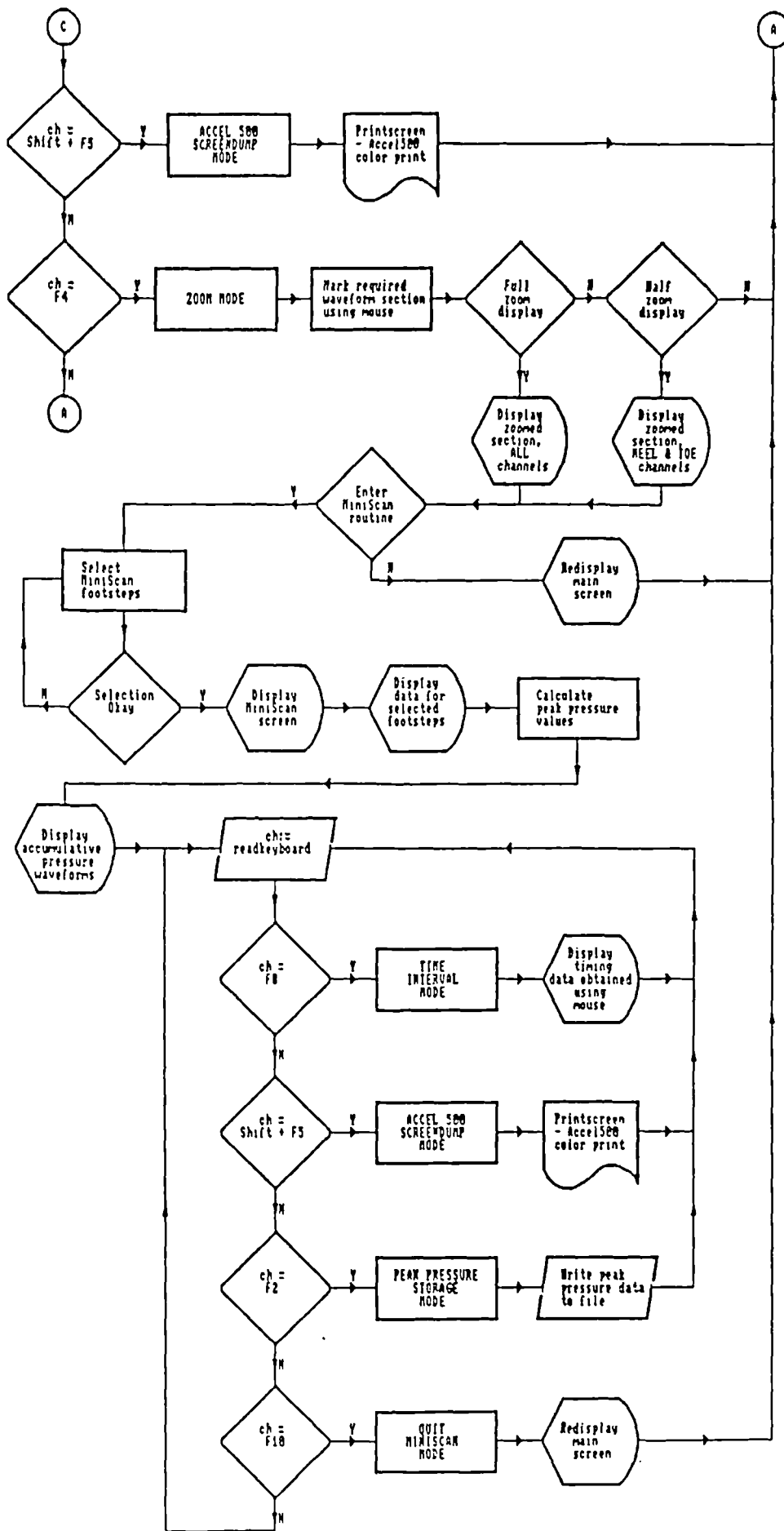


Figure 5.22(c) Flow chart for the data display and analysis program GSPOST (part c)

entering the zoom screen a left and a following right footstep, or vice versa, can be selected and the data from these two steps can then be displayed in a form familiar to a clinical user of foot pressure measurement systems (refer to figure 7.4, section 7.3.1). Close inspection of the pressure-time waveforms for these footsteps is then possible along with the facility to extract peak pressure values. The program also supports a selection of printers and plotters (appendix II), which is an essential requirement for reports, presentation and comparison and of results.

Similarly to gsacqu, the code is structured into four units. Along with the main program (gspost.pas) and the global variable unit (gspost\_g.pas) there are two units containing procedures and functions (gspost\_1.pas and gspost\_2.pas).

### 5.5.3 Software calibration - GSETUP

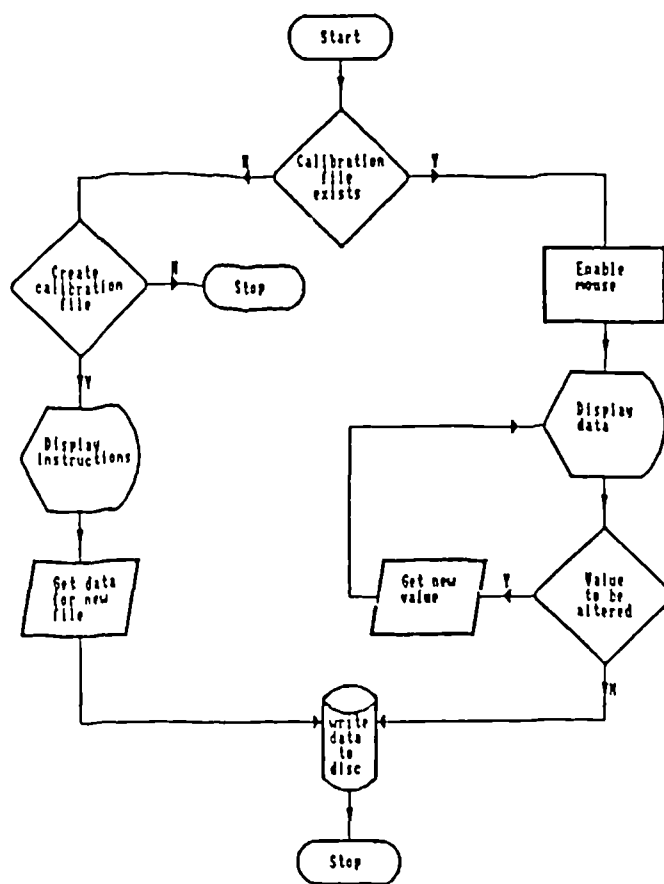


Figure 5.23 Flow chart for the calibration program GSETUP

The program gsetup creates a calibration data file called gsetup.cal if one does not exist in the

working directory, otherwise it permits the alteration of the appropriate calibration data file. Figure 5.23 shows a flow chart of the program.

Basically this calibration file contains the transducer sensitivities and the instrumentation gain in an ASCII format. Both gsacqu and gspost use the information contained in this file to provide calibrated data. It was anticipated that different transducers would be used periodically and so having the main programs read the appropriate data file avoids the problem of having to change calibration constants held within the body of these main programs. Having read the information contained in the file the postacquisition program, gspost, adds a correction factor of 0.45pC/N to all sensitivity values to take into account the variation in transducer sensitivity due to ambient temperature change (section 6.2.5). Gsetup is mouse driven and, having sensed the presence of an existing data file, simply presents the information in one text screen (appendix II) and allows changes to be made quickly and easily. Upon leaving the program the data file is saved to the hard disc.

The program is relatively small (14kbytes) and so all the code is contained in one main file (gsetup.pas).

## 5.6 Conclusions

Charge amplification has been selected as the technique to be used for the electronic system. This decision was made after giving consideration to voltage amplification which was discovered to have several disadvantages in comparison to the preferable charge amplification technique. The main patient equipment was designed as a 16 channel system to process the signals from two sets of eight transducers and supply output voltage signals to a p.c. data acquisition card. In the early stages of project development a calibration unit was constructed which is a single channel unit designed to test and calibrate transducers. A similar dual stage technique was used for the electronic circuitry for both the main equipment and the calibration unit which enabled the relaxation of some design requirements concerning component choice. The two electronic stages are a charge amplifier followed by an augmenting integrator which together simulate a charge amplifier with a frequency response of 0.01 to 200Hz. The elimination of d.c. offsets is carried out using software techniques during analysis of the data and so providing the output offsets were kept below a few hundred millivolts they did not present a problem. The only circuit error requiring careful consideration was random component

generated noise which also determined the accuracy of measurements. It was estimated that accuracies of 2pC and 0.9pC were expected from the main equipment and calibration unit respectively. The smallest input signal to be measured is 1N which is equivalent to 20pC for a typical transducer sensitivity of 20pC/N, and the uncertainty of measurements at this signal level are 10% and 5% for the two units respectively. Typical signal levels are of the order of 30N, giving a corresponding uncertainty of 0.003% and 0.0015% respectively. The requirements for the data acquisition card have been specified after giving consideration to all the relevant parameters and in conclusion the Metrabyte DAS16 card fulfils these requirements. Control of this card is carried out using custom software which has become an essential component of the system, Gaitscan. Three programs have been written which allow the acquisition, display and analysis, and calibration of the data from the transducers. Through the development of this software it was then possible to greatly enhance clinical development of the system because of the highly applied and specialised nature of the system as a whole with this software.

## **Chapter Six**

**6**

# **SYSTEM PERFORMANCE**

## **6.1 Introduction**

In this chapter transducer and hardware system performance is discussed. Results from transducer bench trials are discussed in section 6.2, where calibration measurements are primarily discussed. The performance of the calibration unit and of the main electronic system modules are discussed in sections 6.3 and 6.4 respectively. Measurements carried out in order to determine the maximum data acquisition sampling rate for the particular computer setup used for clinical trials are also discussed in section 6.4.

## **6.2 The transducer**

This section contains details of the performance measurements carried out upon various transducers developed throughout the research. The electronic system has been designed to have a flat response over the required frequency range for gait measurements (chapter 5), which matches the flat response for piezo film. Section 6.2.1 describes the procedure used to verify this flat response for the piezo film transducers. Transducer calibration procedure and results are given in section 6.2.2, together with a comparison of the measured sensitivities with those expected from theoretical calculations, and also the relative performance of the transducers constructed using conducting adhesive and those constructed using non-conducting adhesive. The long and short term repeatability is reported in section 6.2.3, along with a discussion on the accuracy of the calibration technique. During calibration the linearity was checked for each transducer; this and hysteresis is discussed in section 6.2.4. The final three sections are on artifact related transducer performance: the temperature coefficient of the sensitivity has been measured (section 6.2.5), bending artifact is discussed together with estimated errors due to cable flexure (section 6.2.6) and the effect of humidity has also been measured (section 6.2.7).

### **6.2.1 Frequency response**

Free piezo film has a very wide and flat bandwidth of near d.c. to GHz (Kynar technical manual, 1987). In order to check that the transducer response was flat, a mechanical vibration was applied to a transducer using an electromagnetic shaker (supplied with a voltage noise source) fitted with an impedance head, as shown in figure 6.1 (Donarski, 1990). The equipment for these measurements

was set up as shown in figure 6.1.

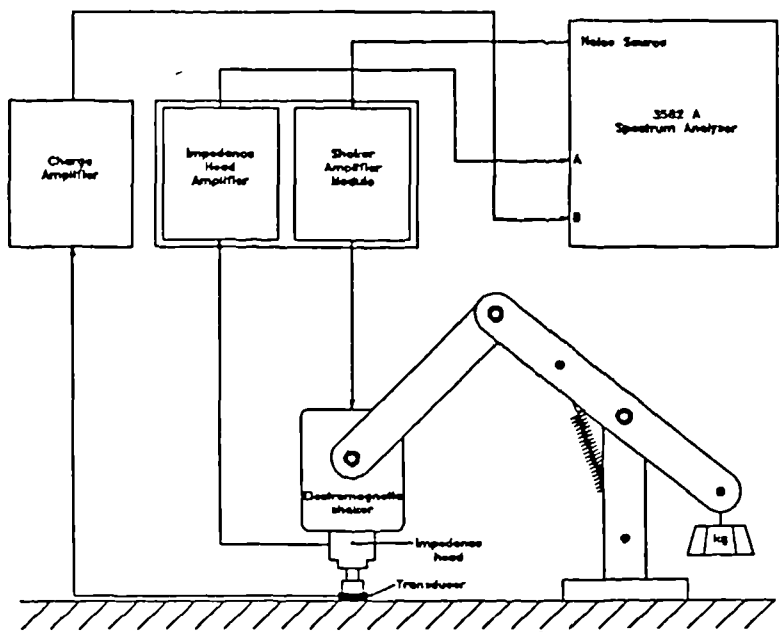


Figure 6.1 Bone resonance equipment used to test transducer frequency response

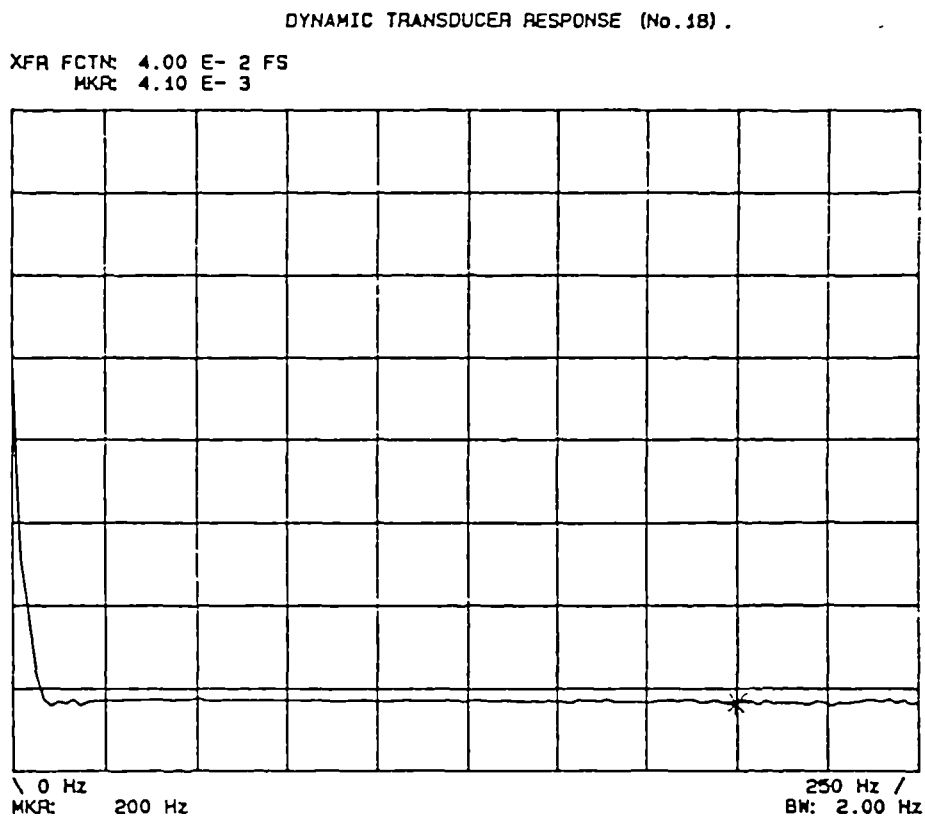


Figure 6.2 The transfer function for a piezo film transducer; applied vibrating force from an electromagnetic shaker and the corresponding charge produced from the transducer.

The equipment was limited to a low frequency cut-off of 8Hz due to internal analogue filters, and so only the transfer function for the response of the transducer in the limited range of 8 to 250Hz could be obtained, and is shown in figure 6.2. These measurements indicated that the transducer response was flat ( $\pm 0.1\text{dB}$ ) over this frequency range. In order to investigate for signals less than 8Hz an impulse measurement was taken so that the time constant of the charge amplifier (one channel of the main patient equipment) with the transducer connected could be calculated. A constant force was applied to the transducer under test and the output signal was allowed to decay to zero. This force was removed and the time constant of the decay of the output signal was measured. Figure 6.3 shows the resulting plot obtained using the Gould 1604 DSO and the exponential decay can be said to obey the following equation:

$$V = V_0 \left( 1 - e^{-\frac{t}{\tau}} \right) \quad (6.1)$$

where in this instance  $V_0 = 617\text{mV}$  and for the point chosen in figure 6.3 (the 63% of decay point),  $V = 389\text{mV}$  and  $t = 16\text{s}$ . The time constant,  $\tau$ , is therefore also 16s and so  $f_{3\text{dB}}$  is calculated to be 0.01Hz.

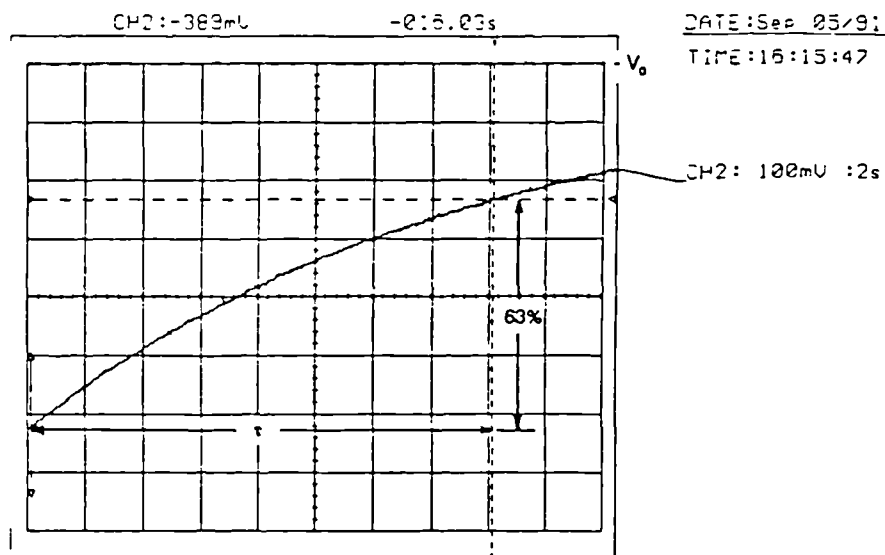


Figure 6.3 Shows the decay of the output voltage from a charge amplifier channel of the main equipment due to an initial force impulse applied to a transducer

This is the cut-off frequency for the equipment and so it can be concluded that the transducer has no effect upon the frequency response of the equipment and it can hence be assumed that the

transducer has a flat frequency response extending down to at least 0.01Hz.

### 6.2.2 Calibration

Before calibrating a transducer, a period of around two weeks was allowed for the adhesive to harden, and following this period each transducer was continually loaded to accelerate any structural *settling in*. This was usually carried out by wearing an insole containing a set of transducers for a day.

A typical calibration curve is shown in figure 6.4; the following is a description of the method used to obtain this calibration information.

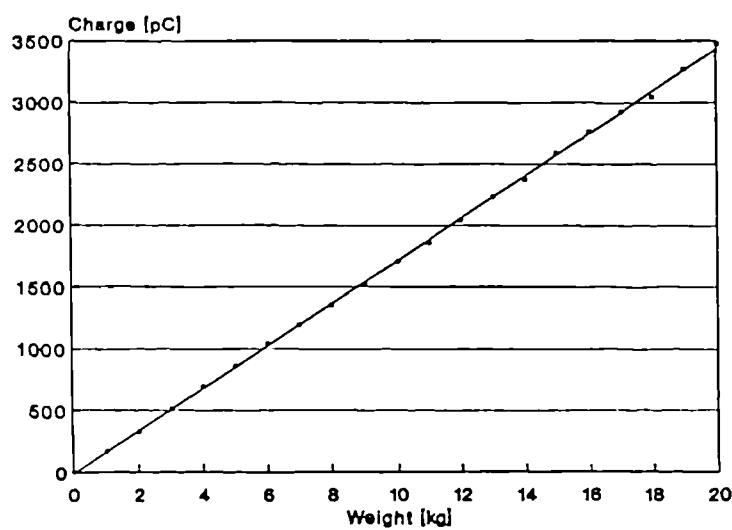
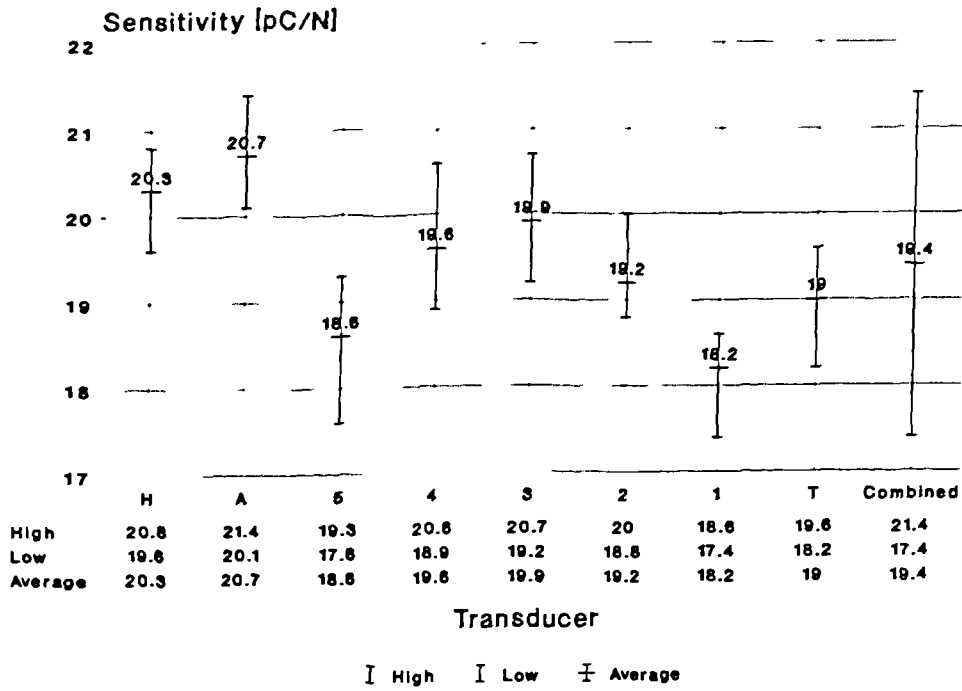


Figure 6.4 Typical transducer calibration curve: sensitivity 17.5pC/N

The technique involved the use of the static calibration jig (section 5.2.4), and the output charge was measured for a range of applied weights (2% uncertainty) using the calibration unit (section 5.2.4) and a Gould 1604 digital storage oscilloscope (4% uncertainty). Unfortunately the calibration jig became unstable for applied weights of greater than 10kg, so a reduced range of 0-10kg was used for routine calibration purposes. This method was slightly modified for further calibration of the same transducers in that having initially checked for linearity (section 6.2.4), it was then only necessary to use one weight rather than a full range in order to check the stability of the sensitivity values.

So that transducer accuracy could be assessed, tests were carried out whereby each transducer was loaded 20 times with a known weight. The weight was applied to the jig, and then removed and the deflection due to this removal of the load was detected. This method was adopted because while

### Type DSHSDN transducers



### Type BHHHDN transducers

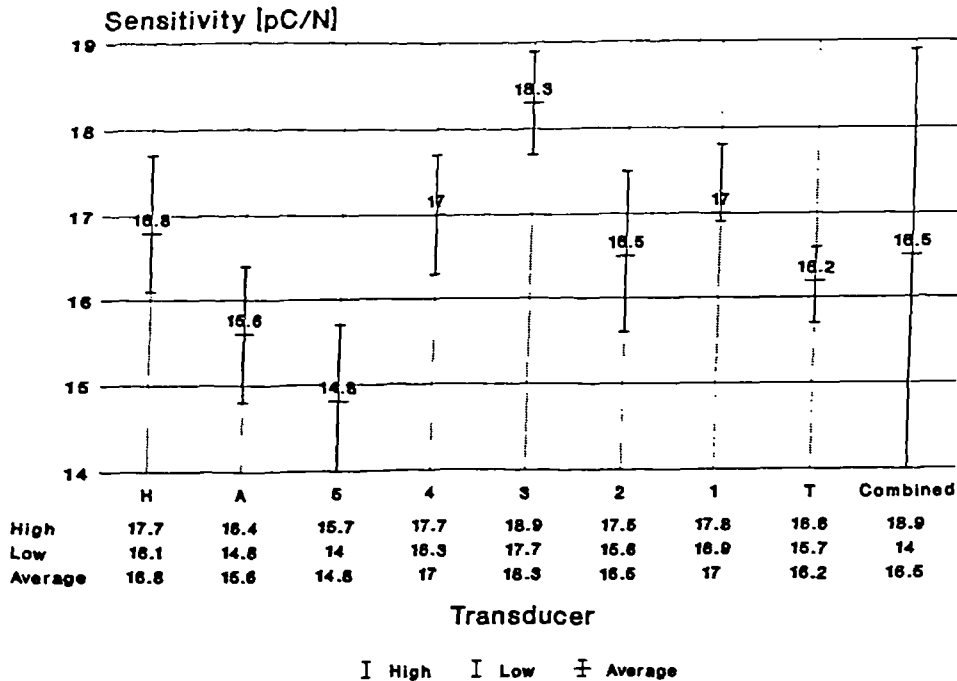


Figure 6.5 Calibration results for both sets of transducers used for clinical trials. The graphs show high, low and average sensitivity values calculated for each transducer, from twenty responses due to an applied weight of 3kg ( $\pm 2\%$ ). Estimated uncertainty for the measurement equipment is 4%.

lifting the load onto the jig it could not be assured that additional loading through the operators arm was not applied. The results from these tests for type DSHSDN and BHHHDN transducers are given in figure 6.5 and these graphs show the highest, lowest and average sensitivity values, calculated from the results. So just considering the spread of measurements about each mean sensitivity value, the worse case uncertainties for both transducer types are +3.9, -5.1% for type DSHSDN and +5.9, -5.6% for type BHHHDN. The measurement equipment uncertainty is estimated to be 4% so it can be seen that most of the uncertainty in these measurements can be attributed to equipment errors.

The other error to consider before the transducer uncertainty can be specified is the fixed  $\pm 2\%$  accuracy for the weights. Therefore in general the transducers can be said to have an accuracy of  $\pm 4\%$  for steady measurement conditions (in section 6.2.3 it will be discussed how this accuracy figure worsens upon repeated removal and replacement of the transducers from the calibration jig).

It can be seen that the two average of the average sensitivity values (19.4 and 16.5pC/N) show a difference of 2.9pC/N. This was thought to be primarily due to the non-conducting epoxy adhesive used for type BHHHDN transducers, and equation 3.20 was used to check this, by calculating a value for the glue layer thickness. So from the results the adhesive factor (equation 3.19) is calculated to be:

$$\nu = \frac{16.5}{19.4} = 0.85$$

Therefore from equation 3.20, the glue layer thickness,  $t_g$ , is estimated to be 15.3 $\mu\text{m}$  which is 4.7 $\mu\text{m}$  less than the estimate discussed in section 3.4.4.1, and so a slightly higher transducer sensitivity has been measured, compared to that predicted.

With reference to section 3.4, the expected transducer sensitivity (or piezoelectric strain constant) was estimated to be somewhere between the two values for  $d_1$  (17pC/N) and  $d_{33}$  (25pC/N). This has been found to be the case, where the average sensitivity figure was measured to be 19.4pC/N (type DSHSDN transducers).

### 6.2.3 Repeatability

In the previous section the transducer accuracy was calculated to be  $\pm 4\%$  for steady measurement conditions, that is, for the transducer undisturbed in the calibration jig. Generally it was discovered

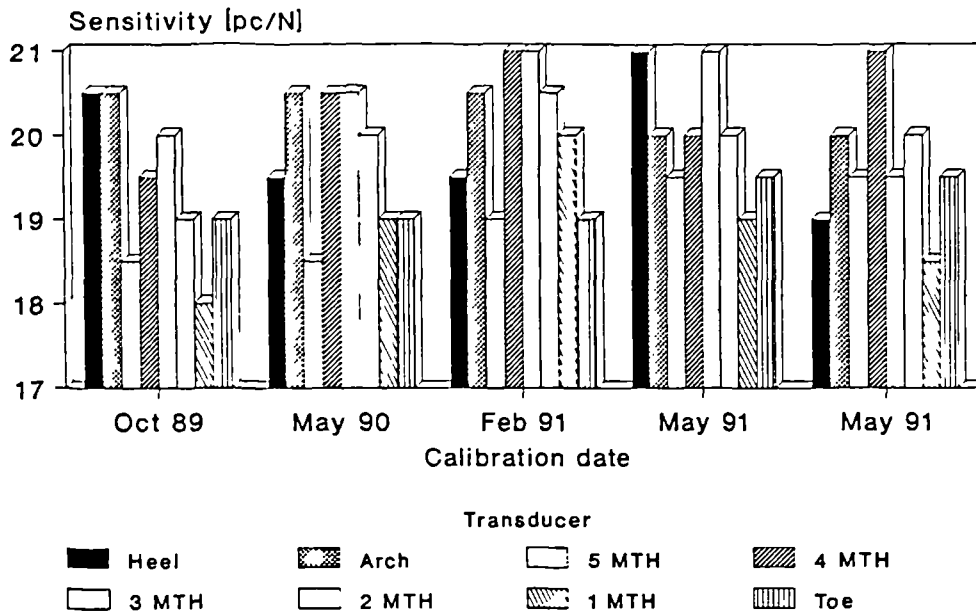


Figure 6.6 Long term repeatability results showing the mean sensitivity values for each of the type DSHSDN transducers used for clinical trials over a period of 1 year 7 months.

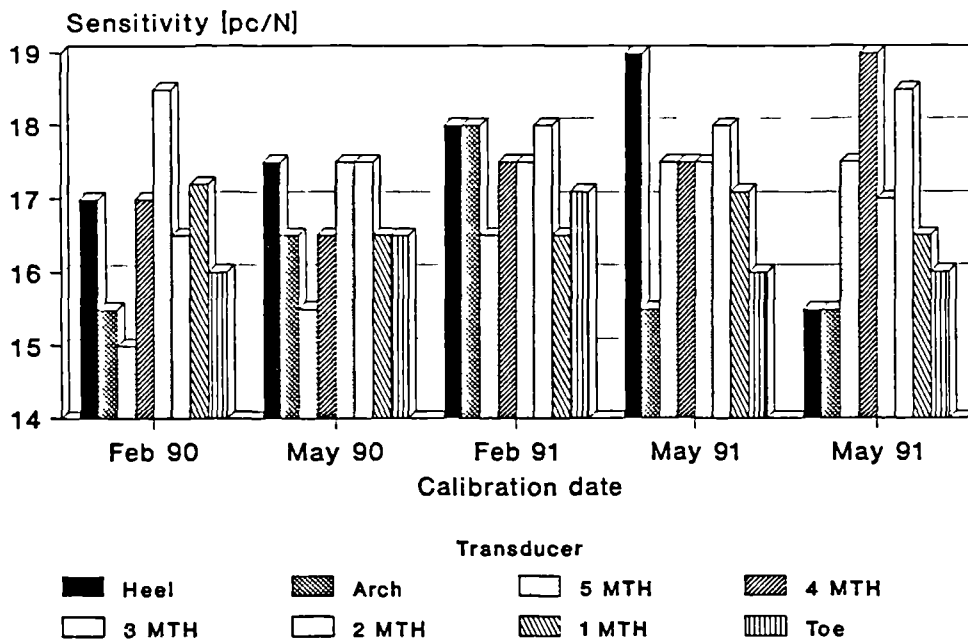


Figure 6.7 Long term repeatability results showing the mean sensitivity values for each of the type BHHHDN transducers used for clinical trials over a period of a 1 year 3 months.

that if a transducer was recalibrated at any time, the repeatability (calculated using the new mean sensitivity) was always within the uncertainty as specified above. In order to assess the transducer repeatability over a length of time, the two sets of transducers used for clinical trials were repeatedly calibrated over a period of a year and a half. Figures 6.6 and 6.7 show the results (mean sensitivity values) in the form of a bar graph for type DSHSDN and BHHHDN transducers respectively. No obvious pattern as in a drop or increase in sensitivity can be noticed from these results, however if a mean value for each transducer is calculated from these results the greatest deviation about this mean is -5, +5% for type DSHSDN and -10, +12% for type BHHHDN transducers. The room temperature was not noted when these measurements were taken, which could account for 3% uncertainty (section 6.2.5), but aside from this the calibration jig was thought to introduce errors and this was checked in the following way. One type DSHSDN transducer was extensively tested by recording the response due to 10 sets of 10 consecutive equal loadings within a one hour period: the transducer was removed from the jig and promptly replaced between each set of measurements.

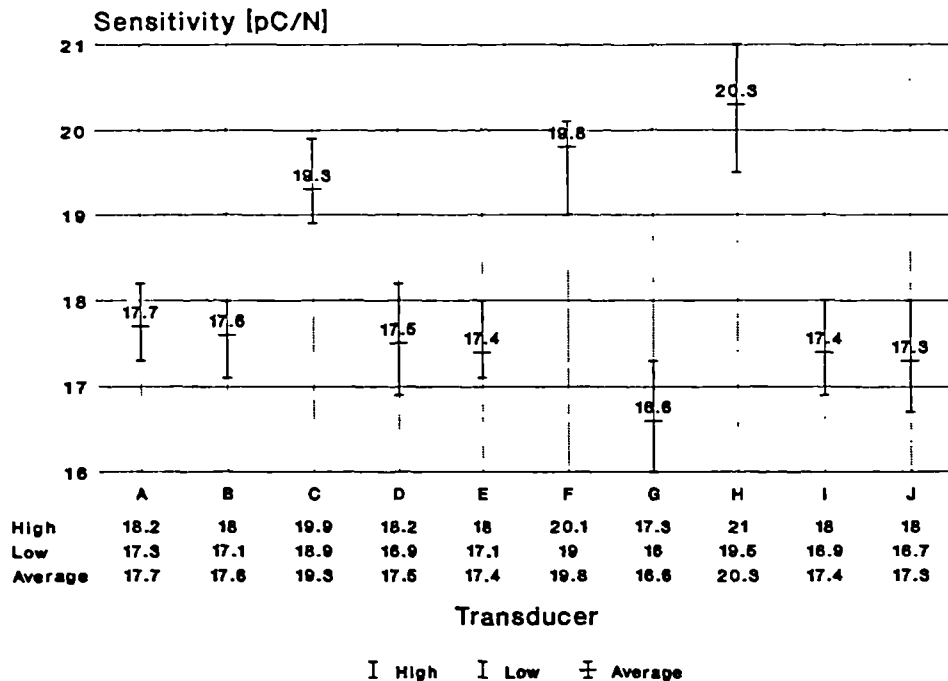


Figure 6.8 Error chart showing the spread of results for the sensitivity values obtained for one type DSHSDN transducer. The transducer was repositioned in the jig and recalibrated 10 times.

Figure 6.8 shows the results, and from these measurements the greatest variation of the mean

sensitivities about the mean for the entire test is -8%, +12%. This agrees with the long term repeatability results for type BHHHDN transducers (figure 6.7), but demonstrates a greater variation in comparison with the long term repeatability for the same transducer type (figure 6.6). This indicates that the way in which the transducers are calibrated is a likely cause of this variation, in that the calibration jig may not be applying exactly equal load each time, and the way in which the load is transmitted to the transducer may also vary. Dynamic calibration methods are discussed in section 8.2.4 that would reduce these uncertainties in the calibration process.

### 6.2.4 Linearity and hysteresis

The linearity for each transducer was initially checked using calibration curves typical of the curve shown in figure 6.4, and in all cases was found to be within 1.5%. The measured sensitivity points used to plot a calibration curve tended to be of random distribution above and below the calibration curve (therefore no non-linear trend), and so the transducers can be said to have a linear response. This agrees with the linear response for free film (Kynar technical manual, 1987), and demonstrates that the transducer design has no effect upon this desired linear response.

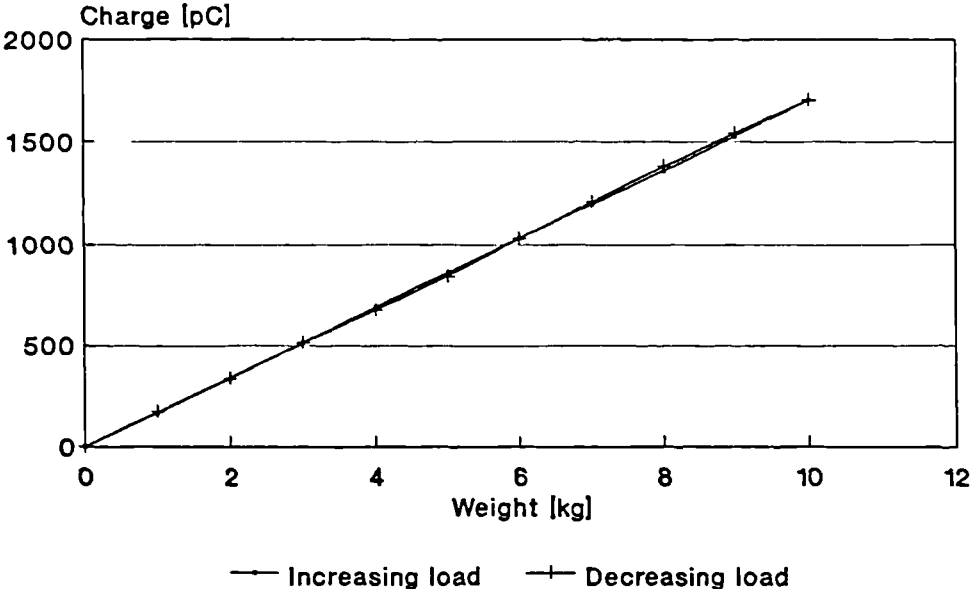


Figure 6.9 Transducer hysteresis

Transducer hysteresis has been measured for an applied load range of 0 to 10kg and a typical result

is given in figure 6.9. Hysteresis is just detectable from these results and was calculated to be less than 1.5%. However the variations in the output signal for the same applied load were within the 4% uncertainty of measurement, and so it can be concluded that there was no significant measurable hysteresis.

### 6.2.5 Temperature coefficient of transducer sensitivity

In order that the effect of ambient temperature upon transducer sensitivity could be investigated, a constant temperature chamber was constructed using several thick cardboard boxes and expanded polystyrene. The chamber was designed so that the transducer calibration jig could be fully contained inside, and so a transducer could then be calibrated in a constant temperature environment, which was adjustable between 5 and 50°C. A small thermistor was attached near to the transducer so that its temperature could be monitored, and the temperature was controlled using a hot air gun and liquid nitrogen. Two type BHHHDN transducers (A and B) were calibrated in the usual way and the results are displayed in figure 6.10. From these graphs, for the operating range of the transducers (10-40°C), the average value for the temperature coefficient was calculated to be  $73\text{fCN}^{-1}\text{K}^{-1}$ . This is less than half the theoretical value for  $d_{33}$  of PVdF ( $180\text{fCN}^{-1}\text{K}^{-1}$ , section 3.5.1), and so this indicates that

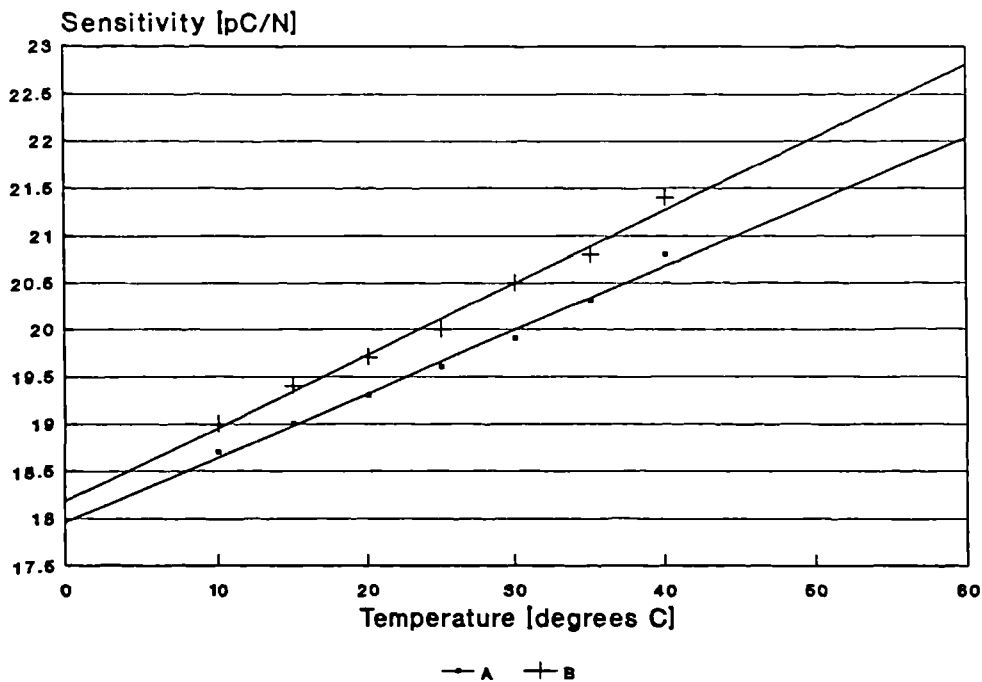


Figure 6.10 Sensitivity variations for two type DSHSDN transducers due to ambient temperature changes.

copolymer film is more temperature stable than PVdF film and/or the transducer is more temperature stable due to its construction, compared to a free element of film (which suggests that secondary pyroelectric effects have been reduced - section 3.5.1).

The in-shoe temperature was measured for twenty subjects and the average temperature was found to be 31.2°C (29-34°C range). If a transducer calibrated at room temperature (25°C) is found to have a sensitivity of 20pC/N then, taking the temperature coefficient of sensitivity to be 73fCN<sup>-1</sup>K<sup>-1</sup>, the error in the detected charge due to an applied load, for the above temperature range, would be +1.5, +3.3%. This error has been reduced by calculating a correction factor for the transducer sensitivities, which is included in the Gaitscan software (section 5.5.3). Each transducer is assumed to be operating at 31.2°C, and so a factor of 0.45pC/N is added to the transducer sensitivities obtained through calibration at 25°C. Therefore by including this correction factor the error has been reduced to -0.8, +1.0% for the above temperature range.

It is possible for room temperature to vary between 18 and 27°C, and therefore there could be a 0.6pC/N sensitivity difference ( $\pm 3\%$  for a transducer with a sensitivity of 20pC/N) between two calibrated results for the same transducer, due to this temperature difference. This is not significant, considering the repeatability results (section 6.2.3), however for future transducer calibration the room temperature is a parameter that should be noted so that this uncertainty can be accounted for, especially if more accurate calibration techniques are used.

#### **6.2.6 Bending tests**

So that the effect of transducer bending could be assessed experiments were carried out to test a transducer under worse conditions, that is, conditions that will not usually be found inside a shoe, as in practice the transducer would be supported by the sole of the shoe.

Two transducers (one type DSHSDN and one type BHHHDN) were initially recalibrated and then tested for uniaxial bending in both directions (in line with the transducer edges), and spherical bending. The static calibration jig was used to apply loading to the transducers and two special styli were fabricated so that the load could be transmitted through a knife edge and a single point, for uniaxial and spherical bending respectively. Another small jig was also constructed to allow the transducers to be supported (0.5mm depth of support) either along two opposite edges, or by all four

edges; to encourage uniaxial or spherical bending respectively, as shown in figure 6.11.

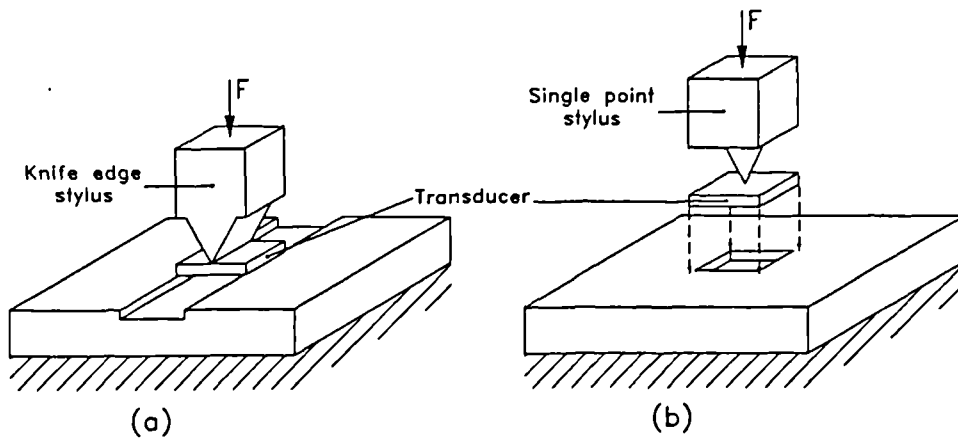


Figure 6.11 Shows the jig used to encourage (a) uniaxial and (b) spherical bending of a test transducer. The static calibration jig was used to apply loading through the special styli.

Many repeated measurements were taken for five loads (1, 3, 5, 8 and 13kg) for each of the transducers, which was necessary because the measurement uncertainty was greater than the small changes in sensitivity caused due to the bending (so practically the errors due to bending are insignificant), which will be discussed.

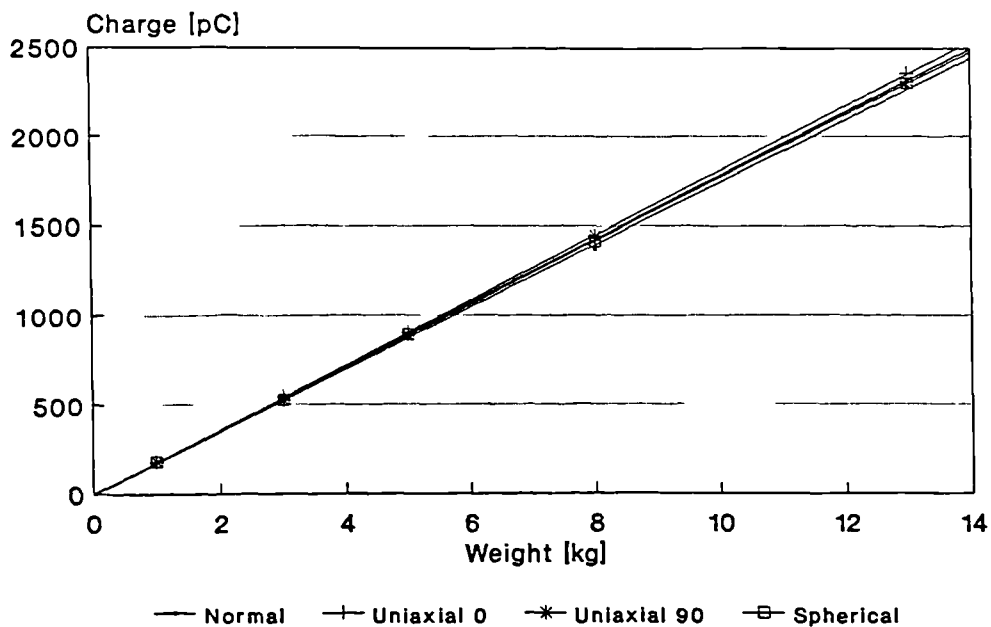


Figure 6.12 Results from bending tests for a type BHHHDN transducer

The results for the type BHHHDN transducer are given in figure 6.12, and from these results there

emerged a trend: the greatest error was found to be due to uniaxial bending in line with the cable groove (uniaxial 0) and the change in sensitivity was 0.5pC/N or 3%. Spherical and uniaxial bending at 90° to the cable groove both produced a change in sensitivity of 0.2pC/N or 1%. In real terms this means that errors due to bending are insignificant as actual errors will be even less than these detected experimentally due to the relaxed in-shoe conditions (inner sole support and distributed applied load). Similar results were also obtained for the type DSHSDN transducer.

#### **Cable noise**

The connecting cable used between the transducers and the amplifiers has been carefully chosen so that flexing of the cable during walking does not introduce significant charge noise into the system. This cable has been tested and it will introduce a maximum noise of 10pC (2.5% of the smallest signal, 20N, to be measured) due to a full 360° bend. The actual amount of cable flexing during walking is virtually unnoticeable so in real terms this error is insignificant.

#### **6.2.7 Humidity susceptibility**

Each transducer was lacquered in order to provide an environmental seal against the harsh conditions to be endured inside a shoe (section 4.3.4).

The in-shoe humidity of 12 subjects was measured, and the average value was found to be 94.8% relative humidity (SD: 5.24). A simple test was devised to assess the effect of a humid environment upon transducer performance with and without lacquer. A sealed vessel containing a saturated solution of potassium sulphate solution was used to create the humid atmosphere (94% RH), into which a transducer could be inserted. All sixteen transducers used for clinical trials (types DSHSDN and BHHHDN, section 4.3.3) were tested and it was found that when lacquered there was no detected electrical response, however there were seemingly random positive and negative charge amplifier output deflections (usually op-amp saturation) for unlacquered transducers. In performing these tests it was intended to show that lacquered transducers were not in any way susceptible to erroneous electrical activity while working in a humid environment, so further tests to determine the cause of the electrical activity for unlacquered transducers were not carried out. Therefore it can be concluded that a mixture of electrochemical and charge leakage effects were the cause of this activity for unlacquered transducers. These tests demonstrate the importance of having a good lacquer layer so that the

transducers are unaffected by the harsh in-shoe environment, which should be maintained by periodic relacquering (section 7.3.6)

### 6.3 Calibration unit

The calibration unit was designed as a single channel charge amplifier and used to investigate early transducer configurations and to calibrate transducers. The transfer function for each gain setting was checked using a Hewlett Packard 3582A spectrum analyser and this is discussed in section 6.3.1. It was also necessary to initially calibrate this unit to obtain gain figures, which would then be used in transducer calibration calculations. Charge gain measurements for all four of the gain settings were taken before the unit was first used and also one year later, again using the spectrum analyser. These measurements are discussed in section 6.3.2.

#### 6.3.1 Frequency response

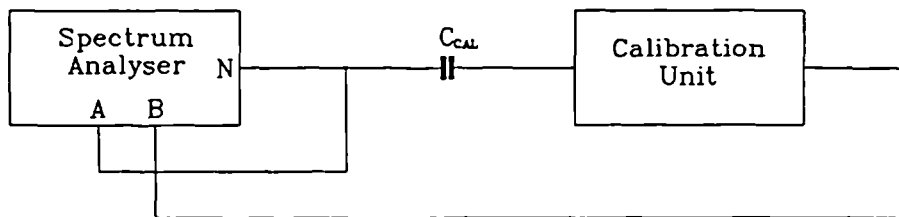
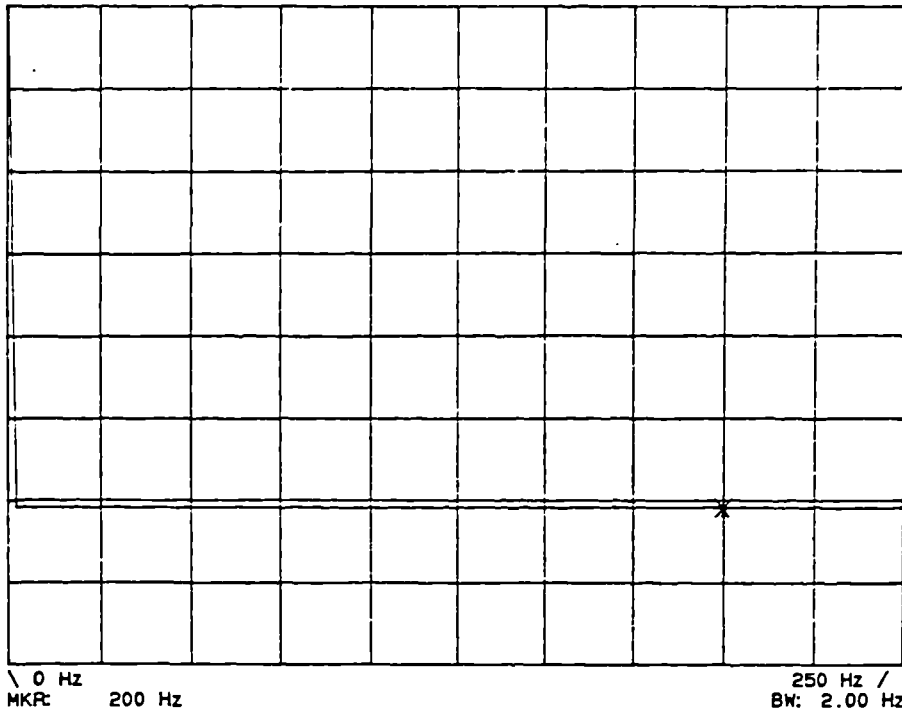


Figure 6.13 Block diagram of the equipment setup used to assess the calibration unit frequency response

For the purposes of equipment calibration, two polystyrene capacitors ( $C_{CAL}$ , in figure 6.13) were soldered in-line into two BNC to BNC connection leads, which were accurately ( $\pm 0.1\%$ ) measured on a bridge instrument (Thurlby CM200). These had values of 110.8pF and 10.02nF. A periodic noise source was taken from the spectrum analyser, N in figure 6.13, and this was fed to one of the calibration capacitors so that a known charge was available at the input of the calibration unit. This noise voltage was also monitored by channel A of the spectrum analyser, and the transfer function was calculated by also monitoring the output of the calibration unit, channel B. Figure 6.14 shows the expected flat response over the desired frequency range, for gain setting Cx1 (0.1V/nC); results

Calibration Unit Frequency Response. Charge Gain 0.1V/nC.

XFR FCTN: 4.00 E- 2 FS  
MKR: 9.51 E- 3



Calibration Unit Frequency Response. Charge Gain 0.1V/nC.

XFR FCTN: 4.00 E- 2 FS  
MKR: 9.60 E- 3

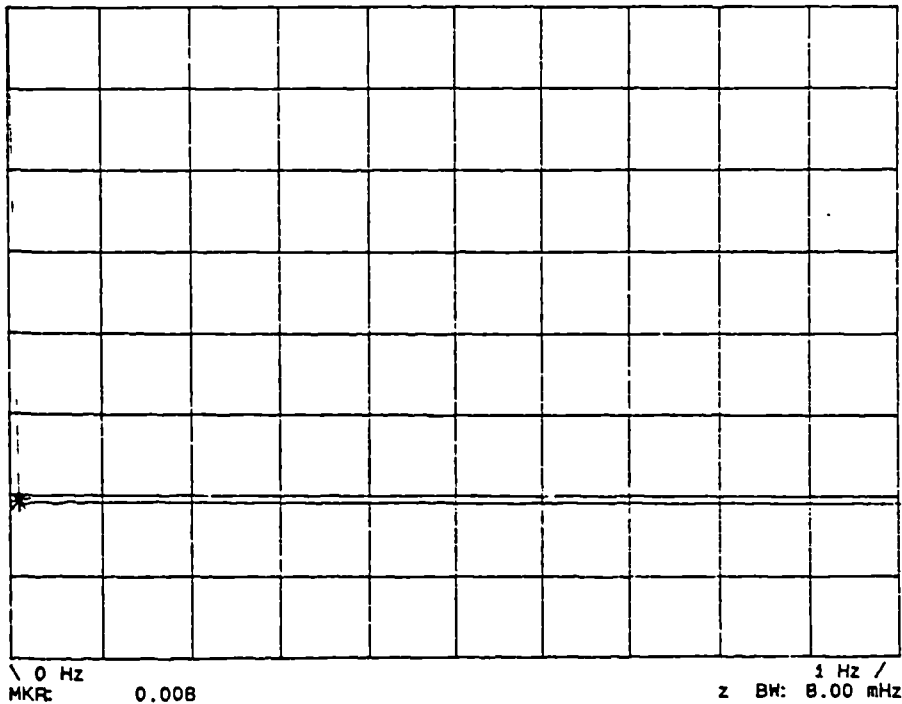


Figure 6.14 Transfer functions for the calibration unit for gain setting Cx1. Shows frequency ranges 2-250Hz and 0.008-1Hz for the top and bottom traces respectively.

for the other gain settings provided the same information. The top trace shows the whole passband, and it can be seen from the bottom trace (0.008-1Hz) that the gain at 0.008Hz is within 0.2dB of the passband gain. All gain settings were measured to be within 1dB of the passband at this frequency.

### 6.3.2 Calibration

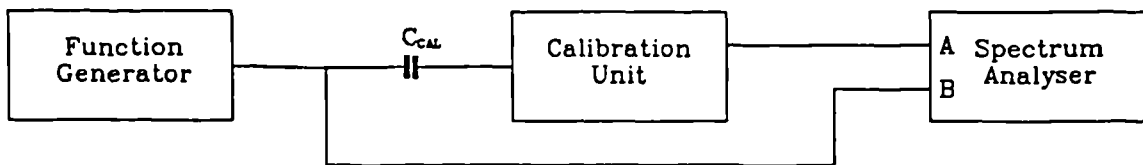


Figure 6.15 Block diagram of the equipment setup used to carry out calibration of the calibration unit.

Having verified that the passband frequency response was acceptably flat for each gain setting, the setup shown in figure 6.15 was used to determine the gain for each setting. The spectrum analyser was used as it was the most accurate piece of equipment available (amplitude uncertainty: +0.05dB, -0.156dB, or +0.5%, -2%, for flat top passband setting). The function generator provided an 80Hz sinusoidal signal which was fed to a calibration capacitor,  $C_{CAL}$ . This signal was also monitored by channel B of the spectrum analyser, and channel A monitored the output from the calibration unit. The gain in V/nC was calculated by taking the ratio of these two signals. A range of charge signals can be detected by each of the calibration unit gain settings, and these are summarised in figure 6.16.

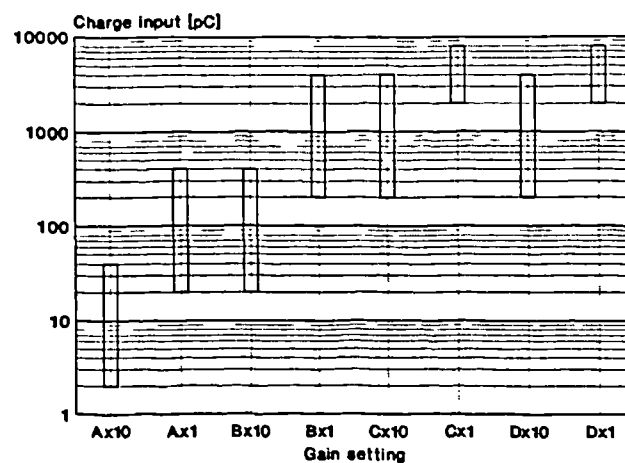
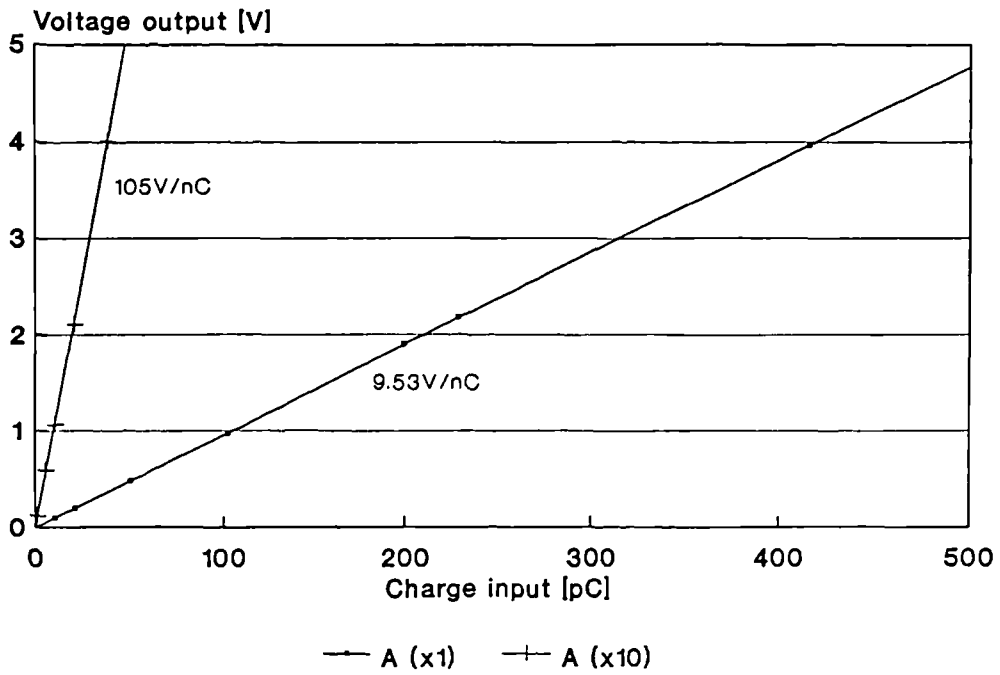


Figure 6.16 Calibration unit gain ranges. Indicates the input charge ranges capable of detection by each of the gain settings.

### Cal unit - range A



### Cal unit - range B

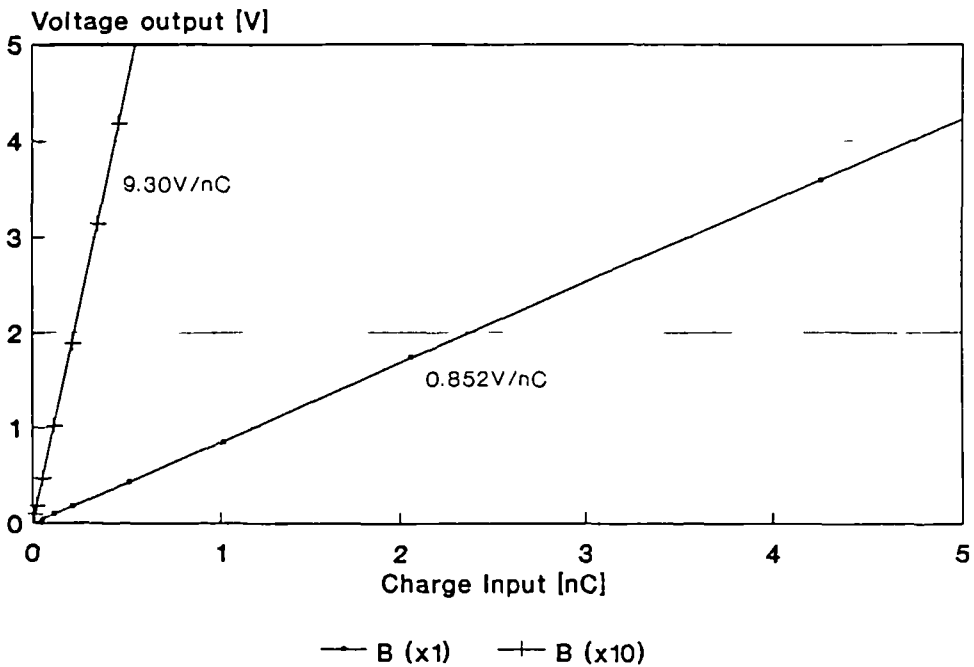
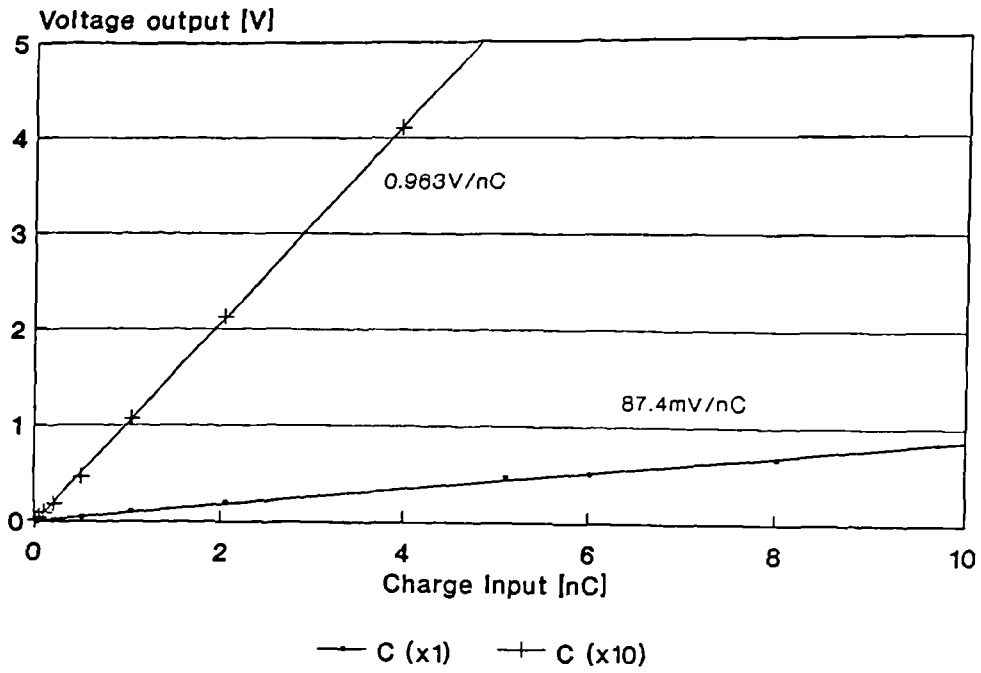


Figure 6.17a Calibration curves for the A and B gain settings

### Cal unit - range C



### Cal unit - range D

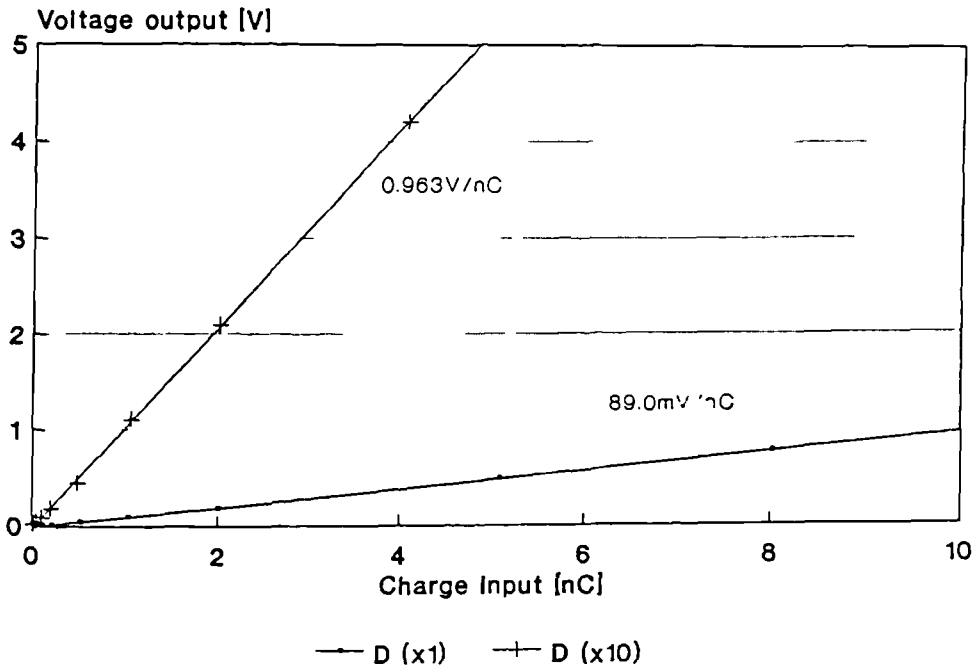


Figure 6.17b Calibration curves for the C and D gain settings

Figure 6.17 shows the calibration curves for all these settings and the corresponding charge gains. These gain values are tabulated in table 6.1, together with the original values which were taken approximately 1 year before.

Gain setting	Charge gain [V/nC]		Deviation from original [%]
	Initial	1 year later	
Ax1	9.75	9.53	-2.3
Ax10	107	105	-1.9
Bx1	0.862	0.852	-1.2
Bx10	9.49	9.30	-2.0
Cx1	0.0862	0.0874	+1.4
Cx10	0.949	0.963	+1.5
Dx1	0.0859	0.0890	+2.4
Dx10	0.946	0.963	+1.8

Table 6.1 Charge gain figures for the calibration unit.

From these results it can be seen that the variations in the measured gains for each gain setting are within the 2.5% uncertainty of measurement for the equipment. These figures were used for transducer calibration calculations and so it can be said that an uncertainty of 2.5% can be achieved for transducer sensitivity figures.

#### 6.4 Electronic system

Initially the frequency response for each channel was adjusted (R4 in figure 5.10) and transfer function plots were obtained. This is discussed in section 6.4.1. For each channel the gain was then adjusted (R3 in figure 5.10) to be equal. The spectrum analyser was used to take these calibration measurements, together with noise measurements, which is discussed in section 6.4.2.

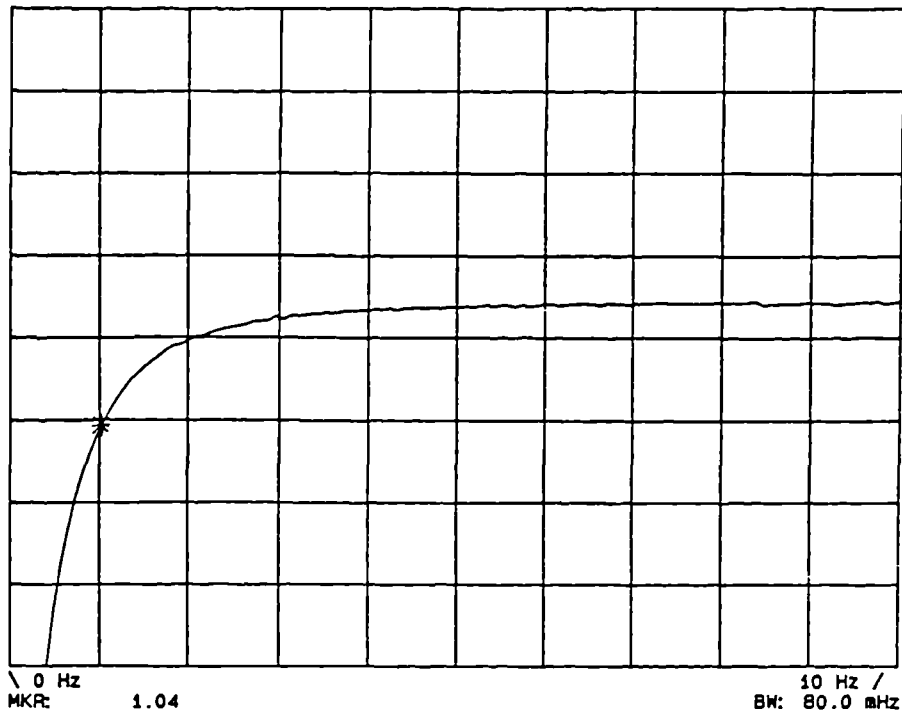
##### 6.4.1 Frequency response

The frequency response for each of the sixteen channels was checked in a similar way to that described in section 6.3.1, for the calibration unit. Figure 6.18 shows the transfer functions for the first

FIRST STAGE - CHARGE AMPLIFIER RESPONSE

XFR FCTN: + 0dB FS  
MKR: - 10.1dB

2 dB/DIV



SECOND STAGE - INTEGRATOR RESPONSE

XFR FCTN: + 10dB FS  
MKR: 2.7dB

2 dB/DIV

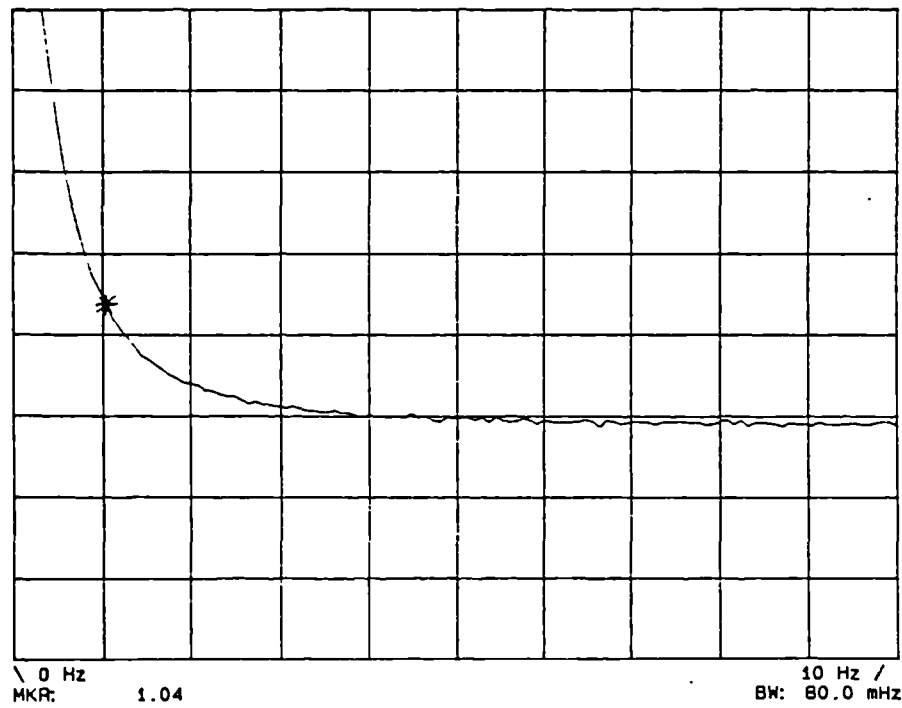


Figure 6.18 Transfer functions for the first and second stage electronics

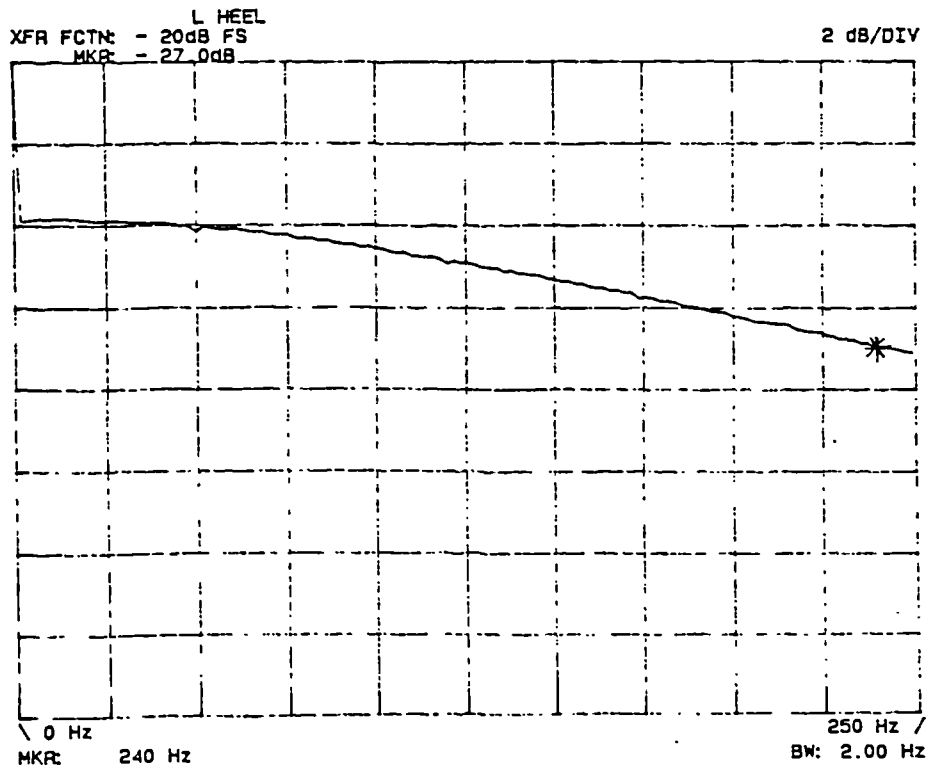
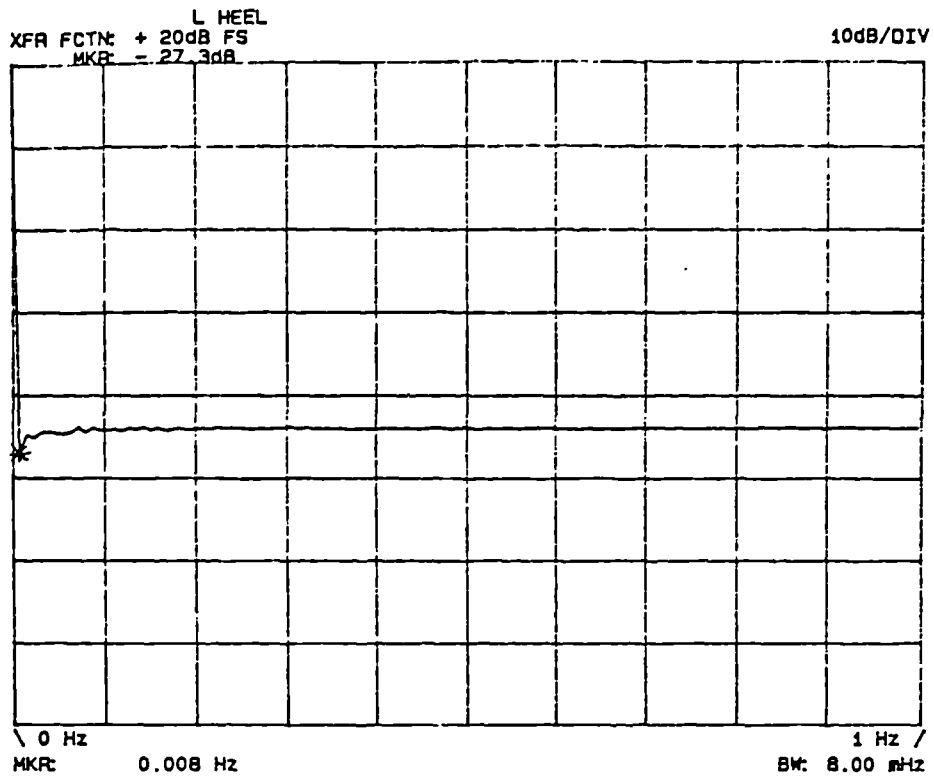


Figure 6.19 Transfer functions for one channel of the main equipment. Shows frequency ranges 0.008-1Hz and 2-250Hz for the top and bottom traces respectively.

and second stage electronics respectively. R4 (figure 5.10) was adjusted so that the second stage 3dB cut-off point coincided with that of the first stage at 1.04Hz. Each channel of the main equipment was setup in this manner so that the combined transfer function showed a flat response in the passband. Figure 6.19 shows this transfer function for one of the channels after having been setup. The low frequency 3dB cut-off point for all the channels was found to be between 0.008 and 0.01Hz, and the high frequency 3dB cut-off points were found to be within 20Hz of 240Hz.

#### 6.4.2 Calibration and noise measurement

Calibration measurements were taken using the setup as described in section 6.3.2. A 30Hz sinusoidal signal was capacitively linked to the input of each channel in turn and the resulting output signal was measured using the spectrum analyser (see figure 6.15). The gain of each channel was therefore able to be calculated and these results are summarised in table 6.2.

Channel	Charge gain [V/nC]		Deviation from original [%]
	Initial	2 years later	
LHeel	0.57	0.56	-2%
LArch	0.57	0.57	0
L5MTH	0.57	0.56	-2%
L4MTH	0.57	0.56	-2%
L3MTH	0.57	0.57	0
L2MTH	0.57	0.56	-2%
L1MTH	0.57	0.57	0
LToe	0.57	0.57	0
RHeel	0.57	0.57	0
RArch	0.56	0.57	+2%
R5MTH	0.58	0.57	-2%
R4MTH	0.57	0.57	0
R3MTH	0.57	0.57	0
R2MTH	0.57	0.56	-2%
R1MTH	0.57	0.57	0
RToe	0.57	0.57	0

Table 6.2 Charge gain figures for the main patient equipment

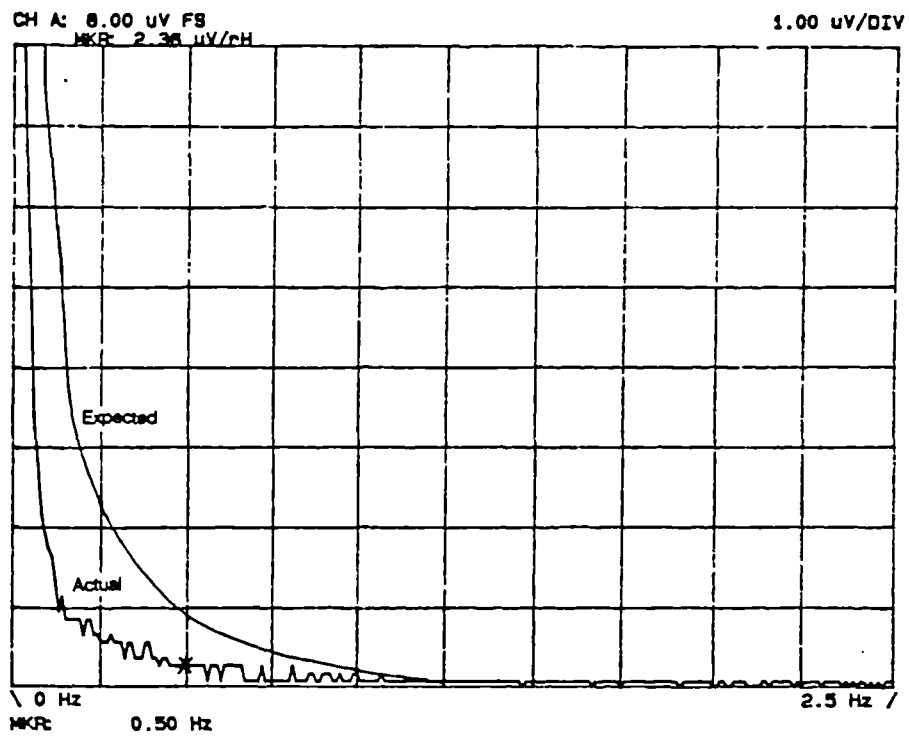
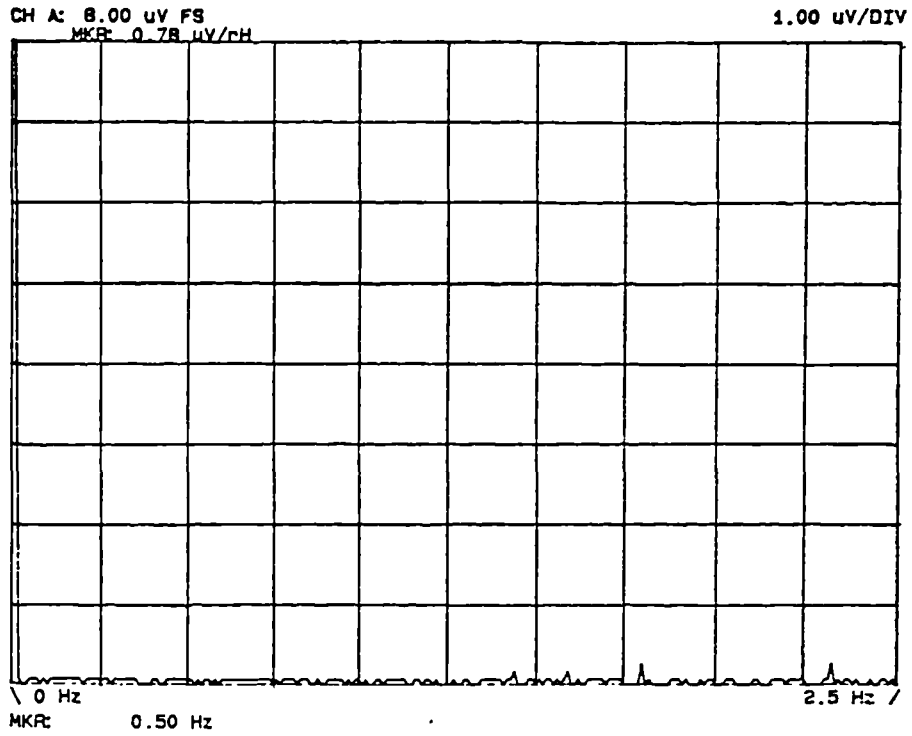


Figure 6.20 Measured noise spectral density for the output of the first stage (top trace - (a)) and the output of the second stage (bottom trace - (b)).

From these results it can be seen that the variations in the measured gains are all within 2% of  $0.57V/nC$  and that the variations over a two year period are within the 2.5% uncertainty of measurement for the equipment.

The theoretically expected noise from the main patient equipment was discussed in sections 5.2.2 and 5.2.3. In order to assess this analysis the noise from the output of the first and second stages was measured using the spectrum analyser. A bandwidth of 0.01 to 2.5Hz was investigated and so the input signals to the spectrum analyser were initially passed through a simple RC bandpass filter (0.008 to 10Hz 3dB cut) to remove the equipment output d.c. offset and any high frequency components of noise that would otherwise have overloaded the spectrum analyser. The results are shown in figure 6.20 and it can be seen that the measured noise from the second stage (figure 6.20b) is less than that which was expected. The output noise from the first stage was estimated to be around  $0.2\mu V/rHz$  and from figure 6.20a it can be seen that the measured noise can be said to be less than  $0.78\mu V/rHz$ , which is the minimum signal that the spectrum analyser is capable of detecting. From these results

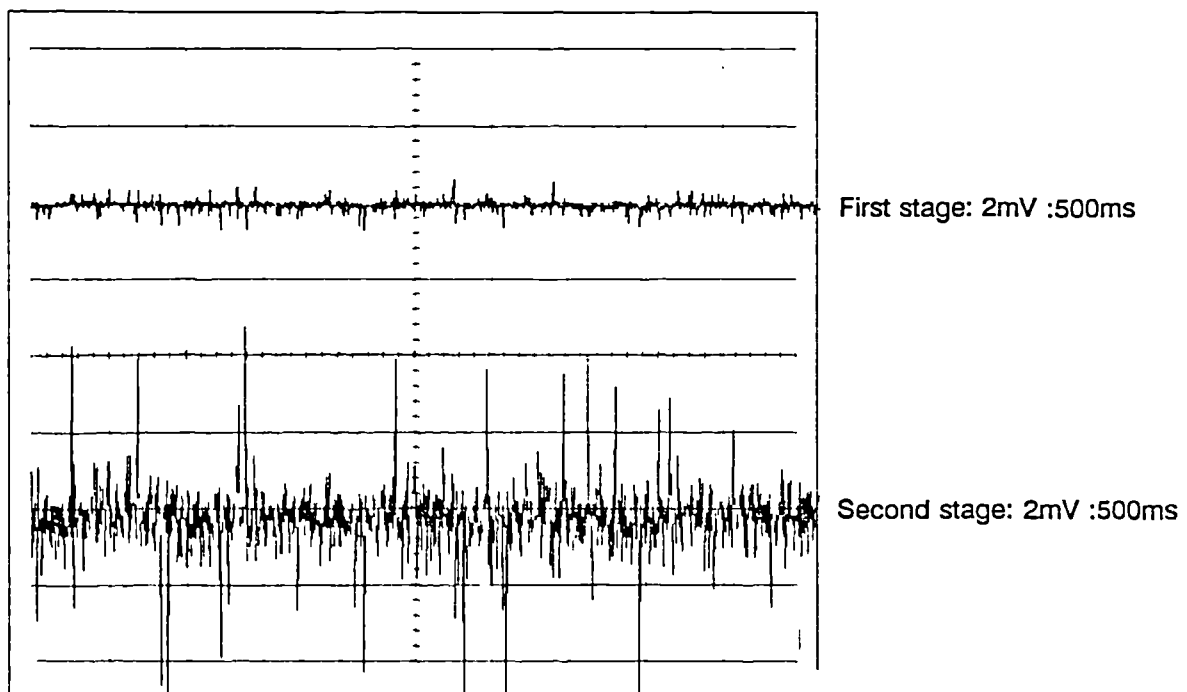


Figure 6.21 Shows the time domain output noise from the first and second stages of the main patient equipment

it can be concluded that the differences in the calculated and measured noise is most likely due to the assumptions made for the calculations of low frequency noise, that is, the extrapolation carried out for the current noise density for the second stage op-amp (OP200) using the manufacturers noise density graphs. It is therefore suspected that the current noise density plot (plot (a), figure 5.13) should have a slope of less than the displayed -20dB/decade. This applies for low frequencies (<1.5Hz) and the measured noise for higher frequencies (>1.5Hz) agrees with what was expected from theoretical calculations. Figure 6.21 shows a time domain noise measurement from the two stages, which is an indicator of the increased output noise from the second stage as compared to the first.

#### **6.4.3 Computer data acquisition**

So that the sampling for data acquisition could be set to a known rate it was necessary to use the on board DAS16 timer and programme the card to sample upon every trigger pulse from this timer (see section 5.5.1). In between samples a small amount of code was executed (procedure *acquire data*, figure 5.21) and the limiting factor for the fastest obtainable sampling rate was the execution time of this code. It was necessary to write a small programme so that the maximum sampling rate could be determined for the particular computer being used. The information obtained from an A/D sample consists of 12 data bits and 4 channel-encode bits. So the simplest way of determining the maximum sampling rate was to acquire data at an initial *safe* rate and gradually increase this sampling rate until samples were missed. This was achieved by decoding the channel number from each sample and consecutively displaying this stream of channel number, starting a new line after each of the sixteen channels had been displayed. From this test it was found that the maximum sampling rate was 15.77KHz for the AT 286 computer being used. Therefore an acquisition rate of 15KHz was chosen, 1KHz less than the original requirement given in section 5.4. This slightly lower rate did not present a problem as initial trials for this work were restricted to walking subjects, and hence to sampling rates of around 4kHz (for a transducer frequency response of 50Hz).

#### **6.5 Conclusions**

In this chapter the transducer and system performance has been discussed.

The electronic calibration unit was built to enable transducer testing and calibration and was used extensively to obtain many of the results contained within the first section of this chapter, transducer performance. The frequency response for this unit was obtained using a spectrum analyser and, as designed, was measured to extend beyond the desired 0.01 to 200Hz range for gait measurements. The unit has eight gain settings, all of which were measured to within an uncertainty of 2.5%. Over a period of one year the calibration of this equipment had not significantly changed.

All areas of transducer performance have been investigated and results have been obtained to illustrate transducer calibration, repeatability, linearity, hysteresis, the temperature dependence upon sensitivity, bending effects and humidity susceptibility. Initial calibration curves were produced for each new transducer from which the charge sensitivities could be calculated. For type DHSHDN and BHHHDN transducers the average sensitivities were measured to be 19.4 and 16.5pCN<sup>-1</sup> respectively. Thereafter repeatability measurements were conveniently taken by repeatedly loading a transducer with a single known weight. For steady state conditions transducer uncertainty has been measured to be 4%. Errors have been discovered in the calibration process that are primarily thought to be due to the mechanical calibration jig. From the repeatability studies it can therefore be said that the transducers are calibratable to within 10%. In addition the linearity and hysteresis studies indicate that these errors to be less than 1.5% respectively. The temperature coefficient of sensitivity has been measured to be 73fCN<sup>-1</sup>K<sup>-1</sup> (for copolymer transducers) which is less than half the expected theoretical value (for PVdF). The conclusion drawn from this is that copolymer is more temperature stable than PVdF and/or the transducer is more temperature stable due to its construction. From the results of this test a compensation factor of 0.45pCN<sup>-1</sup> was calculated which was added to each measured transducer sensitivity (by the Gaitscan software) which thus eliminated a possible 3% error which otherwise would have been due to the difference between the calibration and operating temperatures. Transducer bending tests were necessary so that the errors due to the complex bending could be determined experimentally. Results indicate that the expected error for a worse case situation would be 3%, however for in-shoe conditions this error is expected to be less than 1%. Charge induced due to cable flexing was also estimated and the expected error for a worse case situation was measured to be 2.5% (of the smallest signal, 20N). Therefore the actual error is expected to be insignificant (<1%). Finally, the effect of a humid environment upon the transducer was investigated and no errors

due to electrochemical and charge leakage effects were measured for lacquered transducers. Effects were detected for unlacquered transducers which supports the need for periodic re-lacquering in order to ensure independence from humidity.

Finally, in section 6.4 the performance of the main patient equipment was investigated. Each channel of the equipment was set up so that the 3dB cut-off points for the 1st and 2nd electronic stages coincided and therefore so that the overall frequency response was 0.01 to 200Hz. Each channel was then calibrated to within an uncertainty of 2.5% and an average charge gain of  $0.57\text{V/nC}$  was measured. The calibration of this equipment remained within the 2.5% uncertainty of measurement over a period of 2 years. The circuit noise was theoretically calculated to be predominantly due to the 2nd electronic stage. Noise measurements were taken and this was shown to be true in practice. However, the measured noise was slightly lower than that predicted for frequencies less than 1Hz and this discrepancy was explained back to assumptions made for the theoretical calculations.

In summary the transducer and system performance have together adequately satisfied the requirements stated in previous chapters.

## **Chapter Seven**

**7**

# **CLINICAL MEASUREMENT**

## 7.1 Introduction

In performing clinical trials it was intended to show that the system could provide information which was of use to the orthopaedic surgeon and podiatrist and to show that the system is essentially usable in a clinical setting. In total recordings were taken from 41 subjects who were considered to have a normal gait and 7 subjects with known foot disorders. This chapter contains details of the clinical measurement strategy that was used, also typical results from the recordings will be discussed. Findings and system performance will be discussed in the relevant sections and comments on the clinical validity of Gaitscan will be given in the summarising section, 7.4.

The clinical trials have been an invaluable aid to the development of Gaitscan. Throughout the period of research trials have been periodically carried out at the Brighton Polytechnic department of Podiatry (formerly known as the School of Chiropody and referred to as the School) and Dundee Royal Infirmary (referred to as DRI). Both these centres currently use other gait analysis techniques and systems and are knowledgeable in the field.

The School is an outpatient clinic and teaching department and so has the potential to host detailed clinical studies due to the high volume of treated patients. They make use of a Kistler force plate and a Musgrave colour footprint system, mainly for research purposes, however the instruments receive some clinical use. The work carried out here helped formulate the efficient measurement procedure as detailed in section 7.2 and investigate the effects of a U'ed plantar pad used for relieving the loading on a metatarsophalangeal joint (section 7.3.4).

The Department of Orthopaedic and Trauma surgery of DRI has a dynamic pedobarograph which is in use daily for clinical measurements. Access to patients with varied orthopaedic pathologies was easy however arranging sessions with patients with particular foot disorders required time and planning as they usually had to be called in. An affiliated department, the Dundee limb fitting centre, was able to act as a useful critic while clinical trials were being carried out at DRI supplementing the clinical input to the research. This department makes use of two Kistler force plates embedded in a 7m walkway together with a Vicon video camera system (MIE Ltd) and also a custom developed system enabling EMG measurements. Two particular results obtained from trials at DRI are detailed in section 7.3.2 and 7.3.3.

## **7.2 Measurement procedure**

It is essential that a clinical setting is quiet and private. The mere fact that the patient is to be connected to equipment can arouse his/her anxiety, so a simple explanation was given to each patient during which time the system was being prepared. The painless non-invasive nature of the test was stressed and most importantly it was emphasised that the patient should walk as usually as possible and to try to disregard the presence of the equipment.

It was anticipated that no referral would be made to the results of individual patients thus identifying them, and so no written agreement was required from patients prior to taking measurements. So long as any information is only to be used statistically, the storage of personal information on computer is covered by the universities data protection research registration. Aside from this, a data collection record sheet was devised and used to collect this information, shown in figure 7.1.

As mentioned in the introduction to this chapter, clinical trials have been carried out throughout the development of Gaitscan. During early trials the equipment used in addition to the Gaitscan hardware was as follows: a TEAC MR-3 6 channel cassette data recorder; a Gould 1604 4-channel digital storage oscilloscope and a pc-AT fitted with a Metrabyte DAS16 data acquisition card with CODAS support software. This set up was satisfactory during these early stages of development as only one foot was instrumented, however it quickly became evident that a much more versatile setup was required (see software development, section 5.5). The results presented in this chapter were all obtained from the latest trials, that is, the equipment used was a pc-AT fitted with a Metrabyte DAS16 card, running the Gaitscan suite of programs.

A routine protocol has been followed during trials, and in brief the measurement procedure was as follows:

- (i) Accurate location of the sites of interest
- (ii) Fabrication of measurement insoles
- (iii) Recording data from multiple runs of consecutive footsteps
- (iv) Observation and analysis of results

It is necessary to place the transducers accurately under the correct areas of the foot, namely: heel, lateral arch, metatarsal heads and toe. Care was therefore taken in this initial stage of the measurement procedure and in fabricating the insoles to meet the above requirements. Numerous



techniques could be used to this end; outlined below in the form of a list of instructions is the procedure found to be most suitable:

1. Shape a card insole from standard template shapes to fit exactly ( $\pm 1\text{mm}$ ) inside the subjects shoe. On no account should the insole be able to move once placed inside the shoe.
2. Transfer the locations of the anatomical sites of interest onto the card insole by first accurately locating the sites by palpating the plantar surface of the foot. After marking these sites with a water soluble marker, wet the top surface of the card insole with clinical alcohol solution or spray (e.g. Quick Prep., Stuart Pharmaceuticals Ltd). Finally help the patient to rock to and fro with the card insole placed correctly inside the shoe.
3. This card insole can now be used as a template for both the cork insole and the anatomical site locations.
4. Using rubberised cork of thickness 2mm and double sided tissue tape, or impact adhesive, the marked card insole is adhered to the top surface of the cork, i.e with the anatomical site markings facing upwards<sup>1</sup>. Transducer locating holes can now be punched through both layers in positions corresponding to the anatomical site locations and a hand held square punch measuring 11 x 11mm is used for this purpose.
5. Small adhesive tape pads are placed over the transducer locating holes on the top side of the insole, this provides an anchor for the transducers while placing them in the correct locations from the underside of the insole. A layer of tape cut to the shape of the insole is then adhered to the underside of the insole, so anchoring the transducers and connecting wires in position; Chirofix™ (Smith & Nephew Chiromed) of width 10cm was found to be useful for this purpose. The connecting wires should be routed to the instep and crossed wires should be avoided.
6. The insole is now ready for measurements to be taken. Once placed inside the subject's shoe the connecting wires are passed out alongside the instep of the foot and this should be

---

<sup>1</sup> The thickness of the insole entirely depends upon the thickness of the transducers used, these must, of course, be the same to avoid undesired high or low pressure measuring sites. The materials quoted are for the copolymer type BHHHDN transducers which have a total thickness of 2.8mm.

of little or no irritation to the subject while in locomotion.

It was found that in the clinical situation it was often possible to stagger a Gaitscan test either side of an examination period the patient had originally planned to attend. Once familiar with the system the time necessary to perform a complete test was around 20 minutes, however most of that time is taken constructing the insole. So if this construction could be carried out while the patient was in clinic then a test need only demand 5 minutes before examination to locate the anatomical sites and 5 minutes afterward to take measurements.

After the equipment was correctly interconnected it was necessary to check that all the leads were secured and that the equipment felt comfortable to the subject; the subject is always the best judge of his/her own comfort! The recording of data from multiple runs of consecutive footsteps was carried out by executing the Gaitscan acquire program, gsacqu, and three or four runs of around 10 footsteps were usually taken. Initially the software was written so that the sampling rate was set to 16kHz (200Hz frequency response for each transducer), and this meant that a large amount of data (32kbytes/sec) would be acquired. During normal walking this frequency response is not required as the spectral content of the gait signals is below 50Hz. To show this the signals of ten normal steps from each of the eight transducers were averaged and displayed. The first graph of figure 7.2(i) shows the resulting frequency plot and it can be seen that at 50Hz the signal amplitude is -60dB that of the lower frequencies, indicating that any contribution due to signals greater than 50Hz will be less than 0.1% of the lower frequency signals of interest. The second graph of figure 7.2 shows the frequency plot of an average of ten forced heel strikes (the heel was forcibly slammed to the ground, wearing leather shoes), and this shows the increased frequency content that is expected for increased physical activity. Frequency response requirements for the measurement of physiological signals can also be determined by examining the relative morphology between a raw signal and the same signal after it has been passed through one or more filters. For example, most of the power for an ECG signal is expected to be below 10Hz yet the agreed standard is for equipment to have a frequency response up to at least 100Hz so that the higher frequency components of the signal are faithfully reproduced. A simple test was carried out whereby a typical waveform from a metatarsal head was passed through an adjustable low pass filter. Figure 7.2(ii) shows a raw signal and a signal that had

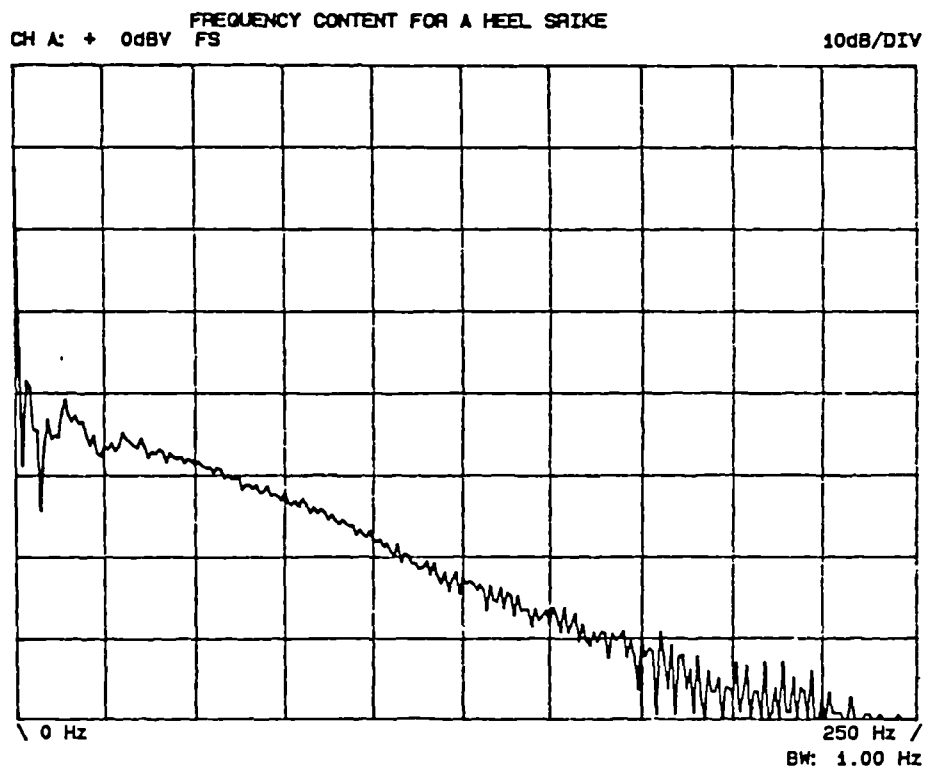
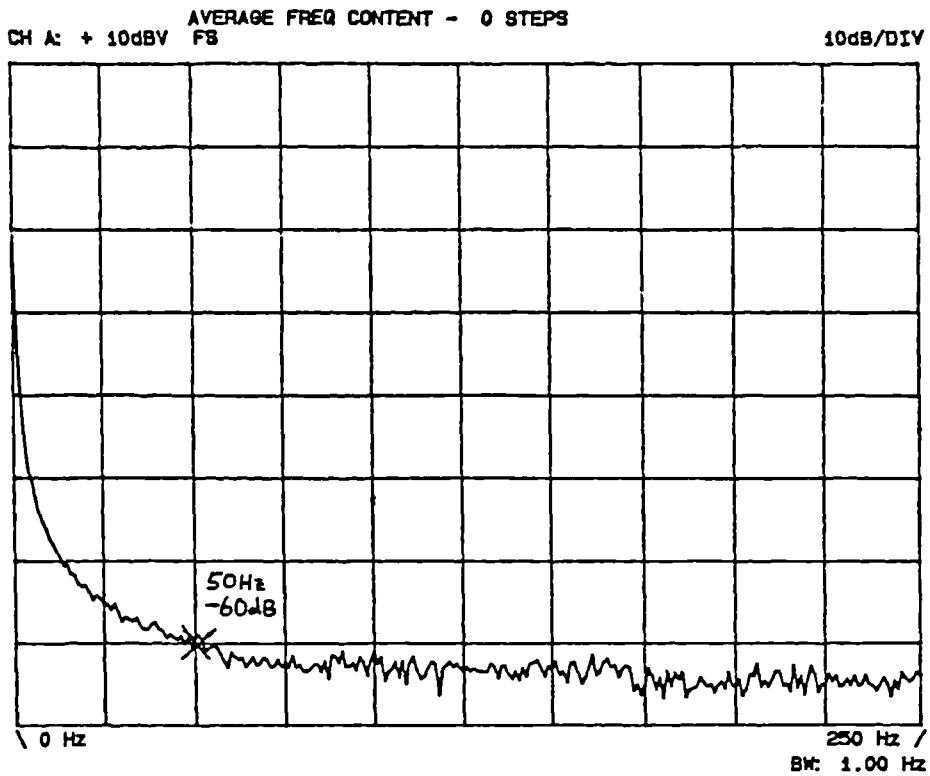


Figure 7.2(i) Spectrum analyser plots showing (a) the frequency content of signals averaged from all eight transducers for 10 normal walking steps and (b) the frequency content of signals averaged from the heel transducer for 10 forced heel strikes.

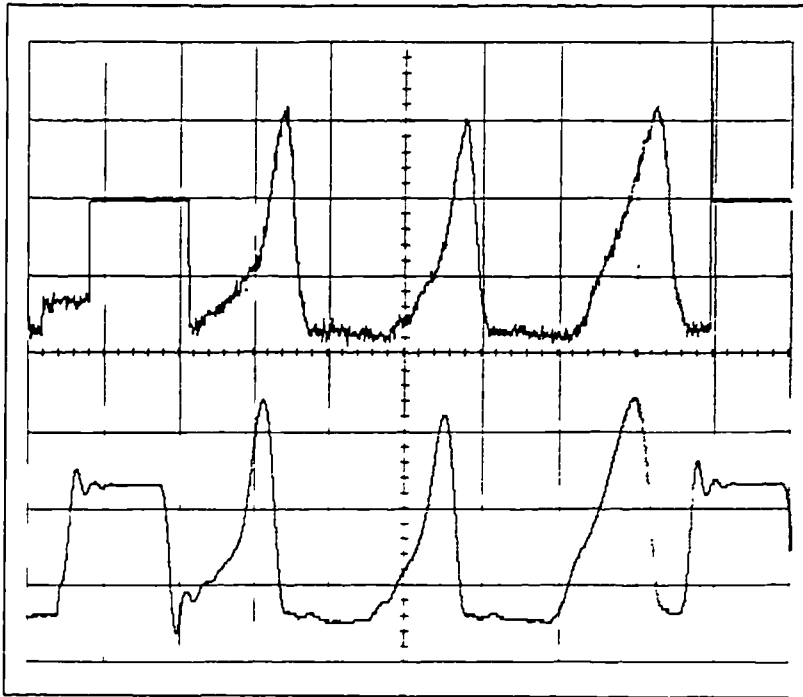


Figure 7.2(ii) A typical signal from a metatarsal head transducer, showing (a) the raw original signal and (b) the same signal after low pass filtering with a 10Hz 3dB cut-off point

been passed through such a filter with a cut-off frequency of 10Hz. Apart from the removal of higher frequency noise the morphology of the filtered signal was not altered for filter cut-off frequencies above 10Hz, however changes were noticed for cut-off frequencies below 10Hz. This result could be related back to the plot of the frequency content for normal walking steps (figure 7.2(i)a) and it can be seen that at 10Hz the signal amplitude is around -46dB. So from these results a 50Hz higher 3dB cut-off point would be suitable for normal walking and a 200Hz higher 3dB cut-off point would be suitable for higher activity. It was therefore decided to have the A/D sampling rate software selectable (corresponding to 50, 100 or 200Hz frequency response for each transducer), in order to optimise data collection so that unnecessary data is not acquired.

On completion of the test the subject was free to go and the observation and analysis of results could be carried out using the Gaitscan postscan analysis program, gspost. Detailed instructions for this program and gsacq can be found in chapters 7 to 9 of the installation and operating manual (appendix II).

### 7.3 Measurement results

In the following sections specific information obtained from clinical measurements will be presented and discussed. Initially typical results for a normal subject will be discussed, and a comparison of these results will be made using measurements obtained from a dynamic pedobarograph (DPBG). Measurement repeatability will next be examined and normal step-to-step variability will be addressed. The following three sections contain results for patients with pathologies: a patient with a knee disorder, another with heel pain and lastly the foot pressure for a normal subject with a false lesion attached under the 2nd MPJ is investigated in order to assess the efficacy of orthotic insole inserts. Finally, problem areas due to artifact and constraints imposed by the measurement system are discussed in the penultimate section of this chapter.

#### 7.3.1 A normal patient

As already mentioned in the introduction (section 1.3.6), in the area of gait analysis *normal* is loosely defined. Probably the most accurate definition is: *"the usual gait of a person considered pathologically normal and who has not had any serious accident or operation affecting the lower limb"*. Most of the subjects investigated throughout this research were considered to be normal. Figure 7.3 shows a typical set of pressure-time waveforms for a normal subject, and figure 7.4 shows a left and a right footstep selected from this set. The peak pressures for each of the eight transducers were obtained using the software, for seven footsteps for each foot. This information was averaged for each transducer and is shown graphically in figure 7.7. To enable these results to be compared with another system, the same subject was walked over a DPBG (DRI) and figures 7.5 and 7.6 show these results for the left and right foot respectively. Having captured the data of a single footstrike, the DPBG software allows the selection of particular areas of interest, labelled 1 to 9 on the foot outlines (figures 7.5 and 7.6). Numerate information is calculated for these areas as peak pressure and average pressure. As the piezo film transducers are sensitive to the average pressure over their area (section 3.4.1), then for comparative purposes the average pressure values obtained from the DPBG should be used. Nevertheless, the marked areas are of different sizes and tend to be greater than 1cm<sup>2</sup>, which therefore means that the Gaitscan results are expected to be some degree higher. The average pressure values obtained from the DPBG are shown with the Gaitscan results in figure 7.7,

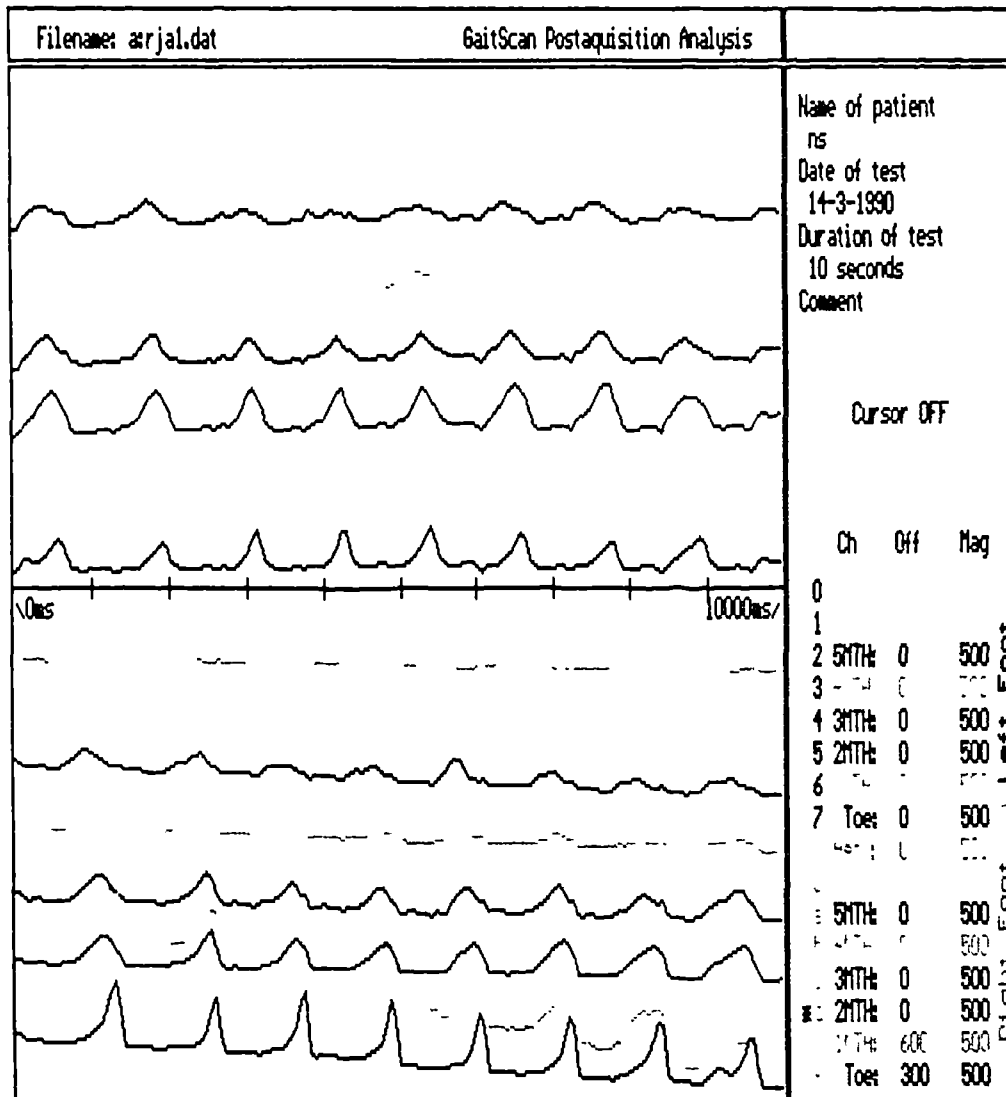


Figure 7.3 The 16 pressure-time waveforms obtained from a 10 second test for a normal subject. The top eight traces show the multiple footstep data obtained from the left foot, while the bottom eight traces show the data obtained from the right foot. Providing the data in this form enables a clear overall picture to be obtained, prior to investigating the data of particular footsteps. Full on-screen manipulation facilities enable the waveforms to be magnified, reduced, zoomed into and superimposed upon one another, and the status of the screen is indicated in the right hand window. To allow quick analysis, a cursor enables time and calibrated amplitude measurements to be taken from the waveforms, shown as disabled.

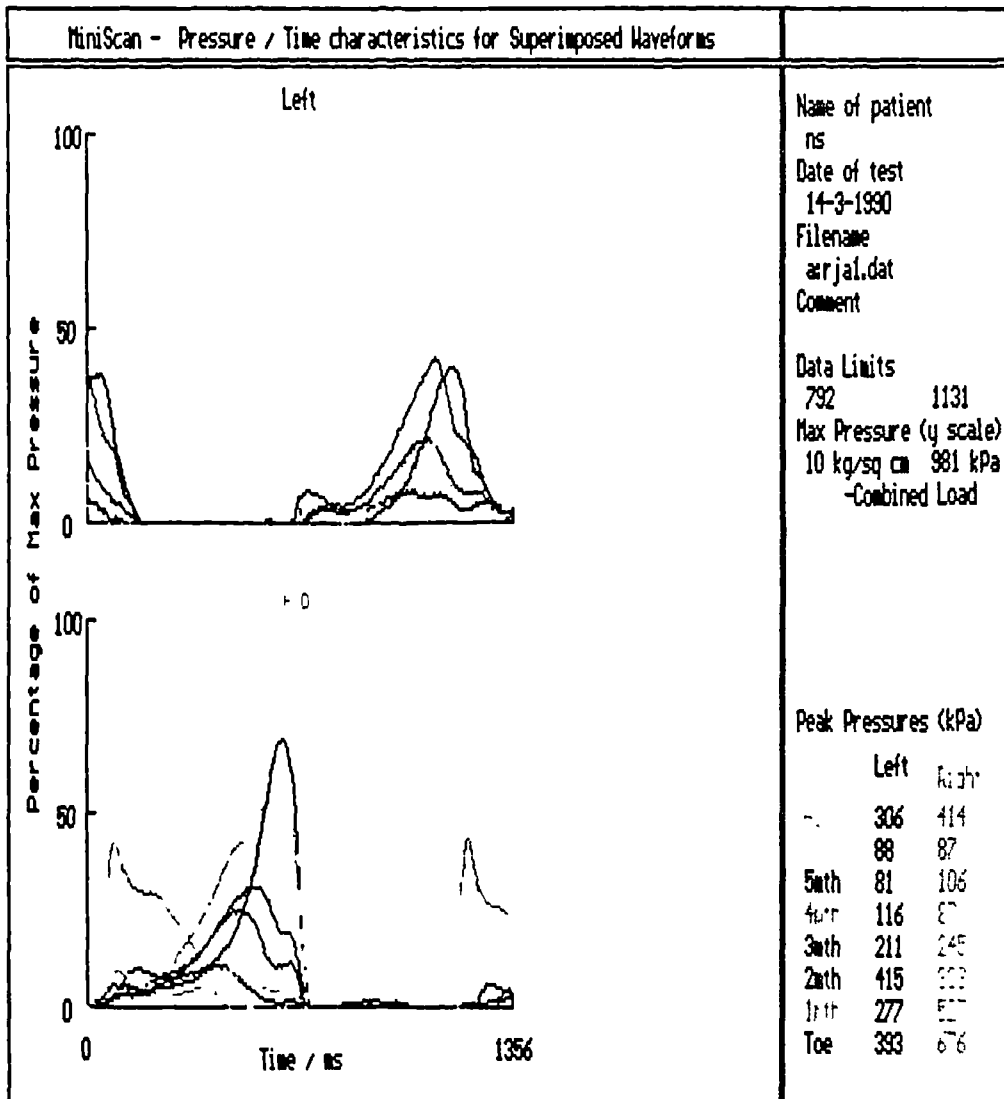


Figure 7.4 The superimposed waveforms for two footsteps. Any two consecutive footsteps can be selected from the main screen (figure 7.3) and displayed quickly in this form - known as the miniscan screen. In the right hand window peak pressure values are displayed for each of the traces, and these can be written to a file. Additional timing information is also shown and once enabled, the mouse is used to pinpoint any part of a waveform and the time from the y-axis to this point is calculated and displayed in milliseconds. Having the two footsteps displayed one above the other allows time duration measurements to be made upon the data from one foot, relative to the data from the other.

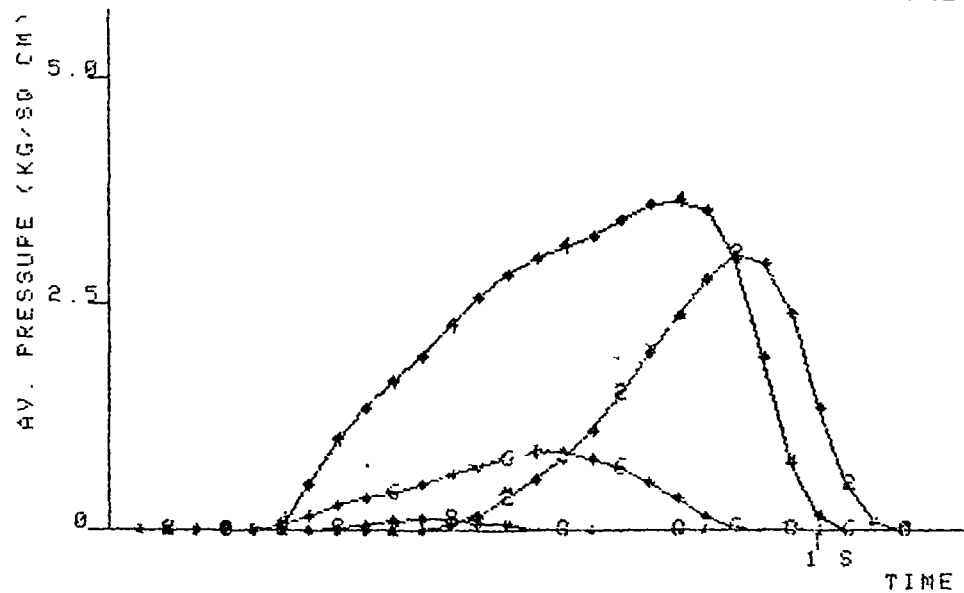
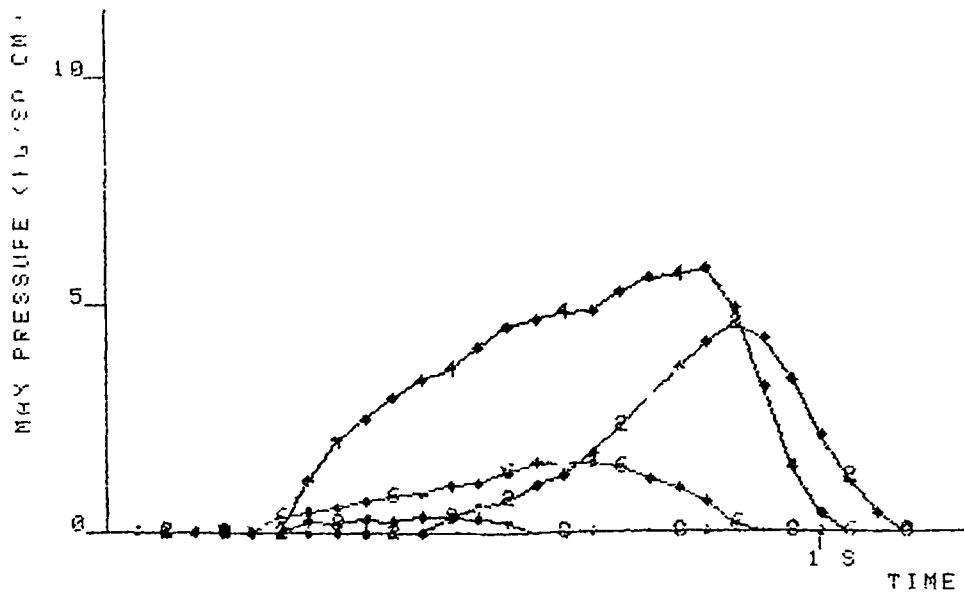


Figure 7.5 DPBG results for the normal subject, left foot. The areas selected for analysis are indicated on the outline of the foot (1 to 9) - the pressure-time graphs are then calculated for these areas.

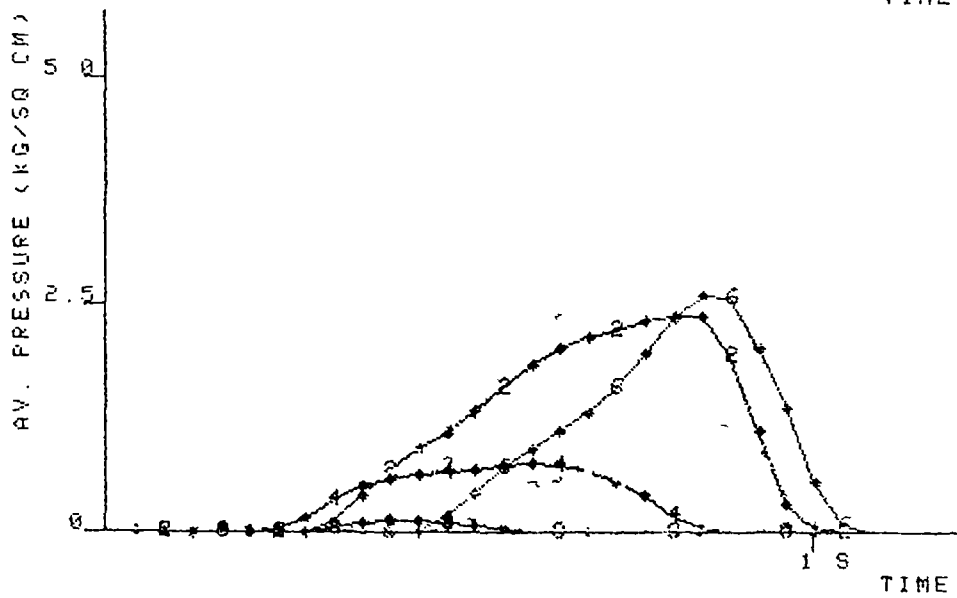
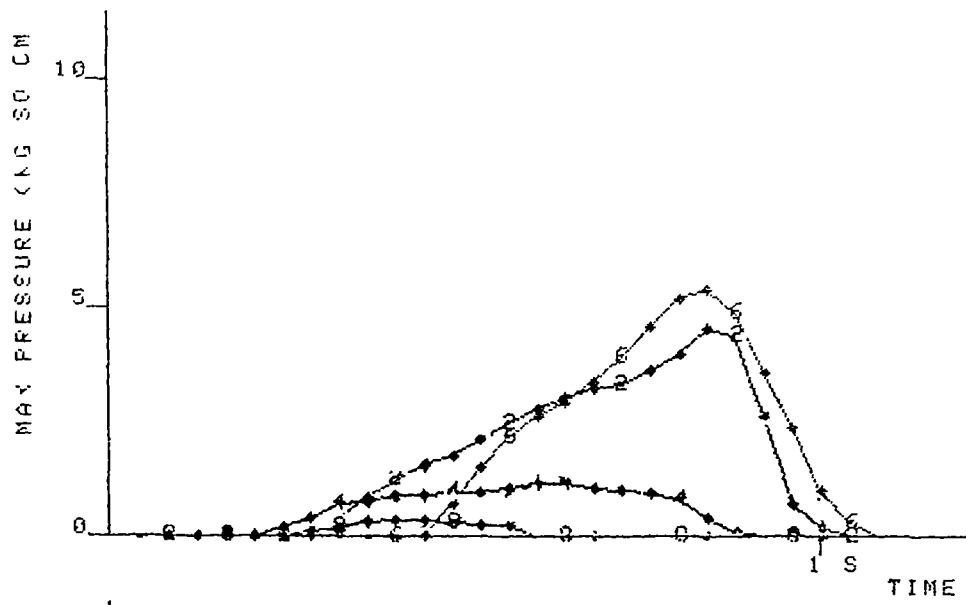


Figure 7.6 DPBG results for the normal subject, right foot.

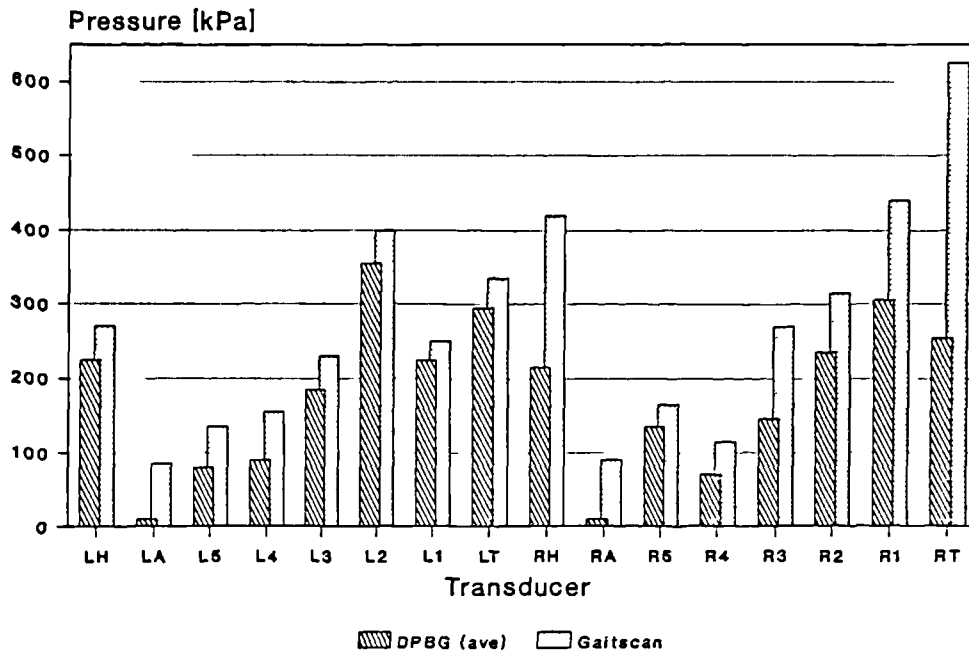


Figure 7.7 Barchart showing the peak values for the average pressure results obtained from all eight areas for both feet for a normal subject: Gaitscan results were obtained by averaging the information from 7 footsteps and the DPBG results were for 1 footstep.

and it can be seen that the Gaitscan results were higher: on average a 28% increase for the forefoot, a 33% increase for the heel and a 90% increase for the lateral arch. The effect upon results due to the DPBG analysis for the relatively large marked areas can be seen by comparing the Gaitscan results with the DPBG peak pressure results: for the forefoot the Gaitscan results are on average down by 31%. Therefore it can be concluded that the in-shoe pressure for normal patient is comparable with the barefoot pressure, measured using a dynamic pedobarograph.

### 7.3.2 Measurement repeatability

In order to evaluate the repeatability of measurements, the possible factors affecting this repeatability needed to be considered:

- Measurement uncertainty
- Normal step-to-step variation
- Accuracy of the fit of the insole inside the shoe
- Accuracy of insole fabrication

The measurement uncertainty was mainly attributed to transducer calibration which amounts to 10% (sections 6.2.2 and 6.2.3). The normal step-to-step variation has been investigated using a DPBG - 10 steps for each foot for the same normal subject have been measured. Various measurements were then taken using Gaitscan to determine the step-to-step variability, the effect of removing and reinserting an instrumented insole and the effect upon results of using a second insole constructed by a different person.

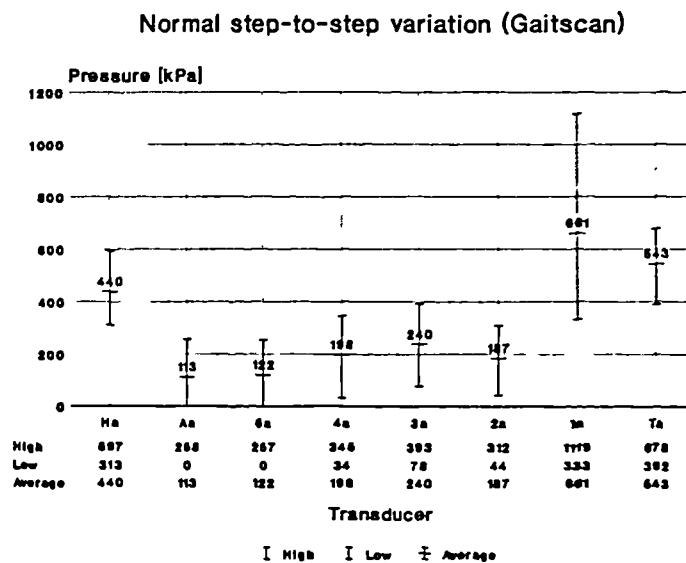


Figure 7.8 Peak pressure values for 21 foot steps for a normal subject obtained using Gaitscan. This indicates the range of the natural variation in peak pressure values that is expected for normal subjects.

Figure 7.8 shows the collected results from 21 steps for a subject (subject A). These results show the greatest variation of the peak pressure from the calculated mean of all the steps. The average of this greatest variation for the metatarsal area is 76%, for the heel 33%, for the arch 114% and for the toe 26%. This therefore indicates the step-to-step variation in peak pressure that is expected for normal subjects. As a comparison similar measurements were taken using the DPBG and figure 7.9 shows the results for a normal subject (subject B). Percentage variation figures for these results are 51% for the metatarsal area, 30% for the heel, 100% for the arch and 54% for the toe. Both of these sets of results are comparable, however it appears that for the shod foot there is a greater normal step-to-step variation in peak pressure for the metatarsal area.

### Normal step-to-step variation (DPBG)

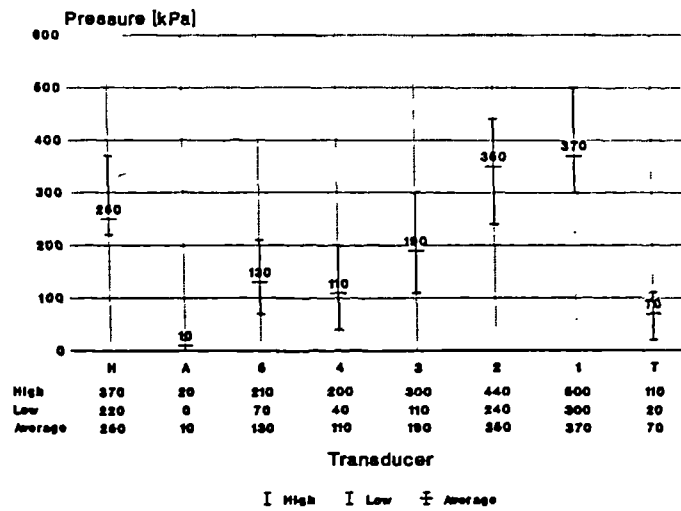


Figure 7.9 Peak pressure values for 10 foot steps for a normal subject obtained using the DPBG. This indicates the step-to-step variability in barefoot peak pressures that is expected for normal subjects.

### Repeatability for repositioned insole

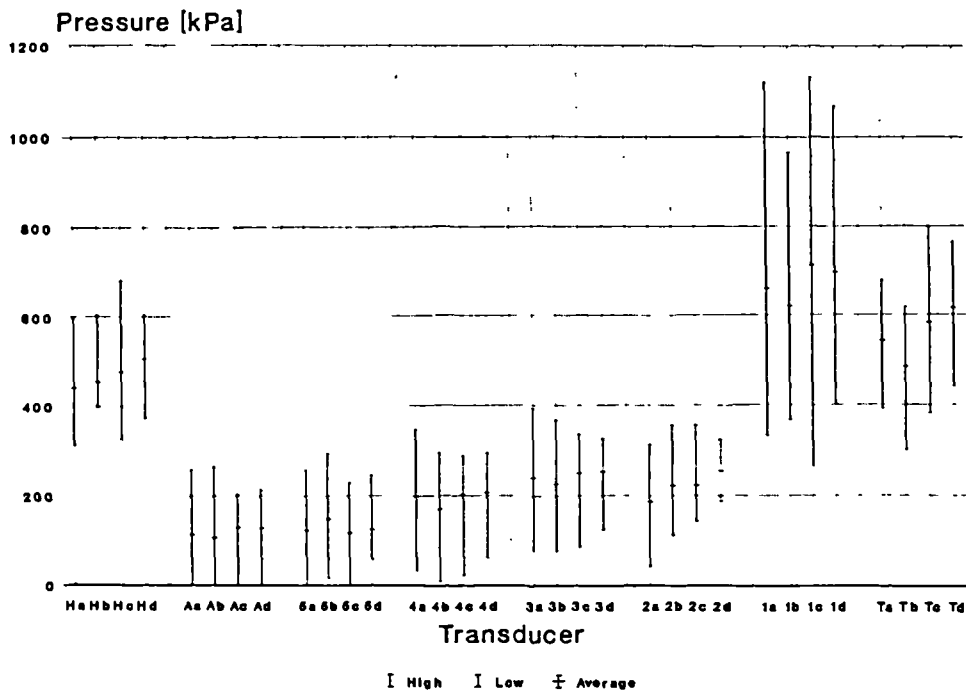


Figure 7.10 Results from repeated measurements with the same insole after having repositioned the insole prior to taken the recordings.

In general it can be concluded from these findings that the information from around 10 footsteps is required in order to establish a picture for a typical footstep in terms of pressure information. So that

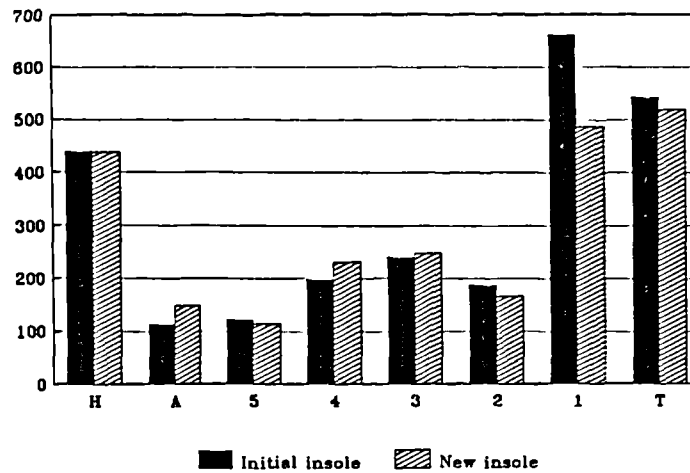


Figure 7.11 Peak pressure values obtained from tests using two different insoles for the same subject. This indicates how the construction of the insole can have an effect upon the measured pressure.

the effect of insole positioning upon measurement repeatability could be assessed the insole used for subject A was taken out of the shoe and repositioned 4 times. Four sets of measurements were taken and around 15 footsteps were analysed for each run. Figure 7.10 shows the results and the variation for the mean values for all transducers is within  $\pm 16\%$ . This indicates that the positioning of the insole and of the foot inside the shoe is likely to cause a change of up to 16% in the mean value of the peak pressures for a transducer. The other test was to have a new insole constructed by a different person. Measurements were taken with this new insole and compared to the results previously taken and described above. Figure 7.11 shows these results and it can be seen that the variation in the mean values is within 17%. This is slightly higher than the variation for the repositioned insole and shows that slight changes in the construction of the insole, i.e. the positioning of the transducers, can have an effect upon the measured peak pressure values.

### 7.3.3 Knee failure and its effect upon foot loading

The patient under investigation was due to have a knee operation in the near future because of a problem that occasionally caused the left knee to collapse without warning. There had also been the

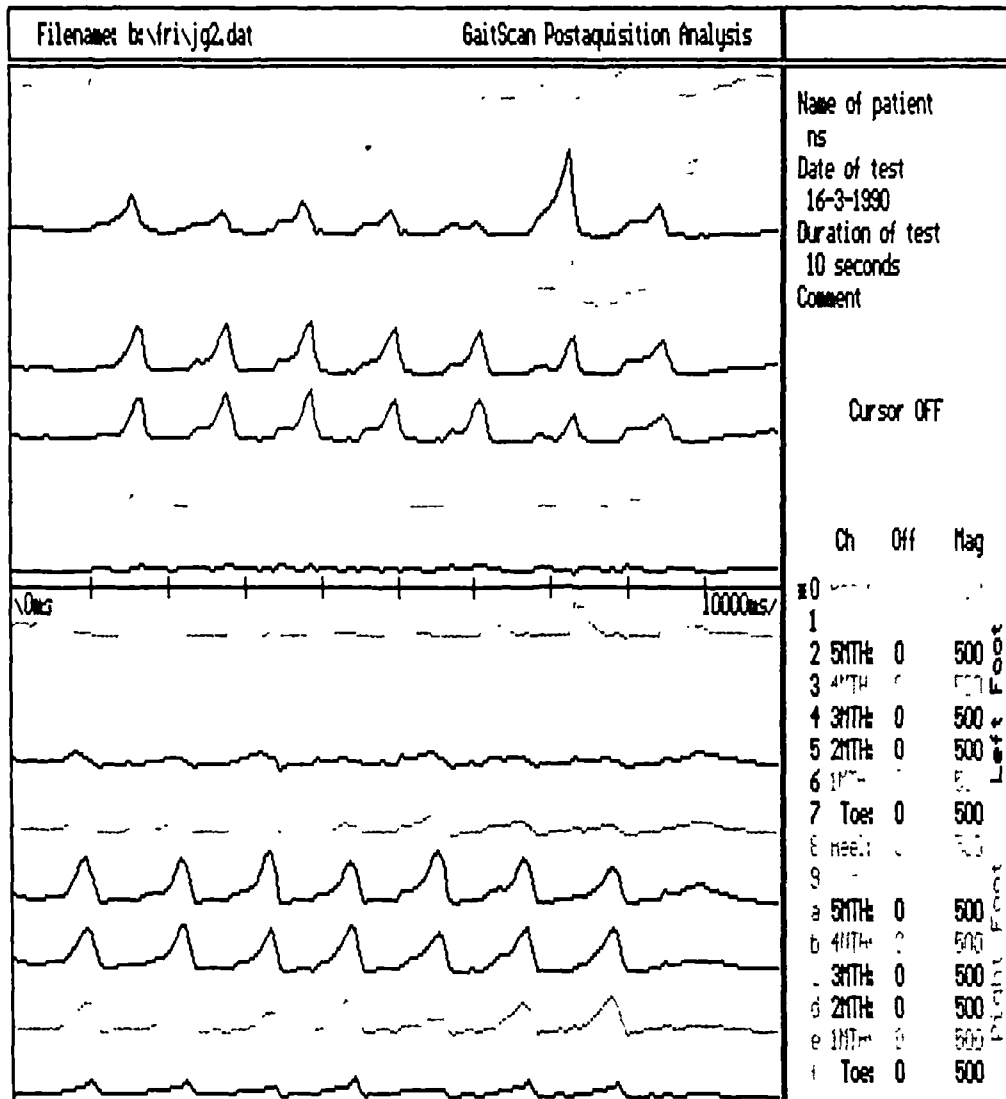


Figure 7.12 The main screen for a patient with a knee disorder. On the sixth step of the left foot the patients knee collapsed and this is shown by a sharp rise in the pressure under the lateral side of the foot.

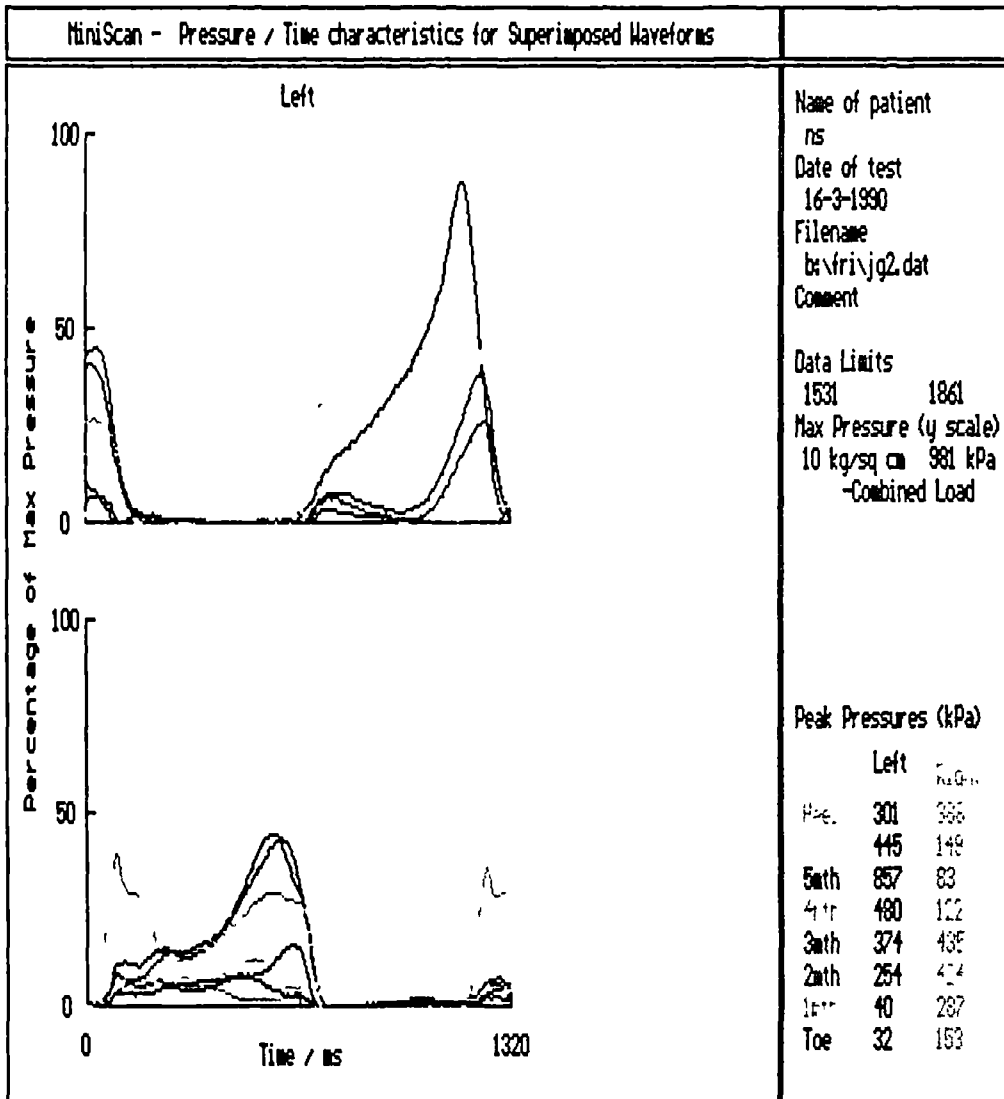


Figure 7.13 The miniscan screen for two selected footsteps of the test shown in figure 7.12. The information shown for the left foot indicates the abnormal pressure experienced by the foot because of the knee collapse.

recent complication of forefoot pain, thought to be related especially as the frequency of knee collapsing incidents had increased. Gaitscan tests were carried out and during the second test the patient's knee collapsed. Figure 7.12 shows the whole test and it can clearly be seen that the left knee collapsed on the sixth step. Figure 7.13 shows this step and the following right step in the expanded miniscan format. From figure 7.12 there are no obvious signs leading up to the incident, which supports the patient's claim that there is no prior warning.

#### **7.3.4 Results from a subject suffering from hindfoot pain**

This elderly subject had a history of forefoot pain and a number of operations had previously been performed in the hope of correcting structural deformities. The subject had returned to the DRI outpatient clinic complaining of pain somewhere in the hindfoot of the right foot while walking. Measurements were taken with the PBG and with Gaitscan. Figure 7.14 shows the results from the PBG which indicate a relatively normal CFP, however the forefoot is flat and loads very evenly, which is due to the dropped arches and callous sites. Figure 7.15 shows the pressure-time waveforms for an initial Gaitscan test. After further clinical consultation it was decided to add a 3mm PPT heel insert into the subject's shoe, and repeat the Gaitscan test. Figure 7.16 shows the results from this test. The subject indicated that the pain, although still remaining, had been reduced with the heel insert in place.

Comparing the results obtained after adding the insert to those obtained before, there was an average overall increase in the peak loading under the MPJ area of 9%, an increase of 37% experienced by the toe and a decrease of 7% under the heel. Adding the insert would have raised the heel slightly and so helped to reform the fallen arches. Also, its presence seems to have redistributed the loading under the foot while walking. The toe is more mobile than any other part of the foot, which could be the reason for the substantial increase in load beneath it - it may well have lied more directly on top of the transducer than it had previously. Another reason for this increase could be because the subject is walking more confidently while experiencing less pain, and so pushing off from the forefoot with more force.

It can be seen that in order to come to a decision as to what treatment to administer for this subject, many factors have had to be taken into consideration, for example, past history, and the presence of

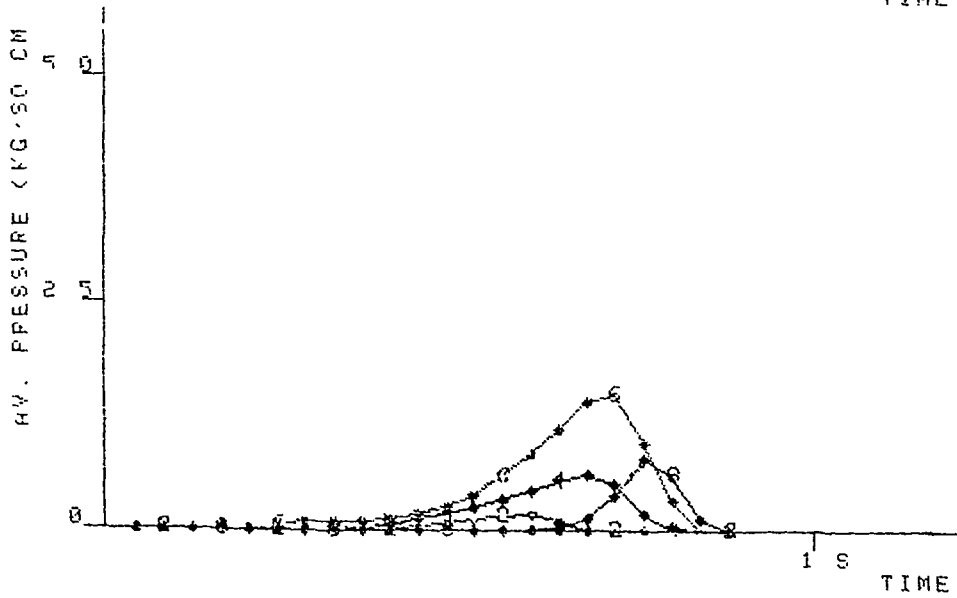
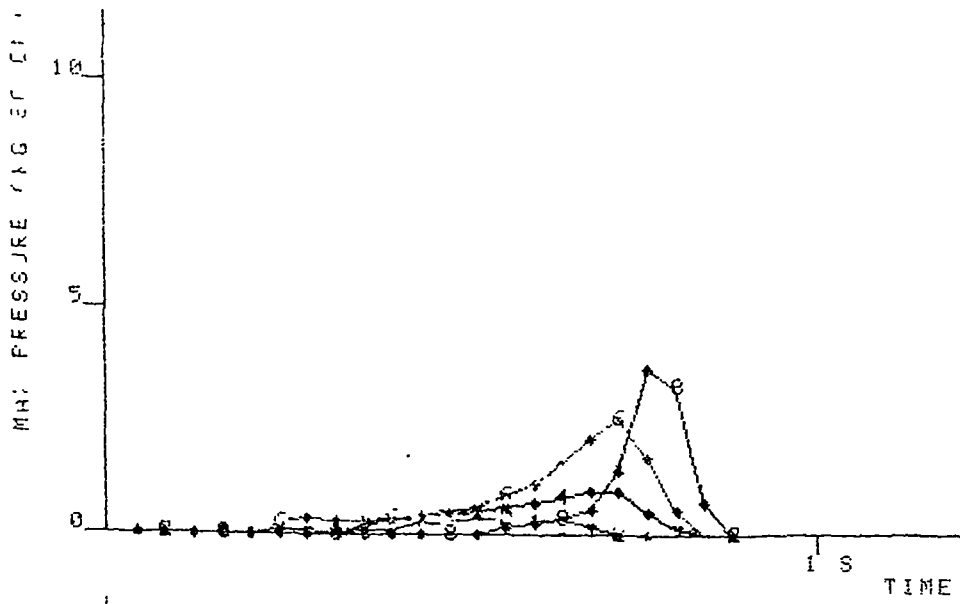
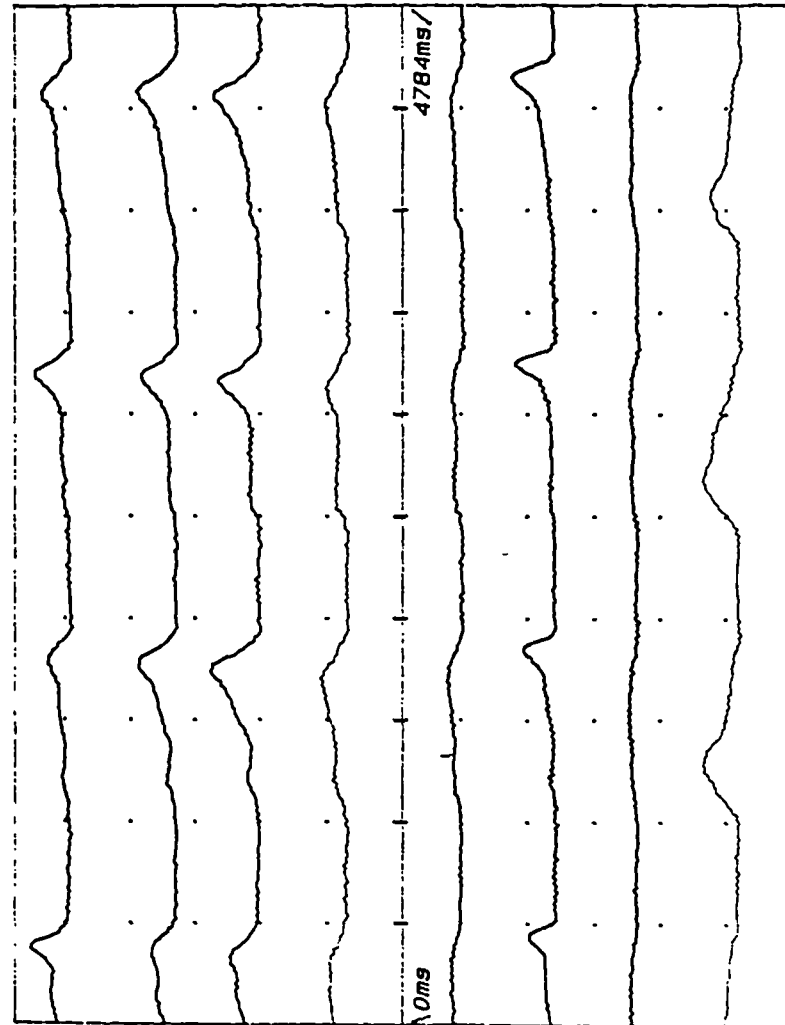


Figure 7.14 DPBG results for a patient with heel pain.

UKC MEDICAL ELECTRONICS LAB  
 ACQUIRED DATA WAVEFORM REPRESENTATION SOFTWARE



Filename :  
 d:\wed\taylor1.dat  
 Name of patient :  
 G. Taylor  
 Date of test :  
 13.9.89  
 Comment :  
 No Inserts

- \_\_\_ 1st MTH
- \_\_\_ 2nd MTH
- \_\_\_ 3rd MTH
- \_\_\_ 4th MTH
- \_\_\_ 5th MTH
- \_\_\_ Great Toe
- \_\_\_ Lateral Arch
- \_\_\_ Heel

Figure 7.15 Initial Gaitscan results for a patient with heel pain.

UKC MEDICAL ELECTRONICS LAB  
 ACQUIRED DATA WAVEFORM REPRESENTATION SOFTWARE

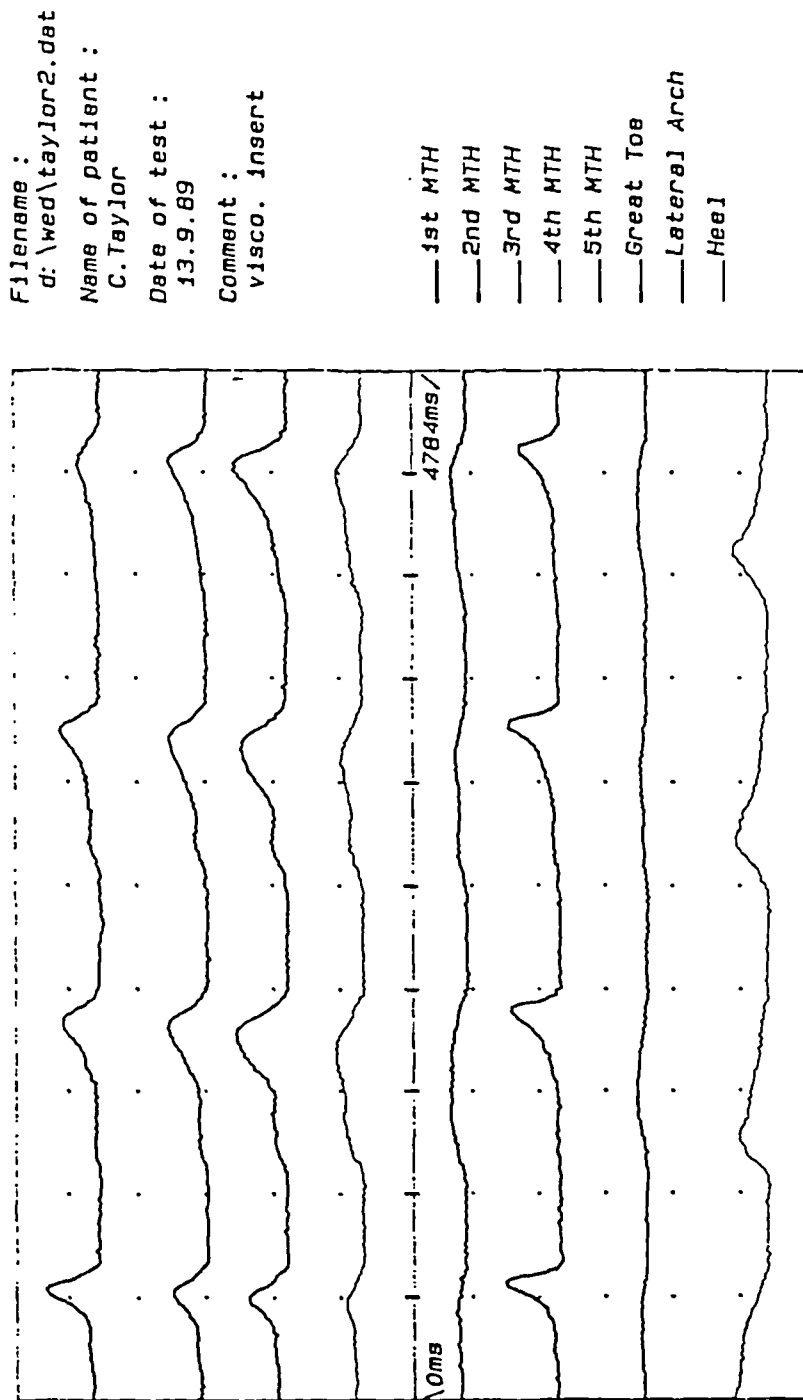


Figure 7.16 Post treatment Gaitscan results for a patient with heel pain.

fallen arches which were best diagnosed using the PBG. In this case measuring the in-shoe loading at certain sites has helped to quantify the effectiveness of the orthotic treatment.

### **7.3.5 Results form orthotic Insole Insert Investigations**

During clinical trials at the Brighton Polytechnic department of Podiatry collaborative work was initiated with a member of staff involved in a project investigating the effect of various insole materials on relieving pressure from lesion sites around the metatarsophalangeal joints. This collaboration was extremely useful in terms of being able to repeat measurements many times for a single subject: in total 87 sets of measurements each of duration 12 seconds were taken. It was also invaluable to have the opportunity to work along side a qualified podiatrist.

The subject had normal feet and so to engineer a pathological condition (such as a callous) a false lesion was formed using a modified golf ball green marker, after many different materials were tried much to the discomfort of the subject. This false lesion measured 1cm in diameter and had a thickness of 3mm, and was taped directly to the plantar surface beneath the 2nd MTH of the right foot. Measurements were initially taken without the false lesion in order to collect normal data, then with the false lesion and subsequent measurements were taken with a U'ed plantar pad in place fabricated from a variety of materials. This orthotic device covered the metatarsophalangeal joint area apart from the lesion site, hence it's name, as the cut-out is in the shape of a U. This is a common podiatric treatment used to relieve high pressure from an area of the foot. The materials used were 3mm and 7mm felt, PPT, Cleron, Sorbothane and closed cell foam.

As a comparative aid for analysis, a Musgrave Footprint system was used to obtain the barefoot plantar pressure distribution with the lesion in place and two pressure map results are shown in figure 7.17. It can be seen that pressure in excess of  $9\text{kg}/\text{cm}^2$  was detected at the site of the lesion and less than  $2\text{kg}/\text{cm}^2$  at the 1st MTH. Whilst this study used all eight transducers located in the usual way, the results and discussion are confined to a consideration of the sensor placed over the 2nd MTH. The peak pressure values for around twenty footsteps for each test were averaged and these results are shown in table 7.1.

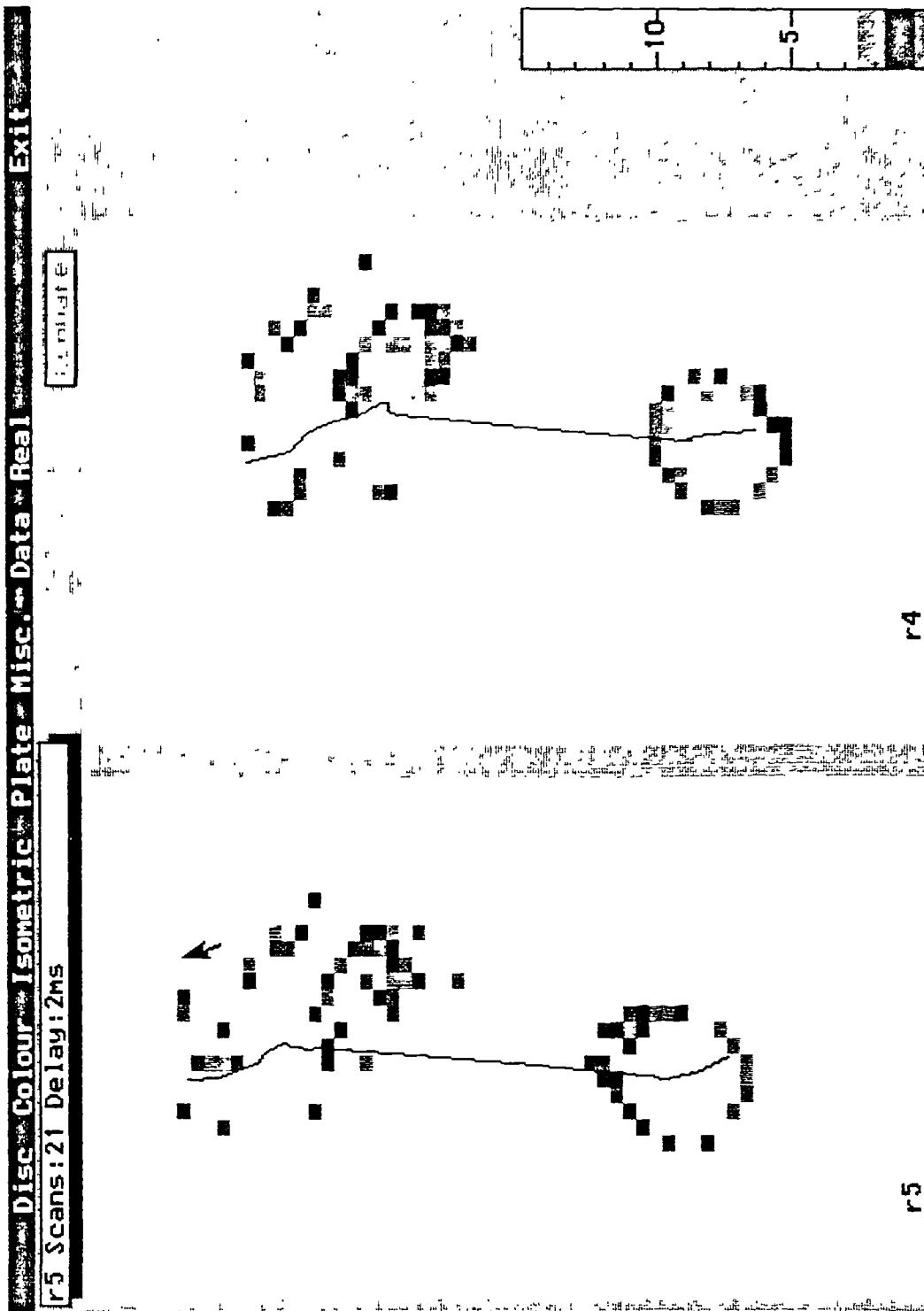


Figure 7.17 Two pressure distribution and CFP results obtained from the Musgrave colour footprint system. Subject is barefoot and wearing the false lesion under the 2nd MTH.

Condition	Peak Pressure values [kPa]	
	Average	S.D.
Normal	520	70
With Lesion	1017	83
Felt (3mm)	742	53
Felt (7mm)	708	46
PPT (6mm)	690	33
Cleron (6mm)	411	46
Sorbothane (6mm)	442	40
Closed Cell Foam (6mm)	390	32

Table 7.1 Results for the orthotic shoe insert tests - average peak pressure values for the 2nd MTH of the right foot

From these results it can be seen that the false lesion caused almost a doubling of the peak pressure compared with the normal reading. In order to further verify this result similar tests were carried out upon the left foot and the pressure values were 503 and 924kPa for normal conditions and with the false lesion respectively. This compares favourably with the results from the right foot and therefore as it was possible to repeat the condition it was then possible to carry out the tests upon different materials to determine whether a U'ed plantar pad could relieve the high pressure caused by the false lesion. The pressure values shown in table 7.1 indicate that the use of a U'ed plantar pad does relieve pressure from an area of high pressure, which at first seems an obvious result. However, in addition these results also give a quantitative indication of the relative effectiveness of the various materials used in relieving this pressure. It may be that lower than normal pressure such as that measured with the 6mm closed cell foam U'ed plantar pad may be as undesirable as a higher than normal pressure. Information of this sort can therefore be seen to provide valuable additional information to aid the selection of a particular material and thickness for the plantar pad.

### 7.3.6 System performance and measurement artifact

The weak point in most of the in-shoe foot pressure measurement systems previously developed commercially or for research purposes has been transducer unreliability. The two sets of transducers

used extensively for clinical trials have been subjected to a fair test of durability, which has included some 500 sets of measurements (each of around 20 footsteps). During this time there have been no failures and just one lead has had to be repaired due to fatigue at the interface with the transducer body. The only continual maintenance that had to be carried out was occasional re-lacquering (section 4.3.4). After around the first 150 trials it was noticed that signals from some of the transducers would be erratic and often cause saturation of the appropriate op-amp. This occurred only when the transducers were placed inside a shoe, and excessive humidity was found to be the cause (section 6.2.7). As this was due to a chipped lacquer layer, re-lacquering cured the problem, and this was carried out periodically after around 100 trials. It is expected that this problem would be eradicated if the modification to transducer design as detailed in section 4.3.4 is carried out. The harnessing of the equipment, after initial redesign following consultation with an orthotics department (DRI), has proved wholly satisfactory. Virtually all patients and subjects tested were confident of walking in their usual manner after only a few practice footsteps.

Figure 7.3 (section 7.3.1) shows the Gaitscan main waveform screen for a trial and there is noticeable baseline drift for channels *1MTH* and *Toe* for the right foot. This is due to temperature artifact, where during the test the transducer is raised or lowered in temperature due to the foot becoming more or less in contact with the transducer. This effect is particularly noticed for the toe transducer where there is more movement inside the shoe compared to the other seven areas. This drift does not present a problem, as long as op-amp saturation is not reached, to the contrary, the fact that a particular area of the foot is losing contact with the transducer could be clinically significant and so should be noted.

#### **7.4 A summery - clinical validity**

It has been shown that Gaitscan can be used in a clinical setting to obtain calibrated information. For a system to be used on a routine basis expense in terms of monetary cost and time must be kept to a minimum. At an estimated retail price of £4k including a computer it is thought that the initial cost could be met by the majority of centres interested in such equipment. In terms of actual clinical use the system is not time demanding, although this applies when an experienced operator is employed to carry out measurements. The results obtained can be effectively compared to those obtained from

other calibrated equipment, such as the DPBG which was used for the clinical trials. And it can be seen that the interface between the foot and the shoe is the important interface to now be investigating, especially now that increasingly more information is available for the barefoot-floor interface. Having successfully carried out the relatively small number of trials described in this chapter, it is clear that the information provided by the system could be of use in biomechanic studies, and so would be of great value in the design of footwear and orthoses. With further system refinement, mainly in the area of data presentation and analysis, it is expected that valuable data on a routine clinical basis could be obtained. The mere fact that quantitative measurements of this sort can now be recorded means that attention may be focused upon new areas, so that ultimately various foot disorders will be able to be quantified more reliably.

## **Chapter Eight**

**8**

# **DISCUSSION AND CONCLUSIONS**

## **8.1 Conclusions**

This chapter contains the conclusions for this thesis, and is split into three sections. Section 8.1 describes the overall conclusions for the work and is split into three areas: transducer development, instrumentation and clinical measurement. Section 8.2 gives details of suggested further work in continuation to this research, and finally section 8.3 provides a succinct concluding précis.

### **8.1.1 Transducer development**

Transducers have been developed using PVdF and copolymer piezoelectric films that are calibratable to within 10%. Piezo film is sensitive to stress in the three orthogonal directions and is also sensitive to shear stress. For this application the film has been incorporated into transducers that are sensitive to vertical stress, that is, stress applied in a direction perpendicular to the plane of the film. Because of the sensitivity to stress in the other directions bending will produce unwanted signals and so stiffening layers have been used which also serve as effective electrodes. It has been shown that error signals due to bending have been reduced to below a percent for the adopted transducer configuration. Fabrication techniques are made difficult due to the extremely inert properties of PVdF. This has been overcome, firstly by making use of copolymer film which is less inert (and less sensitive to bending), and secondly by the use of an etching process that was formally developed for PTFE and achieves a similar result for PVdF. It has therefore been possible to use conventional adhesive techniques for transducer fabrication. The harsh in-shoe environment has imposed several constraints upon transducer design. The transducers were designed as reusable devices and so consequently had to be durable enough to survive through a few hundred uses. Lead breakages and fatigue at the connection with the transducer were found to be a major problem and so a unique connection system was devised which resulted in a highly durable transducer that was capable of enduring in excess of 500 clinical uses. Charge leakage was a potential problem and this was dealt with by the use of a protective lacquer which was used to seal all parts of the sensitive electrode. Periodic lacquering during clinical use thus eliminated these problems.

Through the development of these transducers the in-shoe loading under specific areas of the foot required measuring and this was achieved by constructing an insole for each subject with the

transducers embedded in carefully selected areas that relate to these areas of interest. The information required from a foot pressure measurement system is data on the loading of specific areas of the foot. This was achieved by constructing an insole for each subject whereby each transducer is located at a carefully selected area relating to a specific site of interest. These insoles were constructed using conventional readily available materials.

A simple calibration jig was used so that individual transducers could be tested and calibrated. For stable conditions with the transducer positioned inside the jig a 4% repeatability was obtained. From further repeatability measurements it was found that this jig and method of calibration introduced errors (<10%), contributing to the overall transducer uncertainty of calibration. Hence better than quoted accuracy figures are expected for improved calibration techniques.

The pyroelectric activity of the piezo film resulted in an output d.c. drift because of transducer temperature variations. As expected the transducers constructed using a brass top layer responded more quickly to temperature change than those constructed using a double sided circuit board top layer. On the whole this effect remained acceptable for clinical measurements, and the quicker response is an advantage in terms of transducer stabilisation time. Additionally, to detect the loss of contact between the transducer and the foot may have clinically significant. The other temperature related transducer parameter, the temperature coefficient of sensitivity was investigated and was found to be better than that expected ( $73\text{fCN}^{-1}\text{K}^{-1}$ ) which means that only 1% uncertainty in transducer output is expected due to the in-shoe temperature variations.

### **8.1.2 Instrumentation**

A complete foot pressure measurement system has been designed and built. The requirements for this equipment were initially determined after giving consideration to existing equipment and taking advice from professionals who require such equipment. Exact requirements quickly became apparent after the equipment had been developed to the stage whereby it could be used in the clinic. Sixteen charge amplification channels have been built to receive signals from the eight transducers positioned in each shoe. A novel dual-stage technique has been implemented for these channels whereby the frequency response requirements for the initial stage are relaxed, and compensated for

by the second stage. The accuracy of the circuitry is determined by the random component generated noise and the uncertainty (0.1N) was estimated to be equivalent to 2pC input charge, 10% of the smallest input signal of 1N for a typical transducer sensitivity of 20pC/N. All d.c. errors and drifts do not affect accuracy as software techniques are used to remove these offsets. Custom software was written in Turbo Pascal to control data acquisition and subsequently display, analyse and produce hardcopies for the acquired pressure data. A commercial 12-bit 16 channel data acquisition card was used for data collection purposes which fulfilled the measurement resolution requirements of 1N, and a sufficient acquisition rate of 16k samples/sec was obtained thereby achieving the required 200Hz frequency response for each transducer. An upper 3dB cut-off point of 200Hz was chosen so that the equipment had sufficient bandwidth to capture pressure signals that were expected during high activity such as running. However it has been shown that the required frequency response for normal walking gait is 15Hz, which was concluded by observing the changing morphology of low pass filtered pressure signals: the morphology would alter for filtering less than 15Hz.

### **8.1.3 Clinical measurement**

From the clinical studies carried out during this research it can be concluded that the system can be used as a clinical tool and that meaningful results can be obtained, along side other measurement systems. An efficient measurement protocol has been devised during the clinical measurement periods that demands an acceptable length of time in which to prepare for and carry out measurements. Most of the 48 subjects investigated were regarded as normal and it has been shown that the results obtained for a particular subject are comparable with those obtained for the same subject using a dynamic pedobarograph. The advantages in obtaining foot pressure information for a run of consecutive footsteps has been demonstrated. Considerable step-to-step variation in the observed pressure values between steps has been recorded, and verified using a dynamic pedobarograph. This indicates that average information obtained from observing more than one footstep is necessary in order to obtain a true representative picture of foot pressure. It has been shown that a false lesion can introduce measurable high pressure. This is an important result as it

shows that high pressure caused by areas of callous and dropped metatarsals, for example, will be able to be detected. The most common form of treatment for high metatarophalangeal joint pressure is the use of a U'ed plantar cover, and it was shown that this did indeed reduce loading from the area of concern. Measurements were taken upon a patient with heel pain with and without an additional insole placed inside the patient's shoe. Virtually no measurable difference in pressure was detected upon adding this insole, however the patient indicated less pain and appeared to walk more confidently. This result is important as it demonstrates that for some conditions only a slight change in pressure will result in a desirable outcome, and so very accurate instrumentation is required in order to detect these small changes. More significantly, this shows that foot pressure is not the only parameter that indicates a condition and that in addition other parameters should also be observed.

## **8.2 Outline for future development**

As with most research, this work has thrown up many questions, and in continuation to the work there are areas that would benefit from further research which can be loosely divided into the following categories:

- (i) Further development of Gaitscan.
- (ii) The development of transducers and instrumentation for associated applications.
- (iii) Spin-off applications.
- (iv) The development of combined systems to enable the direct comparison of measurements.

*These areas are discussed within the following sections.*

### **8.2.1 Transducer design and development**

Future development of the discrete piezo film transducer would be in the area of production and manufacturing. Because of the prototype nature of the techniques used to fabricate the transducers for this research they have been meticulously constructed by hand, and efficient fabrication methods would have to be devised so that the project could be taken one step further towards manufacture. There are possibilities for further transducer development for other applications related to this research. For example, the development of transducers for in-shoe shear force measurement, which

is described in section 8.2.2, and secondly the development of a matrix insole incorporating arrays of piezo film sensors, which is described in section 8.2.3. The list does not stop here and there are a diversity of other applications that could benefit from the basic transducer design and development knowledge contained within this thesis.

### **8.2.2 A shear force transducer**

The difficulties of shear force measurement using piezo film have been described in section 3.4.2. Basically because the charge developed across the thin edges of the film due to a directly applied shear force is only in the order of pico-coulombs then sophisticated front-end electronic signal processing is required so that the uncertainty in measurements is kept below an acceptable level (20%). Research into this area is currently being carried out at the University of Kent.

Other methods of shear force measurement using piezo film in an indirect manner are possible. A prototype transducer has been constructed (section 4.4) which provides a signal due to the stretch of an internal piezo film element caused by an applied shear force. Further work upon transducer constructions of this sort is required to verify the technique and to establish whether the design could be miniaturised so that the dimensional requirements for an in-shoe measurement system could be met. There could still of course be spin-off applications if these requirements could not be met.

### **8.2.3 An insole incorporating a matrix of piezo film sensors**

Since completing the research of this thesis, the author has been involved in further research investigating matrix arrays of piezo film transducers with the aim of developing an in-shoe pressure measurement system built around pre-constructed insoles incorporating strategically placed arrays of transducers. This research was a one year pilot study funded by the Scottish Home and Health Department and was carried out at Dundee University. The work undertaken (ref. report # K/RED/4/C/119) was basically a feasibility study and mainly covered the area of transducer development. Outlined below is the justification of the requirements for such a system.

Currently the most popular (and probably the most acceptable) method of measuring plantar pressure distribution is the dynamic pedobarograph. In general this device appears to measure pressure to

within an uncertainty of 10%. However only one random footstep for the barefoot can be measured at any instant, and the device has a relatively low frequency response of 12Hz. It would be desirable to obtain in-shoe pressure distribution information for multiple footsteps thus allowing a pressure picture to be developed for particular areas of the plantar aspect of the foot, such as across the metatarsals. Initial research and development would be carried out upon a small transducer array of 4x4 sensors. Extensive bench and clinical tests could then be performed with this matrix transducer in order to highlight performance difficulties. In response to the findings of these experiments the design requirements for a set of standard, non-customised insoles will be determined. These insoles are expected to contain a maximum of 100 sensors each measuring 6x6mm (requirements for a mens size 12 insole). The insoles will be termed *semi-matrix* insoles in that sensors will only be distributed over the areas of interest (primarily the metatarsal region). It should be noted that the TecScan system is currently able to record 4 seconds of in-shoe data for one foot and so provides in-shoe pressure distribution for the whole of the plantar surface of the foot.

The main difficulties with the development of a matrix insole are related to constructional requirements. In chapter 3 it has been mentioned how bending of the sensor area can yield erroneous data and so it is important to make each sensor site rigid. This requirement is in conflict with that of having a flexible insole of minimal thickness. It is therefore suggested that each sensor site should be individually restrained from bending using small rigid structural elements. Unfortunately delamination of these rigid elements is a potential problem if the insole is used with worn or very compliant shoes. This is because the insole possesses a *chain-mail* type flexibility and extreme local bending, or *spherical bending*, may put high stresses upon adhesive bonds. In order to allow spherical bending and so reduce this problem a very flexible circuit material is desirable so that the necessary insole interconnections can be made and so the flexibility between rigid sensor sites is kept to a maximum. Mechanical and electrical crosstalk, and efficient electrical connection are two very important and substantially interrelated areas of the transducer design. It is essential to minimise mechanical coupling so that an applied force on any one sensor site is not transmitted through the insole layers or through any electrical connection leads to adjacent sensors. Equally as important, it is necessary to minimise electrical (charge) coupling between sensors by careful routing of any electrical

connections. Physical connections to the piezo film surface are of course necessary and will be best achieved using flexible circuit materials with carefully routed conductive tracks, in order to fulfil the above requirements.

Together with this transducer development, work is also being carried out upon the electronic processing of the charge signals from these transducer arrays and software is being developed to acquire and display the data.

#### **8.2.4 System calibration**

To enable calibrated pressure measurement the procedure for system calibration was briefly as follows: the transducers were calibrated using a static loading jig and a range of applied force, resulting in the calculation of an average  $\text{pCN}^{-1}$  sensitivity figure for each transducer. These sensitivity values together with a value for the gain of the electronics were stored in an ascii file, which is used by the Gaitscan suite of programs. Thus the transducer calibration procedure is relatively simple and it has been assumed that the transducers behave in a similar fashion once removed from the bench and placed into the different in-shoe environment. To precisely model the performance of a transducer in the in-shoe environment would be extremely complex, as mentioned in chapter 3, and so more detailed information should be obtained experimentally. Now that the basic calibration techniques have proven successful it is necessary to specialise the experimental techniques in order to obtain this information. There are factors such as the anatomy of the foot, shoe construction and materials, etc, that may influence transducer response and these could be tested if some thought is given to the mechanical construction and capabilities of a testing jig. Transducer bending effects are also virtually impossible to accurately model, however with the aid of a model metatarsal head built into the mechanical jig, and a means for providing backing materials of different compliances to simulate a shoe insole, these effects could be investigated further in order to test new transducer designs. This task would require an accurately calibrated load cell to measure applied load and additional software to correlate the signal from this load cell with the corresponding signal from a transducer under test. A mechanical jig could be designed around a press so that a varying force could be applied to the load cell through the transducer. With automatic calibration techniques in

mind, a computer program could be tasked to calculate a sensitivity figure for the transducer and if interfaced with the Gaitscan software the ascii calibration file could be periodically updated. A quick system check and electronic calibration routine could also be written into this program: if a sine wave of known amplitude is fed through a known capacitance to each channel of electronics in place of the transducers, this effectively simulates an input charge of a known amount. The program could calculate a hardware calibration factor upon monitoring the output of each channel and this information can then be supplied to the Gaitscan software. This work is now being implemented under the research program at the University of Kent.

### **8.2.5 Instrumentation developments**

Further developments would be along the lines of additional equipment to add features to the existing system. Although during clinical trials the use of an umbilical cord has not been a problem, a neater approach would be to collect data remotely using, for example, a portable data recorder carried by the patient. This would also make the system more versatile in that measurements could be taken practically anywhere. For 200Hz transducer frequency response data would have to be stored at 32kbytes/sec, and so for a solid state recorder sufficient memory would have to be available for the desired length of test (640kbytes for 20 seconds). Commercially available recorders tend to have a generalised nature and severe memory and/or acquisition rate restrictions and so a dedicated piece of equipment would have to be designed and constructed.

### **8.2.6 Software developments**

Gaitscan allows minimal data analysis in that just magnitude and timing information for any pressure-time waveform may be obtained. Commercial data analysis software packages such as DADisp and Matlab may be used to perform more complex mathematics upon the data, however this is quite a lengthy process and would normally be used just to enable the requirements for custom software to be determined. The type of data presentation and analysis necessary for foot pressure measurement systems is fairly well known and defined, as detailed in section 2.3.2. However the analysis of multiple footsteps has not been adequately addressed. It has been shown from the results of clinical trials that

pressure distribution patterns vary from step-to-step, especially due to mediolateral sway. So with this in mind an accurate representation of a typical footstep can only be obtained by averaging the data from a run of multiple footsteps. This would be a software task, and user interaction would be necessary so that clinical judgement could be brought into the process. Some thought has been given to the mechanisms that would be involved for the above multiple footstep averaging process: each waveform for single steps from each transducer could be represented by a polynomial equation, having initially defined relevant parameters such as width, height, slope of the waveform, etc. If the entire file was mathematically converted into a list of polynomials and decode information then this would also have the desirable effect of greatly reducing the size of a data file. Once in this form the data could be averaged, manipulated and displayed as desired. So in conclusion the Gaitscan software could be considerably improved in terms of data presentation and analysis so that first, it is on par with existing commercial systems and second, it goes one step further and enables the complex analysis of multiple footsteps.

#### **8.2.7 Combined gait analysis studies**

As has been mentioned (section 1.3), foot pressure measurement is just one area of gait analysis. The measurement techniques used, and so the choice of system, depends upon the type of information that is considered the most appropriate for any one situation / clinical condition (although in practice equipment availability is a major factor in this decision). In the ideal situation many gait parameters would be measured, however the differences between systems in terms of their uncalibrated nature and because of the differences in the type of information produced means that the comparison of information is problematic and very often impossible. To combat these incompatibilities integrated systems are required that enable a wide range of information to be captured, so allowing the comparison of gait parameters. In its simplest form, for example, this would be a common time base. This integrating process would chiefly be a software task involving the *combined data collection from the selected hardware systems, and the associated manipulation, analysis and display of this data.* At Dundee university research of this type is currently being carried out where Gaitscan and an EMG measurement system are being linked up so that in-shoe pressure

and lower limb muscle activity can be correlated. Another suggested project would be the linking of Gaitscan with the dynamic pedobarograph. Presently the areas of interest within the pedobarograph plantar pressure distribution map are selected for analysis without reference to the actual foot. Whereas the Gaitscan transducers are located beneath the same eight areas with reference to the foot. If a template containing this transducer positional information and transducer size could be imported into the pedobarograph system as additional information then, with modifications to the pedobarograph software, exactly the same areas could be selected within the pressure distribution map. This would enable more accurate comparisons between barefoot and in-shoe pressure which could enable, for example, footwear to be quantified more accurately in terms of foot pressure distribution and the effect of this footwear upon this distribution.

#### **8.2.8 Clinical measurement**

The clinical measurements obtained for this work indicate that the system is functionable in a clinical situation and that useful results can be obtained. There is of course huge scope for further clinical measurement which can be conducted in the two distinct areas of normals and pathologies. In the early stages of clinical trials it was discussed that it would be of use to obtain measurements from a patient group with a particular pathology, such as hallux valgus, and this was usually how other research groups have decided upon the criteria for their measurements (section 2.3.3). However a good knowledge of normal foot pressure distribution is required before pathologies can be quantified in terms of the associated divergence (or not) from this normal, and so further clinical trials should be in this area - a comprehensive study of normals. It has been found that normal pressure patterns can be classified into one of 3 or 4 groups, the difference between the groups being different loading patterns transversely across the metatarsophalangeal joints (Foot Society annual meeting, Royal Liverpool Hospital, Nov. 1990). This being the case, computer aided decision making may be of use for the classification of a foot pressure pattern. In addition to the normal patient group two further groups could be investigated. The first, those with anatomical abnormalities, such as rheumatoid arthritis where there are clearly defined callosities caused through metatarsal collapse. And the second, those with apparently normal anatomy but who have foot problems caused by insensitivity

and are known to have high peak plantar pressure, such as diabetics.

For all further measurements it is suggested that as well as the usual age, weight, height, condition, etc, information that should be noted for each subject, footwear should also be a consideration for an in-shoe measurement system such as Gaitscan. It is not yet fully understood how footwear can affect plantar pressure distribution, and so it is reasonable to consider taking measurements where some control over this unknown is possible. This could be achieved through the use of orthopaedic shoes, for example, and for comparative purposes a second set of measurements could also be taken with, for example, the subject's most comfortable pair of shoes. If the information from measurements is recorded in this way then many results could be correlated with the use of data base type software.

### **8.3 Conclusions**

In conclusion, the aims of this research have been met and a bi-pedal in-shoe foot pressure measurement system has been designed, constructed and used in a clinical setting.

The properties of piezoelectric polymer films have been investigated and various transducer designs have been fabricated, with the eventual outcome of the present discrete transducer. Attention has been given to all the constraints imposed by the hostile environment in which the transducer is required to operate, and an exceptional record of reliability has been achieved. An effective insole fabrication technique has evolved during the various trials carried out at two clinical centres and thus eight transducers can quickly be incorporated into an insole, ready for measurements. With an insole positioned in each shoe information is supplied by the sixteen transducers for multiple consecutive footsteps. An electronic system has been designed to detect these signals and to subsequently provide voltage signals to a computer data acquisition card. All the necessary requirements for this instrumentation have been met and an overall uncertainty of 0.1N has been specified. The system would not be complete without the custom designed software which enabled rapid project development at a later stage during clinical trials, due to the more meaningful nature of the results. Essential analysis could be achieved using this software and it has the unique feature of being able to display pressure information for multiple footsteps. This system has been named Gaitscan and has already been of clinical use and furthermore has been incorporated into other research projects as

a research and clinical tool. It is hoped that some of the questions thrown up and the opportunities provided by this study will be the fuel for further research in this or a related field.

## REFERENCES

- Abboud, R., *Evaluation of an inshoe pressure measuring system*, 1989. MSc thesis. Dundee University.
- Charonson, Z., Voloshin, A., Steinbach, T.V., Brull, M.A., and Farine, I., "Normal foot-ground pressure pattern in children," *Clin. Orthopaedics & Rel. Research*, vol. 150, pp. 220-223, July 1980.
- Alexander, I.J., Chao, E.Y., and Johnson, K.A., "The assessment of dynamic foot-to-ground contact forces and plantar pressure distribution: A review of the evolution of current techniques and clinical applications," *Foot and Ankle*, vol. 11(3), pp. 152-67, Dec. 1990.
- Arvan, M. and Brull, M.A., "A fundamental characteristic of the human body and foot. The foot-ground pressure pattern," *J. Biomechanics*, vol. 9(9), pp. 453-457, 1976.
- Arizumi, H., Morita, M., and Yonemoto, K., "A simple method of measuring the footsole pressure of normal subjects using prescale pressure detecting sheets," *J. Biomechanics*, vol. 16(2), pp. 157-165, 1983.
- Arsenault, A.B., Winter, D.A., Marteniuk, R.G., and Hayes, K.C., "How many strides are required for the analysis of electromyographic data in gait?," *Scand J Rehab Med*, vol. 18, pp. 133-135, 1986.
- Arvikar, R. and Seireg, A., "Pressure distribution under the foot during static activities," *Eng. in Med.*, vol. 9(2), pp. 99-103, 1980.
- Barnett, C.H., "A plastic pedograph," *Lancet*, p. 273, Aug. 1954.
- Barnett, C.H., "The phases of human gait," *Lancet*, pp. 617-622, Sept. 1956.
- Bauman, J.H., and Brand, P.W., "Measurement of pressure between the foot and the shoe," *Lancet*, pp. 629-632, Mar. 1963.
- Beely, F., "Zur mechanik des Stehens," *Langenbecks Archiv fur Chirurgie*, vol. 27, pp. 457-71, 1882.
- Betts, R.P., Duckworth, T., and Austin, I.G., "Critical light reflection at a plastic/glass interface and its application to foot pressure measurements," *J. Med. Eng. & Tech.*, vol. 4(3), pp. 136-142, May 1980.
- Betts, R.P., Franks, C.I., and Duckworth, T., "Analysis of pressures and loads under the foot. Part 1: Quantitation of the static distribution using the PET computer," *Clin. Phys. Physiol. Meas.*, vol. 1(2), pp. 101-112, Feb. 1980.
- Betts, R.P., Franks, C.I., Duckworth, T., and Burke, J., "Static and dynamic foot pressure measurement in clinical orthopaedics," *Med. & Biol. Eng. & Comput.*, vol. 18, pp. 674-684, Sept. 1980.
- Betts, R.P., and Duckworth, T., "A device for measuring plantar pressures under the sole of the foot," *Eng. in Med.*, vol. 7(4), pp. 223-228, 1978.
- Beverly, M.C., Horan, F.T., and Hutton, W.C., "Load cell analysis following silastic arthroplasty of the hallux," *Int'l. Orthop.*, vol. 9, pp. 101-104, 1985.
- Bhat, S., Webster, J.G., Tompkins, W.J., and Wertsch, J.J., "Piezoelectric sensor for foot pressure measurement," *IEEE Eng. in Medicine & Biol. Soc. 11th Annual Int. Conf. - Instrumentation for Rehabilitation and Biomechanical measurements*, pp. 1435-6, 1989.
- Boulton, A.J.M., Franks, C.I., Betts, R.P., Duckworth, T., and Ward, J.D., "Reduction of abnormal foot pressure in diabetic neuropathy using a new polymer insole material," *Diabetes Care*, vol. 7(1), pp. 42-46, 1984.

- ransby-Zachary, M.A.P., Stother, I.G., and Wilkinson, R.W., "Peak pressures in the forefoot," *J. Bone & Jt. Surgery*, vol. 72-B(4), pp. 718-21, July 1990.
- Kjaer Bruel, *Piezoelectric accelerometers and vibration preamplifiers*, 1978. Theory and Application Handbook
- ady, W.G., *Piezoelectricity: an introduction to the theory and applications of electromechanical phenomena in crystals*, Dover Publications, New York, 1964. (2nd ed 2 v)
- arlisle, B.H., "Piezoelectric plastics promise new sensors," *Machine Design*, Penton Publishing Inc, Cleveland, Oct. 1986.
- avanagh, P.R., "Technical note: Technique for averaging centre of pressure paths from a force platform," *J. Biomechanics*, vol. 11(4), pp. 487-491, 1978.
- avanagh, P.R., Rodgers, M.M., and Liboshi, A., "Pressure distribution under symptom-free during barefoot standing," *Foot and Ankle*, vol. 7(5), pp. 262-76, Apr. 1987.
- handrasekaran, H., "On the measurement of average foot pressure and ground reactions during walking cycle," *J. Mech. Design*, vol. 102, pp. 683-687, Oct. 1980.
- hatigny, J.V. and Robb, L., "Sensors: making the most of piezo film," *Sensor Review*, vol. 7(1), pp. 15-20, Jan. 1987.
- hoderer, J.D. and Lord, M., *Pedobarographic foot-pressure measurements and their applications*, pp. 173-81. In: *Disability: proceedings of a seminar on rehabilitation of the disabled* (Eds. R.M. Kenedi, J.P. Paul, J. Hughes), Macmillan Press, Baltimore, 1979.
- larke, T.E. and Cavanagh, P.R., "Pressure distribution under the foot during barefoot walking," *Med. Sci. Sport*, vol. 13, p. 135, 1981.
- layton, G.B., *Operational amplifiers*, Butterworth & Co, 1985. (2nd ed.).
- leaver, A.J. and Pantelis, P., "Piezoelectric poly(vinylidene fluoride) films for use in telecommunications," *Proc. Plastics in Telecommunications III, The Plastics and Rubber institute*, pp. 32.1-32.9, Sept. 1982.
- ollis, J.M.F. and Jayson, M.I.V., "Measurement of pedal pressures," *Ann. Rheum. Dis.*, vol. 31, pp. 215-217, 1972.
- rouse, J., Wall, J.C., and Marble, A.E., "Measurement of the temporal and spatial parameters of gait using a microcomputer based system," *J. Biomed. Eng.*, vol. 9(1), pp. 64-68, Jan. 1987.
- tercteko, G.C., Dhanendran, M., Hutton, W.C., and LeQuesne, L.P., "Vertical forces acting on the feet of diabetic patients with neuropathic ulceration," *Br. J. Surg.*, vol. 68, pp. 608-614, 1981.
- unningham, D.M. and Brown, G.W., "Two devices for measuring the forces acting on the human body during walking," *Proc. Soc. Exp. Stress Analysis*, vol. 9(2), pp. 75-90, 1952.
- ario, P. and DeRossi, D., "Tactile sensors and the gripping challenge," *IEEE Spectrum*, pp. 46-52, Aug. 1985.
- ario, P., Bardelli, R., DeRossi, D., Wang, L.R., and Pinotti, P.C., "Touch sensitive polymer skin uses piezoelectric properties to recognise orientation of objects," *Sensor Review*, pp. 194-198, Oct. 1982.
- Derbyshire, B. and Platts, R.G.S., "A shapeable foot-pressure measuring device," *J. Biomed. Eng.*, vol. 11(5), pp. 258-64, May 1989.
- DeReggi, A.S., Edelman, S., and Roth, S.C., "Piezoelectric polymer transducers for dynamic pressure measurements," *Department of transportation, Washington D.C. report no. PB 264125*, June 1976. Kynar information pack, ref. F15.

- DeReggi, A.S., Roth, S.C., Kenney, J.M., and Eldelman, S., "Piezoelectric polymer probe for ultrasonic applications," *J. Acoust. Soc. Am.*, vol. 69(3), pp. 853-859, 1981.
- DeRossi, D. and Domenici, C., "Piezoelectric properties of dry human skin," *IEEE Transactions on Electrical Insulation*, vol. EI-21(3), pp. 511-7, June 1986.
- Dhanendran, M., Hutton, W.C., and Paker, Y., "The distribution of force under the human foot- an on line measuring system," *Measurement & Control*, vol. 11(7), pp. 261-264, 1978.
- Dhanendran, M., *A minicomputer instrumentation system for measuring the force distribution under the feet*, 1979. PhD Thesis, PCL.
- Donarski, R.J., *Bone fracture measurement using mechanical vibration*, 1989. PhD thesis. University of Kent at Canterbury.
- Drganich, L.F., Andriacchi, T.P., Strongwater, A.M., and Galante, J.O., "Electronic measurement of instantaneous foot-floor contact patterns during gait," *J. Biomechanics*, vol. 13(1), pp. 875-880, 1980.
- Duckworth, T., Betts, R.P., Franks, C.I., and Burke, J., "The measurement of pressures under the foot," *Foot and Ankle*, vol. 3(3), pp. 130-141, 1982.
- Durie, N.D. and Shearman, L., "A simplified limb-load monitor," *Physiotherapy Canada*, vol. 31(1), pp. 28-31, 1979.
- Dvorsky, J.E., Kelley, B.A., McCown, R.B., and Renner, G.F., *Active multilayer piezoelectric tactile sensor apparatus and method*, Jan 1987. U.S. Patent No. 4,634,917.
- Feehery, R.V., "Clinical applications of the electrodyneogram," *Clinics in Podiatric Medicine and Surgery*, vol. 3(4), pp. 609-12, Oct. 1986.
- Fox, D.R., Sudworth, K., Booth, M.C., and Penneck, R.J., "A versatile piezoelectric cable," *IEEE Ultrasonics symposium*, pp. 599-602, 1986. (Raychem Ltd, Swindon)
- Franks, C.I., Betts, R.P., and Duckworth, T., "Microprocessor-based image processing system for dynamic foot pressure studies," *Med. & Biol. Eng. & Comput.*, vol. 21, pp. 566-572, Sept. 1983.
- Frost, R.B. and Cass, C.A., "A load cell and assembly for dynamic pointwise vertical force measurement in walking," *Eng. in Med.*, vol. 10(1), pp. 45-50, 1981.
- Gabel, R.H., Johnston, R.C., and Crowninshield, R.D., "A gait analyser / trainer instrumentation system," *J. Biomechanics*, vol. 12, pp. 543-549, 1979.
- Gautschi, G.H., *Piezoelectnc multicomponent force transducers and measuring systems*, 27th June 1978. Transducer '78 conference report, load and force measurement session.
- Gerber, H., "A system for measuring dynamic pressure distribution under the human foot," *J. Biomechanics*, vol. 15(3), pp. 225-227, 1982. A technical note.
- Gifford, G. and Hughes, J., "A gait analysis system in clinical practice," *J. Biomed. Eng.*, vol. 5, pp. 297-301, Oct. 1982.
- Graeme, J.G., Toby, G.E., and Huelsman, L.P., *Operational amplifiers - design and applications*, McGraw Hill, 1971.
- Green, S.L. and Gliddon, J.E.C., *General degree applied maths*, University tutorial press, London, 1966.
- Grieve, D.W. and Rashdi, T., "Pressures under normal feet in standing and walking as measured by foil pedobarography," *Annals Rheumatic Dis.*, vol. 43, pp. 816-818, 1984.
- Grieve, D.W., "Monitoring gait," *Br. J. Hosp. Med.*, pp. 198-204, Sept. 1980.

- Gross,T.S. and Bunch,R.P., "Measurement of discrete vertical in- shoe stress with piezoelectric transducers," *J.Biomed.Eng.*, vol. 10(5), pp. 261-265, May 1988.
- Grundy.M., Blackburn.P.A., Tosh.R.D., McLeish.R.D., and Smidt.L., "An investigation of the centres of pressure under the foot while walking," *J.Bone & Jt.Surgery*, vol. 57-B(1), pp. 98-103, 1975.
- Halvorsen,D., *Personal communication*. (Atochem Ltd)
- Halvorsen,D.L., "Properties and applications of piezo film transducers," *Electronics & Power*, pp. 744-746, Oct.1986.
- Harris,J.D. and Copeland,K., *Orthopaedic engineering*, Biological engineering society, London, 1978.
- Harris,R.I. and Beath,T., *Army foot survey*, National research council of Canada, Ottawa, 1947. Report.
- Helal,B. and Wilson,D., *The Foot*, Churchill Livingstone, Edinburgh, 1988. 2 vols.
- Hennacy,R.A. and Gunther,R., "A piezoelectric crystal method for measuring static and dynamic pressure distributions in the feet," *J.Am.Podiatry Assn.*, vol. 65(5), pp. 444-449, May 1975.
- Hennig,E.M., Cavanagh,P.R., Albert,H.T., and Macmillan,N.H., "A piezoelectric method of measuring the vertical contact stress beneath the human foot," *J.Biomed.Eng*, vol. 4(7), pp. 213-221, 1982.
- Henry,A.P.J. and Waugh,W., "The use of footprints in assessing the results of operations for hallux valgus," *J.Bone & Jt.Surgery*, vol. 57-B(4), pp. 478-481, Nov.1975.
- Hermens,H.J., deWaal,C.A., Buurke,J., and Zilvold,G., "A new gait analysis system for clinical use in a rehabilitation center," *Orthopedics*, vol. 9(12), pp. 1669-1675, Dec.1986.
- Hertzberg,H.T.E., "Some contributions of applied physical arthropology to human engineering," *Annals N7 Academy Sci*, vol. 63(4), pp. 50-7, 1955.
- Holmes-Siedle,A.G., Wilson,P.D., and Verrall,A.P., "PVdF: An electronically active polymer for industry," *Materials & Design J.* Fulmer Yarsley information, a reprinted article.
- Hughes,J. and Klenerman,L., "A clinicians view of foot pressure: A comparison of three different methods of measurement," *Foot and Ankle*, vol. 7(5), pp. 277-84, Apr.1987.
- Humphreys,J., Ward,I.M., McGrath,J.C., and Nix,E.L., "The measurement of the piezoelectric coefficients d31 and d3h for uniaxially oriented polyvinylidene fluoride," *Ferroelectrics*, vol. 67, pp. 131-136, 1986.
- Hutton,W.C. and Drabble,G.E., "An apparatus to give the distribution of vertical load under the foot," *Rheum. phys. Med.*, vol. 11, pp. 313-317, 1972.
- Hutton,W.C., Stott,J.R.R., and Stokes,I.A.F., *The mechanics of the foot and it's disorders*, Blackwell scientific publications, London, 1976. (ed. Klenerman 1977).
- Hutton,W.C. and Dhanendran,M., "A study of the distribution of load under the normal foot during walking," *Intl.Orthop.*, vol. 3, pp. 153-157, 1979.
- Hutton,W.C. and Dhanendran,M., "The mechanics of normal and hallux valgus feet- A quantitative study," *Clin.Orthopaedics & Rel.Research*, vol. 157, pp. 7-13, June 1981.
- Inman,V.T., Ralston,H.J., and Todd,F., *Human Walking*, Williams & Wilkins, Baltimore, 1981.
- Isacson,J., Gransberg,L, and Knutsson,E., "Three-dimensional electrogoniometric gait recording," *J.Biomech.*, vol. 19(8), pp. 627-635, 1986.
- Jaffe,B, *Piezoelectric ceramics*, Academic Press, London, 1971.

- James, W.V., Orr, J.F., and Huddleston, T., "A load cell system in foot pressure analysis," *Eng. in Med.*, vol. 11(3), pp. 121-122, 1982.
- Kaliszer, M., O'Flanagan, S., McCormack, B., Mulhall, J., Heavey, A., and Shehan, J., "Setting the baseline parameters for clinical assessment of foot to ground contact using the Musgrave pressure plate system," *J. Biomed. Eng.*, vol. 11(1), pp. 30-4, Jan. 1989.
- Kawai, H., "The piezoelectricity of poly (vinylidene Fluoride)," *Japan J. Appl. Phys.*, vol. 8, pp. 975-976, 1969.
- Khodadadeh, S., "Quantitative approach to osteoarthritic gait assessment," *Eng. in Med.*, vol. 16(1), pp. 9-14, 1987.
- Kirtley, C., Whittle, M.W., and Jefferson, R.J., "Influence of walking speed on gait parameters," *J. Biomed. Eng.*, vol. 7(10), pp. 282-286, Oct. 1985.
- Klenerman, L., *Personal communication*. (Royal Liverpool Hospital)
- Kljajic, M. and Krejnik, J., "The use of ground reaction measuring shoes in gait evaluation," *Clin. Phys. Physiol. Meas.*, vol. 8, pp. 133-142, 1987.
- Koal, J.G., *Polymer piezoelectric sensor for animal foot pressure*, Feb. 1985. U.S. Patent No. 4,499,394.
- Kobayashi, K. and Yasuda, T., "An application of PVdF film to medical transducers," *Ferroelectrics*, vol. 32, pp. 181-184, 1981.
- Kynar, *Kynar piezo film*, 1983. Technical Manual.
- Kynar, *Oscillating force transducer*, 1987. Kynar information pack ref. F9
- Kynar, *Kynar piezo film*, 1987. Technical Manual.
- Law, H.T., "Microcomputer-based low cost method for measurement of spacial and temporal parameters of gait," *J. Biomed. Eng.*, vol. 9(4), pp. 115-120, Apr. 1987.
- Leduc, A., Reyns, I., Liegois, E., Levray, P.H., and Lievens, P., *Load sharing within the forefoot*, pp. 182-4. In: *Disability: proceedings of a seminar on rehabilitation of the disabled* (Eds. R.M. Kenedi, J.P. Paul, J. Hughes), Macmillan Press, Baltimore, 1979.
- Lerrem, P. and Serek-Hausen, F., "A method of recording plantar pressure distribution under the sole of the foot," *Bulletin of Prosthetics Research*, pp. 118-125, 1973.
- Levens, A.S., Inman, V.T., and Blosser, J.A., "Transverse rotation of the segments of the lower extremity in locomotion," *J. Bone & Jt. Surgery*, vol. 30A, pp. 859-72, 1948.
- Lewis, O.J., "Functional morphology of the joints of the evolving foot," *Symp. zool. Soc. Lond.*, vol. 46, pp. 169-188, 1981.
- Linville, J.G., *PVF2 - Models, measurements, device ideas*, Stanford electronics laboratories, Stanford University, CA., Mar. 1978. Technical Report No. 4834-3.
- Lord, M., "Foot pressure measurement: A review of methodology," *J. Biomed. Eng.*, vol. 3(4), pp. 91-99, Apr. 1981.
- Lord, M., Reynolds, D.P., and Hughes, J.R., "Foot pressure measurement: A review of clinical findings," *J. Biomed. Eng.*, vol. 8(10), pp. 283-294, Oct. 1986.
- Maalej, N., Webster, J.G., Tompkins, W.J., and Wertsch, J.J., "A conductive polymer pressure sensor array," *IEEE Eng. in Medicine & Biol. Soc. 11 Annual Int. Conf. - Position Sensors and Mechano Sensors*, pp. 1116-7, 1989.

- Manley, M., *Discussion contribution plus figure, in Disability.*, pp. 185-190, Macmillan, 1979. ed. Kenedi et al.
- Metrabyte, *DASH-16/16F*, 1986. Technical Manual
- Miller, G.F. and Stokes, I.A.F., "A study of the duration of load-bearing under different areas of the foot," *Eng. in Med.*, vol. 8(3), pp. 128-132, 1979.
- Minns, R.J. and Craxford, A.D., "Pressure under the forefoot in Rheumatoid Arthritis," *Clin. Orthopaedics & Rel. Research*, vol. 187, pp. 235-242, July 1984.
- Minns, R.J., "A conductive rubber footswitch design for gait analysis," *J. Biomed. Eng.*, vol. 4(10), pp. 328-330, Oct. 1982.
- Miyazaki, S., Ishida, A., Iwakura, H., Takino, K., Ohkawa, T., Tsubakimoto, H., and Hayashi, N., "Portable limb-load monitor utilizing a thin capacitive transducer," *J. Biomed. Eng.*, vol. 8(1), pp. 67-71, Jan. 1986.
- Morton, D.J., *The Human Foot*, Columbia Univ. Press, New York, 1935.
- Murray, M.P., Drought, A.B., and Kory, R.E., "Walking patterns in normal men," *J. Bone & Jt. Surgery*, vol. 46A, pp. 335-60, 1964.
- Neubert, H.K.P., *Instrument transducers*, Clarendon press, Oxford, 1975.
- Nicol, K., and Henning, E.M., "Measurement of pressure distribution by means of a flexible, large-surface mat," *Biomechanics VI-A*, pp. 374-380, University Park Press, Baltimore, U.S.A., 1978.
- Nilsson, S. and Planath, I., *Facial injury occurrence in traffic accidents and its detection by a load sensing face*, May 1987. Volvo car corporation report.
- Nix, E.L. and Ward, I.M., "The measurement of the shear piezoelectric coefficients of polyvinylidene fluoride," *Ferroelectrics*, vol. 67, pp. 137-141, 1986.
- Nix, E.L., "A direct method for measurement of the film-thickness piezoelectric coefficient of polyvinylidene fluoride," *Ferroelectrics*, vol. 67, pp. 125-130, 1986.
- Electronics Inc. Novel, *The EMED system, a new measuring process for the diagnostic and therapeutic observation of the foot*, 1987.
- Nye, J.F., *Physical properties of crystals*, Oxford University Press, Oxford, 1957.
- Ohigashi, H., Koga, K., Suzuki, M., Nakanishi, T., Kimura, K., and Hashimoto, N., "Piezoelectric and ferroelectric properties of P(VDF-TrFE) copolymers and their application to ultrasonic transducers," *Ferroelectrics*, pp. 189-202, 1982.
- Olsson, E., Oberg, K., and Ribbe, T., "A computerized method for clinical gait analysis of floor reaction forces and joint angular motion," *Scand J Rehab Med*, vol. 18, pp. 93-99, 1986.
- Park, K., Klaffer, R.D., and Bloomfield, P.E., *A PVdF tactile sensor for industrial robots*, pp. 4.47-4.60, 1987. Pennwalt Corporation information paper No. R13.
- Park, K.T., Klaffer, R.D., and Bloomfield, P.E., "A charge readout algorithm for piezoelectric force transducers," *I.E.E.E. International symposium on the applications of ferroelectrics*, 1986.
- Patel, A., Webster, J.G., Tompkins, W.J., and Wertsch, J.J., "Electronic circuits for capacitive pressure sensors," *IEEE Eng. in Medicine & Biol. Soc. 11th Annual Int. Conf. - Instrumentation for Rehabilitation and Biomechanical measurements*, pp. 1437-8, 1989.
- Payne, P.A., "Transducers, sensors, and instrumentation in clinical biomechanics," *J. Biomed. Eng.*, vol. 11(5), pp. 180-4, May 1989.

- Pedotti,A., Assente,R., Fusi,G., DeRossi,D., Dario,P., and Domenici,C., "Multisensor piezoelectric polymer insole for pedobarography," *Ferroelectrics*, vol. 60, pp. 163-174, 1984.
- Pennwalt,Ltd, *A force transducer*. Invention record No. F9.
- Peruchon,E., Jullian,J.M., and Rabischong,P., "Wearable unrestraining footprint analysis system. Applications to human gait study.," *Med.& Biol.Eng.& Comput.*, vol. 27, pp. 557-65, Nov.1989.
- Pollard,J.P., LeQuesne,L.P., and Tappin,J.W., "Forces under the foot," *J.Biomed.Eng.*, vol. 5(1), pp. 37-40, Jan.1983.
- Pratt,D.J., Bowker,P., Wardlaw,D., and McLaughlan,J., "Load measurement in orthopaedics using strain gauges," *J.Biomed.Eng.*, vol. 1(4), pp. 287-96, 1979.
- Pratt,D.J., "Medium term comparison of shock attenuating insoles using a spectral analysis technique," *J. Biomed. Eng.*, vol. 10(10), pp. 426-9, Oct.1988.
- Quadling,D.A. and Ramsay,A.R.D., *An introduction to advanced mechanics*, G.Bell & Sons, London, 1962.
- Ranu,H.S., "Normal and pathological human gait analysis using miniature triaxial shoe-borne load cells," *Am J Phys Med*, vol. 66(1), pp. 1-11, 1987.
- Ranu,H.S., "A quantitative method of measuring the distribution of forces under the different regions of the human foot: during normal and abnormal gait," *IEEE Eng.in Medicine & Biol.Soc. 11th Annual Int.Conf. - Biomechanics of the Upper & Lower Extremities*, pp. 824-5, 1989.
- Ranu,H.S., "Miniture load cells for the measurement of foot-ground reaction forces and centre of foot pressure during gait," *J.Biomed.Eng.*, vol. 8(4), pp. 175-177, Apr.1986.
- Rehman,I., Patek,P.R., and Gregson,M., "Some of the forces exerted in the normal human gait," *Archives of Physical Medicine*, vol. 30, pp. 698-702, 1948.
- Richardson,P.D., "Piezoelectric polymers," *IEEE Eng. in Medicine & Biol. Magazine*, pp. 14-6, June 1989.
- Robinson,A.L., "Flexible PVF2 film: An exceptional polymer for transducers," *Science*, vol. 200, pp. 1371-1374, June 1978.
- Schwartz,R.P. and Heath,A.L., "The definition of human locomotion on the basis of measurement," *J.Bone & Jt.Surgery*, vol. 29(1), pp. 203-14, 1947.
- Seitz,P., *Personal communication*. (Novel gmbh, Munchen).
- Silvino,N., Evanski,P.M., and Waugh,T.R., "The Harris and Beath footprinting mat: Diagnostic validity and clinical use," *Clin. Orthopaedics & Rel. Research*, vol. 151, pp. 265-269, Sep.1980.
- Simkin,A. and Stokes,I.A.F., "Characterisation of the dynamic vertical force distribution under the foot," *Med.& Biol.Eng.& Comput.*, vol. 20, pp. 12-18, Jan.1982.
- Simmonite,N., *The assessment of plantar padding material in plantar pressure distribution*, 1990. BSc(Hons) Project Report. Brighton Polytechnic.
- Soames,R.W., Carter,P.G., and Towle,J.A., *The rheumatoid foot during gait*, pp. 167-78. In: Biomechanical measurement in orthopaedic practice (Eds. M.Whittle and D.Harris), Oxford Medical Engineering Series 5, Clarendon Press, Oxford, 1985.
- Soames,R.W. and Scott-Flynn,M., "Computer analysis of foot pressure data," *J. Anat.*, vol. 132, p. 473, 1981.
- Soames,R.W., Blake,C.D., Stott,J.R.R., Goodbody,A., and Brewerton,D.A., "Measurement of pressure under the foot during function," *Med.& Biol.Eng.& Comput.*, vol. 20, pp. 489-495, July 1982.

- Stewart,T.P. and Grove,M., "Correlation of pressure sensor systems," *IEEE Eng.in Medicine & Biol.Soc. 11th Annual Int.Conf. - Rehabilitation Engineering II*, p. 1489, 1989.
- Stokes,I.A.F., Hutton,W.C., and Evans,M.J., "The effects of hallux valgus and Keller's operation on the load bearing function of the foot during walking," *Acta Orthop. Belgica*, vol. 41(6), pp. 695-704, 1975.
- Stokes,I.A.F., Faris,I.B., and Hutton,W.C., "The neuropathic ulcer and loads on the foot in diabetic patients," *Acta Orthop. Scand.*, vol. 46, pp. 839-847, 1975.
- Stokes,I.A.F., Hutton,W.C., Stott,J.R.R., and Lowe,L.W., "Forces under the Hallux Valgus foot before and after surgery," *Clin.Orthopaedics & Rel.Research*, vol. 142, pp. 64-72, July 1979.
- Stokes,I.A.F., Stott,J.R.R., and Hutton,W.C., "Force distributions under the foot- a dynamic measuring system," *Biomedical Eng.*, vol. 9, pp. 140-143, Apr.1974.
- Stokes,I.A.F., Hobin,R.A., and Russell,L.H., "The effect of shoe inserts on the load distribution under the foot," *Chiropodist*, pp. 5-12, Jan.1977.
- Stott,J.R.R. and Soames,R.W., "A method for recording the instantaneous pressure distribution under the feet during walking.," *J Anat.*, vol. 132, pp. 472-473, 1981.
- Tappin,J.W., Pollard,J., and Beckett,E.A., "Method of measuring "shearing" forces on the sole of the foot," *Clin.Phys.Physiol.Meas.*, vol. 1(1), pp. 83-85, 1980.
- Teitz,C.C., Harrington,R.M., and Wiley,H., "Pressures on the foot in pointe shoes," *Foot and Ankle*, vol. 5(5), pp. 216-21, 1985.
- Toda,M, "A PVD2 piezoelectric bimorph device for sensing presence and position of other objects," *IEEE Transactions on electron devices*, vol. ED-26(5), pp. 815-817, May 1979.
- Toda,M, "Voltage induced large amplitude bending device- PVF2 bimorph- it's properties and applications," *Ferroelectrics*, vol. 32, pp. 127-133, 1981.
- Tracy,K.B., Montague,E.C., Gabriel, R.P., and Kent,B.E., "Computer assisted diagnosis of orthopaedic gait disorders," *Physical Therapy*, vol. 59(3), pp. 268-277, Mar.1979.
- VanHanswyk,E.P., "The diabetic patient: Orthotic considerations," *Orthotics and Prosthetics*, vol. 33(3), pp. 32-39, Sep.1979.
- Vines,G., "Measuring the weight on your feet," *New Scientist*, vol. 13, p. 24, June 1985.
- Wada,Y. and Hayakawa,R., "A model theory of piezo- and pyroelectricity of poly(vinylidene fluoride) electret," *Ferroelectrics*, vol. 32, pp. 115-118, 1981.
- Wall,J.C., Charteris,J., and Turnbull,G.I., "Two steps equals one stride equals what?: the applicability of normal gait nomenclature to abnormal walking patterns," *Clinical Biomechanics*, vol. 2(3), pp. 119-25, 1987.
- Wang,T.T., Herbert,J.M., and Glass,A.M., *The applications of ferroelectric polymers*, Blackie and Son Ltd, Glasgow, 1988.
- Wamer,C.Y., Wille,M.G., Brown,S.R., Nilsson,S., Mellander,H., and Koch,M., *A load sensing face form for automotive collision crash dummy instrumentation*, pp. 85-93, Feb.1986. 30th Strapp car crash conference; SAE Paper No. 860197; Detroit, MI.
- West,P.M., "The clinical use of the Harris and Beath footprinting mat in assessing plantar pressures," *Chiropodist*, pp. 337-348, Sep.1987.
- West,S.G., "A review of methods of obtaining foot loading data during walking," *Chiropodist*, pp. 84-95, Mar.1987.

- Whiting, M., *Personal communication*. (Sussex school of Podiatry, Eastbourne)
- Willis, J. and Webster, J.G., *Interfacing sensors to the IBM pc*, Prentice-Hall Inc, Englewood Cliffs, 1988.
- Willmott, M., "The effect of a vinyl floor upon walking in elderly patients," *Age and Ageing*, pp. 119-120, 1986.
- Wright, D.G., Desai, S.M., and Henderson, W.H., "Actions of the subtalar and ankle joint complex during the stance phase of walking," *J. Bone & Jt. Surgery*, vol. 46A, pp. 361-82, 1964.
- Yarsley, *Applications briefs relating to piezoelectric and pyroelectric PVdF films*, 1982. Technical Manual
- Zhu, H., Wertsch, J.J., Harris, G.F., Price, M.B., and Alba, H.M., "Pressure distribution beneath sensate and insensate feet," *IEEE Eng. in Medicine & Biol. Soc. 11th Annual Int. Conf. - Biomechanics of the Upper & Lower Extremities*, pp. 822-3, 1989.

## COMMERCIAL REFERENCES

- Atochem Ltd; 22 Ridgeway, Hillend Industrial Park, Dunfirmline, Fife, KY11 5JN, Scotland. *Tel: (0383) 825063* (piezo film).
- Austen Tapes Ltd; Eastland Lane, Paddock Wood, Tunbridge, Kent, TN12 6BU, England. *Tel: (0892) 832141* (3M distributor).
- Avalon Components Ltd; Bowling Green Mill, Street, Sommerset, England. *Tel: (0458) 42244* (orthotic materials).
- Axon Cable Ltd; Unit 7, Ridgeway, Donibristle Industrial Park, Nr Dunfirmline, Fife, KY11 5JN, Scotland. *Tel: (0383) 821081* (coax cables).
- Biokinetics; 6 Wortley Moor Road, Leeds, LS12 4JF, England. *Tel: (0532) 793710* (gait analysis equipment).
- Burr Brown International Ltd; 1 Millfield House, Woodshots Meadow, Watford, Hertfordshire, WD1 8YX, England. *Tel: (0923) 33837* (components).
- BXL Plastics Ltd; ERP Division, 675 Mitcham Road, Croydon, CR9 3AL, England. *Tel: 081 684 3622* (orthotic materials).
- Design Resins Ltd; Unit 13, Carnegie Road, Porte Marsh Trading Estate, Calne, Wiltshire, SN11 9PS, England. *Tel: (0249) 816771* (adhesives).
- Downs Surgical (Escalab) Ltd; Park way Close, Park Way Industrial Estate, Sheffield, S9 4WJ, England. *Tel: (0742) 730346* (gait analysis equipment).
- Electrolube Ltd; Blakes Road, Wargrave, Berkshire, RG10 8AW, England. *Tel: (0734) 404031* (adhesives / materials).
- Entran Ltd; 5 Albert Road, Crowthorne, Berkshire, RG11 7LT, England. *Tel: (0344) 778848* (transducers).
- Focus Ltd; Unit 4, Cheney Manor Industrial Estate, Swindon, Wiltshire, SN2 2PJ, England. *Tel: (0793) 513200* (piezoelectric cables).
- Footman & Co. Ltd; Grove Mill, 475-9 London Road, Mitcham, Surrey, CR4 4YP, England. *Tel: 081 646 2040* (orthotic materials).
- Gilbert and Mellish Ltd; 499-503 Bristol Road, Birmingham, B29 6AU, England. *Tel: 021 471 3055* (orthotic materials).
- GTS Flexible Materials Ltd; Eastern Road, Bracknell, Berkshire, RG12 2UP, England. *Tel: (0344) 54331* (flexible circuit board).
- Habia Cables Ltd; Short Way, Thornbury Industrial Estate, Thornbury, Bristol, BS12 2UT, England. *Tel: (0454) 412522* (coax cables).
- Infotronic Medical Engineering; PO Box 73, 7650 AA Tubbergen, The Netherlands. *Tel: 053-893478* (gait analysis equipment).

Interactive Clinical Research; Avenue des Fauvettes, 2A. Grasmussenlaan - 1950 Kraainem, Belgium. *Tel: 02/721.47.37* (gait analysis equipment).

Interlink Electronics; 535 E.Montecito Street, Santa Barbara, CA, 93103, USA. *Tel: 805-965-5155* (force sensitive resistive film).

John Drew Ltd; 433 Uxbridge Road, London, W5 3NT, England. *Tel: 081 992 0381* (gait analysis equipment).

Keithley Instruments Ltd; The Minster, 58 Portman Road, Reading, Berkshire, RG3 1EA, England. *Tel: (0734) 575666* (computer data acquisition).

Kistler Instruments Ltd; Whiteoaks, The Grove, Hartley Wintney, Hampshire, RG27 8RN, England. *Tel: (025 126) 3555* (transducers).

Kraemer Orthopadie KG; Ronsdorfer Straße 188-190. D-5630 Remscheid 1, Germany. *Tel: (0 21 91) 4 67-0* (gait analysis equipment).

Langer Biomechanics Group UK; Unit 7, The Green, Cheadle, Stoke on Trent, England. *Tel: (0538) 755861* (gait analysis equipment).

Leyland & Birmingham Ltd; Golden Mill Lane, Leyland, Preston, PR5 1UB, England. *Tel: (0772) 421434* (orthotic materials).

Loctite UK; Watchmead, Welyn Garden City, Hertfordshire, AC7 1JB, England. *Tel: (0707) 331277* (adhesives).

Maplin Professional Supplies; PO Box 777, Rayleigh, Essex, SS6 8LU, England. *Tel: (0702) 554171* (components).

Midi Capteurs International Systems; 4, Rue des Libellules - 31400 Toulouse, France. *Tel: 61.25.31.09* (gait analysis equipment).

MIE Medical Research Ltd; 6 Wortley Moor Road, Leeds, LS12 4JF, England. *Tel: (0532) 793710* (gait analysis equipment).

Multicore Solders Ltd; Wood Lane End, Hemel Hempstead, Hertfordshire, HP2 4RQ, England. *Tel: (0442) 233233* (solder paste).

Novel<sub>gmbh</sub>; Beichstrasse 8, 8000 Munchen 40, Germany. *Tel: 089 390102* (gait analysis equipment).

Number One Systems Ltd; Harding Way, Somersham Road, St Ives, Huntingdon, Cambridgeshire, PE17 4WR, England. *Tel: (0487) 494042* (pcb software).

Pennwalt Piezo Film Ltd; 22 Ridgeway, Hillend Industrial Park, Dunfirmline, Fife, KY11 5JN, Scotland. *Tel: (0383) 825063* (piezo film).

Penny & Giles Blackwood Ltd; Blackwood, Gwent, NP2 2YD, Wales. *Tel: (0495) 228000* (gait analysis equipment).

Polysens SpA; Via Donatello, 24 - 50028 Tavernelle, Val di Pesa (Fi), Italy. *Tel: 055/8071580* (gait analysis equipment).

PMI, Bournes Electronics Ltd; 90 Park Street, Camberley, Surrey, GU15 3NY, England. *Tel: (0276) 692392* (components).

RS Components Ltd; PO Box 99, Corby, Northants, NN17 9RS, England. *Tel: (0536) 201234* (components).

Scholl Consumer Products Ltd; 475 Capability Green, Luton, LU1 3LU, England. *Tel: (0582) 482929* (footwear / gait analysis equipment).

Seaton and Price Ltd; 3 Wraxhill Road, Street, Somerset, BA16 0HE, England. *Tel: (0458) 47275* (orthotic materials).

Servodata Ltd; Aico House, Faraday Road, Newbury, Berkshire, RG13 2AD, England. *Tel: (0635) 45373* (force sensitive resistive film).

Smith & Nephew Chiromed; Green Pond Road, London, E17 6EN, England. *Tel: 081 531 4100* (orthotic materials).

Stuart Pharmaceuticals, ICI (Pharmaceuticals) Ltd; Kings Court, Water Lane, Wilmslow, Cheshire, SK9 5AZ, England. *Tel: (0625) 535999* (hospital materials).

TecScan; 451 D Street, 4th Floor, Boston, Massachusetts, USA. (gait analysis equipment).

3M United Kingdom plc; Yeoman House, 57-63 Croydon Road, Penge, London, SE20 7TR, England. *Tel: (0344) 866271* (adhesives / materials).

Verospeed; Stanstead Road, Boyatt Wood, Eastleigh, Hampshire, SO5 4ZY, England. *Tel: (0703) 641111* (components).

W.L.Gore Ltd; Pitreavie Business Park, Queens Ferry Road, Dunfermline, Fife, KL11 5PU, Scotland. *Tel: (0383) 726777* (PTFE etchant).

W.M.Automation; 76 Valley Duff Drive, Carnmoney, Newtownabbey, Co.Antrim, BT36 6PB, N.Ireland. *Tel: (0232) 832055* (gait analysis equipment).

Yarsley, Fulmer Yarsley Ltd; Towers Way, Redhill, Surrey, RH1 2JN, England. *Tel: (0737) 765070* (piezo film).

**Appendix**

**I**

**GENERAL PROPERTIES  
OF PVdF  
AND  
PIEZOELECTRIC  
PVdF FILM**

## General properties of PVdF and PVdF film

(vinylidene) fluoride PVdF is a semicrystalline thermoplastic polymer with excellent chemical, physical and mechanical properties, which result in a wide range of applications in the food, chemical, pharmaceutical and nuclear industries.

Amorphous PVdF has good impact resistance, good abrasion resistance, low creep, outstanding weathering resistance (e.g. unaffected by U.V. light and high stability to gamma irradiation), and exceptional thermal stability, the possible temperature range for operation lying between -50 and 150°C, where no cracking or rupture is observed.

PVdF is a good electrical insulator, having a volume resistivity of  $1.5 \times 10^{13} \Omega\text{m}$ . It has a good electrical breakdown strength of 75 V/ $\mu\text{m}$  and a high dielectric constant, especially when oriented, of around 10. It has rather a high dissipation factor of between 0.015 and 0.02, but is used extensively as a capacitor film. (Kynar Piezo Film technical manual, 1987).

PVdF can be fusion-jointed like polyethylene and polypropylene. It is said to have a fusion temperature of 210°C. It can be processed from 185°C onwards and will withstand temperatures up to 260°C without discolouration. It has excellent flow characteristics and can be processed by extrusion, injection moulding, compression moulding and blow moulding etc. PVdF is flame resistant and self-extinguishing. It is readily manufactured in sheet form in a continuous roll process and can be machined into complex shapes for specific applications. Piezoelectric cable, for example, has been manufactured for hydrophone and geophysical transducer applications (Fox *et al*, 1986; Focus Ltd, Piezotek Sensor Cables).

PVdF like PTFE is outstandingly resistant to most organic acids and bases, aliphatic and aromatic hydrocarbons, organic acids, alcohols and halogenated solvents. It is also resistant to oxidisers and oxygen gases. It is degraded by hot fuming sulphuric acid, some strongly basic primary amines, hot concentrated alkalis and alkali metals. The polymer swells slightly in strong polar solvents such as acetone and ethyl acetate, and is dissolved with difficulty by aprotic polar solvents such as dimethylformamide, dimethylsulphoxide, tetramethylurea or hexamethylphosphotriamide. Other solvents for PVdF include ethylene carbonate, propylene carbonate, dimethylacetamide and N-methylpyrrolidone.

PE has average permeability to small molecules (N<sub>2</sub>, CO<sub>2</sub>, H<sub>2</sub>O etc) but excellent impermeability to larger molecules (aromatics etc).

PE is absolutely non-toxic, and it may be used for food packaging. In addition to its mechanical strength and chemical inertness, PVdF has good "nuclear blast resistance" i.e. shock and radiation resistance. Kureha KF1000 PVdF shows no decrease in tensile strength after exposure to 100 megarads of electron beam irradiation, whereas PTFE shows a 44% decrease at 2 megarads). (Yarsley PVdF applications briefs, 1982). A main commercial use of the material is lining chemical reactors, pipes, valves, pump parts, etc.

From an engineering perspective piezoelectric materials have many differences and PVdF has certain advantages over inorganics such as PZT ceramics, some of the major advantages are detailed below:

Very thin (down to 9µm), self supporting, pinhole-free films are easily produced.

Available as large area (up to 1m<sup>2</sup>), thin films.

Can be laminated to produce bimorph and multimorph elements that multiply transducer response.

The polymer is very flexible, tough and lightweight, and hence can be moulded, stretched or cut to form complex configurations.

Electrodes can be produced on the films in a virtually unlimited variety of patterns.

Low acoustic impedance (a factor of 10 lower than ceramics), therefore the polymer has a good impedance match to water, human tissue and adhesive systems.

Not subject to breakage and loss of dipolar properties when subjected to mechanical impact.

High dielectric strength (75 V/µm) and high operating field strength (30 V/µm a.c.), higher than that of ceramics by a factor of 70.

Resistance to moisture, high humidity and contaminants (0.01% water absorption).

Very broad and flat bandwidth that extends from less than a Hertz to past 10<sup>9</sup> Hz.

Relatively low raw material and fabrication costs compared to those of ceramic and quartz materials, particularly in volume quantities.

As a result of its very low permittivity (1% that of ceramics), the film exhibits  $g$ -constants or voltage output coefficients that are significantly greater than those for ceramics (around 20 times).

to its organic nature, some disadvantages naturally follow, making it inappropriate for certain applications:

Compared to ceramic the material is soft and hence its stiffness is low.

The firm attachment of electrodes to the surface is difficult.

Unlike monocrystals, efficient resonator structures are not feasible.

The stability of the electrical response of the film is lower than that for ceramics (i.e. ageing can cause changes in response).

The Curie point (at which the piezoelectric response disappears) is low at 120°C; the film should only be used for low temperature applications, i.e.  $< 100^\circ\text{C}$ .

As it has a low  $Q$ , it makes a relatively weak electromechanical transmitter when compared to ceramics, particularly at resonance and in low frequency applications.

Its pyroelectric coefficient is about an order of magnitude lower than that of the most commonly used ceramic material (triglycine sulphate), a disadvantage for pyroelectric sensor operation.

**Appendix**

**II**

**GAITSCAN  
INSTALLATION  
AND  
OPERATING  
MANUAL**

# **GAITSCAN FOOT PRESSURE MEASUREMENT SYSTEM**

**version 2.0**

## **Installation and Operating Manual**

**1990**

**A.J.Nevill  
M.G.Pepper**

**Medical Electronics Department  
University of Kent at Canterbury**

**Copyright 1990. All rights reserved.**

## PREFACE

Foot pressure measurement provides valuable information in the quest for complete analysis of human gait.

In the search for accurate assessment of pathological foot conditions and the subsequent successful intervention of a surgical or orthotic nature, it is desirable to be able to quantify the in-shoe load distribution under major anatomical sites of the plantar surface of the foot.

Commercially there is a trend towards barefoot, single foot strike systems. The few attempts at in-shoe pressure measurement have resulted in unreliable data, primarily due to transducer problems.

PVdF and Copolymer piezoelectric film has been designed into novel transducers, sixteen of which have subsequently been incorporated into two insoles. These transducers provide signals allowing absolute measurement of vertical in-shoe loading over multiple footsteps from both feet simultaneously.

Gaitscan has been built around this essential front end which, together with its associated electronics and computer processing, affords data collection of the required in-shoe pressure measurements during gait. Gaitscan also allows retrieval and limited analysis of this comprehensive information, which will be of use to the researcher and to the clinician.

This manual provides instructions for the installation and operation of the Gaitscan data acquisition and postacquisition system. A basic knowledge of MSDOS or PCDOS and the ability to store and retrieve data is assumed. A DOS operating manual should be referred to if problems are experienced in this area.

**Table of Contents**

PREFACE	(i)
Table of Contents	(ii)
Chapter 1 Installation	(1)
Chapter 2 Mouse Support	(2)
Chapter 3 Printer and Plotter Support	(3)
Chapter 4 Manipulation and Use of Data Files	(4)
Chapter 5 Source Code Details	(5)
Chapter 6 Gaitscan Hardware	(6)
Chapter 7 Using Gaitscan	(7)
Chapter 8 Using Gaitscan Acquire - <i>GSACQU</i>	(9)
Chapter 9 Using Postscan Analysis - <i>GSPOST</i>	(10)
Chapter 10 Using Gaitscan Setup - <i>GSETUP</i>	(13)
Chapter 11 Summary of Function Key Utilisation for <i>GSPOST</i>	(14)
Chapter 12 Technical Specifications and System Details	(15)
Appendix I Examples of graphics screens	(16)
Appendix II Standard Insole Templates	(22)

## 1 Installation

### Hardware Installation

The computer system should be set up in accordance with the necessary instruction manuals. All functions, such as printing via the parallel port, etc, should be checked before proceeding to install the Metrabyte DAS16 (or compatible) A/D converter interface card. The following settings must be observed before the A/D card is plugged into a computer expansion slot.

The base address of the A/D card should be set to

**340hex**

as this is the address used by the Gaitscan software. A bank of switches on the A/D card is used for this purpose. The Gaitscan software will not function properly if the interface card is not set to this address or if there is a conflict between other expansion hardware in the computer.

Channel configuration is set so that 16 single ended input channels can be used so this switch is set to the 16 position.

The input signal range is set so that bipolar signals can be acquired, the switch is set to the BIP position.

DMA level 3 is used.

Interrupt level 7 is used.

The input signal level is  $\pm 10V$  so the 5 position dipswitch is set so that all switches are OFF.

Ensuring that the POWER IS OFF, the card may be installed into the computer.

To complete the hardware installation, straightforward connection of the various Gaitscan hardware components is required (see chapter 7), thus completing an electrical path from both insoles to the computer.

### Software Installation

All the necessary Gaitscan files are contained on the floppy disc provided. DOS version 3.2 or greater should be installed along with the two memory resident programs: Integrex dumpega2.com and Microsoft msmouse.com.

To instal Gaitscan insert the floppy disc in drive A:

Type A: ←

Type INSTALL ←

Gaitscan will now be installed on your hard disc in a directory called GS.

## 2 Mouse Support

Gaitscan uses a mouse to drive some of its software functions. The Microsoft mouse driver is required and should be installed during boot up. It is therefore necessary to add a command in the autoexec.bat file, to allow installation each time the computer is turned on. An example is given below:

C: <path> MSMOUSE ←

<path> is the location within the computer's directory structure of the mouse software, e.g. \lib\mouse

A serial mouse is used and is therefore connected to the RS232 serial port, e.g. com1.

### 3 Printer and Plotter Support

Gaitscan can produce hard copies of the obtained waveforms in a number of different ways. The most convenient of these is a screendump facility using the Integrex Colourjet 132 ink-jet printer. To make use of this the driver software, `dumpega2.com`, is required and should be installed during boot up. As with the mouse driver software, it will be necessary to add a command to `autoexec.bat`, such as:

```
C: <path> DUMPEGA2 ←
```

This printer has the advantage of being quiet, a consideration when using Gaitscan in a clinical setting, however the printing time is relatively long at around 4 minutes.

Gaitscan can also support HPGL language plotters, e.g. the Hewlett Packard ColorPro. Existing code supporting this feature is limited and only allows a plot of the main opening screen, which gives concise patient details and plots of the whole test for both feet, i.e. 16 channels over the complete duration of the test. Users with programming knowledge may wish to extend the HPGL plotting capabilities by using the existing procedure as a starting point from which to build upon.

In addition to this plotter support Gaitscan has two further internal hardcopy support features. The first is a colour screen dump to a AMT Accel500 printer/plotter. This method is noisier than the previous two and it takes around 2 minutes to complete a plot. The second internal hardcopy support is a quick screendump facility using a dot matrix printer such as the Epson FX1000. A monochromatic printout is obtained which, for example, may be useful for patient files.

Refer to the *hardcopy functions* section in chapter 9 for the actual commands and instructions for obtaining hardcopies.

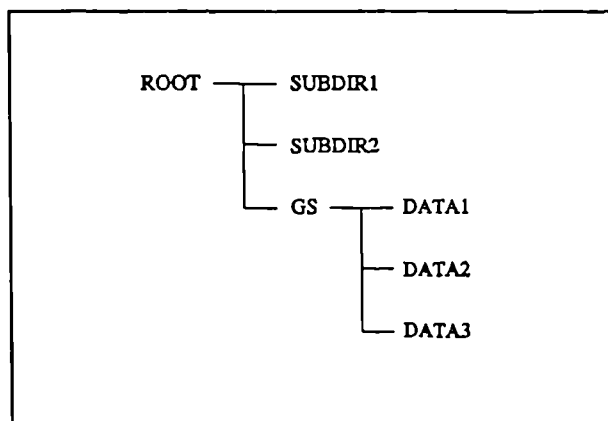
#### 4 Acquisition and Manipulation of Data Files

A directory called GS is created during installation and this holds all the Gaitscan files necessary for operation of the system. If desired all these files could be relocated anywhere within the directory system as long as they are kept together.

##### Acquisition

The program for controlling the acquisition and storage of data is *GSACQU*. One data file is produced for each test which is copied to the hard disc directly after completion of the test. The first thing *GSACQU* will ask for is the path for the data file, i.e. where it will place the data file on the hard disc. In order to avoid confusion and file relocation problems it is suggested that one or a few sub-directories be created from the working directory, GS, in which to hold the data files.

For example the directory tree could look like:



Data1, Data2 and Data3 are subdirectories that will eventually contain Gaitscan data files of certain categories.

*GSACQU* also requires a file name for each test and this is usually the subject's initials. Note that consecutive tests for the same subject do not require repeated file names as each test is indexed with a number increasing from 1. So for example, for a patient under test with the initials of ABC, data files ABC1.DAT and ABC2.DAT will be created if two consecutive tests are performed.

##### Manipulation

The program for controlling the manipulation of the acquired and stored data is *GSPOST*. A second data file is created when *GSPOST* is executed, this has the sole purpose of providing a means of recording the peak pressure values from selected footsteps which can subsequently be printed from DOS. This is intended to be used to save time if this information is required from many footsteps. It is usual to use the same file name as for the original data file. So for data file ABC2.DAT a file named ABC2.GPD will be created.

Gaitscan uses the information held in *GSETUP.CAL* to provide calibrated results. This data file is created and can also be modified by running *GSETUP* and must be present in the working directory for Gaitscan to run.

## 5 Source Code Details

All the software is written in pascal using Borland's Turbo Pascal 5 editor and compiler. The source code is provided on the disc in case the user wishes to make modifications. Basically the software consists of units of code, each unit having a particular purpose. Details of the code is not entered into here, as it should be self explanatory for the knowledgeable programmer.

Below is a list of the names of the units, main program files and executable files for the three Gaitscan programs.

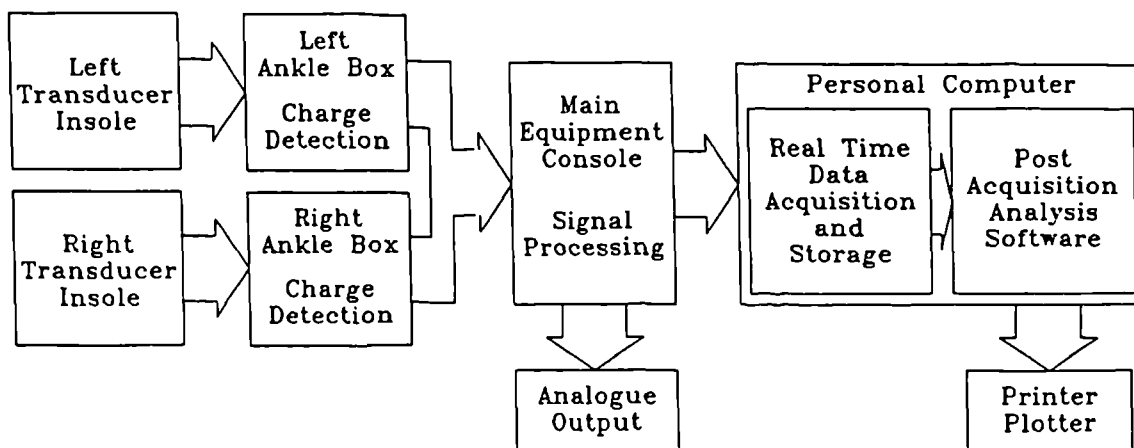
PROGRAM	NAME	DESCRIPTION
Gaitscan Acquire	gsacqu.exe	executable
	gsacqu.pas	main program
	gsacqu_g.pas	global variables
	gsacqu_1.pas	procedures
Postscan Analysis	gspost.exe	executable
	gspost.pas	main program
	gspost_g.pas	global variables
	gspost_1.pas	procedures
	gspost_2.pas	procedures
Gaitscan Setup	gsetup.exe	executable
	gsetup.pas	main program
	gsetup.cal	calibration data

The compiled .TPU files for the program units are not provided, however one other unit is required by Gaitscan and it's compiled version is provided, the name of this compiled unit is given below

worlddr.tpu

If the source code for any program is modified, this unit should be present during compilation otherwise any new executable file will not be created.

## 6 Gaitscan Hardware



System Block Diagram

Basically the equipment can be sectioned into two parts, the main console and the patient units. This equipment is class IB. Which implies that all patient accessible parts are connected to the protective earth conductor of the mains supply and so the equipment is suitable for the external connection of this application.

### Calibration

The transducers supplied have been calibrated but if a calibration unit has been supplied with the equipment this can be used to perform calibration of the transducers. This unit is a single channel charge amplifier with frequency compensation and each transducer can be monitored one at a time while applying a known force. The transducer sensitivity is then calculated in pC/N and this figure is loaded using *GSETUP* into the calibration file *GSETUP.CAL*, and later used by *GSACQU* and *GSPOST*.

### Signal Processing

The electronic circuitry inside the ankle boxes converts the charge signals produced by all the transducers into voltages which are fed to the main equipment console via an umbilical cord. Power for the ankle boxes is also provided through this cord from the main console and interconnection of the umbilical cord to the ankle boxes is provided by a waist box. Signal processing is performed inside the main console to ensure the system has the desired frequency response of 0.01 to 200 Hz. The final signal is then supplied to the computer via a ribbon cable lead.

## 7 Using Gaitscan

In brief the measurement procedure is as follows:

- Accurate location of the sites of interest
- Fabrication of measurement insoles
- Recording data from multiple runs of consecutive footsteps
- Observation and analysis of results

Gaitscan relies upon the accurate placement of the transducers under the bony areas of the foot, namely: heel, lateral arch, metatarsal heads and toe. Care must therefore be taken at this initial stage of the measurement procedure. Numerous techniques can be used to this end; outlined below is the recommended procedure:

1. Shape a card insole from standard template shapes to fit *exactly* inside the subject's shoe. On no account should the insole move once placed inside the shoe.
2. Transfer the locations of the anatomical sites of interest onto the card insole by first marking the plantar surface of the foot with a water soluble marker, then wet the top surface of the card insole with clinical alcohol solution or spray (e.g. Quick Prep.) and finally help the patient to rock to and fro with the card insole placed correctly inside the shoes.
3. This card insole can now be used as a template for both the outer shape and the anatomical site locations.
4. Using rubberised cork of thickness 2mm and double sided tissue tape, or impact adhesive, the marked card insole is adhered to the top surface of the cork, i.e. with the anatomical site markings facing upwards<sup>1</sup>. Transducer locating holes can now be punched through both layers in positions corresponding to the anatomical site locations and a hand held square punch measuring 11 x 11mm is used for this purpose.
5. Small adhesive tape pads are placed over the transducer locating holes on the top side of the insole, this provides an anchor for the transducers while placing them in the correct locations from the underside of the insole. A layer of tape cut to the shape of the insole is then adhered to the underside of the insole, so anchoring the transducers and connecting wires in position; Chirofix™ of width 10cm was found to be useful for this purpose. The connecting wires should be routed to the instep and crossed wires should be avoided.
6. The insole is now ready for measurements to be taken. Once placed inside the subject's shoe the connecting wires are passed out alongside the foot and this should be of little or no irritation to the subject while in locomotion.

In a clinical situation it is often possible to stagger a Gaitscan test either side of an examination period the patient had originally planned to attend. Once familiar with the system the time necessary to perform a complete test is around 20 minutes however most of that time is taken constructing the insole. So if construction can be carried out while the patient is in clinic then a Gaitscan test need only demand 5 minutes before examination to locate the anatomical sites and 5 minutes afterward to take measurements.

Location of the areas of interest is left to the user as he/she is the best person to make this decision. The information required thus determines the placement of the transducers. All foot pressure measuring systems perform analysis upon the areas suggested above, even if more data is initially captured, as is the case for high resolution pressure mat systems.

Before measurements are taken the equipment components should be correctly interconnected and,

---

<sup>1</sup> The thickness of the insole entirely depends upon the thickness of the transducers used, these must, of course, be the same to avoid undesired high or low pressure measuring sites. The materials noted are for the latest Copolymer transducers constructed using a brass top layer, these transducers have a total thickness of 2.6mm.

where necessary, attached to the subject under examination; there follows a description of this procedure.

The transducer wires from each insole collect together in a screw fastening connector which attaches to the corresponding ankle box. These boxes are secured to the distal leg just above the talocrural joint using a special adjustable strap. Once each strap is in place the ankle boxes are attached using the velcro pads. A waist box is secured to the subject using it's ruck-sack style belt and the two connecting wires are attached from this box to the ankle boxes. The final connection is the umbilical cord which links the main equipment console to the waist box. While taking measurements it is important to ensure that all leads are secure and that the equipment feels comfortable to the subject, the subject is always the best judge of his/her own comfort! The main console is linked to the A/D converter card at the rear of the computer using a ribbon cable.

On switch on Gaitscan will take a while to stabilise on account of the increased temperature of the transducers now positioned in the subject's shoes. The time taken to set up the system as described above is usually ample time for the system to stabilise. The subject should now be briefed on the measurement procedure and clearly shown the limits of the walk way.

Data is acquired using the gsacqu program which can be executed by typing

**gsacqu**

The operation of this program is fully described in chapter 8. The data from multiple measurement runs can be acquired to the hard disc of the computer using *GSACQU* and when measurements are complete the subject can be freed from the equipment and released. It may be necessary to record other information depending upon the requirements of the examination, Gaitscan cannot currently store this extra information with the data files and so separate records will have to be kept.

To observe and analyse the results the program *GSPOST* is used and can be executed by typing

**gspost**

All the information from a single run of measurements can be displayed and certain readings can be taken from this file. Chapter 9 explains the capabilities of this program in detail.

## 8 Using Gaitscan Acquire - GSACQU

It is necessary to store all the data from a measurement session to the hard disc of the computer. *GSACQU* is a program that initially captures this information at high speed to the computer's memory and then creates a data file containing the information. This program is executed by typing

### **gsacqu**

Initially the program will prompt for the name of a directory, i.e. where the data file will be saved to. If *return* is pressed the current directory will be used. Following this a file name will be prompted for, see chapter 4 for details on the formation of this data file. The selected directory will be scanned for this file name in case one of that name already exists, the program will not allow an existing file to be over written.

Having successfully created a new data file in which to store the foot pressure information some further information is required before the test can commence. So subsequently the frequency response will be prompted for. The default setting is 50Hz and this is adequate for normal clinical measurements, however Gaitscan has the capability of capturing data at higher rates if, for example, the measurements from a running subject are required. No signal aliasing problems will be encountered as the frequency content of the signals obtained from a subject walking at *normal* speed is less than 50Hz. During running or jumping high frequency signals can be present due to the impulsive nature of the reaction forces experienced by the plantar surface of the foot, and so a higher sampling rate will have to be used. The duration of the test is variable, in the range 1 to 20 seconds, and a value in this range is required. This is to allow for subject to subject variations in walking speed and differences in walkway lengths. Finally some patient details are required. At present this information is not transferred via a data file for later retrieval using *GSPOST* and so this facility is of little or no use and is merely a foundation for further software development, *return* can therefore be pressed in response to each prompt in order to speed up this process.

Once all the required information has been supplied the *pressure level indicators* are displayed. This provides the user with an indication of the functional status of the transducers, i.e whether they are working or not. All that is required is for the subject under test to rock to and fro for the indicators to show relative motion. All the indicators should be in view before measurements are taken.

The next display is a visual indication of the status of the system. *Traffic lights* are displayed and as well as providing information to the user the lights can be used as a patient prompt. Pressing *g* will start data collection and this proceeds for the duration of the test, as defined previously. Once the test has been completed the user is asked whether another test is required: if not the DOS environment is restored; if another is required the original screen is displayed. As extra information the previous files that have been created are also displayed.

Care must be taken to ensure that the hard disc has sufficient space to store the data files that will be created during a test. The system may hang up if this is not observed and a computer *hard reset* will be necessary. Appendix I shows the two graphics screens that will be observed while running *GSACQU*.

## 9 Using Postscan Analysis - GSPOST

The data created by GSACQU can be loaded, the information contained within observed, and to a certain extent analysed, by GSPOST. A demonstration data file, DEMO.DAT is provided and can be used to gain familiarity in using this program. This program is executed by typing

**gspost**

The user will be prompted for the name of the data file to be opened. If the chosen file exists it will be opened and a second file name, for the pressure data file, will be requested. This is an extra file created by GSPOST that will contain peak pressure information of individual footsteps. It is usual for this file to have the same name as the original data file, realized by simply pressing *return*. For example if ABC.DAT is initially opened then the pressure data file ABC.GPD will be created. Before entering the graphics environment of the program an additional comment will be prompted for which, if required, is displayed with the foot pressure waveforms, and also appears on hard copies.

All graphics screens displayed while running GSPOST have a similar layout consisting of three windows, these being a main *waveform* window, a *text* window positioned to the right and a small top *title* window. The graphics screen which GSPOST initially displays is the *main screen* which shows the pressure/time waveforms for the whole test. Any section of this display, i.e. any footstep or selection of footsteps, can be zoomed into and this information can subsequently be shown in the *zoom screen*. It is necessary to superimpose the waveforms on a common set of axes in order to examine the information from a single footstep. The *miniscan screen* displays such information, after the appropriate footsteps have been selected.

The remainder of this chapter is sectioned into three parts. The first explains the functions that can be performed while in the main screen, the second those that can be performed while in the miniscan screen and the final section discusses hardcopy functions. Chapter 11 shows the function key template, in summary to this chapter. It should be noted that certain display conditions are required for some of the functions, this, where applicable, is fully explained in this chapter. Appendix I shows the three graphics screens that will be observed while running GSPOST.

### Main Screen

The information from all sixteen transducers for the whole test is displayed as pressure/time waveforms. The eight waveforms associated with the left foot are displayed in the top half of the waveform window while those associated with the right foot are displayed in the bottom half. Channel labelling is shown in the right text window, along with other file details.

The displayed waveforms can be manipulated on the screen in order to emphasise certain features of the information.

A trace is selected by pressing the corresponding channel index key, i.e 0 to f. For example the 3rd MTH for the right foot is selected by pressing c. The selected trace is shown with a \* to the left of the channel labelling in the text window.

*PgUp* and *PgDn* moves the selected trace up and down the screen, altering the corresponding *offset* value for that trace.

*UpArrow* and *DnArrow* increases and decreases the magnification of the selected trace, altering the corresponding *mag* value for that trace.

*F7* will redraw the selected trace following any alterations of the above nature. Note that the trace is not redrawn automatically.

*Return* will refresh the screen and redraw all traces, this is particularly useful if offset and magnitude

values require changing for more than a couple channels.

*F1* enables the quick measurement cursor. This is useful in order to obtain a quick measurement of the time duration and/or the pressure difference between two points. The mouse is used to select the points which are associated with the selected trace. As an example, if the time taken to reach maximum heel pressure and the value of this pressure are required for the left foot, referenced from heel strike, then the first cursor position (left mouse button) will be positioned at heel strike and the second cursor position (right mouse button) on the peak of the waveform. The selected channel for this example should be 0 and the calculated values will be shown in the text window. To clear the screen of this information and restore normal program operation *return* should be pressed once through with this feature.

*F3* is a function that enables quick footstep referencing, essentially speeding up the process of selecting each footstep for the later display as superimposed waveforms in the miniscan screen. This is accomplished by loading and storing the data points for the beginning and end of each footstep of interest. Display of these selected footsteps is toggled by pressing *shift + F3*. This facility is currently not available for Gaitscan version 2.0.

*F4* enables the mouse cursor for the selection of the zoom limits. The waveform section between the two selected points will be displayed on the *zoom* screen following use of the left and right mouse buttons to select the first and second data points as limits. Once the data points have been selected the user is prompted for continuation on to the zoom screen. This choice is made by clicking the mouse button with the cursor positioned over the desired response, displayed in the text window.

*F9* followed by *return* will enable display of the help screen which contains a summary of the screen manipulation keys and other functions. Striking *return* in this screen will return the user to the main screen.

### Miniscan Screen

A left footstep followed by a right, or vice versa, can be displayed on the same screen in a format such that the pressure/time waveforms for each foot are superimposed. This display format will be familiar to clinicians and other people who have previous experience of other foot pressure measuring systems.

Initially it should be decided which two footsteps to observe, i.e. a left followed by the next consecutive right or vice versa.

*F4* is pressed to enable the zoom cursor and the required footsteps should be contained within the two selected points, using the mouse buttons. On entering the zoom screen all either sixteen channels can be displayed or alternatively just two from each foot. Sometimes it may be desirable to scan through many footsteps, thus time is saved by just displaying four waveforms in total at this stage.

It is necessary to locate *heel strike* and *toe off* accurately for both footsteps before entering the miniscan screen. This is accomplished by first selecting heel strike for the earliest footstep followed by toe off for the same footstep using the left and right mouse buttons respectively. Following this the same procedure is performed for the next footstep. The user will then be prompted for continuation on to the miniscan screen.

As well as the superimposed waveforms, additional information is also available in the miniscan screen. The peak pressure values are calculated for each transducer for the consecutive footsteps and displayed in the text window.

*F2* will store these peak pressure values in the pressure data file, e.g. ABC.GPD.

*F8* will enable the mouse cursor which can then be used to display timing details for the waveforms. All timing information is displayed in milliseconds and is calculated from the y-axis, the time between two points is therefore merely a difference calculation.

*F10* will disable the cursor and so quit from further timing calculations. A second press of *F8* will

refresh the screen and enable a second set of timing measurements to be taken. With the timing cursor disabled a press of *F10* will return the user to the main screen.

### Hardcopy Functions

Reference should also be made to chapter 3 for printer and plotter support features.

The most useful hardcopy feature is the ability to obtain a print/plot of the main miniscan screen. It may be desirable to obtain a print/plot with a white background, instead of the light grey as used for the screen displays. While in the miniscan screen the background colour can be toggled to white, for the purposes of screendump printing, by pressing *shift + F6*. A screen dump using the Integrex ink-jet printer is triggered by the sequence *PrtSc, w, return*. The printer driver software literature should be consulted, as the other facilities available are not described in this manual.

While in the main screen a plot of all sixteen waveforms for the duration of the test can be obtained directly on a HP ColourPro plotter connected to the serial RS232 port, com1. Alternatively a plot file can be created for future plotting or exporting to other packages.

*F5* will enable a monochromatic screendump to a dot matrix printer connected to the parallel port.

*Shift + F5* will enable a colour screendump to an AMT Accel500 printer/plotter connected to the parallel port.

## 10 Using Gaitscan Setup - GSETUP

All the transducers are calibrated and this information is contained in the GSETUP.CAL file along with the polarity of the signal from each transducer and the hardware gain of the system.

*GSETUP* is a mouse driven program that permits creation and alteration of the GSETUP.CAL file. If it does not find a GSETUP.CAL file in the working directory it will prompt for the information required to form a new one. It will not normally be necessary to use this program unless the GSETUP.CAL file has been accidentally deleted or if different transducers are to be used or if a transducer has been replaced.

This program is executed by typing

**gsetup**

Once inside the program a single screen will be displayed. Any calibration figure can be altered by clicking the mouse button with the cursor over the selected figure. A new figure can then be entered, or if *return* is pressed the old figure is restored. On completing any alterations the mouse cursor is placed over the EXIT bar and the button clicked to exit the program and save the modified GSETUP.CAL file. It should be noted that the original file is over written and so it should be copied to another file name before executing *GSETUP* if there is a possibility of requiring this information at a later date.

The transducers are each given a sensitivity measured in pC/N, values of around 20pC/N are typical. The hardware gain has units of V/nC and the value provided is for all channels as the actual individual gains for each channel are within 1% of each other. Gaitscan uses these parameters to calculate calibration factors for each channel and hence V/pC sensitivities for each transducer. Depending upon how the transducers were constructed they provide either a positive or a negative charge signal due to a positive applied force, Gaitscan allows for this by inverting the detected voltage if the transducer provides a negative charge signal. This transducer polarity information is also held in GSETUP.CAL, inside the program this is represented by *n* or *p* characters. Using the wrong polarity will result in an inverted waveform and inaccurate peak pressure calculations.

Appendix I shows the graphics screen that will be observed while running *GSETUP*.

**11 Summary of Function Key Utilisation  
for Postscan Analysis**

	<b>Function Key Alone</b>	<b>Shift + Function Key</b>
<b>F1</b>	Enable Cursor	
<b>F2</b>	Store Peak Pressure Data	
<b>F3</b>	Load Footsteps	Display Loaded Footsteps
<b>F4</b>	Zoom	
<b>F5</b>	Dot Matrix Screen Dump	Accel Screen Dump
<b>F6</b>	Plot	Toggle Background Colour
<b>F7</b>	Redraw Single Trace	
<b>F8</b>	Miniscan Timing	
<b>F9</b>	Help	
<b>F10</b>	Quit	

## 12 Technical Specifications and System Details

### Hardware Requirements

IBM AT or compatible

1M Byte memory

80287 Co-Processor (optional)

Hard Disc Drive - 40MB minimum

360K Byte or 1.2M Byte Floppy Disc Drive

EGA or VGA capabilities

RS232 Serial Port (two recommended)

Parallel Printer Port

MetraByte DAS16 16 Channel High Speed A/D Interface Card (or compatible)

Printer/Plotter (depending upon requirements)

Integrex Colourjet 132 Printer

HP ColorPro Plotter

Dot Matrix Printer (e.g. Epson FX80, FX1000 etc)

Accel 500 AMT Printer/Plotter

Serial Mouse

### Software Support Requirements

DOS Version 3.2 or greater

Integrex IBM PC Screen Dump Program (DumpEGA2)

Microsoft Mouse Driver Version 5.03 or greater

Borland Turbo Pascal Version 5 (if source code editing is required)

### Gaitscan Equipment Specifications

16 Piezoelectric Film Transducers

2 Charge Amplifier Ankle Boxes

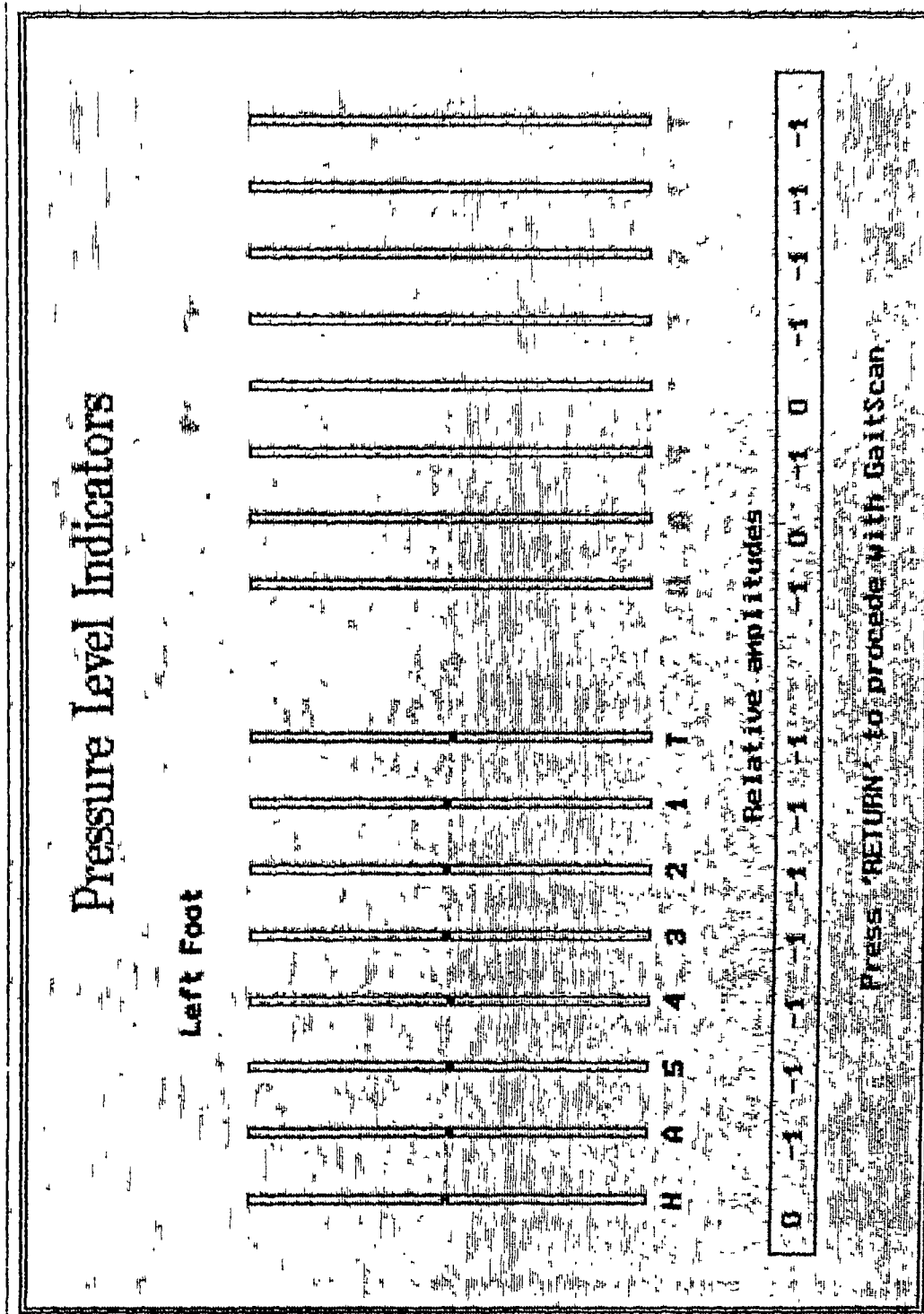
1 Junction Waist Box

1 Main Bench Console

1 Transducer Calibration Unit (optional)

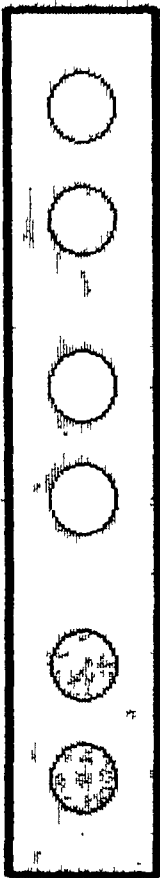
Interconnection Leads

Appendix I Examples of graphics screens



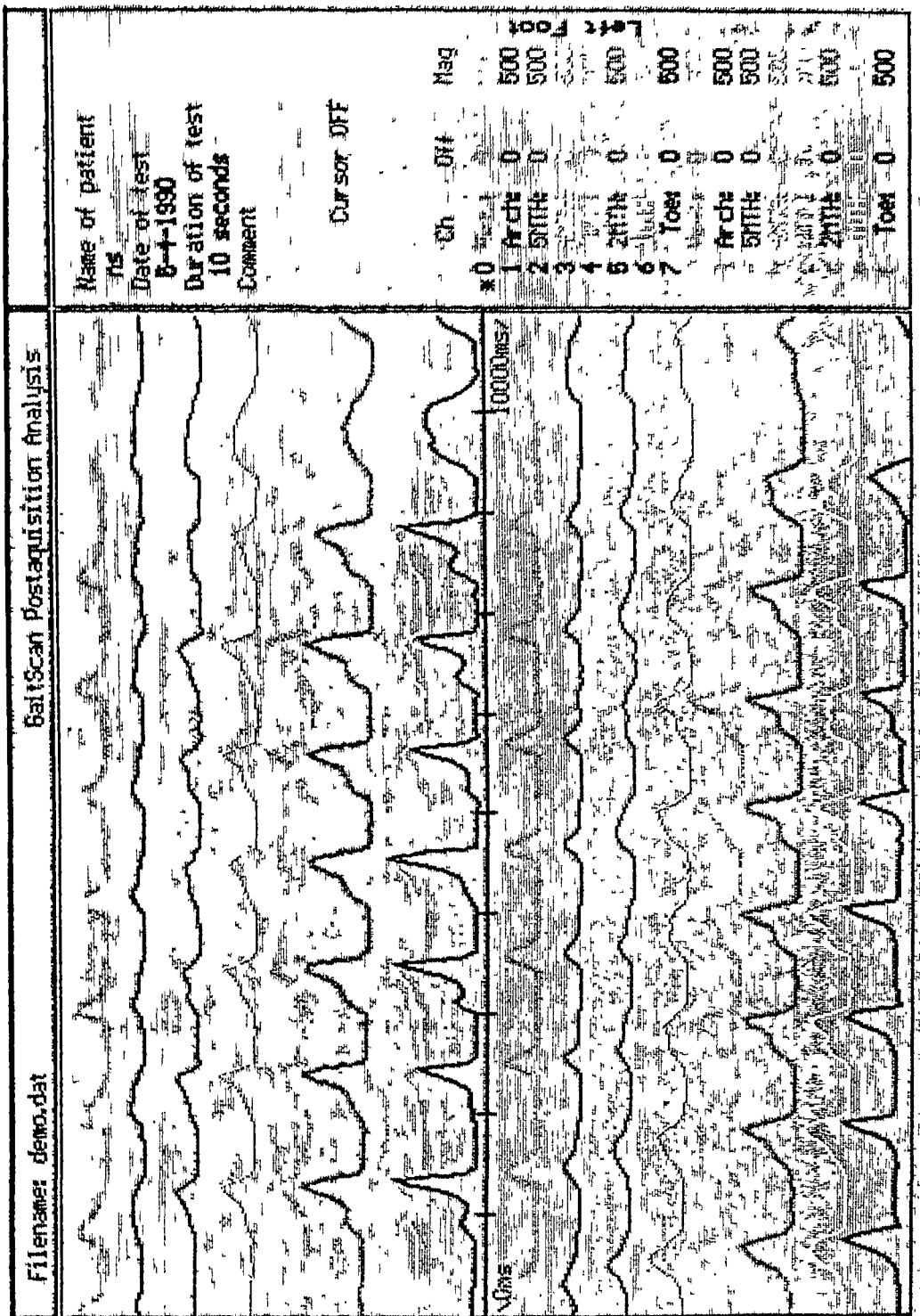
GSACQU Pressure level indicators screen - chapter 8

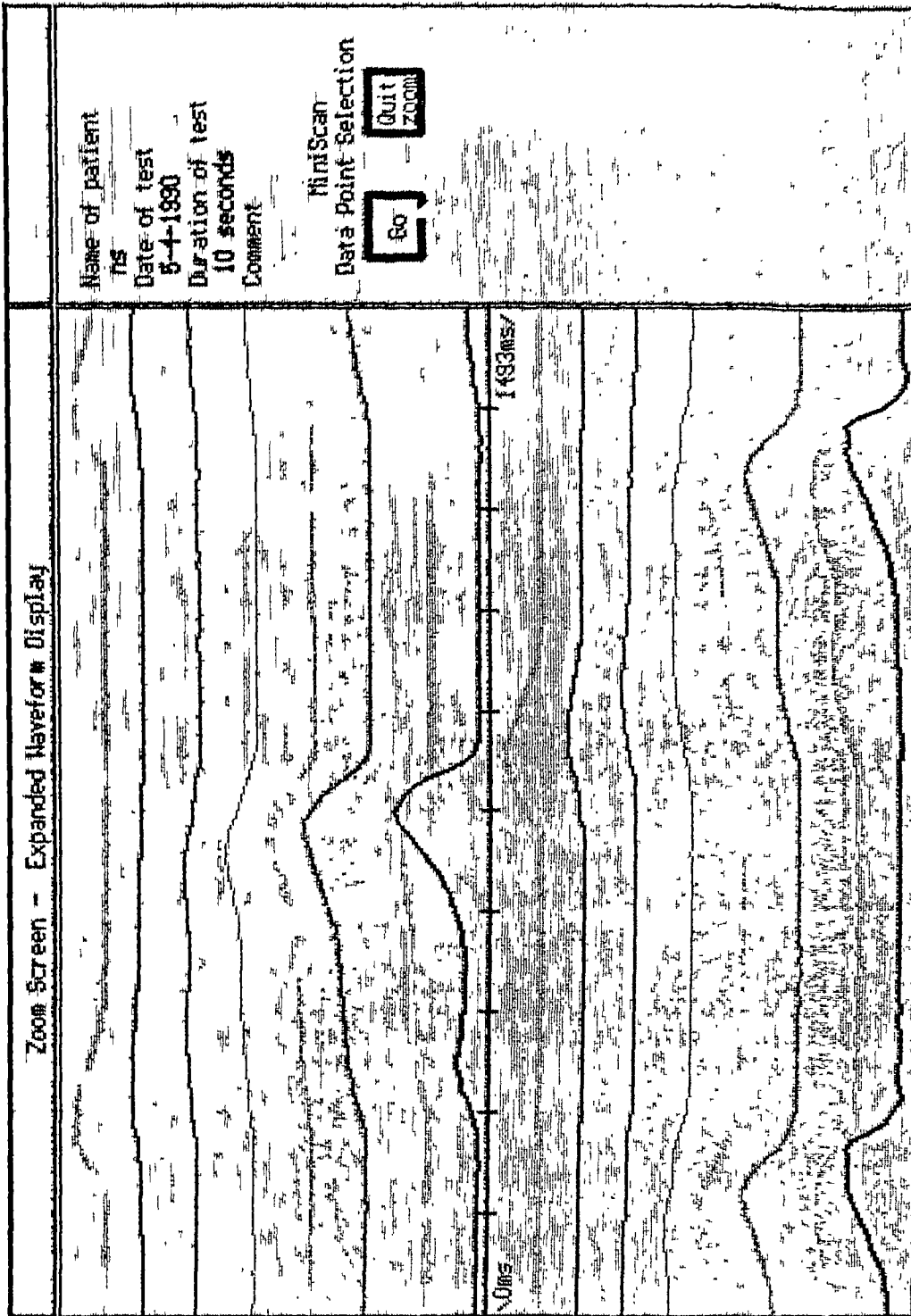
**GaitScan Acquire**



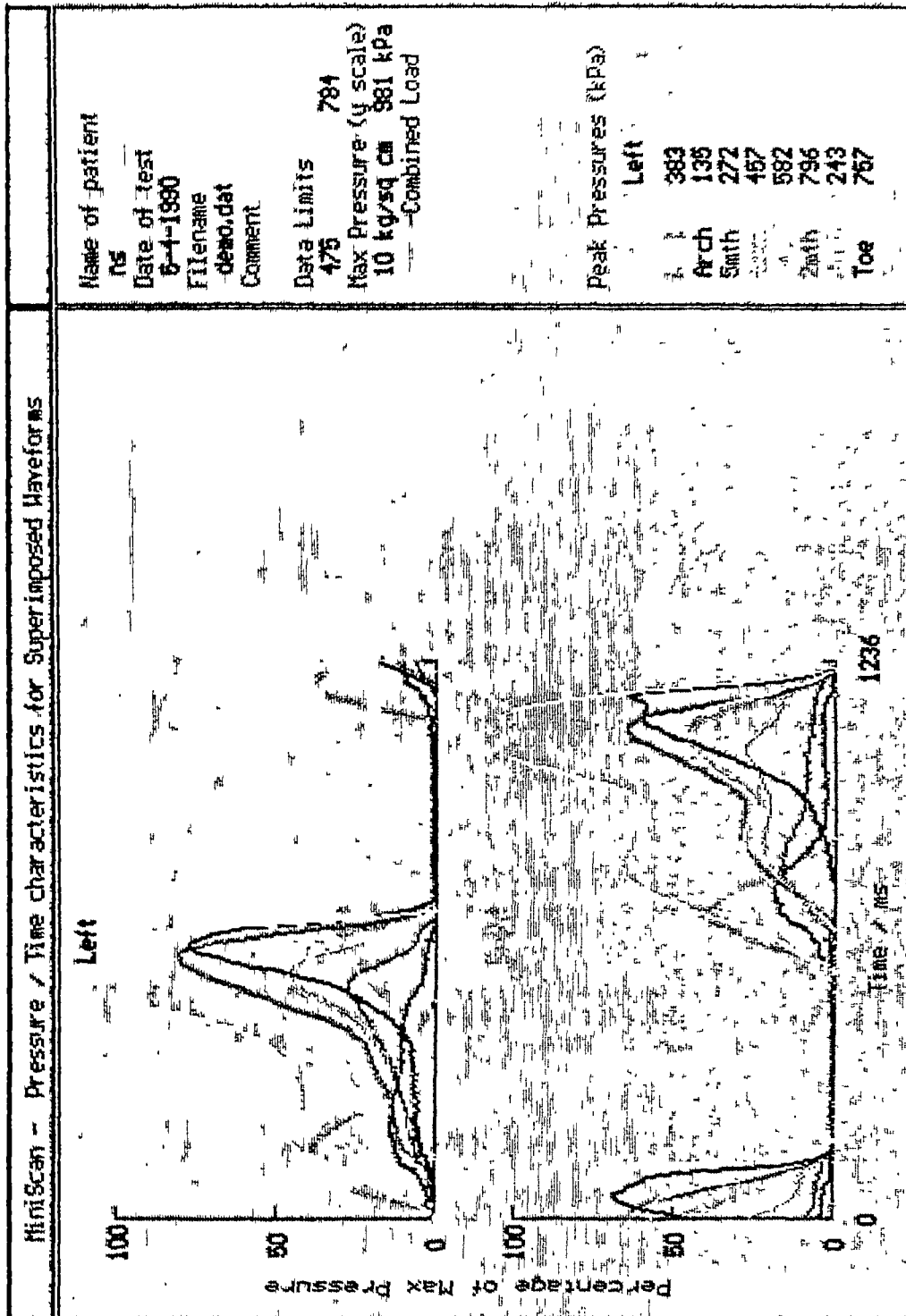
**Ready to Scan BOTH feet.**

Duration of Test	Acquisition Rate	Size of File	Available Heap Memory
second/s	samples/sec	Kbytes	Kbytes

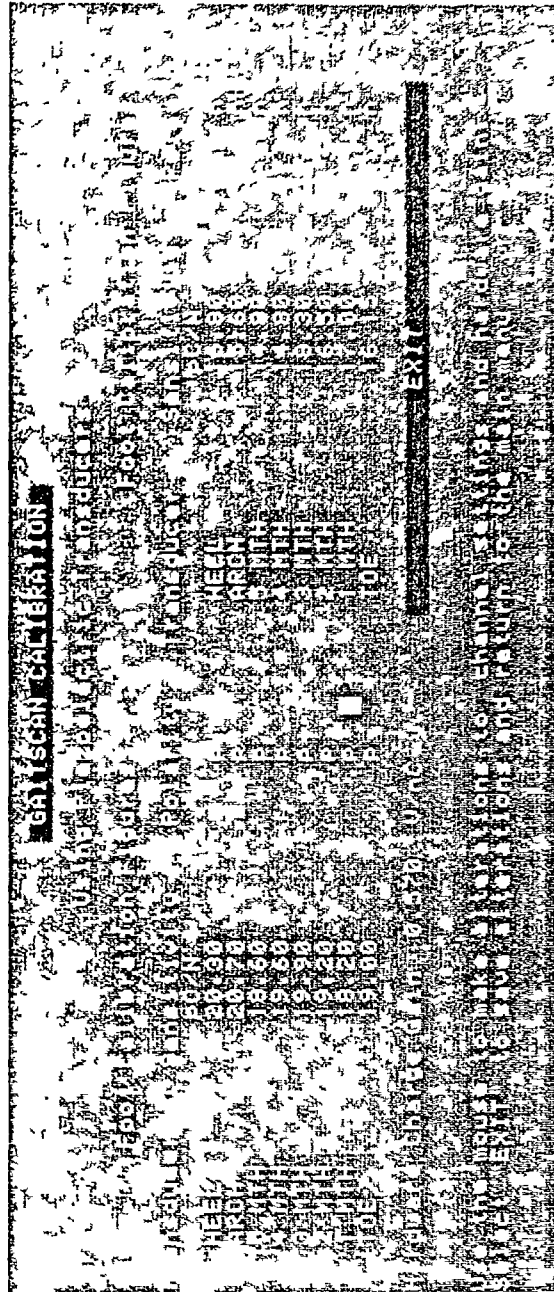




GSPOST Zoom screen - chapter 9



GSPOST Miniscan screen - chapter 9



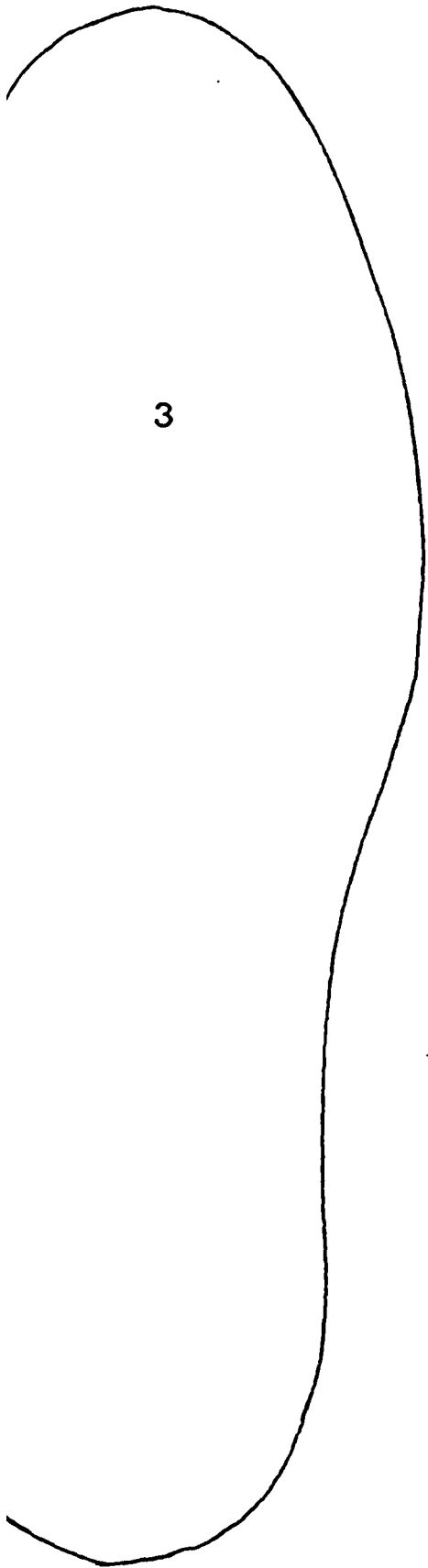
GSETUP Main screen - chapter 10

## Appendix II Standard Insole Templates

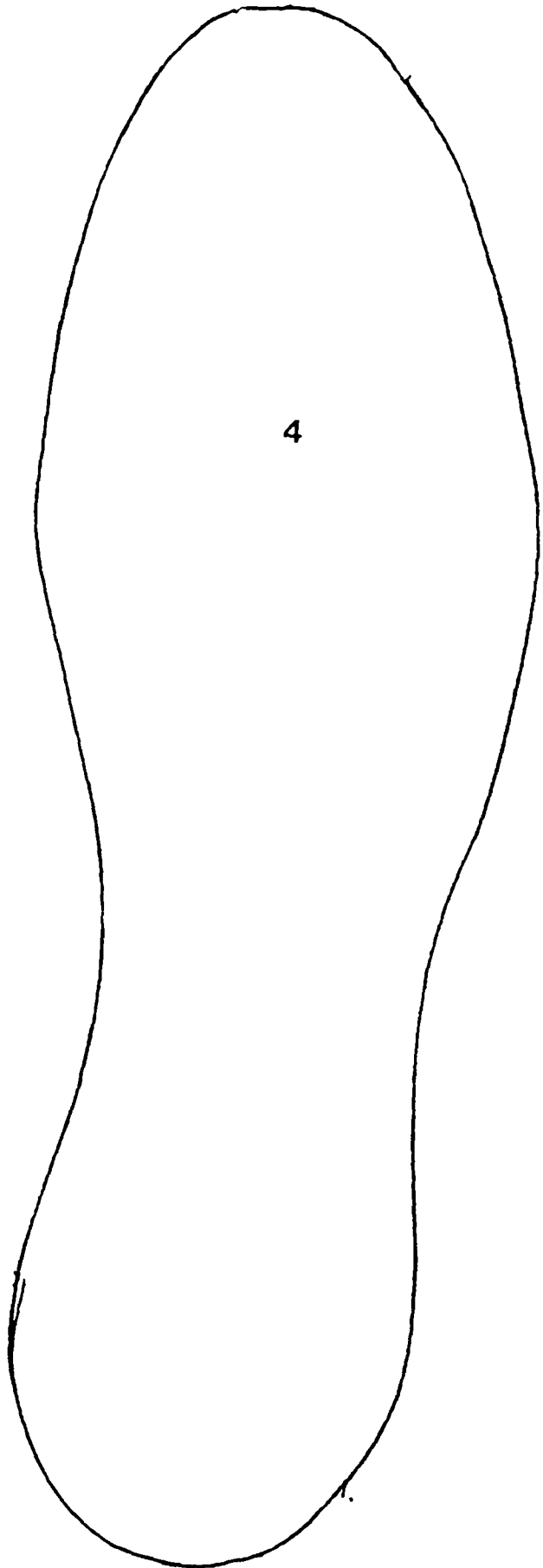
There are of course many hundreds of different shoe designs and shapes, and so insole templates must be considered only as rough guides to the actual shoe insole shape required for any particular shoe.

The shapes provided in this appendix can be used to construct a set of *masters* which can then be used in the clinic. It is recommended to construct these masters from regenerated leather board or a similar material.

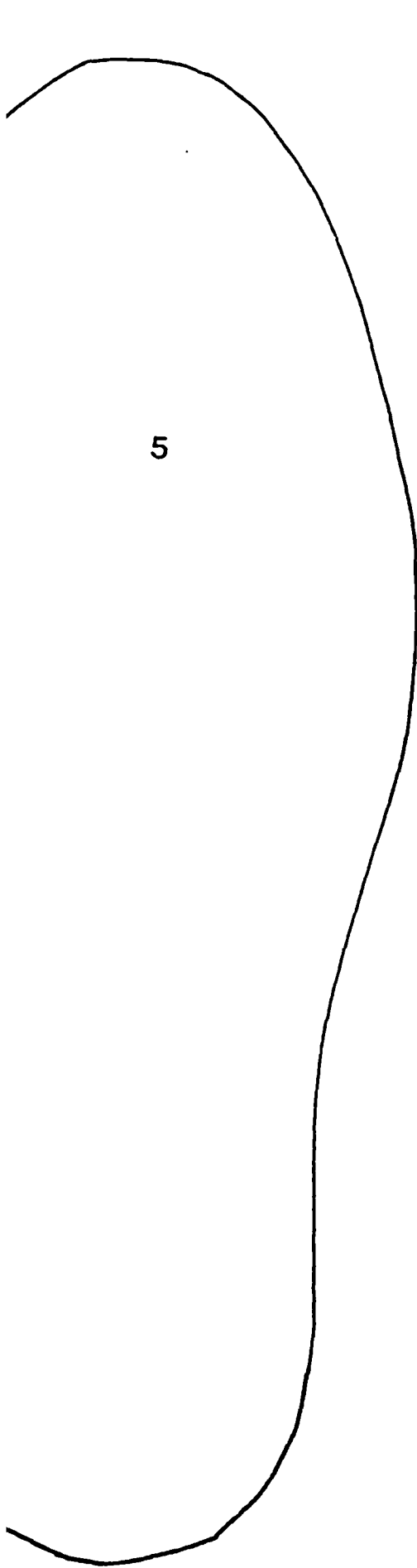
Insole templates are given for the shoe sizes 3 to 11 (approximate sizes).



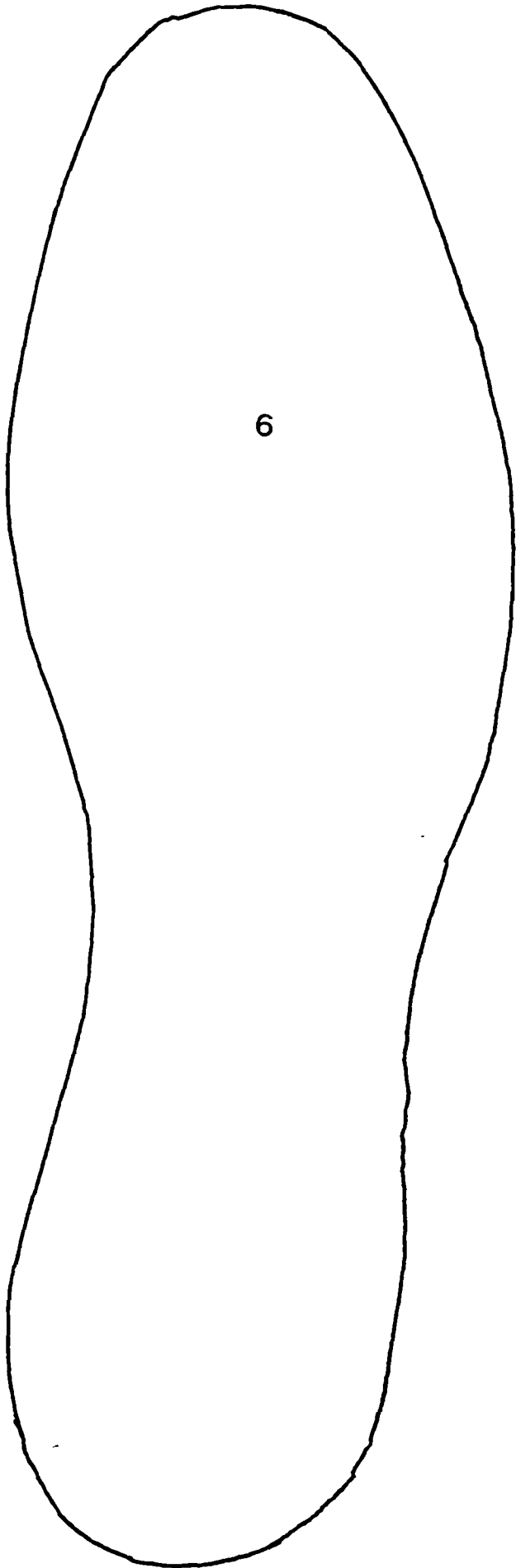
3



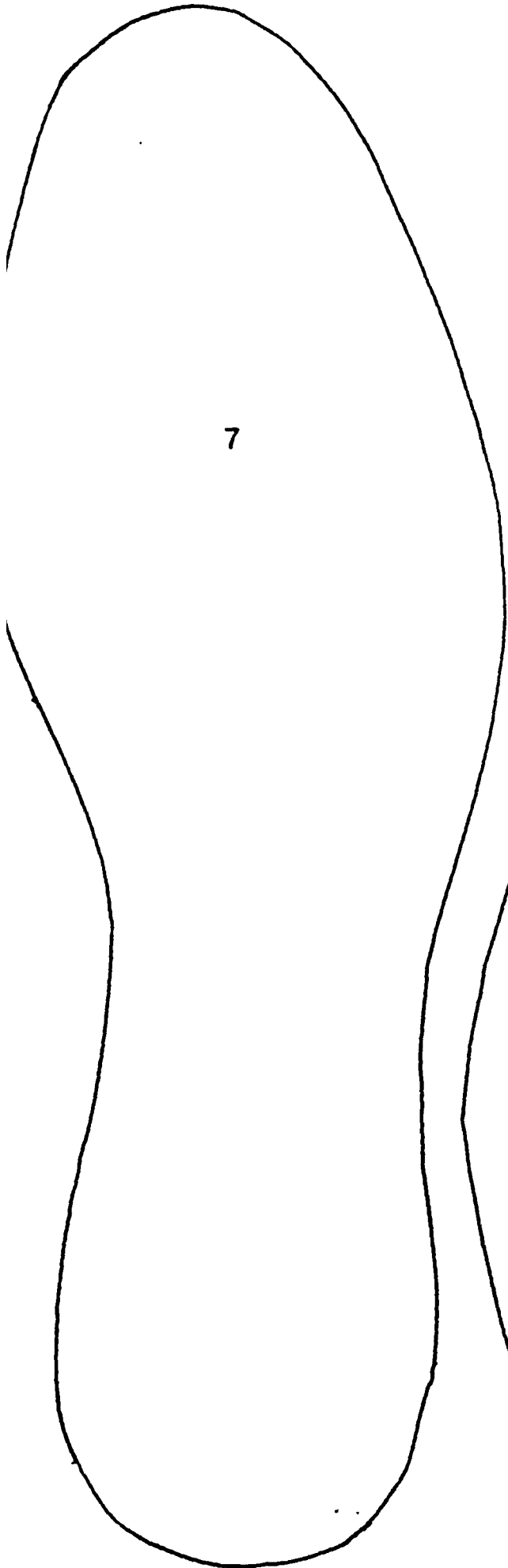
4



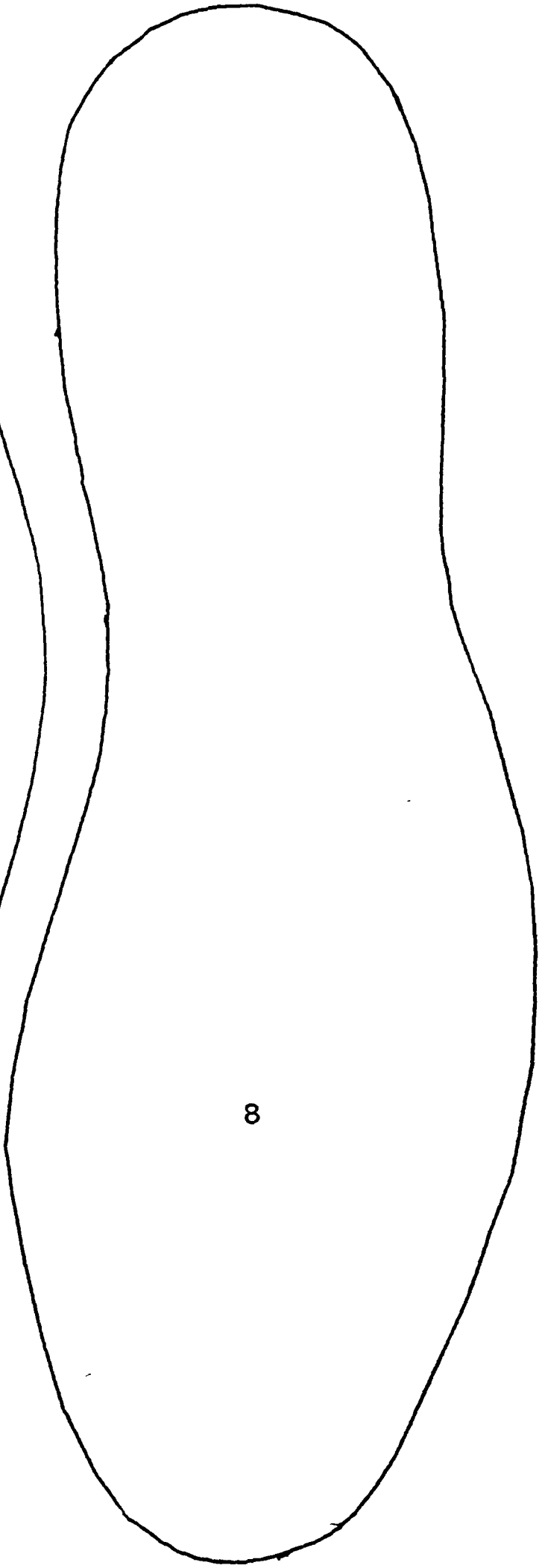
5



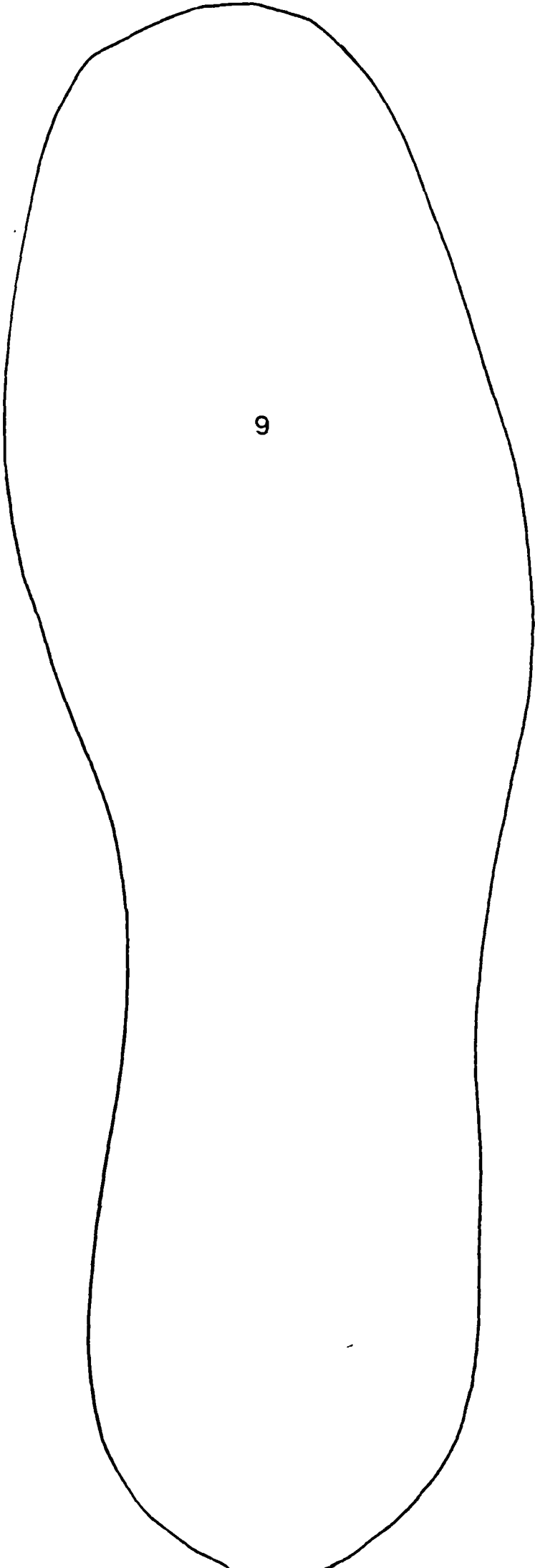
6



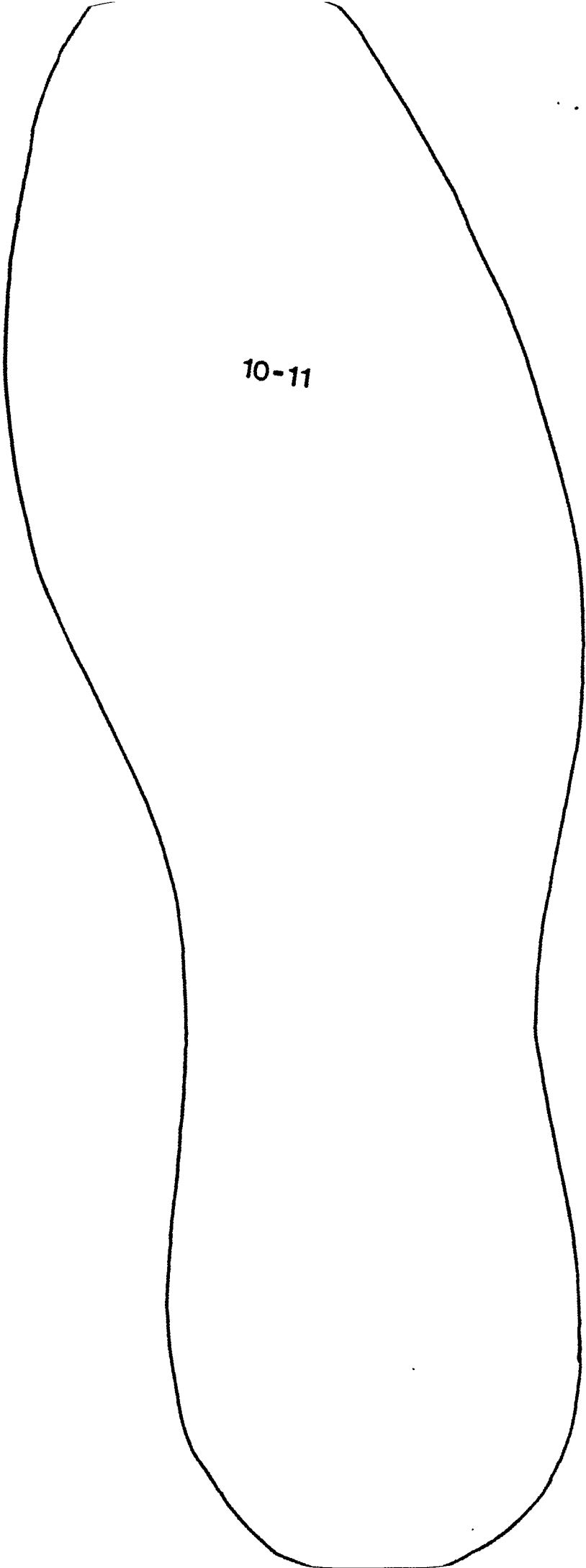
7



8



9



10-11

**Appendix**

**III**

**PRINTED CIRCUIT TEMPLATES  
COMPONENT LAYOUT  
AND CONNECTION DIAGRAMS**

ii Printed circuit templates, component layout and connection diagrams

Insole

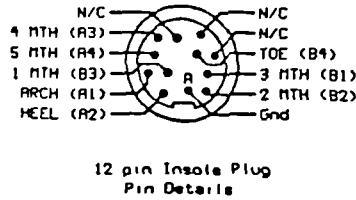


Figure III.1 Pin details for the 12-pin insole plug

Ankle Box

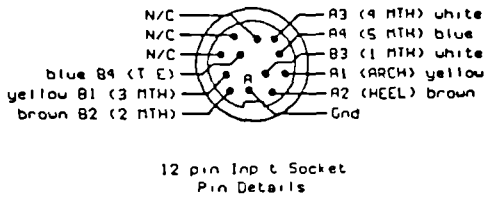


Figure III.2 Pin details for the 12-pin input socket

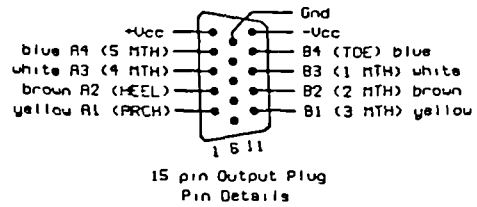


Figure III.3 Pin details for the 15-pin output socket

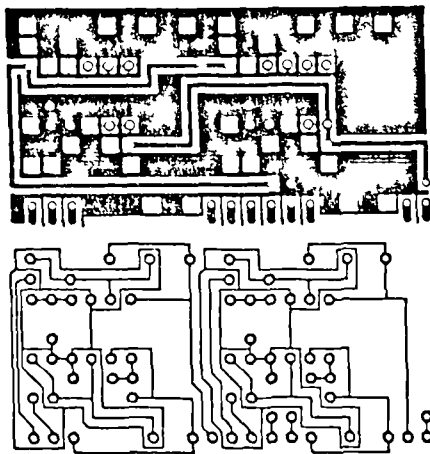


Figure III.4 Top and bottom layer printed circuit templates for an ankle box component card

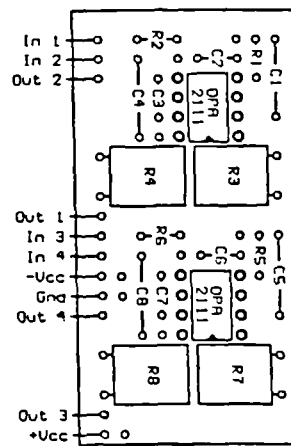


Figure III.5 Component layout diagram for an ankle box component card

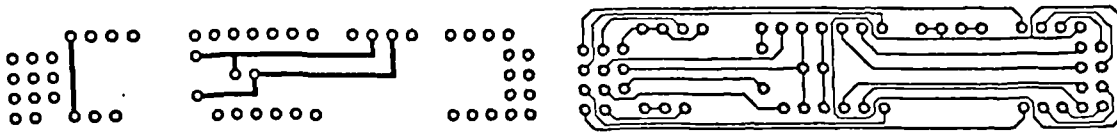


Figure III.6 Top and bottom printed circuit templates for the ankle box mother board

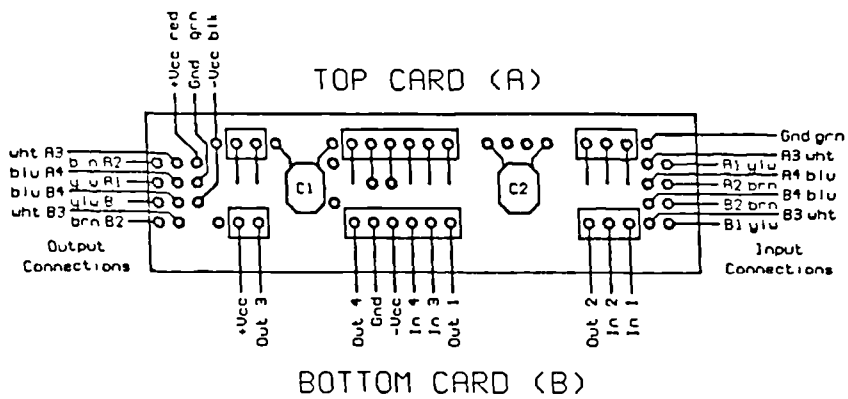


Figure III.7 Ankle box mother board interconnection diagram

Waist box

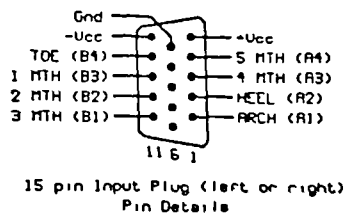


Figure III.8 Pin details for the 15-pin input plug for the left or right foot

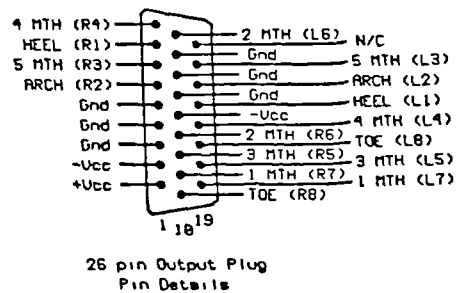


Figure III.9 Pin details for the 26-pin output plug

Main equipment console

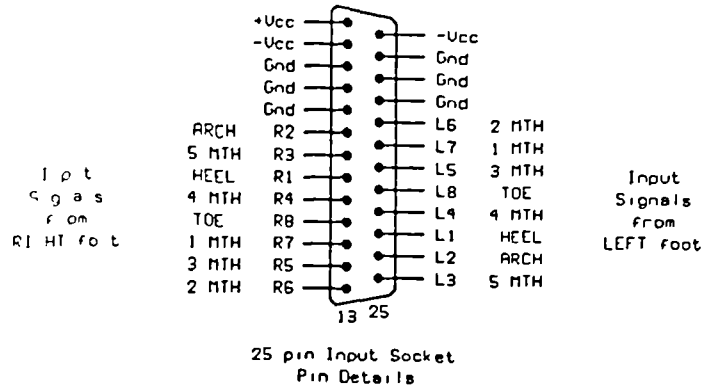


Figure III.10 Pin details for the 25-pin input plug

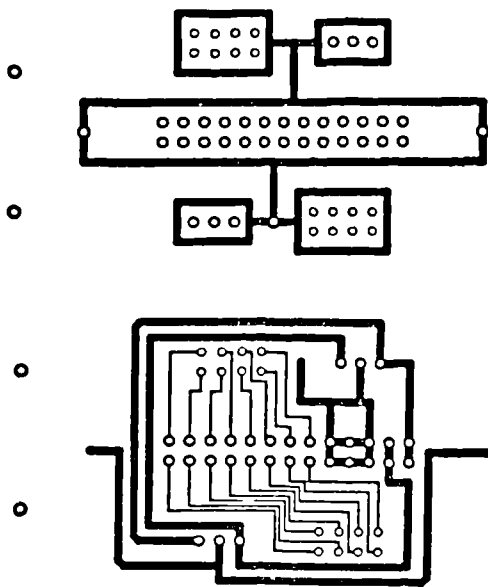


Figure III.11 Top and bottom layer printed circuit templates for the connection back plate

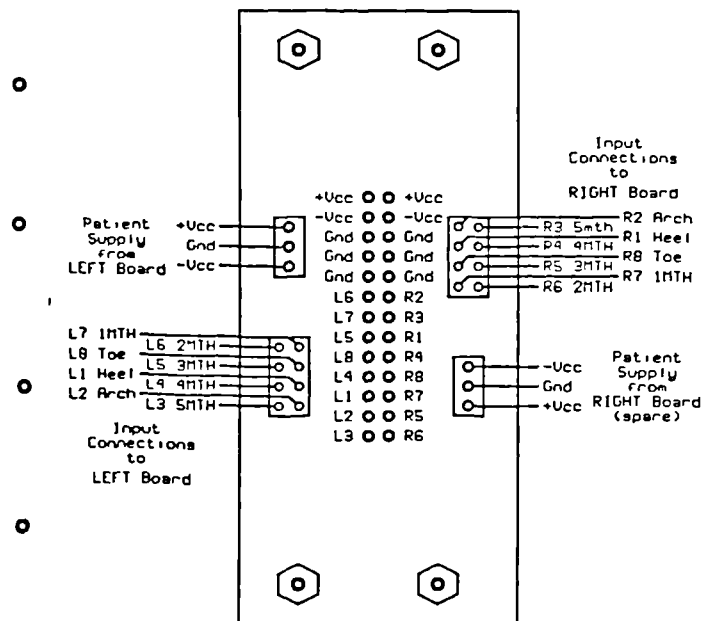


Figure III.12 Connection back plate interconnection diagram

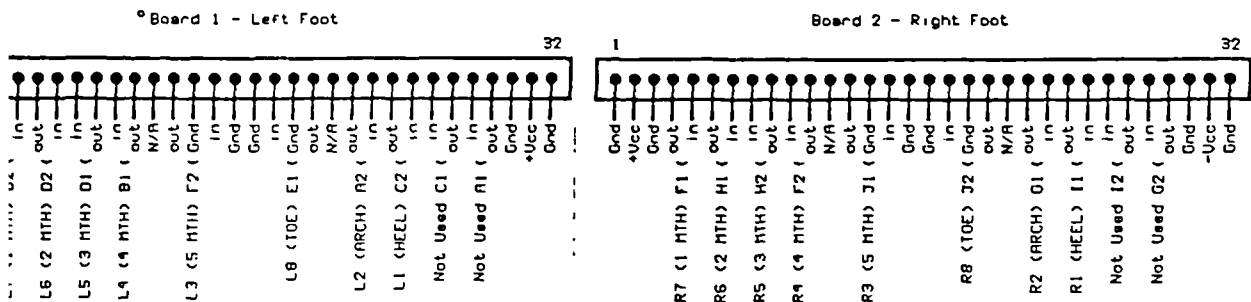
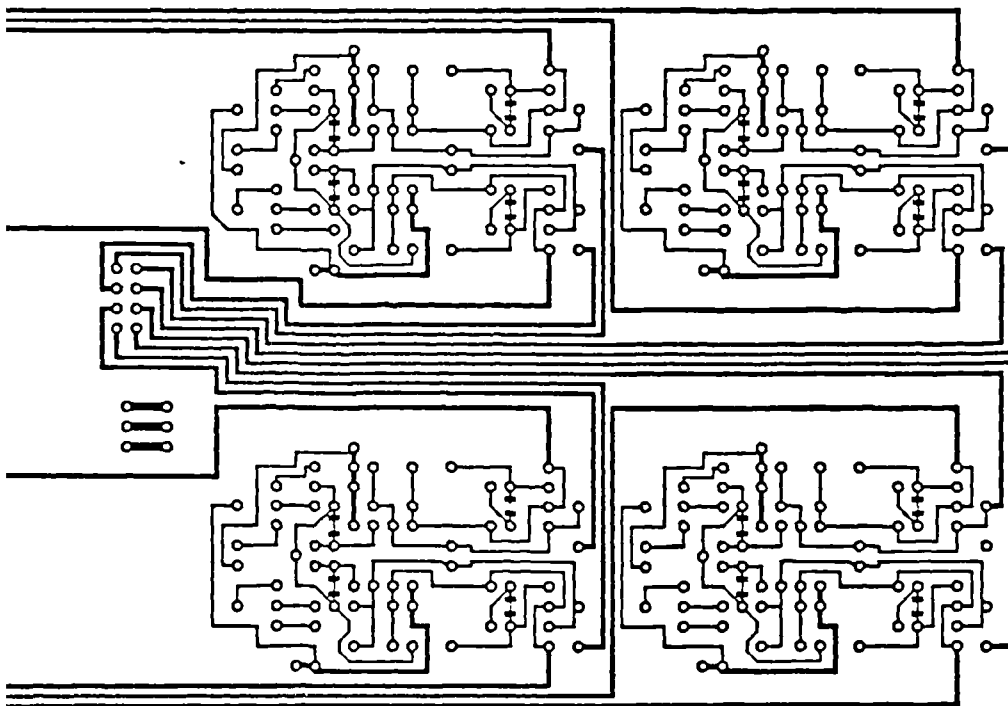
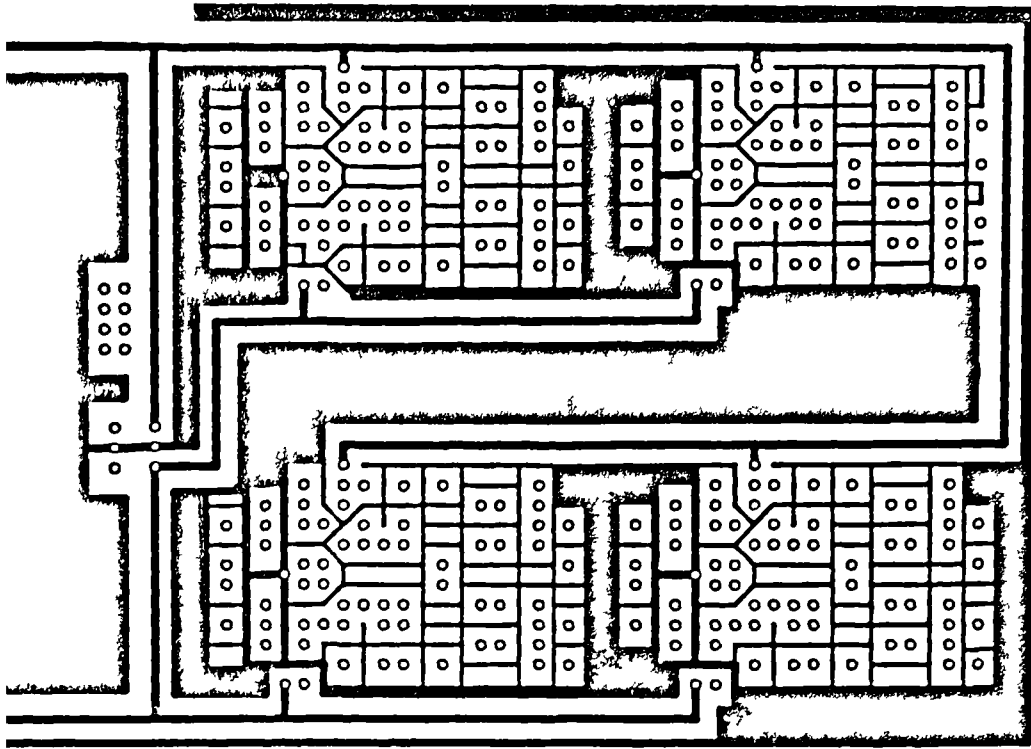


Figure III.13 Main equipment frequency compensation unit connection diagram



4 Top and bottom layer printed circuit templates for the frequency compensation unit

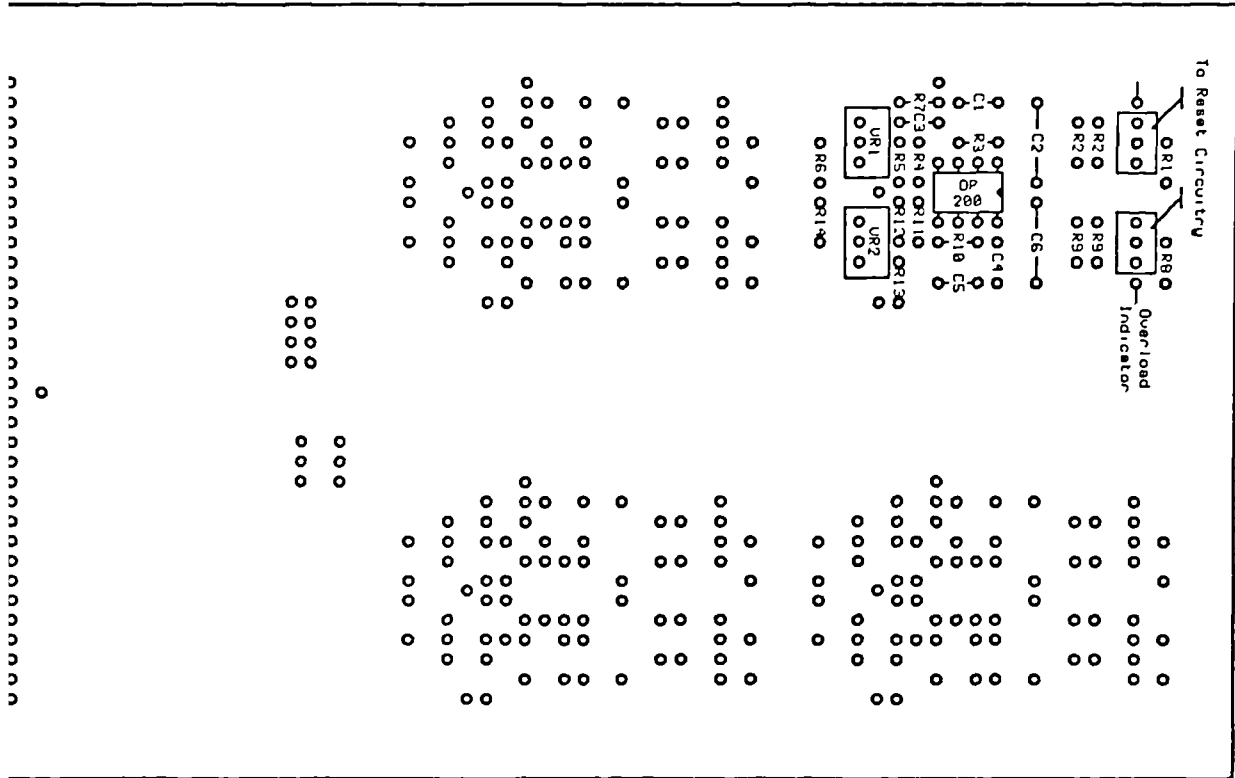


Figure III.15 Component layout diagram for the frequency compensation unit

**Appendix**

**IV**

**TRANSDUCER PROTOTYPE  
CODES**

## Transducer prototype codes

A transducer prototyped during the research has been given a 6 or 7 character code to represent the structure of, and the materials used for, its construction. The first six characters are letters (A - Z) and the seventh is present if the sixth is 'Y' - this is an integer and is an extra code to provide special information for that transducer.

### Format

ABCDEF(n)

- A: Top layer
- B: Top glue layer
- C: Piezo film type including film electrode and treatment details
- D: Bottom glue layer
- E: Bottom layer
- F: Other information 'Y' or 'N' - numeric code present if 'Y'

## Transducer codes

### Top and Bottom layers

- O - None
- D - Double sided circuit board
- B - Brass
- F - Flexible circuit layer

### Glue layers

- A - F241 Toughened Acrylic 2 part adhesive (Perma Bond)
- B - Double sided adhesive tape (non conducting)
- C - Double sided electrically conducting transfer tape (3M 9703)
- D - Cyanoacrylate (Perma Bond)
- E - Cyanoacrylate (Loctite 406 + 757 primer)
- F - Cyanoacrylate (Pacer Tech. Flex Zap)
- G - Quick set epoxy resin (Devcon)
- H - ER 1436 epoxy resin (Design Resins)
- I - ER 1426 epoxy resin (Design Resins)
- J - UR 5048 polyurethane resin (Design Resins)
- K - UR 5062 polyurethane resin (Design Resins)
- L - Photo mount spray adhesive (3M)
- M - Silver loaded epoxy resin (RS)

film

With PTFE etchant treatment

A - 28 $\mu$ m non electroded Kynar PVdF  
B - 28 $\mu$ m silver ink Kynar PVdF  
C - 28 $\mu$ m aluminium/nickel Kynar PVdF  
D - 52 $\mu$ m non electroded Kynar PVdF  
E - 52 $\mu$ m silver ink Kynar PVdF  
F - 110 $\mu$ m non electroded Kynar PVdF  
G - 110 $\mu$ m silver ink Kynar PVdF  
H - 500 $\mu$ m non electroded Kynar copolymer  
I - 500 $\mu$ m silver ink Kynar copolymer  
J - 500 $\mu$ m aluminium/nickel Kynar copolymer  
K - 400 $\mu$ m copper Yarsley PVdF

P  
Q  
R  
S  
T  
U  
V  
W  
X  
Y  
Z

information

N - No other information  
Y - Additional information, code:

1: None  
2: None  
3: None

**Appendix**

**V**

**COSTING**

## Appendix V Costing

The costing for this prototype system has been estimated for August 1991 and is presented in this appendix. The material and labour costs for four areas are considered (transducers, equipment, data acquisition and the computer) and the labour costs have been calculated at a technician rate of £16/hr.

### Transducers

Material costs	- £10
Labour costs:	
Transducer components fabrication	- 2hrs
Preparation	- 1hr
Construction, clean-up	- ¼hr
Soldering, finishing	- ½hr
Total	- 3¼hrs, £60EA
Total costs	- £70EA

Therefore the cost of a set of 16 transducers is estimated to be £1120 and so as the expected life span is 500 uses the estimated cost per use is £2.25. If the transducers were to be manufactured then the use of automated fabrication processes would bring the total assembly time down to around 1hrEA, so without considering tooling costs a set of transducers would cost around £420 (80p per use).

### Equipment

Item	Material costs, £	Labour costs, hrs/£
Ankle box (both)	160	5/80
Waist box	20	1/16
2nd stage unit	100	4/64
Calibration unit	60	3/48
Main enclosure	90	3/48
Power supply	150	1/16
Cables	110	5/80
Total	£690	22hrs/£352
Total costs	- £1042	

**Data acquisition card**

DAS16 (Keithley Instruments Ltd) - £695

Alternative:

PCL718 (Integrated measurement systems) - £600

**Computer**

IBM compatible, AT, VGA, 40MByte HD, floppy - £800

**Total Costs**

All inclusive - £3657

Material only - £2345